

**STRENGTH OF BEAM-COLUMNS IN FLEXIBLY
CONNECTED STEEL FRAMES**

by

John Buick Davison

**A thesis submitted to the
Department of Civil and Structural Engineering
in partial fulfilment of the requirements for the**

Degree of

DOCTOR OF PHILOSOPHY

UNIVERSITY OF SHEFFIELD

June 1987

CONTENTS

	Page
Contents	ii
List of Tables	v
List of Figures	vii
Acknowledgements	xvii
Declaration	xviii
Summary	xx
Notation	xxi
1.0 INTRODUCTION	1.1
References	1.4
2.0 BACKGROUND	2.1
2.1 Introduction	2.1
2.2 Beam to Column Connections	2.1
2.3 Restrained Columns	2.5
2.4 Frame Tests	2.9
References	2.13
3.0 ROTATIONAL STIFFNESS CHARACTERISTICS OF STEEL BEAM TO COLUMN CONNECTIONS	3.1
3.1 The Need for Experimental Data	3.1
3.2 Connection Selection and Design	3.1
3.3 Joint Test Apparatus	3.2
3.4 Fabrication of Test Specimens	3.3
3.5 Assembly and Testing	3.3
3.6 Behaviour of web cleat Connections	3.5
3.7 Behaviour of Flange Cleat Connections	3.10
3.8 Behaviour of Seat and Web Cleat Connections	3.12
3.9 Behaviour of Flush End Plate Connections	3.13
3.10 Behaviour of Extended End Plate Connections	3.18
3.11 The Effect of Lack of Fit and Connection Performance	3.21
3.11.1 Web Cleat Connections	3.22
3.11.2 Flange Cleat Connections	3.24
3.11.3 Flush End Plates	3.26
3.11.4 Extended End Plates	3.29
3.11.5 Extended End Plates to Column Web	3.31
3.12 Conclusions	3.32
References	3.35

4.0	SUBASSEMBLAGE TESTS	4.1
4.1	Introduction	4.1
4.2	Test Apparatus and Instrumentation	4.2
4.3	Test Procedure	4.3
4.4	Summary of Tests Conducted	4.5
4.4.1	Details of Test ST5	4.5
4.4.2	Details of Test ST6	4.7
4.4.3	Details of Test ST7	4.7
4.4.4	Details of Test ST3	4.8
4.4.5	Details of Test ST2	4.9
4.4.6	Details of Test ST8	4.10
4.4.7	Details of Test ST4	4.11
4.4.8	Details of Test ST9	4.11
4.4.9	Details of Test ST10	4.12
4.4.10	Details of Unrestrained Column Tests	4.13
4.5	Discussion of Results	4.15
4.5.1	Behaviour of Connections	4.15
4.5.1.1	Comparison of Joint Test and Subassemblage M- ϕ Response	4.16
4.5.1.2	Joint Action During Column Failure	4.17
4.5.2	Effective Restraint Provided by Connections	4.18
	References	4.23
5.0	FULL SCALE FRAME TESTS	5.1
5.1	Introduction	5.1
5.2	Frames Selected for Study	5.1
5.3	Fabrication and Material Properties	5.2
5.4	Test Arrangement	5.2
5.4.1	Loading Systems	5.3
5.4.2	Instrumentation	5.4
5.4.3	Data Acquisition System	5.6
5.5	Test Procedure	5.7
5.6	Test Frame 1	5.9
5.6.1	Loading History	5.9
5.6.2	Action of Connections	5.10
5.6.3	Effect of Connection Restraint on Beam Moments	5.12
5.6.4	Bending Moment Distribution around the Frame	5.13
5.6.5	Effect of Connection Restraint on Column Capacity	5.13
5.7	Test Frame 2	5.17
5.7.1	Loading History	5.17
5.7.2	Action of Connections	5.17
5.7.3	Effect of Connection Restraint on Beam Moments	5.19
5.7.4	Bending Moment Distribution around the Frame	5.20
5.7.5	Effect of Connection Restraint on Column Capacity	5.21
5.8	Conclusions	5.23
	References	5.25
6.0	COMPARISON OF EXPERIMENTAL BEHAVIOUR WITH ANALYTICAL PREDICTIONS	6.1
6.1	Declaration	6.1
6.2	Introduction	6.1
6.3	Subassemblage Tests	6.1
6.4	Comparison of Frame 1 with SERVER	6.3
6.5	Comparison of Frame 2 with SERVER	6.6
	References	6.8

7.0	DESIGN OF STEEL FRAMES WITH FLEXIBLE CONNECTIONS	7.1
7.1	Availability of Connection Restraint Characteristics	7.1
7.2	Semi-Rigid Connections and Column Design	7.3
7.3	Beneficial Effect of Semi-Rigid Joints on Beam Load Carrying Capacity	7.6
7.4	Frame Analysis and Design with Semi-Rigid Joints	7.8
7.5	Simple Design Method to Include the Benefits of Semi-Rigid Action	7.10
7.6	Conclusion	7.13
	References	7.15
8.0	CONCLUSIONS	8.1
APPENDIX A	DESIGN OF CONNECTIONS	A.1
A.1	Double Angle Web Cleats	A.1
A.2	Top and Bottom Flange Cleats	A.4
A.3	Flush End Plate	A.6
A.4	Extended End Plate	A.9
	References	A.11
APPENDIX B	DESIGN OF FULL SCALE FRAMES	B.1
B.1	Simple Design to BS 449	B.1
B.2	Semi-Rigid Design	B.3
B.3	Design to BS 5950	B.5
APPENDIX C	MATERIAL AND CROSS SECTIONAL PROPERTIES	C.1
C.1	Cross Sectional Properties	C.1
C.2	Tensile Tests	C.1
C.3	Stub Column Tests	C.2
C.4	Residual Stress Tests	C.2
	References	C.4

LIST OF TABLES

Chapter 4

- 4.1 Strain gauge positions.
- 4.2 Subassemblage test series.
- 4.3 Calculation of effective length factor k
- 4.4 Comparison of test and design loads.

Chapter 5

- 5.1 Load increments for application of beam loading.
- 5.2 Loading history of test frame 1.
- 5.3 Distribution of moments at beam loads of 53kN and 116kN (runs 6 and 12).
- 5.4 Distribution of moments at failure of internal column.
- 5.5 Comparison of test and design loads for columns in test frame 1.
- 5.6 Distribution of moments at failure of external column C3
- 5.7 Loading history of test frame 2
- 5.8 Distribution of moments at beam loads of 53kN and 116kN (runs 6 and 12).
- 5.9 Distribution of moments at failure of external column C1
- 5.10 Comparison of test and design loads for columns in test frame 2.
- 5.11 Distribution of moments at failure of internal column C2.

Chapter 6

- 6.1 Comparison of test and analysis column capacities.
- 6.2 Loading history for analysis of frame 1.

Chapter 7

- 7.1 Comparison of effective length ratios from figure 23 of BS 5950

Appendix C

- C.1 Material used in connection tests
- C.2 Material used in subassemblage tests
- C.3 Material used in frame tests

- C.4 Cross sectional properties of columns
- C.5 Cross sectional properties of beams
- C.6 Cross sectional dimensions of angles
- C.7 Material properties of columns, beams and connection components

LIST OF FIGURES

Chapter 2

- 2.1 Variation of moment-rotation characteristics for various types of beam to column connection.
- 2.2 Influence of connection stiffness on beam moment distribution.
- 2.3 Influence of connection restraint on the strength of axially loaded columns.
- 2.4 Test arrangement used by Bergquist (2.41)
- 2.5 Details of rigid joint ed frames tested by Yura and Lu (2.55) .

Chapter 3

- 3.1 Details of test connections.
- 3.2 Joint test apparatus.
- 3.3 Seat and web cleat connection under test.
- 3.4 Method of rotation measurement.
- 3.5 Experimental M- ϕ curve for web cleat connection to column web (JT/02)
- 3.6 Experimental M- ϕ curve for web cleat connection to column web (JT/03).
- 3.7 Rotation of web cleat connection.
- 3.8 Experimental M- ϕ curve for web cleat connection to column web (JT/012B).
- 3.9 Experimental M- ϕ curve for web cleat connection to column flanges (JT/04).
- 3.10 Experimental M- ϕ curve for web cleat connections to column flanges (JT/05).
- 3.11 Experimental M- ϕ curve for web cleat connection to column flanges (JT/06).
- 3.12 Comparison of M- ϕ curves for web cleat connection to column web and column flanges.
- 3.13 Distortion of column flanges produced in web cleat test
- 3.14 Typical M- ϕ Curve for Web Cleat Connections.
- 3.15 Experimental M- ϕ curve for flange cleat connection to column Web (JT/07).

- 3.16 Experimental M- ϕ curve for flange cleat connection to column flanges (JT/08).
- 3.17 Moment v horizontal slip of flange cleats in test JT/07.
- 3.18 Moment v horizontal slip of flange cleats in test JT/08.
- 3.19 Comparison of M- ϕ curves for flange cleat connection to column web and column flanges.
- 3.20 Typical M- ϕ curve for flange cleat connection to column web.
- 3.21 Bending of top flange cleat in test JT/08.
- 3.22 Bending of bottom flange cleat in test JT/08.
- 3.23 Column flange deformation produced by flange cleats.
- 3.24 Extent of deformation of column flanges in test JT/08.
- 3.25 Experimental M- ϕ curve for seat + web cleat connection to column web (JT/09).
- 3.26 Experimental M- ϕ curve for seat + web cleat connection to column flanges (JT/10).
- 3.27 Deformation of column flanges in test JT/10.
- 3.28 Distortion of web cleats in test JT/10.
- 3.29 Comparison of M- ϕ curves for seat and web cleat connections to column web and column flanges.
- 3.30 Comparison of M- ϕ curves for flange cleat and seat cleat with web cleat connection to column flanges.
- 3.31 Typical M- ϕ curve for web and seat cleat connections.
- 3.32 Typical M- ϕ curve for flush end plate connections.
- 3.33 Experimental M- ϕ curve for flush end plate connection to column web (JT/11)
- 3.34 Experimental M- ϕ curve for flush end plate connection to column web (JT/11B).
- 3.35 Test JT/11B - failure of M16 grade 4.6 bolts.
- 3.36 Failed bolts from test JT/11B.
- 3.37 Deformation of column flange produced by flush end plate connection.
- 3.38 Deformation of column flanges produced by flush end plate connection.

- 3.39 Experimental M- ϕ curve for flush end plate connection to unstiffened column flanges (JT/12).
- 3.40 Experimental M- ϕ curve for header plate connection to JT/14.
- 3.41 Extended end plate connection prior to testing.
- 3.42 Experimental M- ϕ curve for extended end plate connection to stiffened column flanges (JT/13).
- 3.43 Experimental M- ϕ curve for extended end plate connection to stiffened column flanges (JT/13b).
- 3.44 Typical M- ϕ Curve For extended end plate connection to stiffened column flanges.
- 3.45 Comparison of extended end plate connection tests with similar connection tests by Packer and Morris.
- 3.46 Deformation produced on extended end plates.
- 3.47 Comparison of extended end plate connection test with test with tests conducted at BRE incorporating backing plates.
- 3.48 Web cleat lack of fit test (CT/01).
- 3.49 Additional instrumentation on test CT/01.
- 3.50 Experimental M- ϕ curve for web cleat connection with oversized holes through beam web.
- 3.51 Experimental M- ϕ curve for flange cleat connection with holes in the beam flanges (CT/02).
- 3.52 Test CT/02 in progress.
- 3.53 Deformed shape of deliberately distorted flush end plate (CT/03).
- 3.54 Lack of fit introduced into end plates.
- 3.55 Experimental M- ϕ curve of distorted flush end plate connection (CT/03).
- 3.56 Experimental M- ϕ curve of distorted flush end plate connection with grade 8.8 bolts (CT/05).
- 3.57 Extended end plate (CT/04).
- 3.58 Deformation of column flanges produced by tightening grade 8.8 bolts (CT/04).
- 3.59 Experimental M- ϕ curve for extended end plate connection with deliberate lack of fit - grade 8.8 bolts.

- 3.60 Experimental M- ϕ curve for distorted extended end plate connection with HSFG bolts.
- 3.61 Distorted extended end plate test with HSFG bolts prior to preloading (CT/06).
- 3.62 Distorted extended end connection with fully torqued HSFG bolts.
- 3.63 Deformation of column flanges at end of test CT/06.
- 3.64 Test arrangement for tests C7/07 and C7/08.
- 3.65 Experimental M- ϕ curves for extended end plates to the column web (CT/07/08).
- 3.66 Typical M- ϕ curves for a range of connections to the column web.
- 3.67 Typical M- ϕ curves for a range of connections to the column flanges.

Chapter 4

- 4.1 'I' shaped subassemblage.
- 4.2 Subassemblage test rig.
- 4.3 Test specimen under load.
- 4.4 Beam end restraints to prevent in-plane rotation.
- 4.5 Beam end restraints.
- 4.6 Location of strain gauges.
- 4.7 Restraints to prevent out-of-plane action.
- 4.8 Local deformation produced by flange cleats - ST5.
- 4.9 Total axial load v. central displacement - ST6.
- 4.10 Total axial load v. central displacement - ST7.
- 4.11 Improved restraints at mid-height.
- 4.12 Improved restraints at third points.
- 4.13 Total axial load v. central deflection - ST3.
- 4.14 Total axial load v. central deflection - ST2.
- 4.15 Total axial load v. central deflection - ST8.
- 4.16 Total axial load v. central deflection - ST4.
- 4.17 Load buckling of column flange - ST4.

- 4.18 Local buckling of column flange - ST4.
- 4.19 Total axial load v. central deflection - ST9.
- 4.20 Total axial load v. central deflection - ST10.
- 4.21 Effective length of pin-end column tests - ST1.
- 4.22 Model for estimating degree of restraint in test ST1.
- 4.23 Comparison of moment-rotation curves from joint test and subassemblage test ST4.
- 4.24 Comparison of moment-rotation curves from joint test and subassemblage test ST7.
- 4.25 Comparison of moment-rotation curves from joint test and subassemblage test ST8.
- 4.26 Comparison of moment-rotation curves from joint test and subassemblage test ST6.
- 4.27 Moment and axial load interaction for test results.
- 4.28 Typical moment-rotation response of a semi-rigid connection.

Chapter 5

- 5.1 Frame 1 (major axis) before testing.
- 5.2 Frame 2 (minor axis) before testing.
- 5.3 Out-of-plane action bracing locations.
- 5.4 Frame nomenclature.
- 5.5 Hydraulic beam loading arrangement.
- 5.6 Column head loading arrangement.
- 5.7 Frame instrumentation.
- 5.8 Strain gauge positions.
- 5.9 Illustration of rotation device.
- 5.10 Beam and column rotation devices in position.
- 5.11 Rotation measurement at column base
- 5.12 Displacement of measurement system.
- 5.13 Initial shape of frame 1.
- 5.14 Initial shape of frame 2.
- 5.15 Distortion of connection due to beam loading.

- 5.16 Moment-rotation curve for joint C.
- 5.17 Moment-rotation curve for joint E.
- 5.18 Moment-rotation curve for joint F.
- 5.19 Moment-rotation curve for joint G.
- 5.20 Moment-rotation curve for joint H.
- 5.21 Moment-rotation curve for joint I.
- 5.22 Moment-rotation curve for joint J.
- 5.23 Moment-rotation curve for joint K.
- 5.24 Moment-rotation curve for joint L.
- 5.25 Deflected shape of frame 1 at runs 12, 17 and 22.
- 5.26 Deflected shape of frame 1 at runs 12, 17 and 26.
- 5.27 Applied beam load against bending moment for beam 2.
- 5.28 Applied beam load against bending moment for beam 3.
- 5.29 Applied beam load against bending moment for beam 4.
- 5.30 Applied beam load against bending moment for beam 5.
- 5.31 Applied beam load against bending moment for beam 6.
- 5.32 Bending moment distribution in beam 3 as beam loads are applied.
- 5.33 Applied beam load against central deflection for beam 2.
- 5.34 Applied beam load against central deflection for beam 3.
- 5.35 Applied beam load against central deflection for beam 4.
- 5.36 Applied beam load against central deflection for beam 5.
- 5.37 Applied beam load against central deflection for beam 6.
- 5.38 Moment distribution around frame 1 at runs 6 and 12.
- 5.39 Moment equilibrium at joints in frame 1 at end of beam loading.
- 5.40 Total load in column against central deflection - column 4.

- 5.41 Total load in column against central deflection - column 5.
- 5.42 Total load in column against central deflection - column 6.
- 5.43 Total load in column against central deflection - column 7.
- 5.44 Moment distribution around frame 1 at failure of central column.
- 5.45 Moment distribution around frame 2 at failure of external column.
- 5.46 Moment-rotation curve for joint A.
- 5.47 Moment-rotation curve for joint B.
- 5.48 Moment-rotation curve for joint C.
- 5.49 Moment-rotation curve for joint D.
- 5.50 Moment-rotation curve for joint E.
- 5.51 Moment-rotation curve for joint F.
- 5.52 Moment-rotation curve for joint G.
- 5.53 Moment-rotation curve for joint H.
- 5.54 Moment-rotation curve for joint I.
- 5.55 Moment-rotation curve for joint J.
- 5.56 Moment-rotation curve for joint K.
- 5.57 Moment-rotation curve for joint L.
- 5.58 Deflected shape of frame 2 at runs 12, 16 and 27.
- 5.59 Deflected shape of frame 2 at runs 12, 27 and 36.
- 5.60 Applied beam load against bending moment for beam 1.
- 5.61 Applied beam load against bending moment for beam 2.
- 5.62 Applied beam load against bending moment for beam 3.
- 5.63 Applied beam load against bending moment for beam 4.
- 5.64 Applied beam load against bending moment for beam 5.
- 5.65 Applied beam load against bending moment for beam 6.
- 5.66 Bending moment distribution in beam 3 as beam loads are applied.

- 5.67 Applied load against central deflection for beam 1.
- 5.68 Applied load against central deflection for beam 2.
- 5.69 Applied load against central deflection for beam 3.
- 5.70 Applied load against central deflection for beam 4.
- 5.71 Applied load against central deflection for beam 5.
- 5.72 Applied load against central deflection for beam 6.
- 5.73 Moment distribution around frame 2 at runs 6 and 12.
- 5.74 Moment equilibrium at joints in frame 2 at end of beam loading.
- 5.75 Moment distribution around frame 2 at failure of column in position 1.
- 5.76 Total load in column against central deflection - column 1.
- 5.77 Total load in column against central deflection - column 1.
- 5.78 Total load in column against central deflection - column 1.
- 5.79 Moment distribution around frame 2 at failure of central column.
- 5.80 Total load in column against central deflection - column 5.
- 5.81 Total load in column against central deflection - column 6.

Chapter 6

- 6.1 Comparison of analytical and experimental load-deflection response - ST2.
- 6.2 Comparison of analytical and experimental load-deflection response - ST3.
- 6.3 Comparison of analytical and experimental load-deflection response - ST4
- 6.4 Comparison of analytical and experimental load-deflection response - ST6.
- 6.5 Comparison of analytical and experimental load-deflection response - ST7.
- 6.6 Comparison of analytical and experimental load-deflection response - ST8.

- 6.7 Comparison of analytical and experimental load-deflection response - ST9.
- 6.8 Comparison of analytical and experimental load-deflection response - ST10.
- 6.9 Comparison of analytical and experimental load-deflection curve for test ST6 with lateral load introduced at midheight.
- 6.10 Comparison of analytical and experimental load-deflection curve for ST6 with residual stress and moment-rotation curves from test data.
- 6.11 Comparison of analytical and experimental load-deflection curve for test ST7 with lateral load introduced at midheight.
- 6.12 Moments at the head of column in test ST4.
- 6.13 Moments at the head of column in test ST8.
- 6.14 Moments at the head of column in test ST9.
- 6.15 Computer models for frame 1 and frame 2.
- 6.16 Linearised moment rotation characteristic used in the analysis of frame 1.
- 6.17 Comparison of predicted and test load-deflection response of beam 6.
- 6.18 Bending moment distribution under full beam loading.
- 6.19 Deflected shape produced by beam loading.
- 6.20 Bending moment distribution prior to failure of central column.
- 6.21 Deflected shape prior to failure of central column.
- 6.22 Bending moment distribution prior to failure of external column
- 6.23 Deflected shape prior to failure of external column.
- 6.24 Load-deflection response of column 4 for 10mm and 30mm eccentricities at the column head.
- 6.25 Comparison of moment rotation response of connections to an internal and external column.
- 6.26 Bending moment distribution under full beam loading.
- 6.27 Deflected shape produced by beam loading.

- 6.28 Comparison of predicted and test load-deflection response of beam 3.

Chapter 7

- 7.1 Interaction plot of axial load and moment for an I section bent about the major axis.
- 7.2 Interaction plot of axial load and moment for an I section bent about the minor axis.
- 7.3 Influence of boundary conditions at the remote ends of beams in limited subassemblages on the axial capacity of columns.
- 7.4 Flow chart for computerised design method for semi-rigid braced frames.
- 7.5 Determination of effective lengths using modifications to the method in BS 5950 appendix E.2.

Appendix C

- C.1 Tensile test - Load against time.
- C.2 Stub column test in progress.
- C.3 Stress-strain curve for column C16.
- C.4 Stress-strain curve for column C17.
- C.5 Sectioning of universal column section to determine residual stress pattern.
- C.6 Residual stress patterns for columns C4, C11, C13, C14 and C15.

ACKNOWLEDGEMENTS

The project described in this report has been a pleasure to work on due to the co-operative spirit of all those involved. I would like to acknowledge the helpful assistance provided by the project supervisors, Dr D A Nethercot and Dr P A Kirby, the support of the technical staff in the department and in particular the practical advice and know-how supplied willingly by Mr John Surr. My appreciation is also extended to the Building Research Establishment for not only the use of their excellent laboratory, but also for the help of Mr P Sims, Dr D Moore and Mr D Jenkins, in organising and conducting the two large frame tests.

Analysis of the frame test results was facilitated by the use of a powerful frame analysis program developed at the Politecnico di Milano, Italy. I am grateful to Professor R Zandonini and Dr C Poggi for their permission for its use and also for the helpful discussions I have had with them.

Analysis of the subassemblage test results was conducted by Mr A M Rifai. I am grateful to him for allowing me to present some of the results of his work in a comparison of the experiments with analytical predictions.

Financial support of the project was provided by the Science and Engineering Research Council, the Constructional Steel Research and Development Organisation (which has now been abolished and its activities are encompassed in those of the new Steel Construction Institute) and the Construction Industry Research and Information Association. The British Steel Corporation supplied all the required materials free of charge.

The typing of this report is the work of Miss J Stacey, to whom I express my thanks.

DECLARATION

Except where specific reference has been made to the work of others, this thesis is the result of my own work and includes nothing which is the outcome of work done in collaboration. No part of it has been submitted to any University for a degree, diploma or other qualification.

The experimental work described herein has formed the basis for several technical papers which are detailed below:

Davison, J.B., Kirby, P.A. and Nethercot, D.A., 'Rotational response of steel beam-to-column connections', International Conference on Steel Structures, Budva, Yugoslavia, September 1986.

Davison, J.B., Kirby, P.A. and Nethercot, D.A., 'Column behaviour in PR construction - experimental behaviour', ASCE Convention, New Orleans, September 1986 (also submitted to the Journal of Structural Engineering, AISC, 1987).

Nethercot, D.A., Davison, J.B. and Kirby, P.A., 'Connection flexibility and beam design in non-sway frames', ASCE Convention, New Orleans, September 1986.

Davison, J.B., Kirby, P.A. and Nethercot, D.A., 'Rotational stiffness characteristics of steel beam to column connections', Journal of Constructional Steel Research, Vol. 7, 1987 (in press).

Davison, J.B., Kirby, P.A. and Nethercot, D.A., 'Effect of lack of fit on connection restraint', Journal of Constructional Steel Research, Vol. 7, 1987 (in press).

Davison, J.B., Kirby, P.A. and Nethercot, D.A., 'Semi-rigid connections in isolation and in frames', State of the Art Workshop, Connections and the Behaviour, Strength and Design of Steel Structures, Cachan, France, May 1987.

Kirby, P.A., Davison, J.B. and Nethercot, D.A. 'Large scale tests on column subassemblages and frames', State of the Art Workshop, Connections and the Behaviour, Strength and Design of Steel Structures, Cachan, France, May 1987.

SUMMARY

This thesis describes an experimental study undertaken to examine the influence of joint resistance to in-plane moments on the performance of steel columns and complete frames. The principal objective of the tests was to provide experimental data against which sophisticated computer analysis programs may be verified.

Details of the experimental study of 22 joint tests, eight column subassemblages, and two three storey, two bay steel frames are reported. It is demonstrated that all beam to column connections have an inherent degree of stiffness and that their moment-rotation characteristics are non-linear. The load carrying capacity of columns, confined to buckle in-plane, is shown to be enhanced considerably by the resistance to rotation provided by simple beam to column connections. In frames incorporating flange cleat connections the beams and columns can sustain greater loading and deflect less than is predicted by current design models. The assumptions of pin-ended columns and simply supported beams are shown to be conservative.

Comparisons of the results of the column and frame tests with two finite element analysis programs are presented. The use of computer programs for semi-rigid design as well as the development of a simple approach are discussed.

NOTATION

In this thesis the following notation has been used. Notation peculiar to the Appendices is described therein.

C	initial stiffness of a connection
C*	effective stiffness of a connection
E	modulus of elasticity of steel
I	second moment of area of a section
K	joint restraint coefficient
k	ratio of effective and actual column length (L_E/L)
L	column length; beam span
L_E	effective length
M	moment applied to a joint or member
M_{Cx}, M_{Cy}	moment capacity of a section about the major and minor axes in the absence of axial load
M_p	plastic moment of a section ignoring local buckling
P	applied axial load
P_{Cx}, P_{Cy}	compressive resistance about the major and minor axis
P_y	squash load of a section
P_c	compressive strength
P_y	yield stress of steel
W	point load applied to a beam
w	uniformly distributed beam load
β	connection to beam factor
β^*	effective β value
λ	slenderness ratio
ϕ	connection rotation (radians)

1.0 INTRODUCTION

Structural steel frames have become increasingly popular in recent years. The cost of steel, the speed of erection of steel frames and their inherent versatility have all contributed to make steel attractive to clients and architects. In contrast to the 'hi-tec' image of many new steel framed buildings the permissible stress methods of design normally used have been in existence for many years. Presently designers are being encouraged to adopt a new design philosophy, that of limit states, in several new steelwork codes (1.1, 1.2).

Despite the apparent sophistication of the new codes and the progress that has been made in the analysis of steel frames using computer programs, steelwork design still centres around simplifying assumptions about the interaction of structural members. In braced frames in particular the design of columns is dependent on the designer's estimation of an effective column length based on an assessment of the performance of the beam to column connections. Transfer of load through the connection is then calculated from the eccentricity of the beam end reaction. In unbraced frames the adoption of so called rigid connections allows the designer to perform a detailed analysis of the frame using elastic, elasto-plastic and second order elasto-plastic computer programs. Thus one of the first decisions a designer must make is whether to assume the connections will function as pins, in the so called simple design approach, or as fully rigid moment resisting joints in the rigid design method.

The fact that connections do not act either as perfect pins or as fully rigid will not surprise the reader. Nor did it escape the notice of researchers Wilson and Moore (1.3) seventy years ago who

reported an investigation into the flexibility of riveted structural connections. Testing of beam to column connections has continued ever since. These investigations have conclusively demonstrated that 'simple' connections, those designed only to carry the beam end reaction, do in fact possess a degree of rotational stiffness and 'rigid' connections have some flexibility. Though some connections closely approximate to one of the two extremes the majority lie somewhere in between. In recognition of this many connections are now classified as 'semi-rigid'.

The beneficial effects of the semi-rigid nature of connections were realised fifty years ago and attempts to take advantage of the connection restraint in reducing beam sizes were made (1.4). However the influence of the restraining effect of connections on column behaviour has only relatively recently been researched (1.5).

With the wider availability and increased power of computers, interest in the incorporation of the semi-rigid nature of joints into analysis programs has been widespread. Numerous analytical studies of the influence of connection stiffness in member and frame stability have been undertaken. Tests against which the computer models may be compared have unfortunately been left far behind. Thus the need for an experimental study of the effects of joint flexibility in steel frames is manifest.

The principal purpose of the investigation detailed herein was to examine experimentally the behaviour of full size columns and frames incorporating simple connections and to assess the influence of the inherent stiffness of the joints on stability. Moment-rotation characteristics of the joints are of fundamental importance in understanding the behaviour of steel frames. An accurate prediction

of the $M-\phi$ curve for a particular connection is not possible so the first phase of the test programme was directed towards determining the $M-\phi$ relationship for several commonly used beam to column connections.

The second phase comprised the examination of the effect of connection stiffness on the load carrying capacity of a limited column subassemblage. Finally the performance of two full size, two bay, three storey frames was studied.

References

- 1.1 BS 5950
'The Structural use of steelwork in buildings'
Part 1, Code of Practice for Design in Simple Continuous
Construction : Hot Rolled Sections, London, British Standards
Institution, 1985.
- 1.2 AMERICAN INSTITUTE OF STEEL CONSTRUCTION
'Load and resistance factor design'
First Edition, 1986.
- 1.3 WILSON, W.M. and MOORE, H.F.
'Tests to determine the rigidity of rivetted joints in steel
structures'
University of Illinois, Engineering Experimental Station,
Bulletin No. 104, Urbana, USA, 1917.
- 1.4 PD 3343 SUPPLEMENT NO. 1 to BS 449 : PART 1
'The use of structural steel in building'
British Standards Institution, 1971.
- 1.5 JONES, S.W., KIRBY, P.A. and NETHERCOT, D.A.
'Effect of semi-rigid connections on steel column strength'
Journal of Constructional Steel Research, Vol. 1, No. 1, 1980,
p. 38-46.

2.0 BACKGROUND

2.1 Introduction

In 1929 the Steel Structures Research Committee was appointed to review the then present methods and regulations for the design of steel structures and to investigate the application of 'modern' theory of structures to the design of steel structures. The steel industry of the day hoped that the work of the Committee "would yield a more exact knowledge of the strains in a given structure and could be expected to lead to the adoption of a precise factor of safety with consequent higher standards of design. The outcome would be the more efficient economic and extended uses of steel" (2.1). The work undertaken by the Committee formed the basis of BS 449 'Specification for the Use of Structural Steel in Building' (2.2), first published in April 1932, but it also highlighted a fundamental problem with the analysis and design of steel framed structures; how best to account for the interaction of the beam and column members due to the fixity of the connections. This quandary identified in the early 1930's has received attention at various times over the last 50 years and has become more widely appreciated but the interaction of components of a frame is not commonly accounted for in steel frame design, simplified, easier to handle solutions being preferred.

The work of the Steel Structures Research Committee (a summary of which may be found in reference 2.3) and that of Young and Jackson (2.4) in Canada provided the impetus for much research into the action of joints, and later the performance of restrained columns and complete structural frames. The following sections briefly describe notable achievements in past research into the above aspects of frame behaviour.

2.2 Beam to Column Connections

A vast number of tests on the behaviour of beam to column connections have been conducted since Wilson and Moore (2.5) first investigated the response of riveted connections in 1917. A history of research into moment-rotation tests is reported in reference (2.6). Additionally Goverdhan (2.7) has collected a large number of test data and provides $M-\phi$ curves, numeric data and useful information in a single document. Nethercot (2.8) has also summarised the available test data and supplies comprehensive tables containing details of over 700 experimental investigations. The Structural Stability Research Council recognised the importance of collecting all the available data on connection tests in order to investigate ways of incorporating their semi-rigid nature into design and analysis. They have produced a comprehensive bibliography (2.9), which is also available stored on disk, to enable the reader to identify references to tests on connections of a particular type. Chen and Kishi (2.10) have also recently produced a comprehensive collection of data on joint tests.

The tests conducted confirm that all connections possess some rotational stiffness, the degree of which is a function of the type, size, and exact details of the joint. Figure 2.1 illustrates the range of moment-rotation, or $M-\phi$, curves which occur for the popular types of connections. The ideals of fully fixed and pinned are represented by lines coincident with the ordinate and abscissa respectively. In practice fully fixed connections are restricted to fully welded and stiffened connections, the more popular extended end plate connection does possess some flexibility. At the opposite extreme very flexible connections for example the single sided web plate (which is popular in North America though it is little used in

the United Kingdom) and double web cleats may carry modest moments. This inherent stiffness has a beneficial effect on the strength and deflection of notionally simply supported beams. Consider figure 2.2. A truly simply supported beam spanning a distance L and subjected to a total load W must sustain a moment of $WL/8$ at the midspan and no moment at the supports. The fully fixed beam has moments of $WL/12$ and $WL/24$ at the built-in ends and midspan respectively. A beam having 'semi-rigid' connections (a term which embraces all types of connection) would cause a reduction in the moment at the centre of the beam, compared with the simply supported case, as the connections resist the beam end rotations and attract some moment. The potential benefits of connection stiffness in reducing the moment and deflection at the centre of a beam, and hence the required beam size, were realised in the 1930's by researchers in Britain and the United States. Methods of incorporating these benefits were proposed in semi-rigid design methods (2.11, 2.12).

In order to incorporate the effects of the semi-rigid connection into design a knowledge of the $M-\phi$ response is a prerequisite. Attracted by the potential economies, a strong research effort into the response of typical beam to column connections and proposed design procedures was initiated. This early work concentrated on the popular riveted construction methods. The development of connections using bolts and welding (2.14) made much of this early test data obsolete, and many investigations into the new types of connection were undertaken (2.15 - 2.19).

As researchers tested connections the attraction of being able to predict their response, dependent on geometrical size and layout, material properties and bolt types became evident. Sommer (2.20)

fitted non dimensional polynomial curves to a series of test data for web cleat connections, and used a size effect factor to apply the function to connections of a similar type but differing sizes. Frye and Morris (2.21) developed the work to embrace several types of connection. However, though good agreement between the functions and test data was achieved, extrapolation beyond the size and exact details of the connections tested has had limited success. More recently finite element techniques have been used to predict the behaviour of various types of connection (2.22-2.24), but once again the results can be unreliable when applied to similar connections of a different size or varied detail.

It is therefore apparent that at present the only reliable way to find the $M-\phi$ relationship for a particular connection is by structural testing. This obviously prevents the widespread use of semi-rigid design methods, but recent developments should help to remove this obstacle. Firstly the large body of test data which has been created is now more readily available. This will allow investigations into the likely variability of the $M-\phi$ response for connections to be undertaken and standard, lower bound curves to be produced. Secondly, the effects of semi-rigid joints on both columns and complete frames can be accurately predicted by computer models (see section 6). These models may be used to examine the sensitivity of structures, and structural elements, to the precision of the $M-\phi$ data and thereby verify the suitability of particular standard curves. Work already conducted in this area suggests that for large frames the overall performance is not particularly sensitive to the precise $M-\phi$ curve (2.25). Finally, a move towards the adoption of standard connection details would reduce the number and variability of connec-

tions used in practice and also make the provision of guidance on the expected performance of the connection much easier. In Australia standard connection details are already available (2.26), and the merits of their use are discussed in reference (2.27).

The purpose of the joint test series detailed in Chapter 3 was to provide $M-\phi$ data for a range of practical connections for use with the beam and column sections to be used in column and frame tests. This data was subsequently used in analysing the results of the column and frame tests, but the series also provided the opportunity to examine the relative performance of connections, which were all suitable for the same beam and column sections and tested in the same manner.

2.3 Restrained Columns

In 1759 Euler derived the solution of the elastic buckling of a perfectly straight, centrally loaded, pin-ended column. Since then analytical and experimental investigations have been undertaken to examine the effects of initial crookedness, residual stress, load eccentricity, material properties and section shape on the strength of a member in compression. As a result, knowledge of the behaviour and strength of the pin ended column is extensive. Ballio and Mazzolani provide a historical record of research into the behaviour of columns which started with Eione of Alexandria in 75 B.C. (2.28).

Design practice has relied upon understanding of the pin-ended column to produce safe column designs. In braced structures, with simple connections between beam and column, the column has been assumed to act as a pin-ended column of length equal to the storey height. Column curves relating the slenderness ratio of the column to a safe working stress have then been used to calculate a safe working

load. This method has been in general use for many years. However, in many structures 'rigid' connections are used, in some cases to eliminate the need for bracing, so in order to use a similar design approach, and the same column curves, in situations where the pin-ended column assumption is not acceptable the concept of an 'effective' column length was developed. The real column restrained by connected members is replaced by an 'effective' length of pin-ended column, chosen to have the same strength as the real restrained column. The effective length is usually estimated by the designer from considerations of the relative size of members and the type of beam to column connections. This is an obvious limitation of the method, and one which has been recognised for many years. The recent trend towards limit state methods of design has reinforced the need for column design to include the effect of restraint from the adjacent structural members which becomes of increased importance as the column approaches failure.

The first attempt to include the effect of connected members or column stability made use of a limited, rigid jointed subassemblage, comprising the column and four beams. A series of nomographs, or alignment charts were provided which enabled the designer to calculate an effective length for a column forming part of a rigidly jointed structure. This method is in popular use today and variations of it appear in many structural codes (2.29, 2.30). As discussed in section 2.2 most connections fall in between the extremes of 'pin' and 'rigid'. Consequently neither the simple method of design assuming pin ended columns, nor the method just described for rigidly jointed structures, are appropriate in many cases. De Falco and Marino (2.31) were the first to try to modify the alignment charts for use with

semi-rigid connections. The method used the initial tangent stiffness of the connection. Reference 2.32 details a method which incorporates the initial tangent stiffness of the connection and beam flexibility into column design for American practice.

The problem of the end restrained column has been investigated recently by several researchers, notably by Chen (2.33), Jones et al (2.34) and Razzaq and Chang (2.35). These studies have shown, mainly by analytical investigations verified by some experimental results, that the stiffness of the restraining connection is a major factor in column strength. Fig. 2.3 illustrates the column strength curves for members with a variety of end conditions. The effect of the connection stiffness is evident, particularly at high slenderness. Noteworthy too is the fact that the connections used are of the simple type, i.e. those which would normally be considered to act as pins in design. The potential for economies to be made in structural design by incorporating the beneficial, and as yet neglected, effect of the semi-rigid nature of simple shear connections is clear.

Although much attention has been focussed on the problem of end restrained columns in recent years it has been mainly of an analytical nature (2.34,2.36,2.37). The question of whether the expected improvements in performance of restrained columns over pin ended columns are evidenced in practice has not been as thoroughly investigated.

In the early 1960's Galambos (2.38) examined experimentally the behaviour of columns with end moments applied through loading devices and later tested column and beam subassemblages with welded joints (2.39) to provide verification of restrained column theories proposed for use in the plastic design of multi-storey frames.

Experiments on laterally loaded beam-column subassemblages, again with rigid connections between the beam and column, were reported by English and Adams (2.40). Probably the most significant contribution to the experimental evidence of the restraining characteristics of simple connections was provided by Bergquist in 1977 (2.41). Bergquist tested five subassemblages, each comprising of a column and four beams, connected with web cleats to the column web. The tests, designed to examine the influence of the connections on the column buckling load, have been the only source of data for comparison of analysis techniques and have consequently been used by many researchers. However the self contained beam loading arrangement adopted by Bergquist, illustrated in figure 2.4, used tension cables to apply loads to the beams which resulted in an unrealistic load pattern. Examples of the connections used in the study were tested separately, but the cleats were bolted to a reaction frame rather than the column section to be used in the subsequent subassemblage tests.

Since this project was initiated the work of Cuk (2.42) in Australia has been completed. A series of nine tests on three storey beam columns, subjected to bending moments and axial loads was tested.

Clearly the number of experimental investigations into the action of restrained columns, particularly those which incorporate simple connections and the effect of the finite length of the beams, are limited. It was the purpose of this project to add to the experimental evidence that beam to column connections have a pronounced effect on the load carrying capacity of columns. A series of ten column subassemblage tests covering the spectrum of connection

stiffness, buckling about major and minor axes, with loading applied through the beams as well as axially in the column, was performed and is described in detail in Chapter 4.

2.4 Frame Tests

The earliest tests conducted on steel frames were carried out in the 1920's in the United States. Strain measurements were taken on the columns of two buildings, the Equitable Building, Des Moines, Iowa (2.43) and the American Insurance Union Building, Columbus, Ohio (2.44). The results of the tests showed observed stresses that were consistently greater than those calculated, the discrepancy being attributed to some error in the theory; although the strain gauge device used, a Berry gauge, appears not to have been particularly accurate and there were problems with temperature corrections which were necessary.

In Britain the work of the Steel Structures Committee during the 1930's covered an extensive range of tests on actual building frames and an experimental frame. The purposes of the tests (2.45) were to investigate the effects of the lack of fit at column splices, the moments transmitted by the beam-to-column connections, the reduction in beam span stresses due to the restraint offered by the connection, the influence of the column base to foundation interface and the effect of concrete encasement. The first tests conducted were on the Geological Museum in South Kensington (2.46). Measurements of strain were taken on the bare steel frame under load and also for the frame when encased in concrete, the results are presented in reference (2.47). The interesting feature is that the observed readings

more closely resembled the strains expected within a rigidly jointed frame than one with assumed pin joints and moments calculated assuming an eccentric beam reaction.

Next Baker studied a number of three storey frames specially erected at the Building Research Station (2.48). A three dimensional frame two 16' bays wide, and one 16' bay deep, with three 8' storeys was erected using 8" x 4" x 18 lb/ft steel joints throughout (2.49). The test frame incorporated frames with columns bent about both major or minor axes and used a variety of riveted connection details. The results of the tests on this experimental frame demonstrated that the bending moment distribution around the frame when subjected to vertical loads was similar in form to that of a rigidly jointed frame, but the magnitude of the moments in the column were less than those predicted by a rigid frame analysis.

Having gained experience with the experimental frame three London buildings were tested during construction, the Cumberland Hotel (2.50) at Marble Arch, Euston Offices (2.51) and a block of London flats (2.52). Tests were carried out on the bare steel frames under point loads, after the floors had been constructed, after the columns had been encased and finally when the structure was complete. All the structures behaved very nearly as rigidly jointed frames, which made nonsense of the main assumptions inherent in BS 449 design methods. The implications of the experimental observations are discussed in reference 2.53 and outlined in reference 2.3 and 2.54.

In America interest in plastic design prompted a study by Yura and Lu (2.55) into the ultimate load carrying capacity of braced multi-storey frames. Maximum load tests were conducted on four braced frames, each with the same geometry and member sizes but with the

loading conditions varied. All the tests reached or exceeded the maximum load predicted by plastic theory and demonstrated that plastic methods could be applied to the design of braced multi-storey frames.

Figure 2.5 (taken from reference 2.55) illustrates the test frames investigated. Notice that the connections are heavily welded and are at the 'rigid' end of the spectrum of beam to column connection stiffness. Details of the apparatus used to load the frames may be found in reference 2.56 along with a list of references of rigid steel frame testing conducted in the United States from the 1940's to the early 1960's.

In 1964 a Joint Committee of the Institute of Welding and the Institution of Structural Engineers reported a simplified design method for fully rigid multi-storey welded steel frames (2.57). In order to verify the method tests were conducted on a full-scale 3 storey, 2 bay by 1 bay rigid jointed frame fabricated from rolled steel sections of Grade 43 steel. The tests were reported in The Structural Engineer (2.58). A second report (2.59) permitted the use of a higher grade steel and a second, more extensive frame was tested, the results of which are reported by Smith and Roberts (2.60). These tests were conducted in the large structures laboratory at the Building Research Station.

Taylor reports on an experimental study of continuous columns (2.61). Nineteen two-bay three-storey 1/3 to 1/2 scale steel frames were tested. Rigid joints were again used for the beam to column connections. Beams framing into the column's minor axis (on one side only) were pinned at their remote ends. No in plane sway was permitted during testing. Loading was applied to the central column, the major axis beams at midspan and to the minor axis beams in four of

the tests. The tests were designed to study the effect on the collapse load and behaviour of a continuous column, of minor axis restraint, slenderness ratio, the relative importance of loads applied to the major and minor axis beams, and the relative importance of single and double curvature bending of a column about its major axis.

The tests conducted on steel frames since the 1930's have concentrated on rigid frames. Recent interest in the semi-rigid nature of connections and their influence on frame behaviour and developments in computer analysis have been restricted by the lack of experimental data on modern structures with simple connections. The aim of the full scale tests conducted in this project was to provide experimental evidence of the restraint characteristics of simple connections and demonstrate the contribution they make towards a more beneficial distribution of bending moments in the beams and the effect they have on the collapse load of columns. It is also envisaged that the data will be used to verify the predictions of semi-rigid analysis programs which have been recently developed.

In the period since this project was started a report of work by Stelmack et al (2.62) has been published. The purpose of the study reported therein was to provide experimental documentation of the validity of analytical methods for predicting the response of flexibly connected steel frames. Ten tests on two frames, a two storey single bay, and a two bay, single storey, were conducted. The results showed good correlation with the predicted response. However the scope of the work was limited because neither the tests nor the analysis extended beyond the elastic range.

References

- 2.1 STEEL CONSTRUCTION RESEARCH COMMITTEE
First Report, Department of Scientific and Industrial Research,
HMSO, London, 1931, page 1.
- 2.2 BRITISH STANDARDS INSTITUTION
'The use of structural steel in buildings'
Part 2, London, BS 449, 1969.
- 2.3 BAKER, J.F.
'Early steelwork research'
Journal of Constructional Steel Research, Vol. 1, No. 1,
September 1980, p. 3-9.
- 2.4 YOUNG, C.R. and JACKSON, K.B.
'The relative rigidity of welded and riveted connections'
Canadian Journal of Research, 1934, 11, No. 1, p. 62-100.
- 2.5 WILSON, W.M. and MOORE, H.F.
'Tests to determine the rigidity of riveted joints in steel
structures'
University of Illinois, Engineering Experimental Station,
Bulletin No. 104, Urbana, USA, 1917.
- 2.6 JONES, S.W., KIRBY, P.A. and NETHERCOT, D.A.
'The analysis of frames with semi-rigid connections - a state-
of-the-art report'
Journal of Constructional Steel Research, Vol. 3, No. 2, 1983,
p. 2-13.
- 2.7 GOVERDHAN, A.V.
'A collection of experimental moment-rotation curves and
evaluation of prediction equations for semi-rigid connections'
Masters Thesis, University of Vanderbilt, Nashville, Tennessee,
December 1983.
- 2.8 NETHERCOT, D.A.
'Steel beam to column connections - a review of test data and
their applicability to the evaluation of the joint behaviour of
the performance of steel frames'
CIRIA Project Record, RP 338, 1985.
- 2.9 STRUCTURAL STABILITY RESEARCH COUNCIL
'Connections bibliography'
Task Group 25, Third Draft, March 1987.
- 2.10 KISHI, N. and CHEN, W.F.
'Data base of steel beam to column connections'
Volumes I and II, Structural Engineering Report No.
CE-STR-86-26, School of Civil Engineering, Purdue University,
1986.

- 2.11 STEEL STRUCTURES RESEARCH COMMITTEE
Second Report, Department of Scientific and Industrial Research,
HMSO, London, 1934, p. 177-199 and Third Report, 1936, p.
364-393.
- 2.12 RATHBUN, J.C.
'Elastic properties of riveted connections'
Transactions of American Society of Civil Engineers, 1936, 101,
p. 524-63.
- 2.13 PD3343 Supplement No. 1 to BS 449 : Part 1
'The use of structural steel in building'
British Standards Institution, 1971.
- 2.14 MUNSE, W.H.
'Fifty years of riveted, bolted and welded steel construction'
Journal of Construction Division, American Society of Civil
Engineers, September 1976, 102, CO.3, p. 437-47
- 2.15 MUNSE, W.H., BELL, W.G. and CHESSON, E.
'Behaviour of riveted and bolted beam-to-column connections'
Journal of the Structural Division, American Society of Civil
Engineers, 1959, 85, March, ST3, p. 25-50.
- 2.16 SHERBOURNE, A.N.
'Bolted beam-to-column connections'
The Structural Engineer, 1961, 39, June, No. 6, p. 203-210.
- 2.17 BAILEY, J.R.
'Strength and rigidity of bolted beam-to-column connections'
Conference on Joints in Structures, University of Sheffield,
1970.
- 2.18 LEWITT, C.W., CHESSON, E. and MUNSE, W.H.
'Restraint characteristics of flexible riveted and bolted
beam-to-column connections'
Engineering Experimental Station Bulletin No. 500, University of
Illinois, January 1969.
- 2.19 LIPSON, S.L.
'Single-angle welded-bolted connections'
Journal of the Structural Division, American Society of Civil
Engineers, 1977, 103, March, ST3, p. 559-571.
- 2.20 SOMMER, W.H.
'Behaviour of welded header plate connections'
Master's Thesis, University of Toronto, Ontario, 1969.
- 2.21 FRYE, M.J. and MORRIS, G.A.
'Analysis of flexibly connected steel frames'
Canadian Journal of Civil Engineers, September 1975, 2, No. 3,
p. 280-91.
- 2.22 KRISHNAMURTHY, N., HUANG, H., JEFFREY, P.K. and AVERY, L.K.
'Analytical $M-\phi$ curves for end-plate connections'
ASCE, January 1979, p. 133.

- 2.23 LIPSON, S.L. and HAGUE, M.I.
 'Elastic plastic analysis of single-angle bolted-welded connections using the finite element method'
 Composites and Structures, December 1978, No. 6, p. 533-45.
- 2.24 TONG, C.S.
 'The elastic-plastic behaviour of semi-rigid connections in steel structures'
 Ph.D. Thesis, Hatfield Polytechnic, June 1985.
- 2.25 POGGI, C and ZANDONINI, R
 'Behaviour and strength of steel frames with semi-rigid connections'
 Flexibility and Steel Frames, ed. W.F. Chen, ASCE, 1985, p. 57-76.
- 2.26 HOGAN, T.J. and THOMAS, I.R.
 'Standardised structural connections'
 Part A, Institute of Steel Construction, 2nd Edition, October 1981.
- 2.27 McCORMICK, M.M.
 'Background to AISC standard connections'
 BHP Melbourne Research Laboratory Report MRL 39/1, March 1974.
- 2.28 BALLIO, G. and MAZZOLANI, F.M.
 'Theory and design of steel structures'
 Chapman and Hall, London, 1983, p. 371-378.
- 2.29 BS 5950 'The structural use of steelwork in buildings'
 Part 1, Code of Practice for Design in Simple Continuous Construction : Hot Rolled Sections, London, British Standards Institution, 1985.
- 2.30 AMERICAN INSTITUTE OF STEEL CONSTRUCTION
 'Load and resistance factor design'
 Manual of Steel Construction, First Edition, 1986.
- 2.31 DE FALCO, F. and MARINO, F.J.
 'Column stability in type 2 construction'
 Engineering Journal, American Institute of Steel Construction, 1966, 13, 4th Quarter, 109-115.
- 2.32 BJORHOVDE, R.
 'Effect of end restraint on column strength - practical applications'
 Engineering Journal, American Institute of Steel Construction, 1984, 21, 1st Quarter, 1-13.
- 2.33 CHEN, W.F.
 'End restraint and column stability'
 Journal of the Structural Division, ASCE, Vol. 106, No. ST11, November 1980, p. 2279-2295.

- 2.34 JONES, S.W., KIRBY, P.A. and NETHERCOT, D.A.
'Effect of semi-rigid connections on steel column strength'
Journal of Constructional Steel Research, Vol. 1, No. 1, 1980,
p. 38-46.
- 2.35 RAZZAQ, Z. and CHANG, J.G.
'Partially restrained imperfect columns'
Additional Papers, Conference on Joints in Structural Steelwork,
Teesside, April 1981, Pentech Press Ltd, p. 6.57-6.80.
- 2.36 SUGIMOTO, H. and CHEN, W.F.
'Small end restraint effects on strength of H-columns'
Journal of the Structural Division, ASCE, Vol. 108, No. ST3,
March 1982, p. 661-681.
- 2.37 SHEN, Z.Y. and LU, L.W.
'Analysis of initially crooked end restrained steel columns'
Journal of Constructional Steel Research, Vol. 3, No. 1, 1983,
p. 10-18.
- 2.38 VAN KUREN, R.C. and GALAMBOS, T.V.
'Beam-column experiments'
Journal of the Structural Division, ASCE, Vol. 90, April 1964,
p. 223.
- 2.39 LAY, M.G. and GALAMBOS, T.V.
'The experimental behaviour of restrained columns'
Welding Research Council, Bulletin No. 110, November 1965,
p. 17-38.
- 3.40 ENGLISH, G.W. and ADAMS, P.F.
'Experiments on laterally loaded steel beam-columns'
Journal of Structural Division, ASCE, Vol. 99, ST7, July 1973, p.
1457-1470.
- 3.41 BERGQUIST, D.J.
'Tests on columns restrained by beams with simple connections'
Report No. 1, American Iron and Steel Institute Project No. 189,
Department of Civil Engineering, The University of Texas,
Austin, Texas, January 1977.
- 2.42 CUK, P.E.
'Flexural-torsional buckling in frame structures'
Ph.D. Thesis, School of Civil and Mining Engineering, University
of Sydney, Australia, 1984.
- 2.43 FULLER, A.H.
'Measurement of stresses in four steel columns of the Equitable
Building, Des Moines, Iowa'
Iowa State College of Agriculture and Mechanic Arts, Engineering
Experiment Station, Bulletin No. 72, Ames (Iowa), 1924.
- 2.44 MORRIS, C.T.
'Dead load stresses in the columns of a tall building'
Ohio State University, Engineering Experimental Station,
Bulletin No. 40, Columbus, 1928.

- 2.45 FABER, O.
'Strains in buildings - statement of the problem and of the first tests contemplated'
First Report of the Steel Structures Research Committee, HMSO, 1931, p. 69-70.
- 2.46 BAKER, J.F.
'Examination of building in course of erection'
First Report of the Steel Structures Research Committee, HMSO, London, 1931.
- 2.47 FABER, O.
'Report on observed stresses in a steel frame structure at the Museum of Practical Geology, South Kensington'
Second Report on the Steel Structures Research Committee, HMSO, London 1934, p. 44-60.
- 2.48 BAKER, J.F.
'An investigation of the stress distribution in a number of three-storey building frames'
Second Report on the Steel Structures Research Committee, HMSO, 1934, p. 241-318.
- 2.49 LOBBAN, C.H.
'Measurement of stresses in experimental frame'
First Report of the Steel Structures Research Committee, HMSO, 1931, p. 191-193.
- 2.50 BAKER, J.F.
'An investigation of the stress distribution in the steel framework of a modern hotel building'
Final Report of Steel Structures Research Committee, HMSO, London, 1936, p. 8-139.
- 2.51 BAKER, J.F.
'An investigation of the stress distribution in the steel framework of a modern office building'
Final Report of Steel Structures Research Committee, HMSO, London, 1936, p. 140-227.
- 2.52 BAKER, J.F.
'An investigation of the stress distribution in the steel framework of a modern residential flats building'
Final Report of Steel Structures Research Committee, HMSO, London, 1936, p. 228-249.
- 2.53 BAKER, J.F.
'A review of tests on three existing buildings'
Final Report of Steel Structures Research Committee, HMSO, London, 1936, p. 228-249.
- 2.54 BAKER, J.F.
'The steel skeleton - Volume 1 - Elastic behaviour and design'
Cambridge University Press, 1954.

- 2.55 YURA, J.A. and LU, L.W.
'Ultimate load tests on braced multistorey frames'
Journal of the Structural Division, ASCE, Vol. 95, NO. ST10,
October 1969, p. 2243-2264.
- 2.56 YARIMCI, E., YURA, J.A. and LU, L.W.
'Techniques for testing structures permitted to sway'
Experimental Mechanics, August 1967, p. 321-331.
- 2.57 Joint Committee Report on Fully-rigid Multi-storey, Welded Steel
Frames
Institution of Structural Engineers, December 1964.
- 2.58 WOOD, R.H., NEEDHAM, F.H. and SMITH, R.F.
'Tests on a multi-storey rigid steel frame'
The Structural Engineer, Vol. 46, No. 4, April 1968, p. 107-120.
- 2.59 Second Joint Committee Report on Fully-rigid, Multi-storey,
Welded Steel Frames
Institution of Structural Engineers, May 1971
- 2.60 SMITH, R.F. and ROBERTS, E.H.
'Test of a full-scale rigid-jointed multi-storey frame in
high-yield steel (BS 4360, Grade 50)'
BISRA Open Report, Report No. EG/A/17/71
- 2.61 TAYLOR, D.A.S.
'An experimental study of continuous columns'
Proceedings of the Institution of Civil Engineers, Vol. 53,
1972, p. 1-7.
- 2.62 STELMACK, T.W., MARLEY, M.J. and GERSTLE, K.H.
'Analysis and tests of flexibly connected steel frames'
Journal of Structural Engineering, ASCE, Vol. 112, No. 7, July
1986, p. 1573-1588.

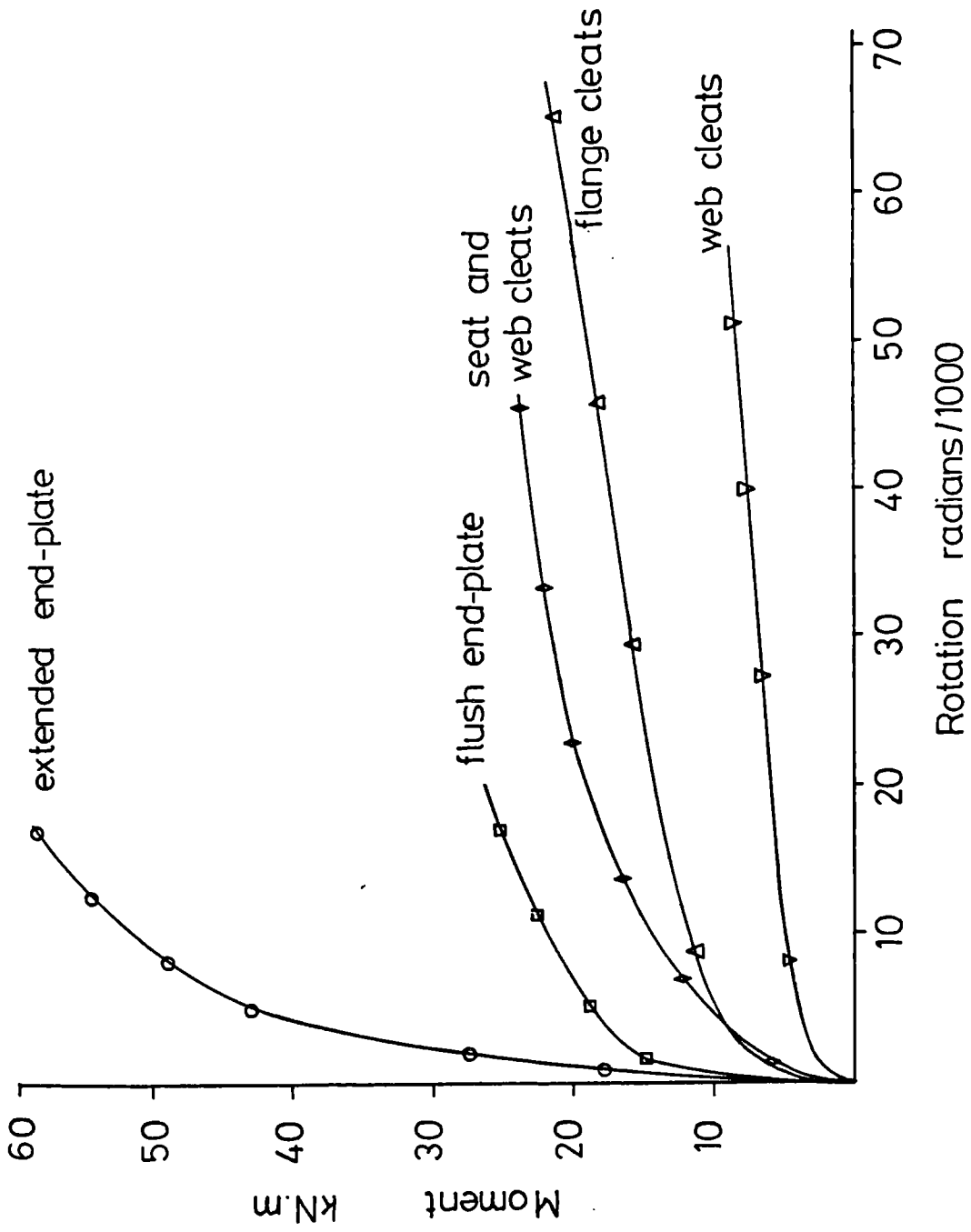


FIGURE 2.1 Variation of moment-rotation characteristics for various types of beam to column connection

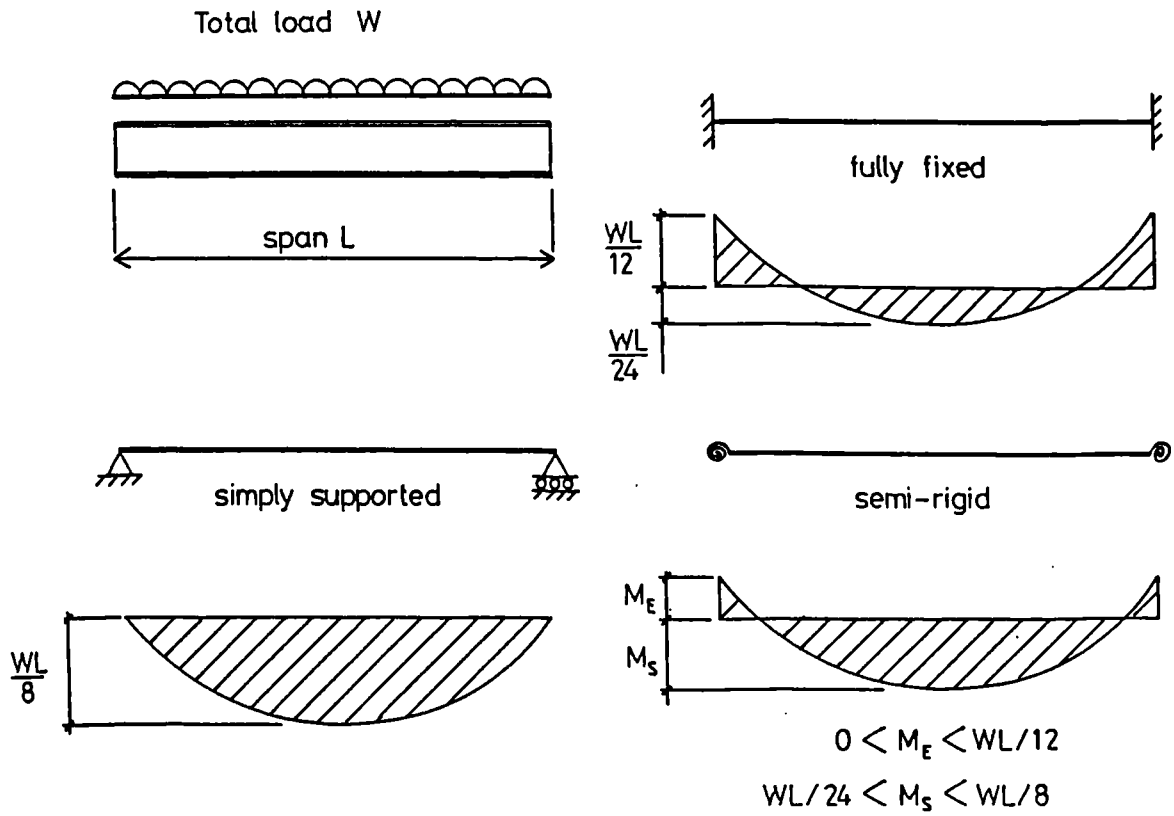


FIGURE 2.2 Influence of connection stiffness on beam moment distribution

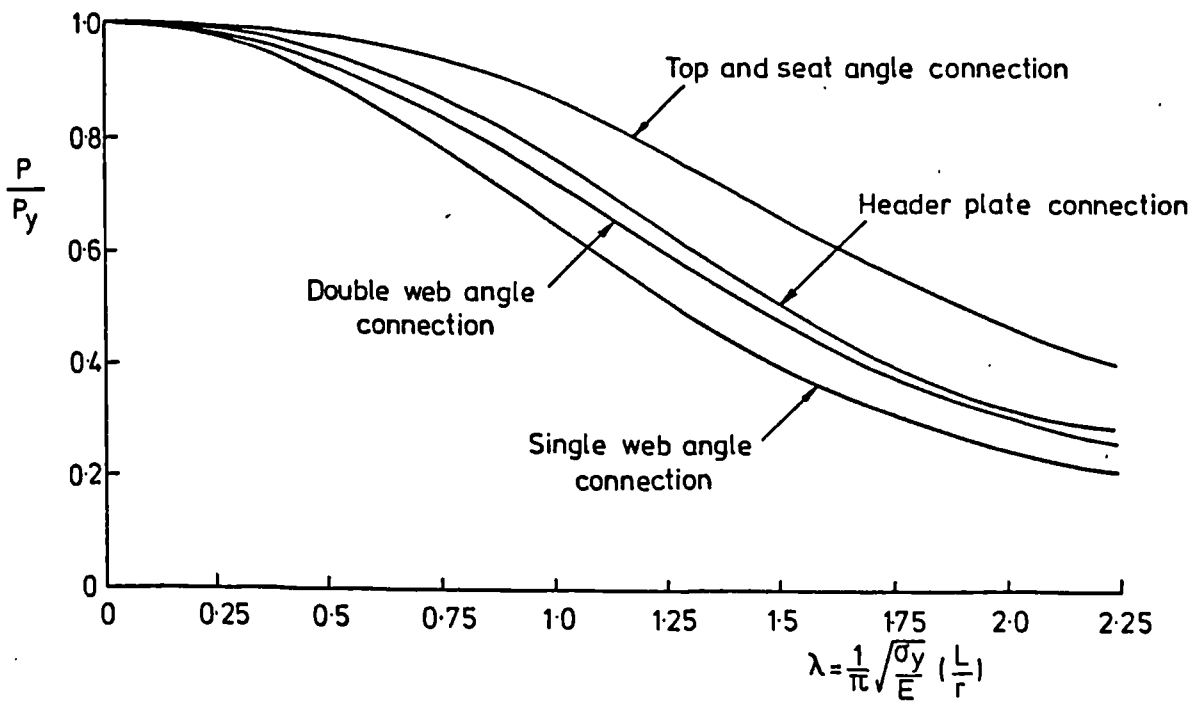


FIGURE 2.3 Influence of connection restraint on the strength of axially loaded columns

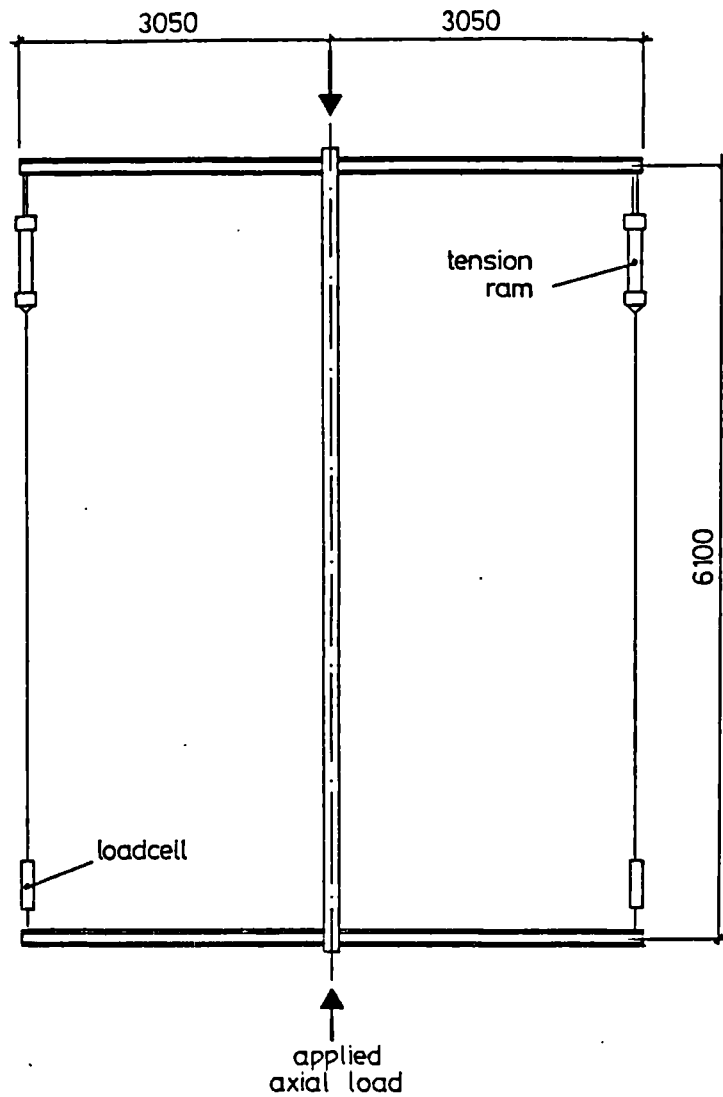


FIGURE 2.4 Test arrangement used by Bergquist (2.41)

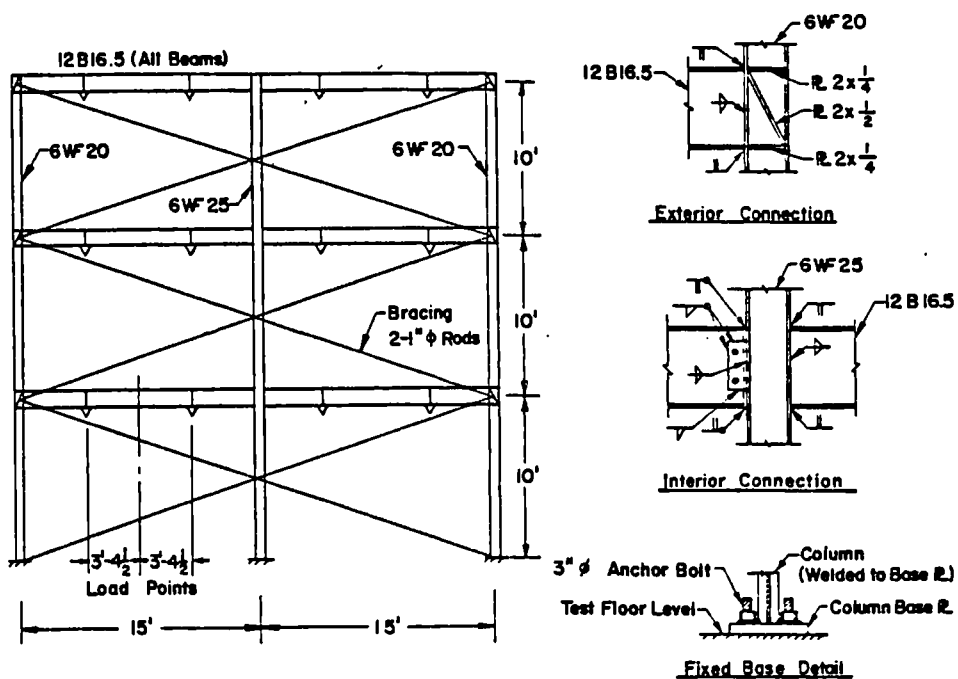


FIGURE 2.5 Details of rigid jointed frames tested by Yura and Lu (2.55)

3.0 ROTATIONAL STIFFNESS CHARACTERISTICS OF STEEL BEAM TO COLUMN CONNECTIONS

3.1 The Need for Experimental Data

Since connections are statically indeterminate and attempts at rigorous analytical study have met with limited success, the need for experimental data to provide the moment-rotation relationship of connections is self-evident. Many researchers have fitted their data with mathematical expressions quite closely, but invariably constants which are peculiar to each connection and dependent on many design variables are required; these can only be determined by experiment. An accurate representation of the non-linear moment-rotation behaviour of the connections to be used in the subassemblage and frame tests was essential, so a series of joint tests to provide this data was undertaken.

It is noteworthy that a great deal of previous experimental work conducted on joint behaviour was concerned with connections that are now obsolete, so experimental data on connection types in common use at present should be of considerable interest.

3.2 Connection Selection and Design

A recent survey (3.1) of beam to column connections used throughout the construction industry in the U.K. revealed that web cleats, flange cleats, combined seat and web cleats, and flush and extended end-plates are presently in common use. These types cover the spectrum of connection response, from the very flexible web cleats to the relatively rigid extended end-plate. An example of each was selected for study. The complete test series is summarised in table 3.1 and figure 3.1 details each of the connections.

Both the web cleat and flange cleat connections were designed for shear only to the permissible stress method described in the AISC handbook, "Design of Structural Connections" (3.2). It is common practice to employ flush end-plates as shear connections and to base their design on the shear capacity of a number of bolts, checking the bearing resistance of the column flange and end-plate thickness. A flush end-plate of 12mm thickness employing six M16 bolts was selected as being representative for the size of members used. The moment capacity of this joint was then calculated using the method proposed by Horne and Morris (3.3). The plastic moment of the beam section was used as the design moment for the extended end-plate connection, which was undertaken using the recommendations of Mann and Morris (3.4). Design calculations for each connection are provided in Appendix B.

3.3 Joint Test Apparatus

A cruciform test arrangement was chosen, rather than a cantilever type, since the former requires a less extensive test rig and also provides some indication of the variability of nominally identical connections. Load was applied to the column by a 500 kN screw jack. The reaction of each beam was measured at a distance of 1000mm from the column face or web for the major and minor axis tests respectively. Figure 3.2 illustrates the main features of the test apparatus, whilst figure 3.3 shows a seat and web cleat specimen under test.

When performing connection tests to determine the moment-rotation response it is the relative rotation of the beam to the column that is required (3.5). Rotations were therefore measured at a point on the centreline of each beam and on the column. The method of rotation measurement used at each of the three positions is illus-

trated in figure 3.4. 'T' bars, tack welded to the cruciform, were attached to three LVDTs by a system of wires and pulleys. Rotation of the specimen and 'T' bar resulted in a change in the initial wire lengths L_1 , L_2 , L_3 to new lengths l_1 , l_2 , l_3 . The changes in length were measured by the movement of the LVDTs and the new wire lengths in the revised geometry were used to compute the new position and rotation of the bar. The rotation of each joint was then computed. By positioning the 'T' bars as near as practicable to the connection the contribution to rotation made by the beam's curvature can be minimised. An obvious limitation of this system is that no quantitative information on the contributions of the individual components of the connection is obtained. However, since the objective of the tests was to obtain the overall moment-rotation response of a series of connections, rather than to study connection behaviour in detail, the method was deemed suitable. The data were recorded and processed by a microcomputer based data logging system developed at the University.

3.4 Fabrication of Test Specimens

Details of the materials used throughout the test series, i.e. section sizes and tensile test results are recorded in Appendix C.

3.5 Assembly and Testing

The test specimens were assembled in the rig. This was found to be the best way to ensure that the column was vertical and the beams were set at 90° degrees to it. When bolting up the connections no attempt was made to centralise the bolts in the bolt holes. Two grades of bolts were used, 4.6 and 8.8; all were 16mm in diameter. In this series of tests the bolts were not required to be fully torqued. A decision on the method of bolt tightening was necessary. As will be discussed later, the first three tests were tightened with an ordinary

spanner, or a socket and short ratchet. A torque wrench was used for the remaining tests. After careful consideration it was decided that some measure of control of tightening would be beneficial. In the field bolts are tightened to 'hand-tight'. The most enlightening definition of this condition is found in the Australian code (3.6), where 'snug-tight' is defined as 'the tightness attained by a few impacts of an impact wrench or the full effort of a man using a standard podger spanner'. Clearly 'hand-tight' is extremely variable; and the question of what is a reasonable value to adopt is raised.

In order to find what torque should be applied, the bolts tightened in the first three tests were checked with the torque wrench. A figure of 160 N.m (120lb.ft) was suggested by the bolt manufacturer as a reasonable torque, and one that the technician had applied with ordinary hand tools. This figure is approximately 50% of the torque required to bring the M16 grade 8.8 bolt up to its proof load. It was found that the location of the bolt affected the torque applied in the first three tests - for example, it appeared to be easier to apply a torque to a bolt when the spanner was pushed down, rather than pulled up. This variability was eliminated by use of the torque wrench in subsequent tests. The adoption of a torque control method of bolt tightening was used to ensure consistency between tests in each of the phases of the project, not to develop frictional forces in the connections.

Having assembled the test specimen the rotation bars were welded to the beams and columns. The load cells were positioned on the beams at a distance of 1 metre from the column face (or web for the minor axis tests), and the test piece was slowly lifted by the screw jack

until the load cells were just nipped into place. The initial lengths of all nine transducer wires, and the end clearance of the beam from the column face were recorded.

Data logging was then commenced. The tests were started very slowly to allow the apparatus to settle into place, but without applying much load. The speed of the jack was then increased to a suitable rate. The data logging equipment takes a reading of all channels at pre-set time intervals; scan time intervals of 45-60 seconds were used. A total of 120 scans could be accommodated in the computer memory, giving a total test time of 1.5 to 2 hours.

The above procedure was typical of most of the tests conducted. Details peculiar to the testing of each connection type are described in the following sections, along with some comments on connection behaviour.

3.6 Behaviour of Web Cleat Connections

The behaviour of web cleat connections was studied in seven tests (JT/01-06 and 01B). The results of the first test are not reported because the load cells were not working properly, though the test proved to be a useful pilot.

In tests JT/02 and 03 the bolts, which were M16 grade 8.8, were tightened with either a spanner or a small socket and ratchet. No method of tightness control was employed. The resulting moment-rotation curves are shown in figures 3.5 and 3.6. It is apparent that very little resistance to rotation was encountered till a rotation of 0.01 radians (0.57°) had been exceeded. A fairly constant connection stiffness of the order of 130 kN.m/rad. was achieved for rotations in the range of 0.01 to 0.05 radians. Beyond this range the bottom flange of the beam came into contact with the column and the

connection stiffened up considerably. In test JT/03 the connection was loaded and unloaded several times. The unloading and loading stiffness at different levels are approximately equal and linear (1835 kN.m/rad.) but once the connection was loaded above its current maximum level it followed the original non-linear moment-rotation curve. It is also noticeable from test JT/03 that the deformations produced by a moment are largely inelastic and irrecoverable.

The interesting feature of these tests was the apparent lack of stiffness at low levels of moment. Many of the tests reported in the past have used high strength bolts torqued to quite high levels, certainly higher than those achieved by simple hand tightening. The importance of bolt tightness in beam web connections was reported in two papers by Richard (3.7, 3.8) in which a series of tests were conducted to investigate the behaviour of single plate framing connections with slotted holes. 7/8" diam. A307 bolts were used and for comparative purposes tests were conducted with the bolts hand tight (i.e. tightened with a spanner), and finger tight. An earlier series of tests had been conducted with higher strength bolts, A325 and A490, in a fully torqued condition. Irrespective of the number of bolts the moment resisted by the connection was zero or near zero when finger tight bolts were used, but was progressively larger for hand tight A307, and fully torqued A325 and A490 bolts. This led Richard to the conclusion that the moment generated by the connection was primarily a result of a clamping force between the connection plate and the beam web. In Richard's test, since slotted holes were used, no bearing of the bolts could occur. It appears that the same mechanism of moment transfer is developed in web cleat connections, the bolt force induces a frictional force between the cleats and beam

web and allows only limited amounts of slip to occur. This need only be the case until the bolts move into bearing. The amount of rotation that can occur before the bolts move into bearing will depend on the ratio of bolt to hole size, the position of the bolt in the bolt holes, the number of bolts, and the bolt layout. In the two bolt connection detailed the bolts to hole size ratio is relatively small, and the distance between the bolts is quite large. Therefore the rotation experienced before the connection begins to load can be easily accommodated by the clearance of the bolts in their respective holes. Not until this 'slack' has been removed will the connection begin to exhibit resistance to rotation. Figure 3.7 illustrates the possible rotation if the bolts were centrally positioned in perfectly aligned holes. Since the experimental results showed unresisted rotation for about 0.015 radians the actual slip per bolt must have been of the order of 0.75mm.

How much rotation may occur before the connection begins to load is significant. For example, consider a 254 × 102 × 22UB spanning 5m under full elastic loading, the rotation of its ends is given by

$$\phi = \frac{\omega L^3}{24EI}$$

$$\begin{aligned} \text{which for } \omega = 11.9 \text{ kN/m} &= \frac{11.9 \times 25 \times 5 \times 10^9}{24 \times 210 \times 10^3 \times 2867 \times 10^4} \\ &= 0.0103 \text{ radians} \end{aligned}$$

Notice that this rotation is of the order of that which may occur essentially unresisted by the connection.

Some concern was felt that the results above are inconsistent with those reported by several other researchers. In order to check if the method of bolt tightening adopted, i.e. tightening as tight as possible with hand tools, was the cause of the difference a further test was conducted but with the bolts tightened to 160 N.m (120 lb.ft) with a torque wrench. As discussed in section 3.5 this value was selected as a typical hand-tight figure and not as a torque to fully tension the bolts. The result of this test JT/01B, is shown in figure 3.8.

In contrast to tests JT/02 and 03, the bolts in test JT/01B were sufficiently tight to prevent slip occurring in one large movement. Instead the bolts moved gradually into bearing as a series of small slips took place. This can be seen from the moment-rotation curve where the connection resists moment immediately. It is therefore evident that the bolt tightness does affect the behaviour of web cleats.

In the first two minor axis tests access to the two bolts was limited, and it is possible that because of this tightening of the bolts was not as effectively achieved as for example in a major axis test where all the bolts were more readily accessible. By using the torque wrench all bolts were assured the same torque, regardless of their location. Normal fabrication practice is to bolt cleats onto beam webs in the shop, thereby ensuring that they are secure. However since no control of this operation is required, and the cleats may be loosened during erection, the wisdom of relying on this bolt tightness is called into question.

Tests JT/04 to 06 were conducted with web cleats fixed to the column flanges. The moment-rotation curves for these three tests are shown in figures 3.9 to 3.11. In all three tests the bolts were grade 8.8 M16's, tightened to 160 N.m.

During test JT/04 a great deal of noise was heard as the test proceeded. These loud cracks coincided with sudden drops in the load.

In figure 3.9 these sudden reductions in load are readily apparent. The test apparatus was deflection controlled - so sudden slips caused the load to drop off, and the screw jack had to travel further before additional load could be applied. This accounts for the erratic nature of the moment-rotation curve. More commonly joint tests are conducted in a 'load control' system, so if slip occurs the load remains constant but a sudden increase in deflection would be observed.

Test JT/05 was conducted to examine the response of the connection under decreasing loads. Similar to test JT/03, the connection unloaded and reloaded with the same stiffness, and rejoined the original $M-\phi$ curve when the current maximum moment was exceeded.

Joint test JT/06 was assembled as test JT/04 yet the resulting moment-rotation curve shows a much smoother relationship. In this test there were few noticeable slips and the bolts moved gradually into bearing. A comparison is made between this test and the minor axis test, JT/01B, in figure 3.12. The major axis connection is initially less stiff than the minor axis test, due to the deformation of the column flanges. The minor axis connection does not deform at very low loads, giving a greater initial stiffness. The distortion of the flanges produced by the web cleats can be seen in figure 3.13. Though the ductility of the two connections is produced by different

deformation patterns, i.e. in a major axis test the column flanges may distort, but in a connection to the column web the cleats must deform, once the bottom flange comes into contact with the column the behaviour is similar. The increase in stiffness which occurs when the beam bottom flange comes into contact with the column arises at too great a rotation and is accompanied by too much deformation to be of any practical use. For the tests conducted a rotation of about 0.075 radians was achieved before contact with the column, but the exact amount will of course depend on the connection geometry, particularly the end clearance of the beam.

In order for the experimental data to be of use in analysing the results of the subassemblage tests typical major and minor axis connection moment-rotation curves have been refined. The analytical methods used in Chapter 6 require experimental data points to which curves are then fitted. In order to obtain reasonable curves the data points have been reduced in number and the 'saw-tooth' effects smoothed out. Figure 3.14 shows the typical moment-rotation curves to be used in subsequent analysis.

3.7 Behaviour of Flange Cleat Connections

The popularity of this type of connection is probably due to its simple fabrication and its usefulness during erection. The seat, a bottom flange cleat, is either welded or bolted to the column in the fabrication shop. Once the columns are erected, beams may be rested on the cleats, bolted in place, and the top, restraining, cleat then bolted up. In practice the choice of welding or bolting the cleats to the column will be dependent on the fabricator's machinery - if an automatic drilling machine is available they will be bolted to the

column. The decision to bolt the cleats to the column in these tests was based at least partly on the necessity of keeping welding to a minimum.

Two tests incorporating flange cleats were performed; JT/07 and 08, the moment rotation curves for which are shown in figures 3.15 and 3.16.

In order to set up the tests so that the top flanges of the beams were level, and at 90° to the column it was found to be easier to set up the connection using the top cleat first. Once the beams were level and the column vertical the seat cleat was securely fixed to the bottom flange of the beam and then bolted to the column. All the M16 grade 4.6 bolts were then systematically tightened from 80 N.m to 160 N.m in 40 N.m increments. The method of assembly though different from that used in practice, should not affect the resulting moment-rotation curves because the bottom cleat was fixed tightly to the beam flange before bolting the cleat to the column, thus ensuring good contact between the cleat and the beam flange.

In both tests the relative movement between the beam flanges and the cleats was measured. In test JT/07 this was monitored by recording the distance between the edge of the cleat and a point on the beam flange with a digital calliper, and in test JT/08 a Huggenburger dial gauge was used. Test JT/07 examined the effects of unloading the connection, but test JT/08 used monotonic loading.

Initially rotational movement was due to continuous slipping of the bottom flange on the seat cleat. Little movement of the top cleat was seen. This movement continued until the bolts in the beam flange came into bearing on the edge of the seat cleat holes; about 1.2 to 1.4mm of movement had occurred. Once the bottom bolts were in bearing

the top suddenly slipped about 0.8mm and continued to slip a further 0.8mm, until a sudden large slip of 1.2mm brought the top bolts into bearing. The pattern of movement of top and bottom cleats can be seen in figures 3.17 and 3.18. Figure 3.19 compares the behaviour of the two tests. The major axis test has a lower initial stiffness than the minor axis connection due to the flexibility of the column flanges.

The unloading stiffness of the connections is once again considerably greater than the loading stiffness once initial deformation has started to occur. Figures 3.21 to 3.24 show the deformation of the flanges and cleats of test JT/08.

An idealised moment-rotation curve for both major and minor axis connections is presented in figure 3.20. Here the data have been conditioned to give a smooth curve suitable for use in analysis.

3.8 Behaviour of Seat and Web Cleat Connections

A recent review (3.9) of steel beam to column test data noted that none was available for bottom flange and web cleat connections, figure 3.1. Test JT/09 and JT/10 were conducted to study this type of connection.

The connection was assembled from the same angle sections as the flange cleat tests, but the top flange cleat was replaced by two web cleats. M16 grade 4.6 bolts were used throughout, in 18mm diameter holes, and were all tightened to 160 N.m. Both tests were conducted with monotonically increasing load.

Test JT/09 clearly illustrates a disadvantage of the cruciform type of testing method employed. The right-hand beam dipped by large amounts and was influenced by the behaviour of the left-hand beam. As can be seen from figure 3.25 the left-hand beam had a reasonably smooth moment-rotation curve, except for a large slip at 15 kN.m, but

the right-hand beam displayed very erratic behaviour. Results of the major axis test JT/10 are plotted in figure 3.26. The ductility of the connection appears to be provided by the deformation of the column flanges and the web angles. A photograph of this test is shown in figure 3.27, and of the minor axis test in figure 3.28.

A comparison of the moment-rotation characteristics of major and minor axis bottom flange and web cleat connections is made in figure 3.29. Surprisingly the major axis test has the greater stiffness. This is certainly the opposite of what was expected, and it may be due to the variability of the tests rather than a true indication of their respective behaviour.

Figure 3.30 compares the flange cleat and bottom flange plus web cleat connection tests. Both have similar initial tangent stiffnesses, but the top flange cleated connection softens at a lower moment. Once the connections have started to soften the top flange cleated connection has a slightly higher inelastic stiffness, which is probably due to the longer lever arm compared to the web cleated connection. Figure 3.31 presents smoothed moment-rotation curves for web and seat cleat connections.

3.9 Behaviour of Flush End Plate Connections

The flush end plate is currently the most popular type of connection, principally because of its straightforward fabrication, although convenience in containing the joint within the beam depth is also a factor. This type of connection is often used simply as a shear joint, for example in eaves beam connections, and no advantage is taken of its inherent stiffness. The design of this connection (as presented in Appendix A3), was based on the shear capacity of the connection, though the design moment capacity was also checked.

Three tests were conducted on flush end plates JT/11 minor, JT/11b minor and JT/12 major. Where possible the end plates and columns were drilled together to ensure alignment of the holes. E43 electrodes were used to weld the end-plates to the beams. A 4mm continuous fillet weld was provided. All the end plates were welded by an experienced welder, but may not be typical of those produced in a fabrication shop since the welder's experience was not wholly derived from the welding of structural sections. After welding the end plates to the beams the plates were examined for distortion. They were unaffected by the welding, the only irregularities appeared to be along the plates' free edges where shearing them had caused some slight curvature. During assembly of test specimens JT/11 and JT/12 the bolt holes were aligned by pushing two 18mm diameter bars through two sets of holes and then bolting the beams in place with the remaining four bolts. The bars were then removed and the remaining bolts inserted. Obviously on site such precautions would not be taken, but for these tests it ensured that the plates were not in bearing on the bolts initially and allowed some investigation of vertical slip. In test JT/11b the above procedure was not followed because the end plates were not drilled as a set with the column, and consequently the alignment of the holes was not as good. In this test the beams were offered up to the column and the bolts inserted, so it is likely that the connection was bearing on the bolts initially. Some grinding of the edges of the plates in the web connection tests (JT/11 and 11b) was necessary to clear the root radii at the column's web-flange junction.

Figure 3.32 shows the average moment-rotation curve for test JT/11. The curve is initially virtually linear up to a moment of about 30 kN.m (35% of M_p). After this the curve bends in a rounded knee due to the distortion of the end plates, and begins to level off at a moment of between 46.5 kN.m (left-hand beam) and 46.1 kN.m (right-hand beam) - see experimental curves in figure 3.33. Once the maximum was obtained on the right-hand beam there was a loud crack and sudden drop off in load, and the left-hand beam was forced to follow the decrease in load as the right-hand connection continued to rotate under decreasing loads. Inspection of the connection after the test revealed that the web weld at the level of the tension bolts had failed. This was unexpected.

A repeat test was conducted, JT/11b, to verify the result and to examine whether web weld failure was typical. The moment-rotation curves for test JT/11b are shown in figure 3.34.

Notice from the figure that the initial stiffnesses are again almost linear up to a moment of about 30 kN.m. The rounded knee brings the curve round to maximum moments of approximately 51.1 and 49 kN.m. Soon after attaining this peak load a loud crack heralded a sudden reduction in load. After the test it was apparent that bolt stripping had been the cause of failure. Figure 3.35 shows the three bolts when the specimen had been unloaded. The top nut had been pulled along the bolt the end of which was about 2mm short of being flush with the edge of the nut. The middle bolt had become flush with the nut, whilst the bottom bolts projected through the nut by about two threads, approximately 3mm. Figure 3.36 shows the three bolts set against a full scale diagram of the distortion of the end plates at

failure. The 5mm and 7mm clearances between the end plates and column web were measured before the removal of the load at the end of the test.

Tests JT/11 and 11b highlight a problem that occurs with cruciform testing. The two connections cannot act independently and irregularities in behaviour of one connection produce corresponding irregularities in the other. For example in test JT/11b the left-hand beam showed a negative rotation at about 46 kN.m - see figure 3.34. Clearly this would not occur in a building, but with the cruciform arrangement the column may move and alters the balance of one side of the test to the other.

It is interesting to note that neither of the minor axis tests appeared to suffer from vertical slip. This is not surprising in test JT/11b where the bolts may have been in bearing from the start of the test, but in test JT/11 it would suggest that the clamping force developed by the compressive component of the applied moment was sufficient to prevent slip occurring. However the ratio of moment to shear in these tests was not particularly severe, and it is likely that in a more heavily loaded connection some slip may occur.

Test JT/12 was conducted to investigate the behaviour of a flush end-plate connected to the unstiffened flanges of a light column. As expected the flexibility of the column's flanges considerably reduced the connection's initial stiffness, and appreciably increased its ductility. Figures 3.37 and 3.38 give some indication of the relative amounts of distortion suffered by the column flanges and the end plate. Figure 3.39 shows the experimental moment rotation curves for the test. Quite large differences in the maximum capacities and plastic stiffnesses of the left and right-hand connections were

observed. Maximum moments of 23.0 kN.m and 29.6 kN.m and plastic stiffnesses of 290 kN.m/radian and 625 kN.m/radian were achieved for the left and right-hand beams respectively. Figure 3.32 is the average of the two curves which gives a clearer picture of the connection's initial stiffness and the negative rotations recorded at the right-hand connection have been rationalised. An initial tangent stiffness of approximately 20,000 kN.m/radians was recorded. Some difference in the behaviour of the two connections may be due to the presence of washers adjacent to the column flange on the right-hand connection, but on the left side the bolts were inserted with the head of the bolt on the inside of the flange. The effect of the presence of washers was noted previously in a series of tests by Chesson and Munse (3.10).

Undoubtedly the difference between the two sides is not wholly attributable to the bolts. Throughout the test series some differences in response and maximum moment capacity have been present and this suggests that the apparatus imparts some bias into the connection test. Control in setting up the end-plated connections was very limited, so the possibility of the column not being vertical, or the beams not set at the same level arises. With the cleated connections careful alignment could be achieved due to the tolerances in the connection elements, but this was not so with the stiffer connections.

Joint test JT/14 was conducted to determine what contribution the flange welds make to the behaviour of a flush end-plate connection. A flush end-plate, identical to those in tests JT/11 and JT/12 was welded to the beams with a 4mm continuous fillet weld down each side of the web only. The bolt spacing and plate overall size were the same as the all-welded flush end-plates (even though header plates

are usually plates of a smaller depth than the beam's depth) in order to make direct comparison with the flush end-plate tests possible. The experimental moment-rotation curve is shown in figure 3.40.

Surprisingly the connection performed almost as well as the fully welded connection, the maximum moment was 43.6 kN.m which compares well with 46.5 kN.m and 51.1 kN.m recorded in tests JT/11 and JT/11b respectively. The average of the two sides was 88% of the average of the four flush end-plate connections, and 53% of the beam's plastic capacity. A comparison of tests of header plates and double web cleats conducted by Sommer (3.11) showed a very similar behaviour between the two connection types. This was not the case in these tests leading to the conclusion that the plate depth is an important factor in the behaviour of header-plates since it controls the amount of rotation which can occur before the beam flange comes into bearing on the column.

3.10 Behaviour of Extended End Plate Connections

The extended end plate connection, with a row of tension bolts outside the beam flange, has a greater moment capacity than a flush end plate due to the increased lever arm of the resultant tensile force. Despite the disadvantage of the connection projecting above the beam's top flange the extended end plate has become very popular for connections required to transfer beam moments into columns. Many investigations have been undertaken to study the effects of changing the various components in the connection (3.12), but in this series of tests the objective of conducting the extended end plate connection was to find experimentally its moment-rotation relationship. Though

the connection closely approximates rigid behaviour it provides an upper bound to the 'semi-rigid' connections under study in this project.

A "rigid" connection, designed to carry the beam's fully plastic moment, was fabricated as shown in figure 3.1. The design, based on a method by Mann and Morris (3.4) is contained in Appendix A4. Due to the relatively thin column flanges (approximately 7mm) compared to the 15mm thick end plate considerable stiffening of the column was necessary. Figure 3.41 shows the test specimen prior to testing. High strength tensile bolts, grade 8.8 M16, were used and tightened to 150 N.m. This torque was applied to ensure the bolts were all consistently tightened and was insufficient to 'fully torque', or prestress, the bolts.

The moment-rotation curve for the extended end plate test, JT/13, is shown in figure 3.42. Maximum moments of 53.5 and 49.9 kN.m were achieved by the right and left-hand beams respectively. The behaviour of the connection was non-linear throughout, but with a knee occurring at about two-thirds of the beam's plastic capacity. A slip occurred at a quite high load and was thought to be the onset of failure. Since the test was not adequately shielded for destructive testing the test was stopped. However on dismantling the specimen there were no signs of imminent failure and the only sign of distress was the distorted column flanges. The specimen was reassembled and retested as test JT/13b. Figure 3.43 shows the moment-rotation curve. Reloading the connection resulted in a near linear response up to the moment at which slip occurred in test JT/13. Failure of test JT/13b was due to weld failure. The beam top flange weld to the end plate on the right-hand side failed. This was not unexpected since the 4mm

continuous fillet weld was small and the design calculations showed it to be a possible failure mode. The actual mode of failure was not regarded as particularly important in these tests because the connection response at levels of load and rotation significantly lower than those at failure was sought. Tests by Johnstone and Walpole (3.13) which studied the effect of loading and unloading extended end plate connections showed the unloading and subsequent reloading behaviour of the connections to be approximately linear up to the current maximum moment, where the curve then rejoins the original moment-rotation relationship. By overlaying the results of test JT/13b and test JT/13 the curve shown in figure 3.44 was achieved.

A series of tests by Packer and Morris (3.14) involved testing nominally identical specimens, except for column size. A reduction in column flange thickness reduced the initial connection stiffness appreciably, and changed the shape of the moment-rotation curve. The tests incorporated 254 × 102 × 22UB beams and 152 × 152UC columns of serial weights 23,30 and 37 kg/m. 16mm diameter HSFG bolts were used to bolt the 15mm extended end plates to the columns which were stiffened at the level of the top and bottom beam flanges. The moment-rotation curves are shown in figure 3.45. A direct comparison of behaviour between Packer and Morris tests and test JT/13 is not possible due to the different bolts used and the pattern of column stiffening. However the behaviour observed in test JT/13 would appear to be closer to the curve obtained for the 9.5mm thick column flanges than that for those 6.5mm thick (152 × 152 × 23UC) due to the more efficient stiffening employed. It also seems likely that the 'ordinary' 8.8 M16 bolts perform as well as HSFG bolts.

Figure 3.46 shows the deformation produced in the test. Considerable deformation of the thin column flanges is evident, but only slight deformation of the beam end plates occurred. Before the specimen was assembled the end plates bent towards the beam, the magnitude was about 1mm at the plate's top edge. This curvature was removed during bolting up and was not evident when the specimen was dismantled after the test.

The use of backing plates has been the subject of recent research because they can provide a cheaper alternative to the time consuming, and therefore costly, conventional methods of column stiffening. A series of tests were conducted at BRE to study the effects of backing plates on the behaviour of a 15mm thick extended end plate bolted to 152 × 152 × 23UC. The beams, column and method of testing were very similar to those used in this test series. Figure 3.47 shows the moment rotation characteristics of a connection to an unstiffened column, a column stiffened with backing plates, and the conventionally stiffened column JT/13. Notice that the conventionally stiffened column has a greater initial stiffness than the column stiffened with backing plates and is more linear up to about 40 kN.m. Unfortunately test JT/13 was not continued as far into the plastic region as the BRE tests since weld failure occurred. However the use of conventional column stiffening is very time consuming and does not appear to give large increases in connection stiffness compared with that which may be achieved by the much simpler, and cheaper, use of backing plates.

3.11 The Effect of Lack of Fit on Connection Performance

Some degree of lack of fit, arising from rolling tolerances, fabrication and erection deviations, is inherent in all structural

frames and designing for perfect fit is impractical. Numerous on site disagreements over the quality of fit-up achieved in end plate connections arise. For this reason CIRIA investigated the problem of fit-up in connections - and presented their findings in Report No. 87 (3.15). Consideration was given to the problem of lack of fit in end plate connections incorporating HSFGB bolts in this report, but what effect does lack of fit of end plate connections have when ordinary, not fully torqued, bolts are used? During steelwork erection lack of fit is often rectified by enlarging bolt holes. What effect does this have on 'simple' connections? Since neither of these questions were addressed in CIRIA Report No. 87, CIRIA sponsored eight lack of fit tests at Sheffield University. These subsidiary tests were conducted in the same manner as the main joint test series and enabled a direct comparison to be made between nominally 'perfect' and deliberately imperfect connections.

3.11.1 Web Cleat Connections

Web cleat connections have an inherent degree of tolerance due to their use of bolts in clearance holes. However on occasion it is necessary to open up the holes through the beam web to accommodate lack of fit, perhaps due to a shortfall in beam length, or misalignment of holes. Test CT/01 was conducted to investigate the effect of increasing the diameter of the holes through the beam web from 18 to 20mm. The holes in the cleat and column remained at 18mm diameter, and the connection was identical to the major axis web cleat test (JT/04-06) specimens. In addition to the automatic logging of moment and rotation, four dial gauges were used to measure the rotation of the left-hand beam relative to the column flanges and the relative rotation of the cleat to the beam web - see figures 3.48 and

3.49. The connection was assembled in the test rig and levelled before tightening the bolts. No special measures were taken to align the cleat and beam holes or to centralise the bolts, but it was observed that the connection rested in bearing on the bolts as would be the case in practice. All the bolts were grade 8.8 M16, and the tightening procedure discussed in section 3.5 was followed. The moment-rotation relationship is shown in figure 3.50.

Comparing the results with those obtained for the 'perfect' connection in test JT/06 it is apparent that the larger holes do influence the connection's response. The behaviour of the right and left-hand beams was very similar and can be summarised as follows. Initially the connection responded almost linearly up to a moment of 3 kN.m, thereafter it began to rotate with little increase in moment. The connection must have been slipping but no audible slips were observed until the rotation reached 7.5×10^{-3} radians. Up to a rotation of about 40×10^{-3} radians the connection carried increasing loads but slipped on numerous occasions in a rather erratic and noisy manner. Between 40×10^{-3} and 70×10^{-3} radians, the connection sustained increasing moment with a uniform increase in rotation. A maximum moment of 7.5 kN.m was recorded at a rotation of 70×10^{-3} radians at which point the test was terminated.

Turning to the moment-rotation curve for test JT/06, presented in figure 3.11, a similar pattern of behaviour is evident but the amount of slip is considerably less and a maximum moment of 9.5 kN.m was attained at a rotation of about 65×10^{-3} radians. In neither test did the bottom flange of the beam come into contact with the column flange.

Clearly with larger holes through the beam web the potential for slip is much greater and it would appear that the full amount of slip is produced. Theoretically the top and bottom bolts, if central through the holes, would allow 3mm of slip, resulting in a rotation of 60×10^{-3} radians. In the experiment the rotation at which independent slips ceased was 40×10^{-3} radians, which suggests that the connection was set up in a less favourable position than the idealised model.

For connections required to act as pins, or designed as such, the effect of oversized holes through the beam web is not significant.

However if the connection's behaviour was of importance in the design, for example in reducing the span moment and/or deflection, or to provide restraint to a column, then the effect of the larger holes, which reduces the moments carried by the connection by around 30%, would be detrimental.

3.11.2 Flange Cleat Connections

The second test in the CIRIA lack of fit series CT/02, was a top and bottom flange cleat connection identical in all respects to test JT/08 except that the holes in the beam flanges were increased to 20mm diameter. All the bolts were grade 46 M16, and were tightened to 160 N.m. In order to monitor the relative slip between the beam and cleats two dial gauges were mounted on the left-hand beam's flanges and recorded the movement of a small metal upstand welded to the cleats - see figure 3.52.

Figure 3.51 shows the behaviour of the specimen during the test. The dial gauge readings were helpful in providing insight into the connection's response as the test proceeded and the following mode of behaviour was observed. From the start of the test the top cleat

slipped steadily until about 3mm of movement had taken place in the dial gauge with the bottom cleat remaining almost stationary. At about 10 kN.m the top and bottom cleats both moved slowly to give the curved central portion of the moment-rotation curve. A loud bang accompanied a sudden 2mm slip of the bottom flange cleat at a moment of 17.7 kN.m. The top cleat had moved some 4mm by this time. A drop in load due to this large slip can be seen on the moment-rotation curves for both the left and right-hand beams. The connection load then increased until another slip at the bottom of about 1.5mm caused the load to plummet to a value corresponding to a moment of 10.3 kN.m. From that point onwards the top cleat steadily moved a further 0.5mm, and the bottom a further 1.8mm. The remaining irregular behaviour was due to the right-hand beam slipping at the bottom cleat.

A comparison of the lack of fit connection's response with the nominally perfect connection test JT/07 shows that, as for the web cleat tests, the potential for slip is both greater and fully developed by the connection. Totals of 4.5mm and 6.1mm of slip were experienced by the top and bottom cleats respectively, compared with 2.8 and 1.2mm in the 'perfect' test. Clearly the amount of slip which can occur will depend on the relative positions of bolt holes and bolts, and consequently will be subject to wide variation. Another difference between the two tests was the mode of behaviour -in the 'perfect' test the top cleat did not slip until the bolts in the bottom cleat were in bearing, whereas, as explained above, the top cleat slipped first and then forced the bottom cleat to slip in the lack of fit test. It is likely that the mechanism developed will depend on the relative magnitude of the frictional forces created between the top and bottom cleats with the beam flanges, although it

is probable that the top cleat would slip first in a real beam-column connection due to the greater frictional force developed on the bottom cleat by virtue of the beam end reaction.

Unless the flange cleat connection was to be used as a semi-rigid connection the effect of large holes in the beam flanges is not important and, even where the restraint provided by the connection is to be relied upon, the imperfect connection still managed to attain a similar maximum moment and at a comparable rotation.

3.11.3 Flush End Plates

During the welding process distortion of the end plate frequently results. The pattern and amount of distortion depends on the welding process, the shape and thickness of the end plate and the degree of care taken in fabrication. Distortion may be controlled by careful tacking and positioning of welds, but in some cases it is almost inevitable that some distortion will occur. Many disputes arise when badly distorted end plates are fitted up on site, perhaps because daylight can be seen through the connection, or the plates are not pulled up fully against the column. In connections incorporating HSFG bolts this clearly leads to confusion - after all HSFG bolts derive their name from the means by which they are supposed to carry shear loads, and if the plates are not in full contact can the necessary shear force be developed? This particular problem was dealt with in CIRIA Report No. 87. However many end plates do not employ HSFG bolts and the effect of initial lack of fit on these connections was not studied.

In order to investigate the effect of distortion on flush end plate connections a further test, CT/03, was conducted using the same details as JT/11. In the case of the original test series very little

distortion of any end plates was encountered, mainly because of the light welds and relatively heavy end plates. It was therefore necessary to distort the end plates after welding them to the beams. A pattern of distortion similar to that produced by welding was formed in the end plates by heating the plates and hammering them into shape. The distorted shape can be seen in figure 3.53 and diagrammatically in figure 3.54.

A torque of 160 N.m was applied to all 6 M16 grade 4.6 bolts when assembling the test. Grade 4.6 bolts had been selected for the previous test series as the connection was designed to carry only shear, and although JT/11b had shown that bolt failure was likely it was necessary to keep all parameters the same in test CT/03 in order to isolate the effect of lack of fit. As the test was a minor axis one (a major axis test would doubtless result in flange deformation similar to JT/12) it was impossible to see how well the plates pulled together. After tightening the bolts it appeared that not all the distortion in the vicinity of the central pair of holes was removed because the nuts on these two bolts were flush with the end of the bolt whereas the bolts in the top and bottom rows projected a few millimetres through the nuts.

Figure 3.55 shows the results of the test in the form of a moment-rotation curve. Failure of the test occurred by bolt thread stripping. A comparison of this test with JT/11b shows a similarity of behaviour in terms of initial stiffness and the rotation at failure but the lack of fit test failed at a lower moment. The average moment in test CT/03 was 43.3 kN.m compared with 49.6 kN.m in test JT/11b, and in test JT/11, although the failure was caused by a weld, the bolts must have been very near to their ultimate load as evidenced by

the levelling off of the moment-rotation curve at a maximum of 46.2 kN.m. With so small a number of tests it is not possible to draw definite conclusions but it appears likely that the effect of lack of fit was not drastic and the reduction in capacity may have been due to the variability between tests rather than the lack of fit. A possible cause for concern would occur if the bolts in such a connection were tightened excessively in an attempt to eliminate the unsightly lack of fit. If they were loaded well beyond their elastic limit (which would be possible with some badly distorted plates and ordinary bolts) then they may not have sufficient capacity to carry either the shear load for which they were designed nor the moment that would be produced due to the beam end rotation. The permissible shear capacity of an M16 grade 4.6 bolt, for example, is halved if the bolt tension is increased from 7 to 19 kN. In such a connection it would be better to simply tighten the bolts hand tight, as required for ordinary bolts, and make no attempt to remove the distortion.

A further flush end-plate was tested in test CT/05 to examine what effect a higher strength bolt has on connection performance. The end-plate was distorted in the same manner as CT/03 and assembled with 6 M16 grade 8.8 in place of the 4.6 bolts all torqued to 160 N.m.

Figure 3.56 shows the experimental moment-rotation curve. Maximum moments of 61.8 kN.m and 68.0 kN.m were observed for the left and right hand beams respectively. A comparison of figures 3.55 and 3.56 demonstrates that little difference in behaviour up to moments of about 55% M_p was observed for the two connections with different grade bolts. At around 45 kN.m the grade 4.6 bolts were stripped but the higher grade bolts were capable of sustaining larger moments. Where

bolt failure is the failure criterion using a higher grade bolt does not affect the initial response of the connection but does permit a longer plastic plateau at a higher value of moment.

3.11.4 Extended End Plate

As explained in sections 3.11 and 3.11.3 the need to examine the effect of lack of fit on connections incorporating untorqued bolts has been identified. A test identical to test JT/13 was conducted but with a deliberately deformed end plate. The distortion can be clearly seen in figure 3.57, where the specimen was set up with the bolts finger tight, and also diagrammatically in figure 3.53. Distortion was produced in the same way as for the flush end plate test. All the bolts were tightened to 160 N.m. Notice from figure 3.58 that not all the distortion was removed by the bolts, and in fact even at higher loads it is unlikely that the distortion would be eliminated because the flanges of the column had already started to bend.

A comparison of the resulting moment-rotation curve, figure 3.59, and that for the nominally perfect test, figure 3.42 shows a good correlation. The peak moments were 57.5 kN.m and 58.1 kN.m respectively. Test CT/04 was stopped because the beams were beginning to fail by lateral torsional instability and the channels providing the beam end reactions were showing signs of distress, but it is likely that the test would have failed by weld failure as test JT/13b.

Examination of the results of the two tests suggests that the lack of fit in the test did not adversely affect the connection's performance. Where the friction between the plates is not important, i.e. in connections not incorporating HSPG bolts, distortion of end plates appears not to be a problem. This conclusion is in accordance

with CIRIA Report No. 87 which states that "where HSFG bolts are used as high tensile bolts in moment connections poor contact is unlikely to matter structurally. Lack of fit does not affect the ultimate tensile capacity. Sufficient slip resistance will normally be generated by the compression component of the applied moment. Slip is not normally a design criterion for such joints".

As further verification of CIRIA Report No. 87 an extended end-plate connection, test CT/06, incorporating distorted end plates, but with HSFG bolts was tested. The end plates were distorted in the same way as test CT/04. M16 HSFG bolts were fully torqued and inspected by using load indicating washers. Some distortion of the relatively thin column flanges took place.

Figure 3.61 shows the test specimen with the bolts just nipped into place. The column flange distortion produced by tightening the HSFG bolts to their proof load can be seen in figure 3.62. Notice that not all of the plate distortion was removed. The performance of the connection was similar to test CT/04, which incorporated grade 8.8 bolts. Figure 3.60 gives the moment-rotation curve, and a comparison of this with figure 3.59 shows that the connection with HSFG bolts has a greater initial stiffness than the 8.8 bolt connection. Figure 3.63 records the deformed shape of the specimen at the end of the test.

A recent piece of research in Australia (3.16) noted that pretensioning of bolts increased the initial connection stiffness, but the ultimate capacity remained the same. In test CT/06 some increase in strength over the grade 8.8 bolt connection is noticeable. However this may be due to variability between the tests due to different fit-up, or material properties. Without more extensive testing it is not possible to completely explain this increase in strength.

It would appear from this single test that the use of HSFG bolts with a distorted end-plate produces little difference in the general behaviour of the connection compared with that of a connection incorporating grade 8.8 bolts. Although a 'perfect' connection with HSFG bolts was not tested it is felt that the effect of plate distortion in a moment connection incorporating HSFG bolts will be minimal because the mechanism of load transfer is not dependent on the frictional force developed between the end-plate and column flanges.

3.11.5 Extended End Plates to Column Web

The final two tests dealt with a distorted (CT/07) and a perfect (CT/08) extended end plate connection, both with grade 8.8 bolts, attached to a thick plate to simulate a connection to a 'rigid' flange or to each side of a column web see figure 3.64. The tests were conducted in a large Amsler machine and were load controlled. The magnitude of the rotations measured was very small and since the method of rotation measurement used (as described in section 3.3) was designed to record rotations over a wide range it was therefore not sensitive to very small changes. For these reasons the moment-rotation curves shown in figure 3.65 for tests CT/07 and CT/08 are probably less accurate than those reported earlier. However, they do indicate that the presence of lack of fit was not significant. They also give some indication of the contribution of flange distortion to the moment rotation response of the other extended end plate connection tests.

The $M-\phi$ responses of the two connections to the column flanges have a rounded knee which commences at about 30 kN.m (35% of the fully plastic beam moment) followed by a ductile plateau. In contrast the responses of the connections to the column web are virtually linear up to about 75% of fully plastic beam moment before

some yielding of the end plates and bolts causes a reduction in stiffness. The difference is attributable to the contribution of flange distortion to connection flexibility.

3.12 Conclusions

A set of connections suitable for use with a 254 × 102 × 22UB and 152 × 152 × 23UB have been tested and their moment-rotation characteristics measured. Figures 3.66 and 3.67 display the typical behaviour of each connection type, and the range of connection stiffness is readily apparent. The reason for testing the connections was to provide moment-rotation data for subsequent use in analysing the behaviour of subassemblages and frame tests but the following conclusions may be drawn from the test programme.

1. The web cleat connections showed very flexible behaviour until the beam bottom flange came into contact with the column. Bolt tightness appears to be a significant factor in the initial response of this type of connection.
2. Tests conducted on flange cleat connections showed this type exhibits an almost bi-linear moment-rotation response. The initial curve is approximately linear up to a moment of about 15% of the beam's fully plastic moment at which point the curve's slope quickly decreases and a second almost linear phase is encountered. Connections to the column web are stiffer than those to the column flanges since the latter are able to produce some distortion of the column.
3. Seat and web cleat connections behave in a similar way to flange cleat connections. They have a similar initial connection stiffness; but a slightly lower inelastic stiffness.

4. The effect of lack of fit resulting from enlarged bolt holes in cleated connections does not appear to cause a significant reduction in strength. Its effect is confined to allowing more slip to occur during moment transfer. In connections designed to provide 'simple support' this is clearly of no concern. If the semi-rigid behaviour of the connection was to be utilised in the design of the beams or columns then the detrimental effect on the moment-rotation response should be considered. In such a case the use of HSPG bolts to prevent slip between the beam and cleats would be a possible, if not always convenient, way of ensuring that the enlarging of the bolt holes would not adversely affect the structural performance.
5. Flush end plate connections are currently very popular. The tests conducted showed large differences in behaviour between connections to the column web and unstiffened column flanges. In the case of the connection to the column web, failure was caused by stripping the threads of bolts. For the major axis test the comparatively thin column flanges produced a much more flexible connection and failure was by excessive deformation of the column. Substituting grade 8.8 bolts for grade 4.6 enabled the connection to the column web to extend further into the plastic range but did not appear to affect the response of the connection. A flush end plate welded only to the beam web and connected to the column web had a similar moment-rotation response to those welded to the beam flanges.
6. Lack of fit in the form of distortion in flush end plates does not significantly change the response of the connection, except perhaps if the bolts are overtightened in order to remove the

plate distortion. Where ordinary grade bolts are used it would be preferable to handtighten only rather than attempt to pull in the distortion.

7. Much research has already been conducted on the behaviour of extended end plates. The three extended end-plate connections conducted in this test series show that the use of HSFG bolts in preference to grade 8.8 bolts has little beneficial effect on the moment-rotation behaviour.
8. In extended end plate connections the effect of distortion of the plates does not appear to cause a significant difference in the moment-rotation response. This applies to connections incorporating either HSFG or grade 8.8 bolts.
9. It must be remembered that the importance of lack of fit in any connection is related to the desired mechanism of load transfer. If HSFG bolts are used in a connection to transfer shear by the frictional forces developed by the two or more contact surfaces then the effect of distortions which prevent the surfaces mating is important. If a cleated connection is required to carry a given moment and not rotate excessively then the effect of enlarged bolt holes in this case may be significant. In such cases the designer must consider the implications carefully.

References

- 3.1 JENKINS, W.M.
'Local failures in steelwork structures'.
BRE Contract F3/2/256, Research Report, Hatfield Polytechnic.
- 3.2 HOGAN, T.J. and THOMAS, I.R.
'Standardised structural connections',
Part B : Design of Structural Connections, Australian Institute
of Steel Construction, 2nd Edition, October 1981.
- 3.3 HORNE, M.R., MORRIS, L.J.
'Plastic design of low rise frames'.
Granada Publishing Ltd, 1981.
- 3.4 MANN, A.P. and MORRIS, L.J.
'Limit design of extended end-plate connections'.
Proc. Am. Soc. Civ. Engrs., J. Struct. Div., No. 105, No. ST3,
March 1979, p. 511-525.
- 3.5 JONES, S.W., KIRBY, P.A. and NETHERCOT, D.A.
'The analysis of frames with semi-rigid connections - A
state-of-the-art report'
Journal of Constructional Steel Research, Vol. 3, No. 2, 1983,
pp. 2-13.
- 3.6 AUSTRALIAN STANDARD AS 1511-1984
'Use of high-strength bolts in structures'.
- 3.7 RICHARD, R.M., GILLETT, P.E., KRIEGH, J.D., LEWIS, B.A.
'The analysis and design of single plate framing connections'.
AISC, Eng. Journal, 2nd Quarter 1980, p. 38-52.
- 3.8 RICHARD, R.M., KRIEGH, J.D., HORMBY, D.E.
'Design of single plate framing connections with A307 bolts'.
AISC, Eng. Journal, 4th Quarter, 1982, p. 209-213.
- 3.9 NETHERCOT, D.A.
'Steel beam to column connections - a review of test data and
their applicability to the evaluation of the joint behaviour of
the performance of steel frames'.
CIRIA Report Record, RP 338/1985.
- 3.10 LEWITT, C.W., CHESSON, E., MUNSE, W.H.
'Restraint characteristics of flexible rivetted and bolted
beam-to-column connections'.
University of Illinois, College of Engineering, Engineering
Experimental Station, Bulletin 500.
- 3.11 SOMMER, W.H.
'Behaviour of welded header plate connections'.
Ph.D. Thesis, University of Toronto, January 1960.
- 3.12 SHERBOURNE, A.N.
'Bolted beam to column connections'.
The Structural Engineer, Vol. 91, No. 6, June 1961, p. 203-209.

- 3.13 JOHNSTONE, N.D. and WALPOLE, W.R.
'Behaviour of steel beam-column connections, made using bolted end plates'.
Bulletin of the New Zealand National Society for Earthquake Engineering, Vol. 15, No. 2, June 1982, p. 82-92.
- 3.14 PACKER, J.A. and MORRIS, L.J.
'A limit state design method for the tension region of bolted beam to column connections'.
The Structural Engineer, Vol. 55, No. 10, October 1977, p. 446-458.
- 3.15 MANN, A.P. and MORRIS, L.J.
'Lack of fit in steel structures'.
CIRIA Report 87, 1981.
- 3.16 YEE, Y.L.
'Prediction of non-linear behaviour of end-plate eave connections'.
Ph.D. Thesis, Monash University, Victoria, Australia, Nov. 1984.

TEST NUMBER	CONNECTION TYPE	AXIS	CONNECTION COMPONENTS	BOLT GRADE	COMMENTS
JT/01	Web cleats	Minor	80x60x8 RSA	8.8	Random bolt tightness
JT/01B	Web cleats	Minor	80x60x8 RSA	8.8	
JT/02	Web cleats	Minor	80x60x8 RSA	8.8	Random bolt tightness
JT/03	Web cleats	Minor	80x60x8 RSA	8.8	Random bolt tightness
JT/04	Web cleats	Major	80x60x8 RSA	8.8	
JT/05	Web cleats	Major	80x60x8 RSA	8.8	
JT/06	Web cleats	Major	80x60x8 RSA	8.8	
JT/07	Top and bottom flange cleats	Minor	80x60x8 RSA 125x75x8 RSA	4.6	Unloading behaviour obtained
JT/08	Top and bottom flange cleats	Major	80x60x8 RSA 125x75x8 RSA	4.6	
JT/09	Bottom flange and web cleats	Minor	80x60x8 RSA 125x75x8 RSA	4.6	Slip in R.H. beam
JT/10	Bottom flange and web cleats	Major	80x60x8 RSA 125x75x8 RSA	4.6	
JT/11	Flush end-plate	Minor	265x125x12 M.S. Plate	4.6	Premature weld failure
JT/11B	Flush end plate	Minor	265x125x12 M.S. Plate	4.6	Bolt thread stripping
JT/12	Flush end-plate	Major	265x125x12 M.S. Plate	4.6	
JT/13	Extended end-plate	Major	350x135x15 M.S. Plate	8.8	
JT/13B	Extended end-plate	Major	350x135x15 M.S. Plate	8.8	Re-test of JT/13
JT/14	Header plate	Minor	265x125x12 M.S. Plate	4.6	End-plate welded to beam web only

TABLE 3.1 Summary of connection tests

TABLE 3.1 continued

TEST NUMBER	CONNECTION TYPE	AXIS	CONNECTION COMPONENTS	BOLT GRADE	COMMENTS
CT/01	Web Cleats	Major	80×60×8 RSA	8.8	Holes through beam web enlarged from 18 to 20mm diameter
CT/02	Flange Cleats	Major	80×60×8 RSA	4.6	Holes through beam flanges enlarged from 18 to 20mm diameter
CT/03	Flush End Plate	Minor	265×125×12 M.S. Plate	8.8	Distorted 12mm flush end plate. Test failed due to bolt thread stripped.
CT/04	Extended End Plate	Major	350×135×15 M.S. Plate	8.8	Distorted 15mm extended end plate. Test stopped due to lateral torsional buckling of beams.
CT/05	Flush End Plate	Minor	265×125×12 M.S. Plate	8.8	Distorted 12mm flush end plate.
CT/06	Extended End Plate	Major	350×135×15 M.S. Plate	HSFG	Distorted 15mm extended end plate. Bolts pre-loaded using load indication washers.
CT/07*	Extended End Plate	Minor	350×135×15 M.S. Plate	8.8	Beams and end plates from test CT/08 retested. Failed by weld failure.
CT/08*	Extended End Plate	Minor	350×135×15 M.S. Plate	8.8	Undistorted 15mm end plate. Test failed due to local buckling of beam web under the reaction point.

* different test arrangement

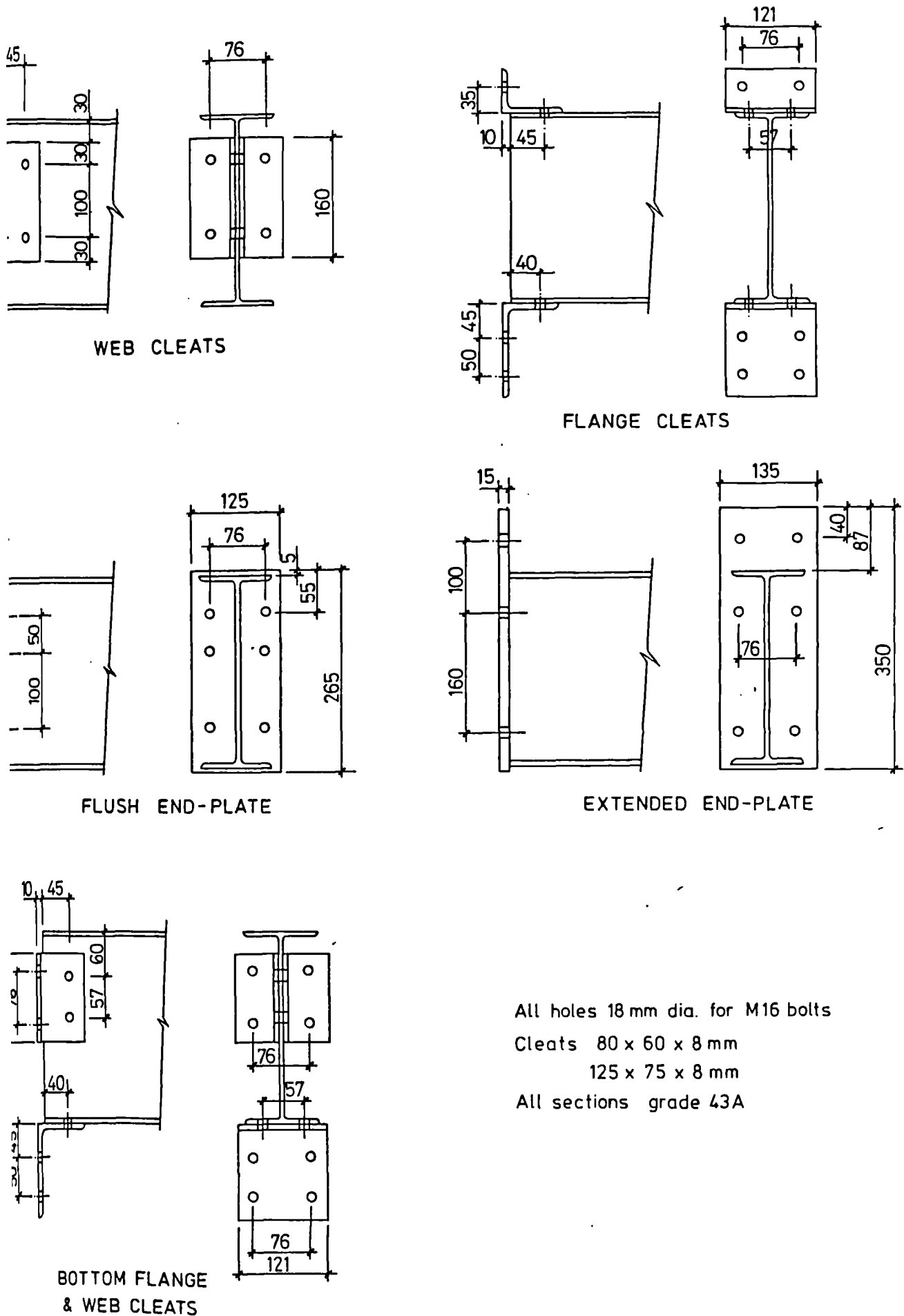


FIGURE 3.1 Details of test connections

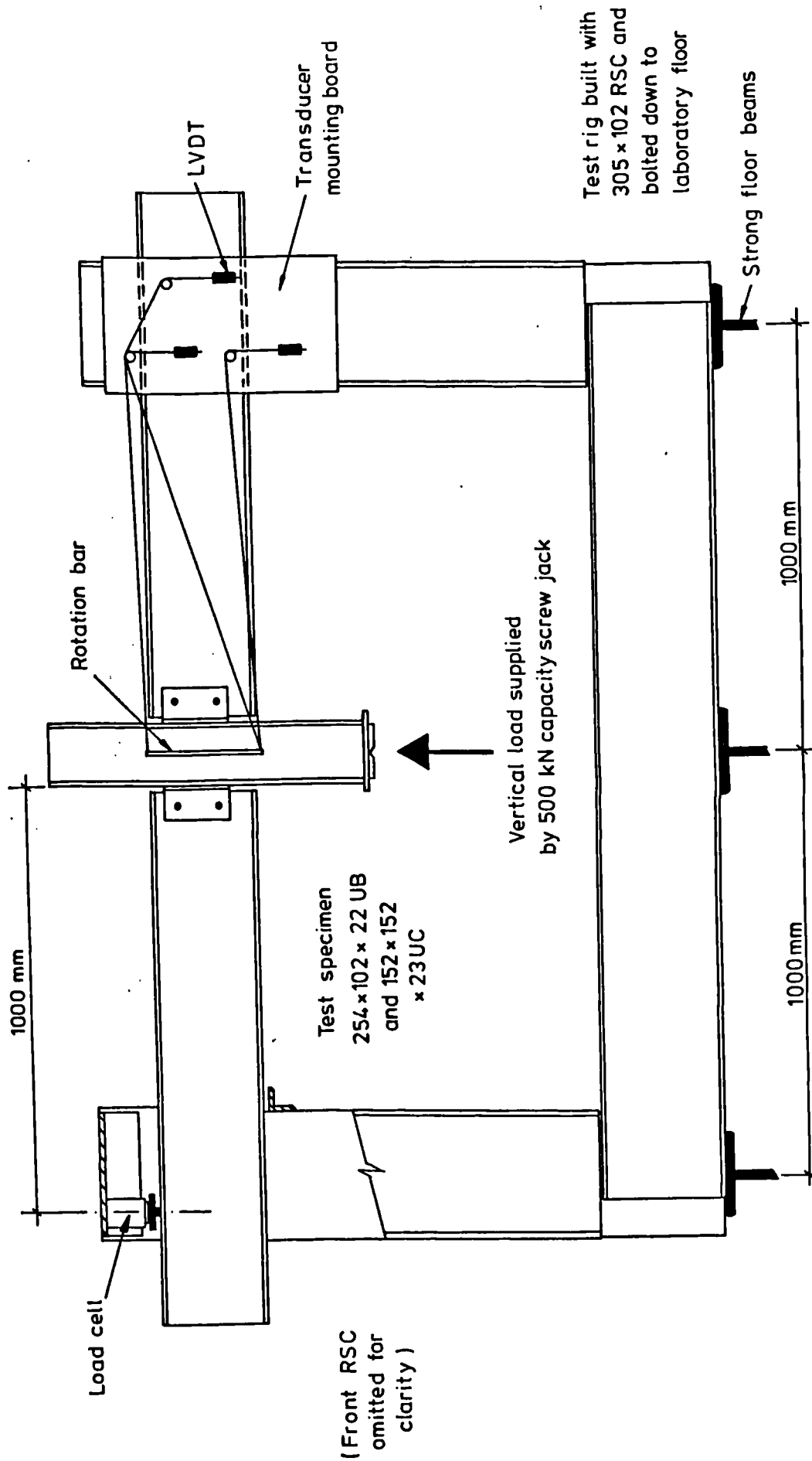


FIGURE 3.2 Joint test apparatus

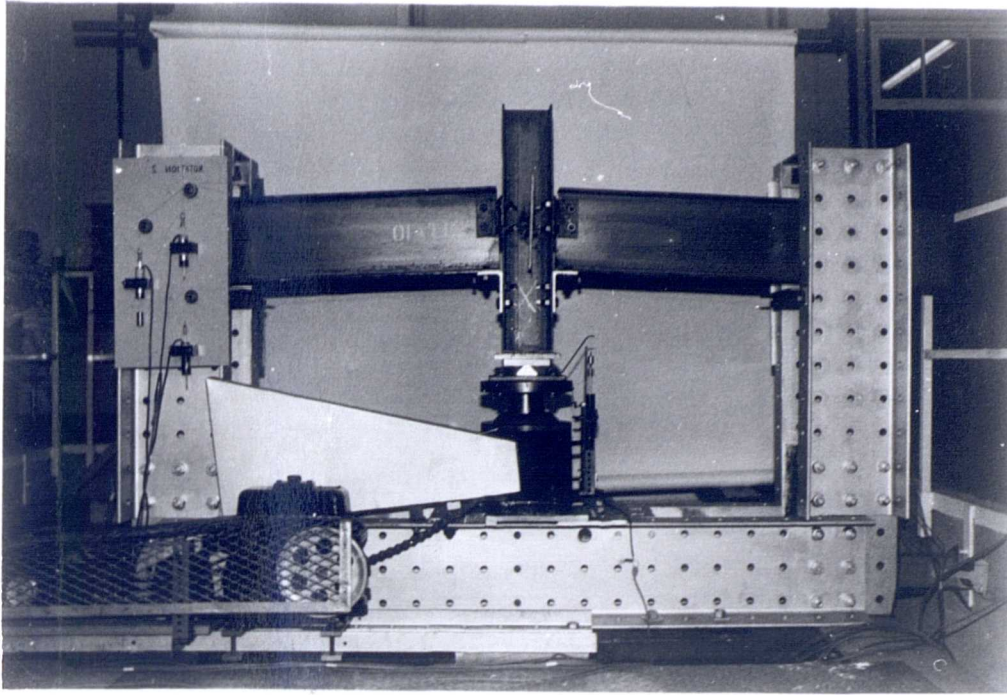


FIGURE 3.3 Seat and web cleat connection under test

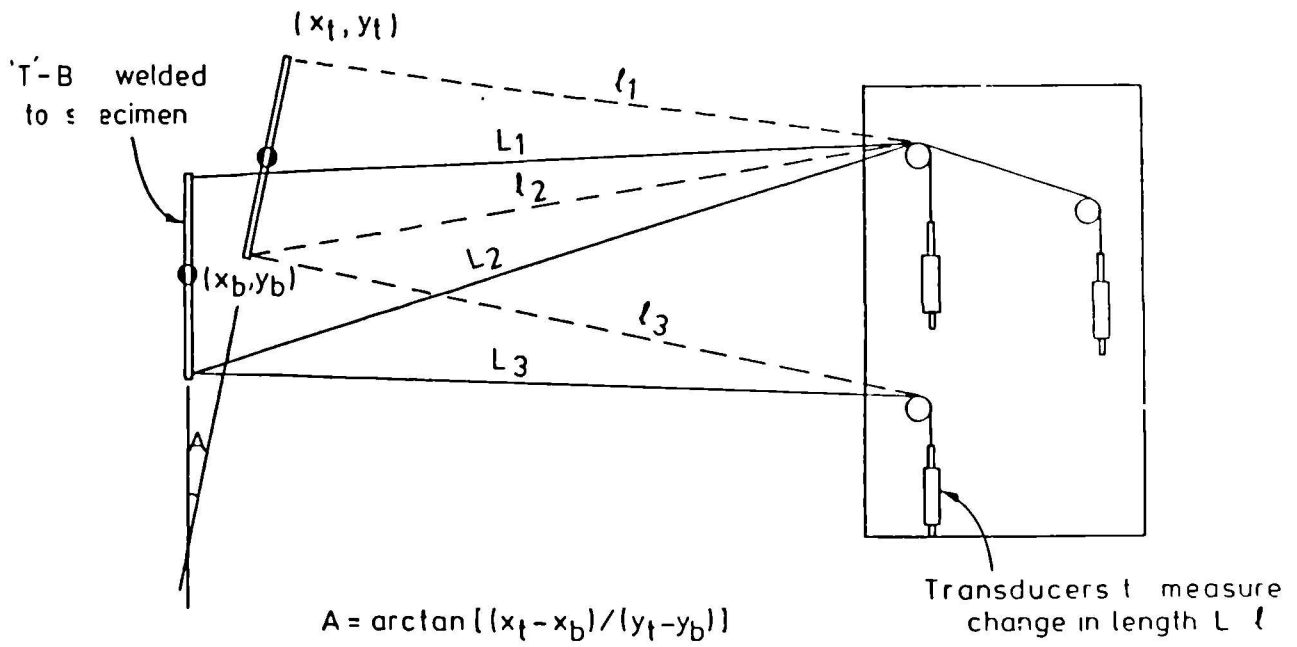


FIGURE 3.4 Method of rotation measurement

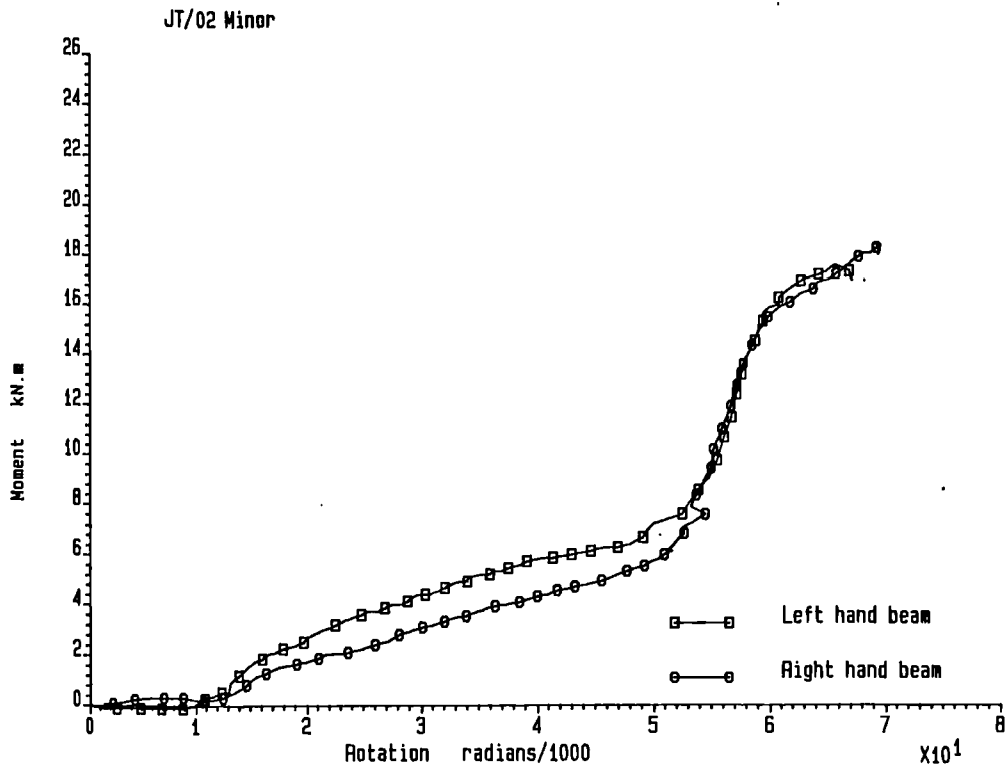


FIGURE 3.5 Experiment M- ϕ curve for web cleat connection to column web (JT/02)

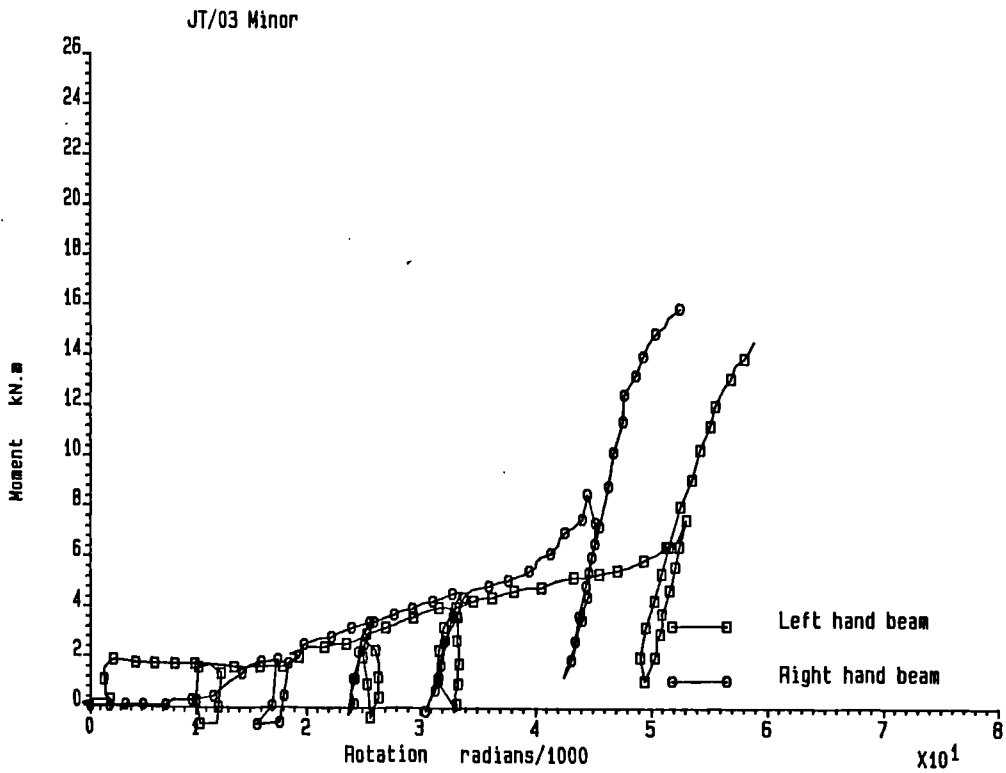
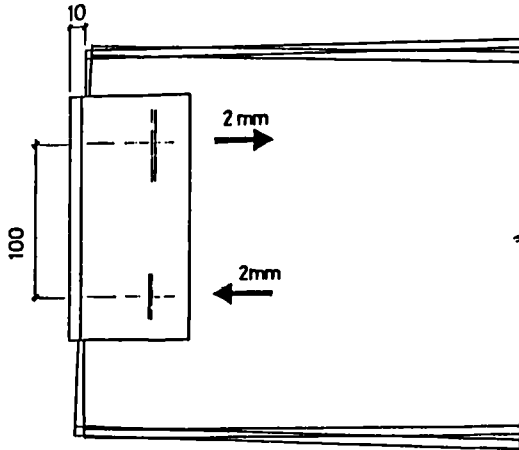


FIGURE 3.6 Experimental M- ϕ curve for web cleat connection to column web (JT/03)



Bolts are 16mm diameter. Holes in cleats and beam web are 18mm diameter clearance holes. If the bolts are central in the bolt hole then the maximum horizontal slip per bolt is 2mm.

The rotation due to a slip of 2mm at the top and bottom bolts is therefore,

$$= \frac{2 + 2}{100} = 0.04 \text{ radians}$$

FIGURE 3.7 Rotation of web cleat connection

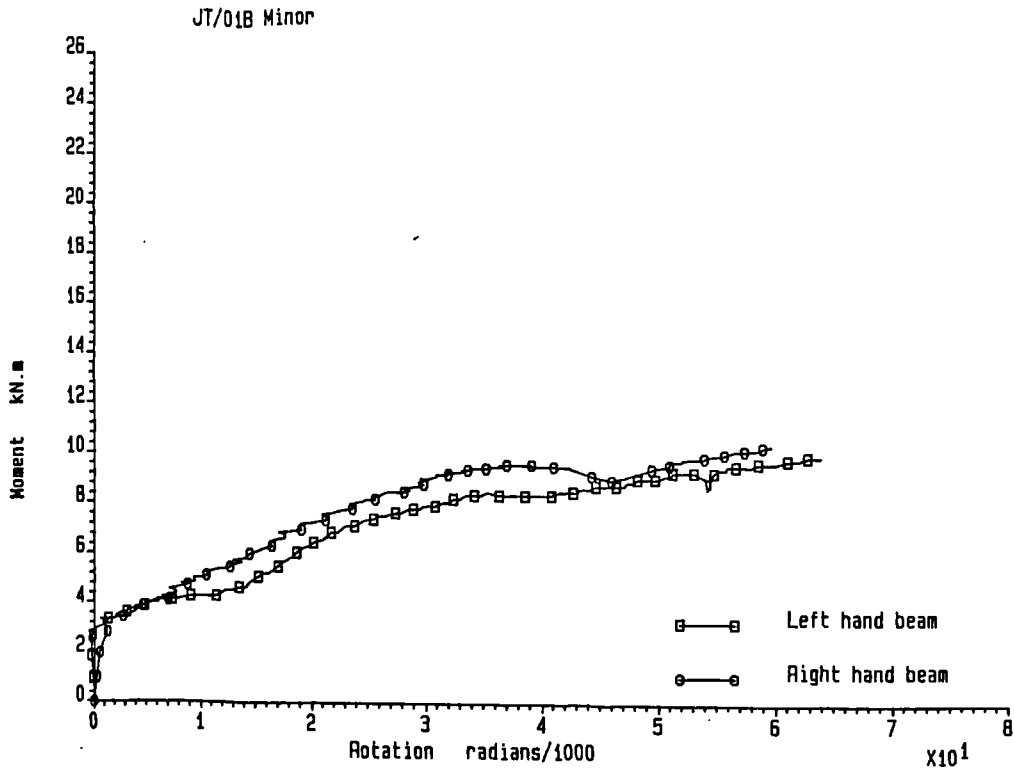


FIGURE 3.8 Experimental M- ϕ curve for web cleat connection to column web (JT/01B)

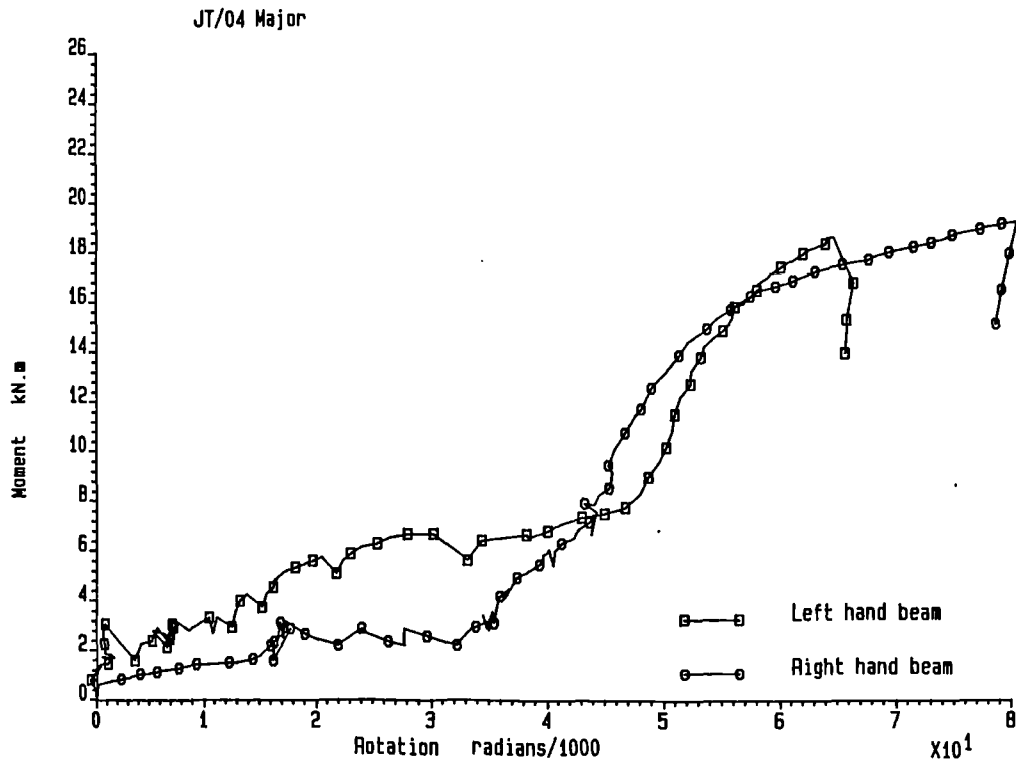


FIGURE 3.9 Experimental M- ϕ curve for web cleat connection to column flanges (JT/04)

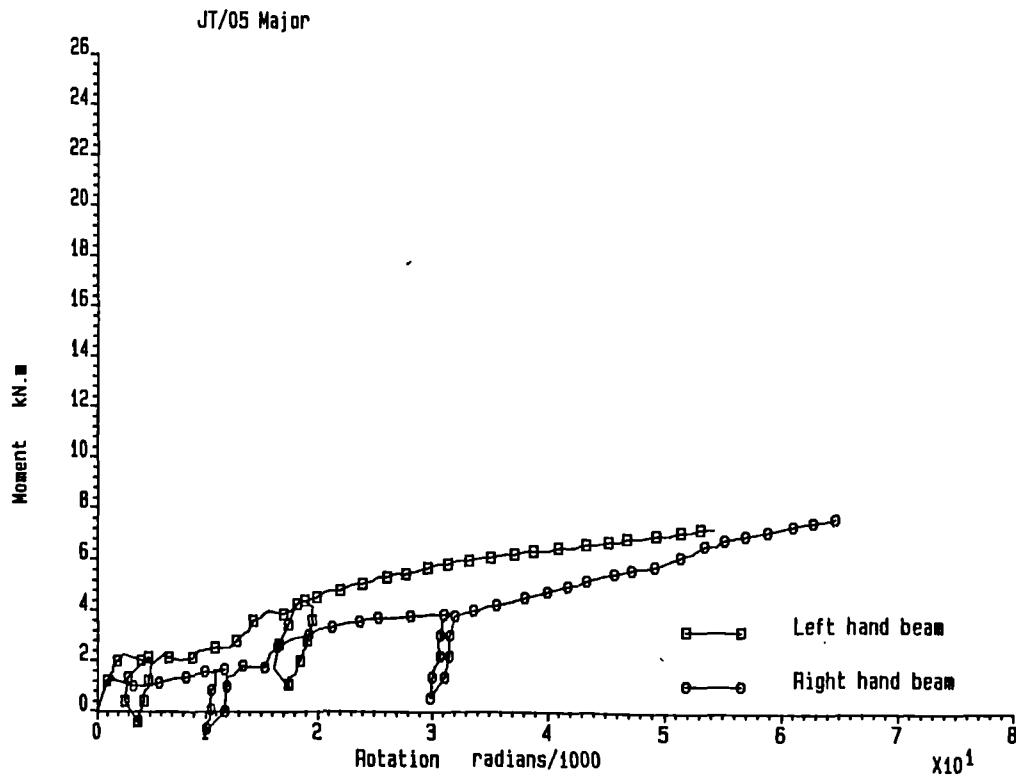


FIGURE 3.10 Experimental M- ϕ curve for web cleat connections to column flanges (JT/05)

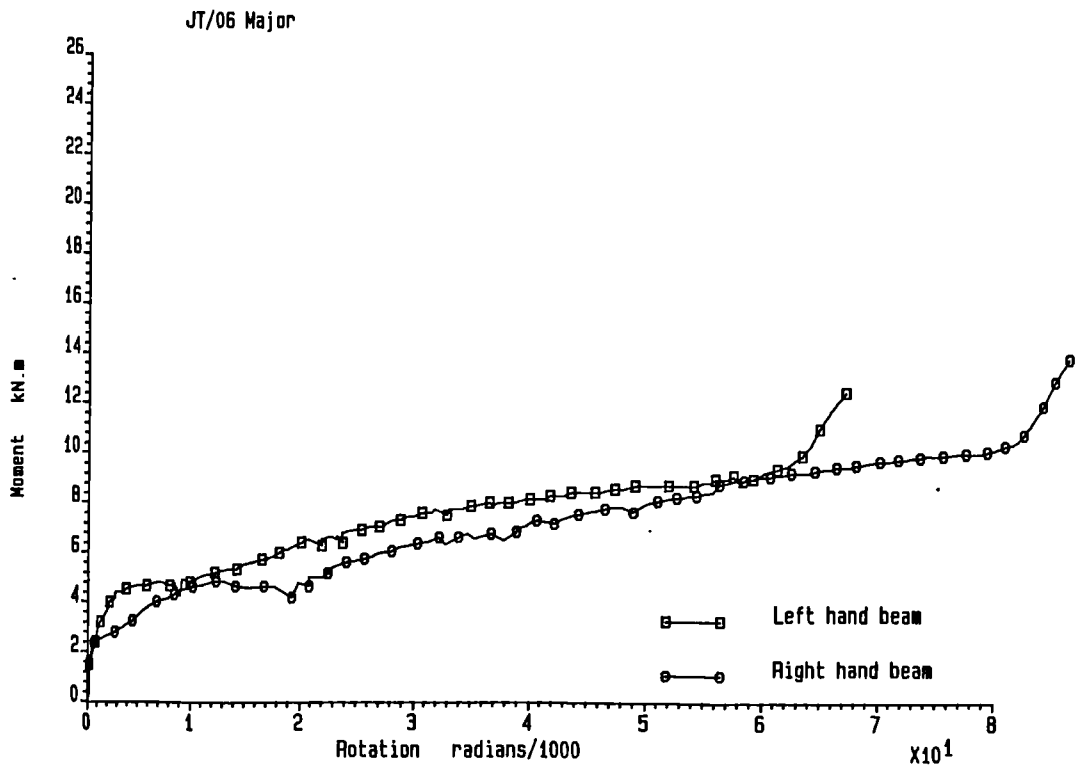


FIGURE 3.11 Experimental M- ϕ curve for web cleat connection to column flanges (JT/06)

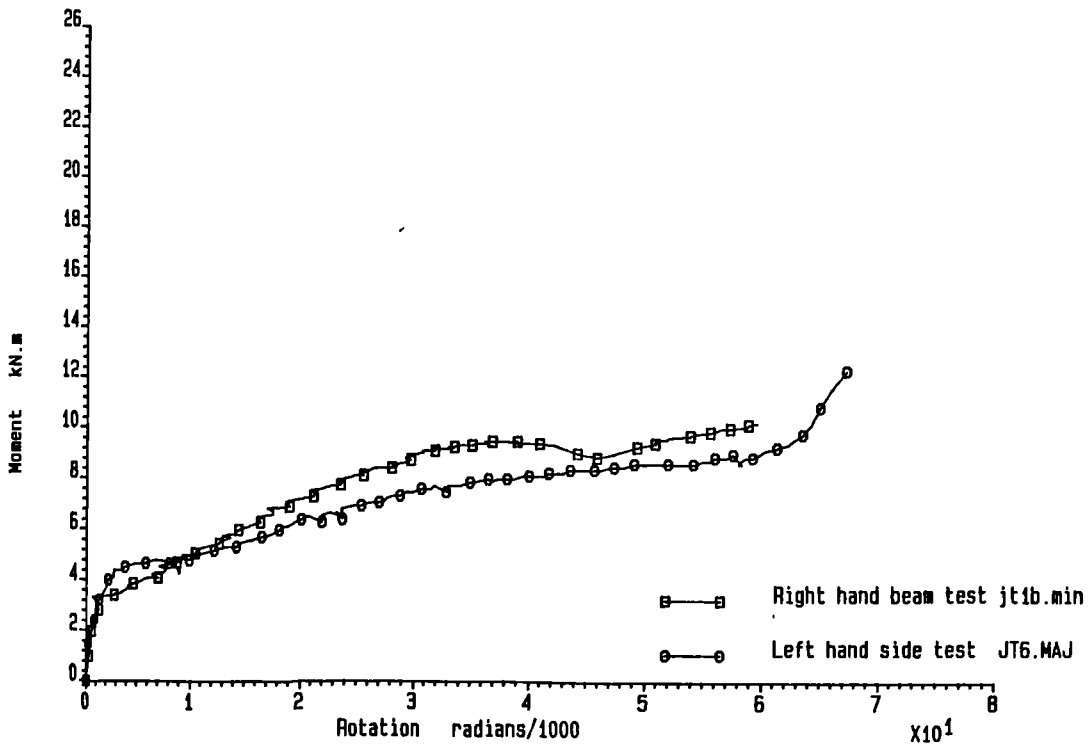


FIGURE 3.12 Comparison of M- ϕ curves for web cleat connection to column web and column flanges



FIGURE 3.13 Distortion of column flanges produced in web cleat test

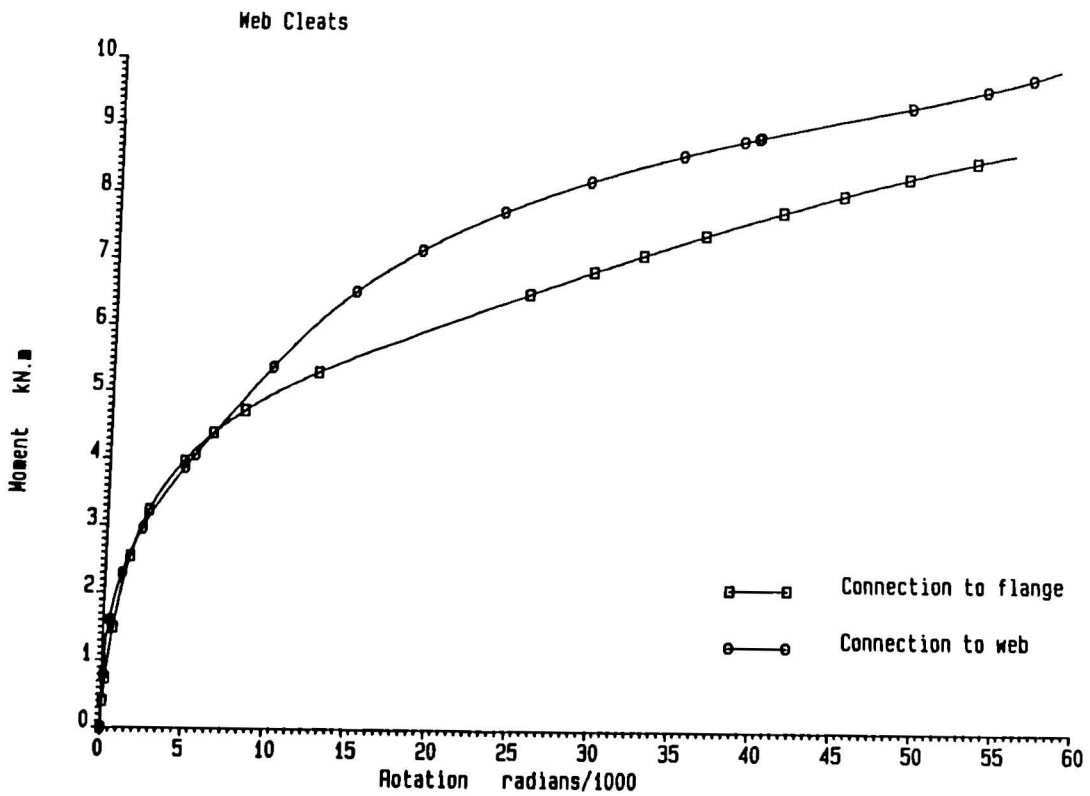


FIGURE 3.14 Typical M- ϕ curve for web cleat connections

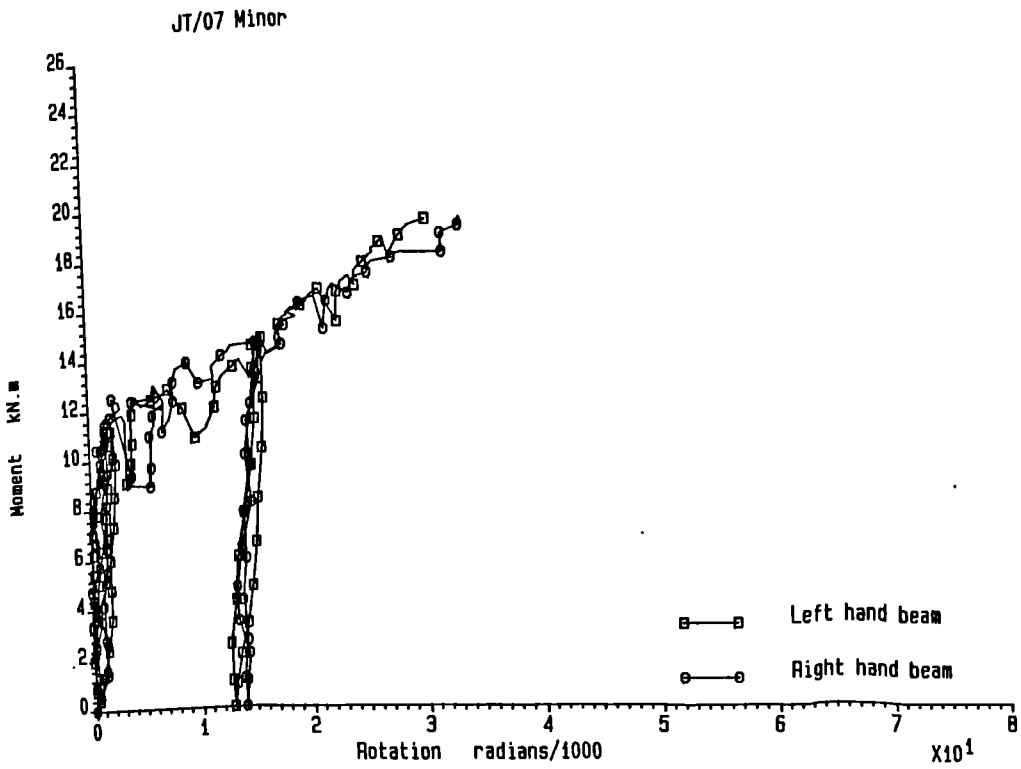


FIGURE 3.15 Experimental M- ϕ curve for flange cleat connection to column web (JT/07)

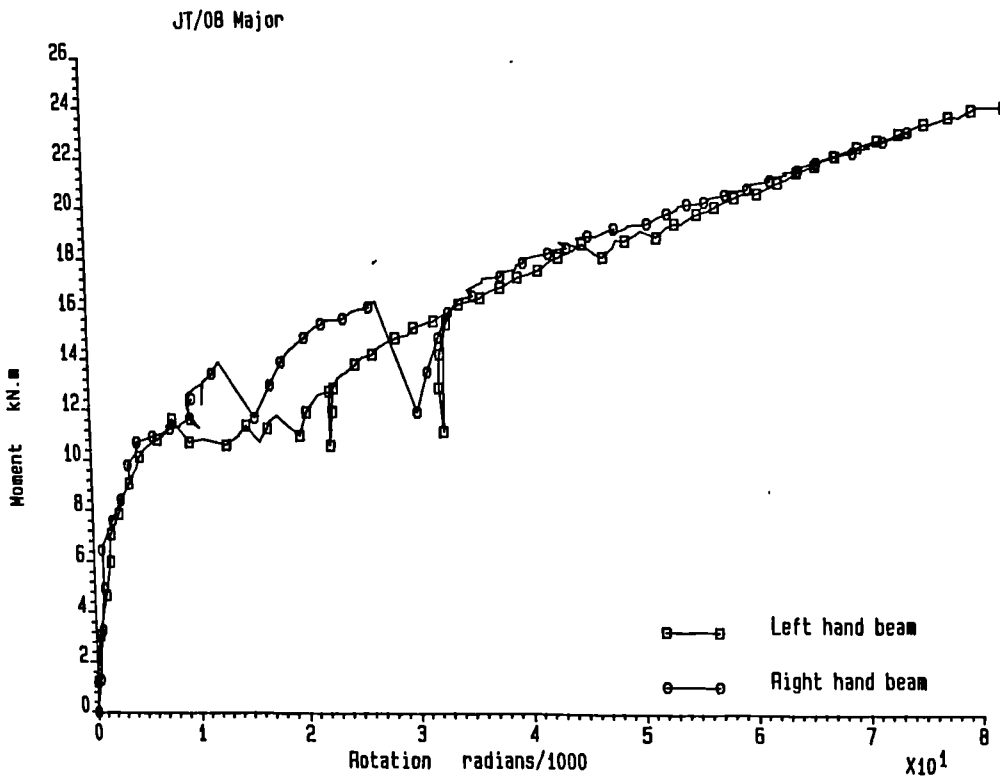


FIGURE 3.16 Experimental M- ϕ curve for flange cleat connection to column flanges (JT/08)

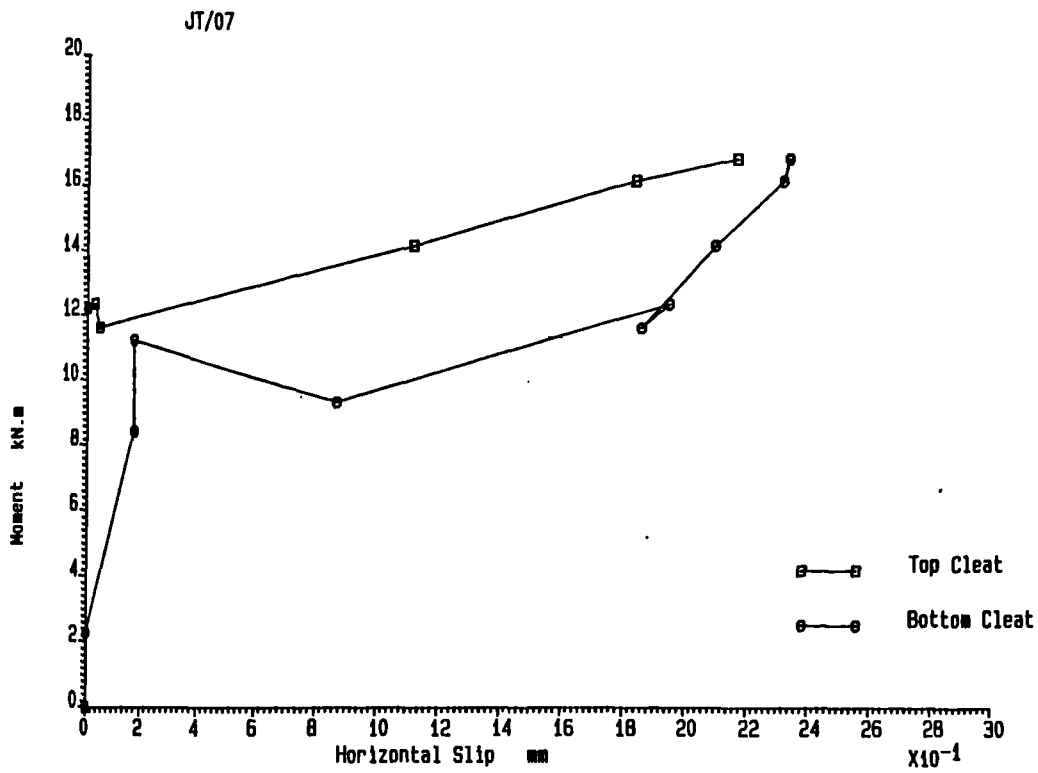


FIGURE 3.17 Moment v horizontal slip of flange cleats in test JT/07

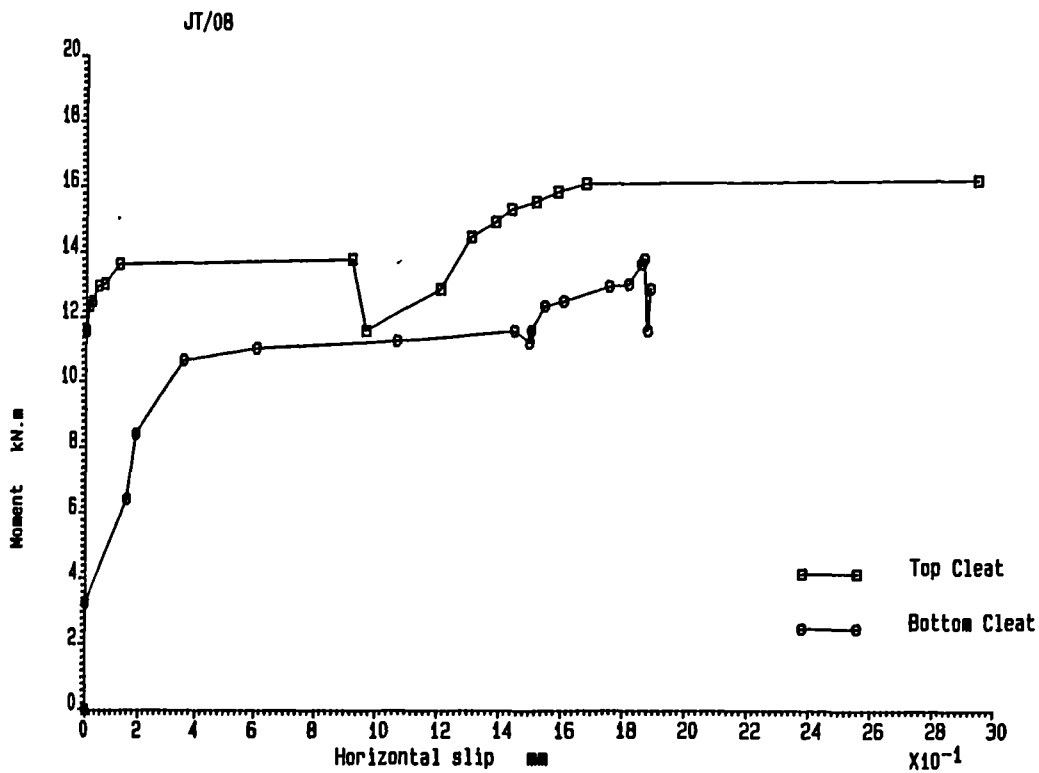


FIGURE 3.18 Moment v horizontal slip of flange cleats in test JT/08

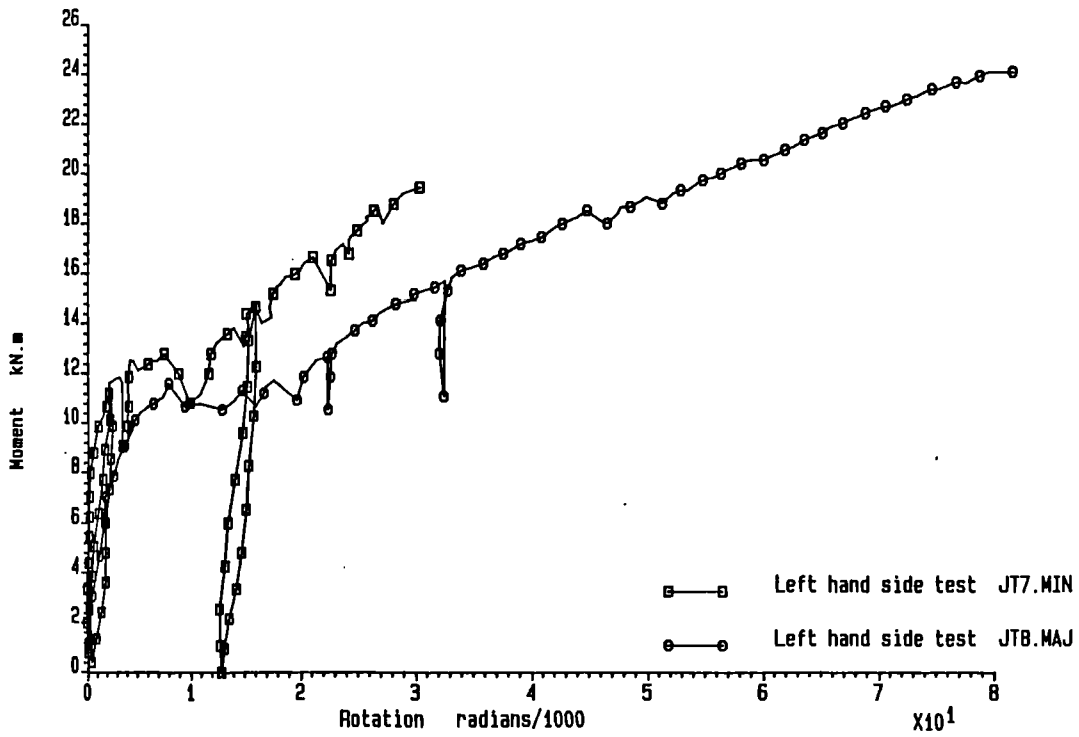


FIGURE 3.19 Comparison of $M-\phi$ curves for flange cleats connection to column web and column flanges

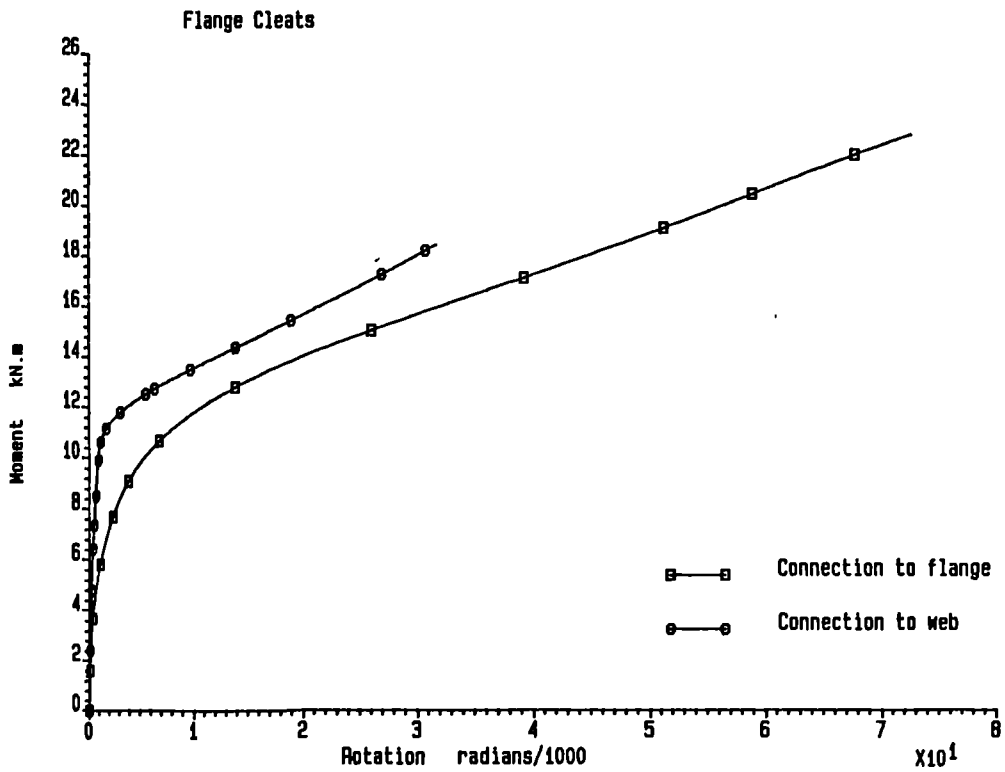


FIGURE 3.20 Typical $M-\phi$ curve for flange cleat connections

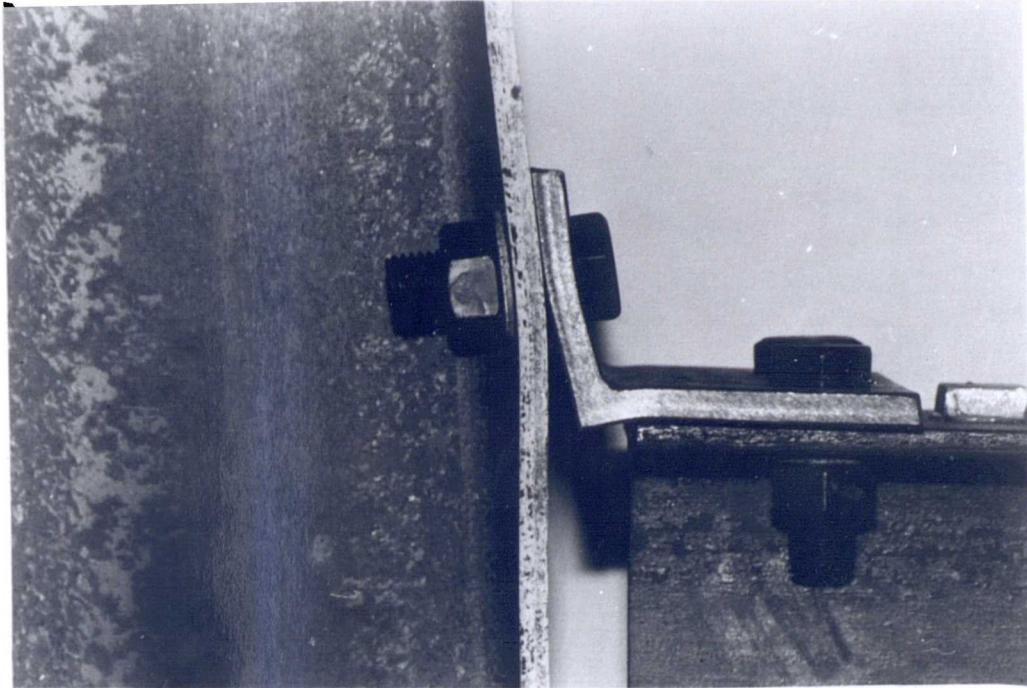


FIGURE 3.21 Bending of top flange cleat in test JT/08

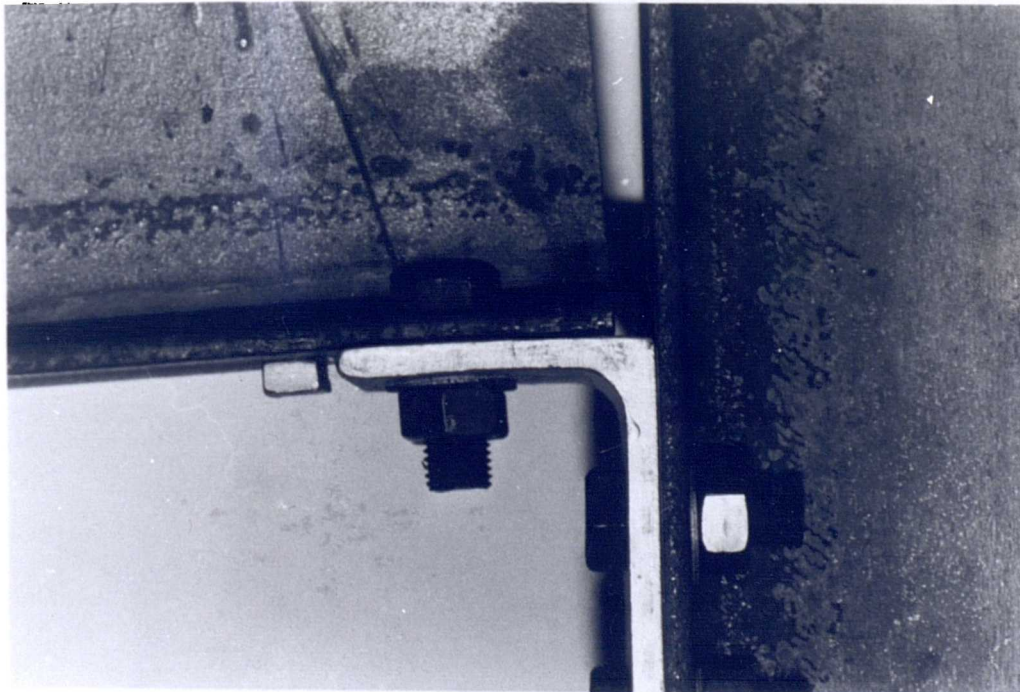


FIGURE 3.22 Bending of bottom flange cleat in test JT/08

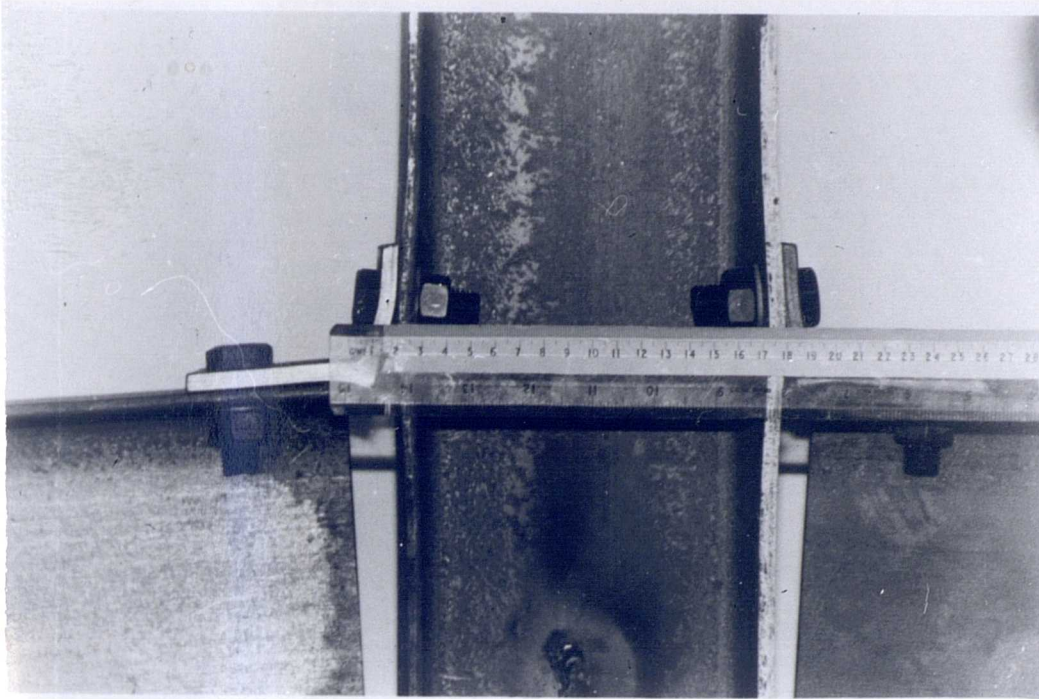


FIGURE 3.23 (above)
Column flange deformation
produced by flange cleats



FIGURE 3.24 (left)
Extent of deformation of
column flanges in test
JT/08

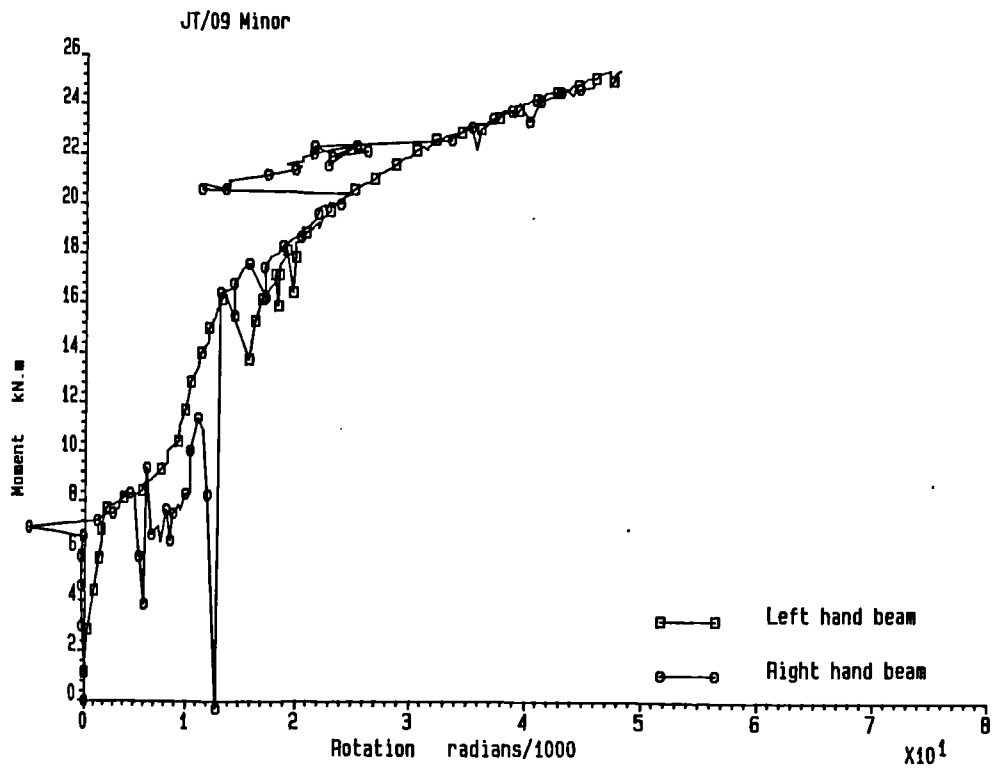


FIGURE 3.25 Experimental M- ϕ curve for seat + web cleat connection to column web (JT/09)

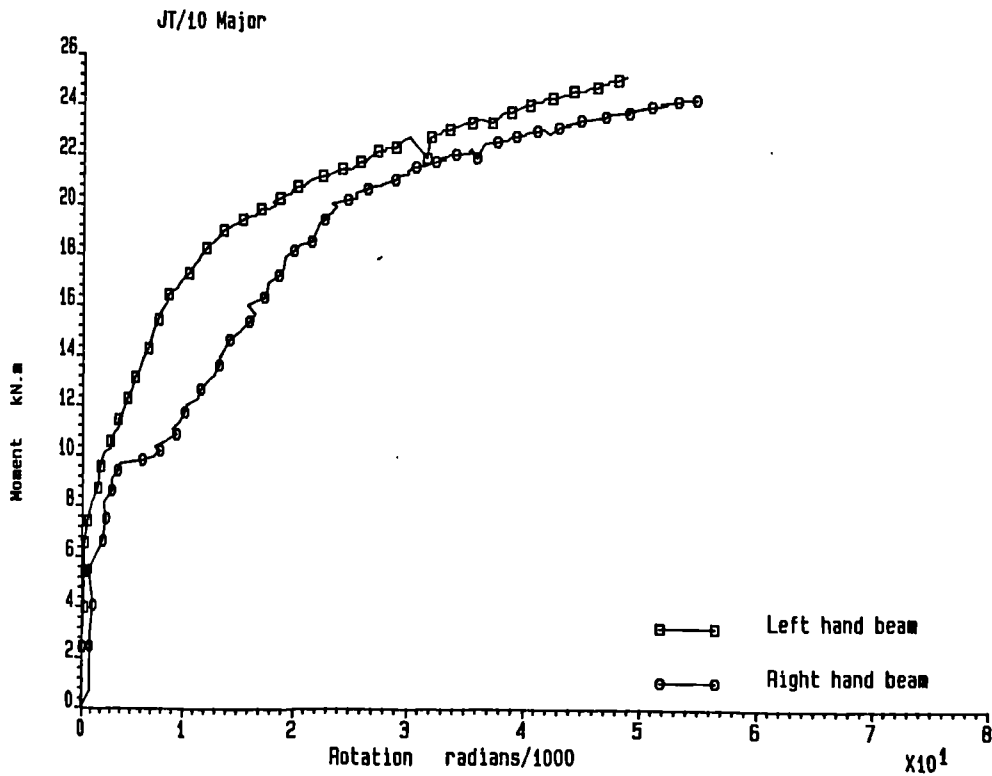


FIGURE 3.26 Experimental M- ϕ curve for seat + web cleat connection to column flanges (JT/10)

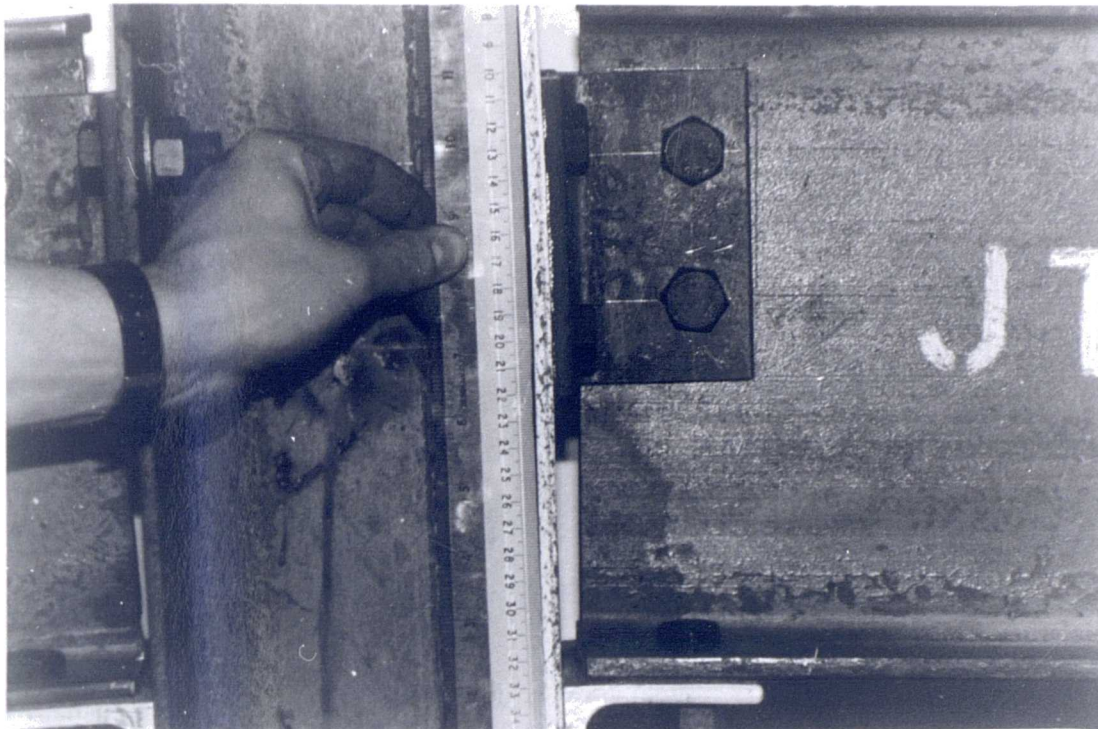
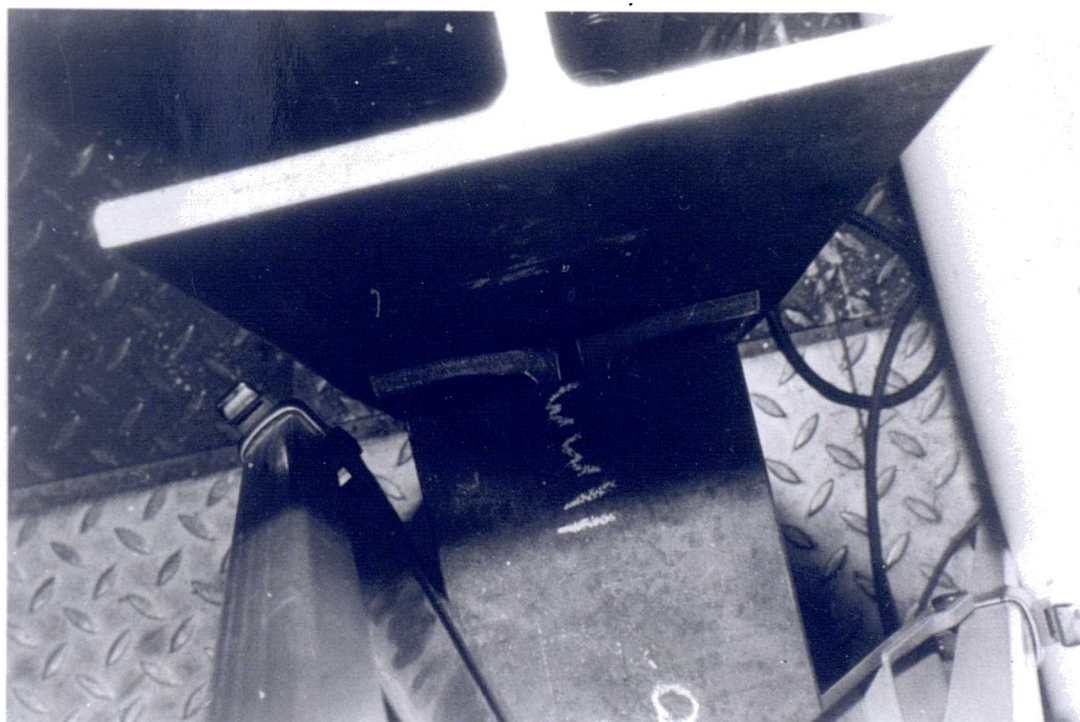


FIGURE 3.27 Deformation of column flanges in test JT/10



. i t r t i n f w e b c l e a t s i n T e s t J T 1 0

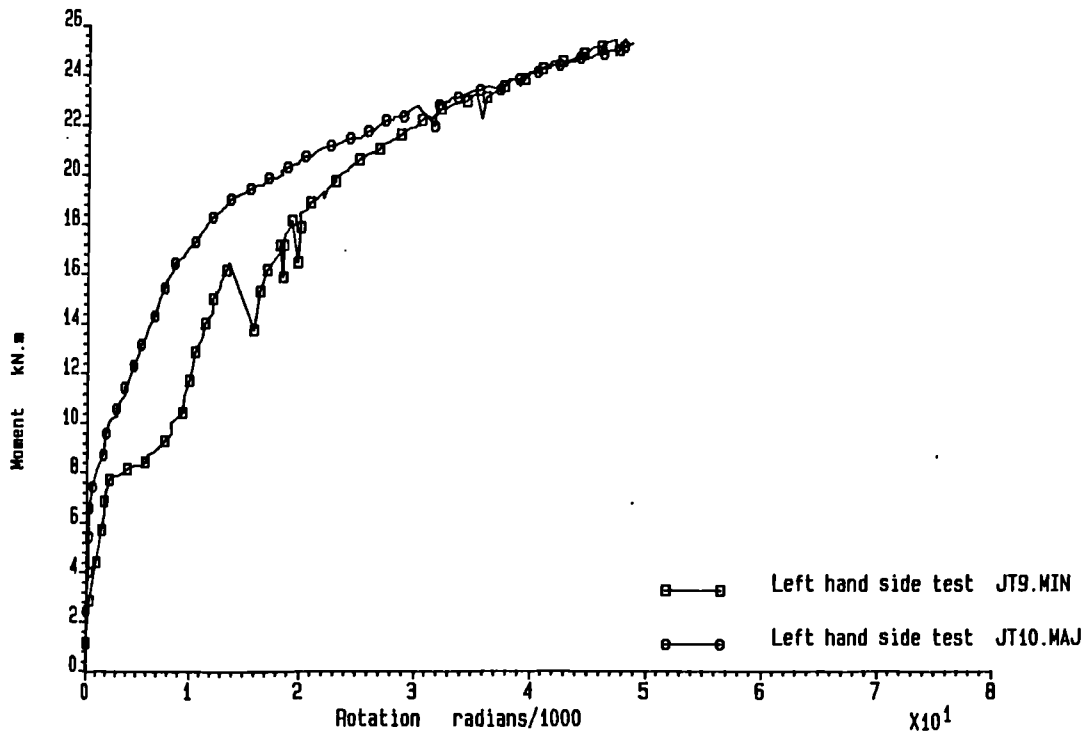


FIGURE 3.29 Comparison of $M-\phi$ curves for seat and web cleat connections to column web and column flanges

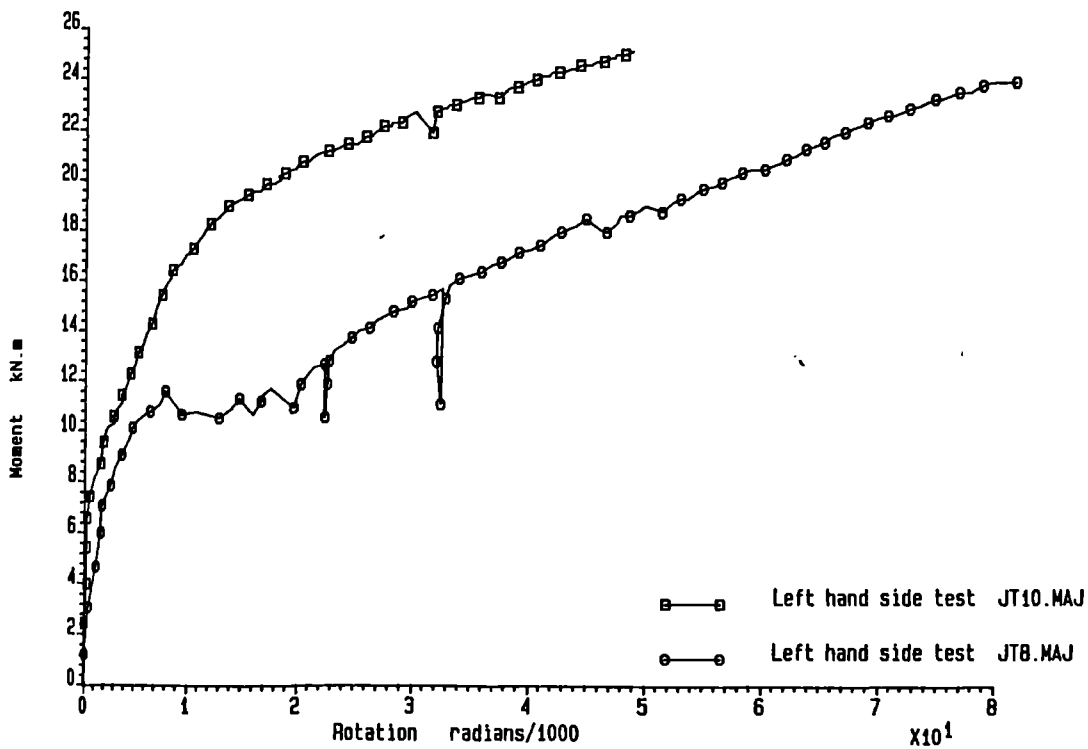


FIGURE 3.30 Comparison of $M-\phi$ curves for flange cleat and seat cleat with web cleat connections to column flanges

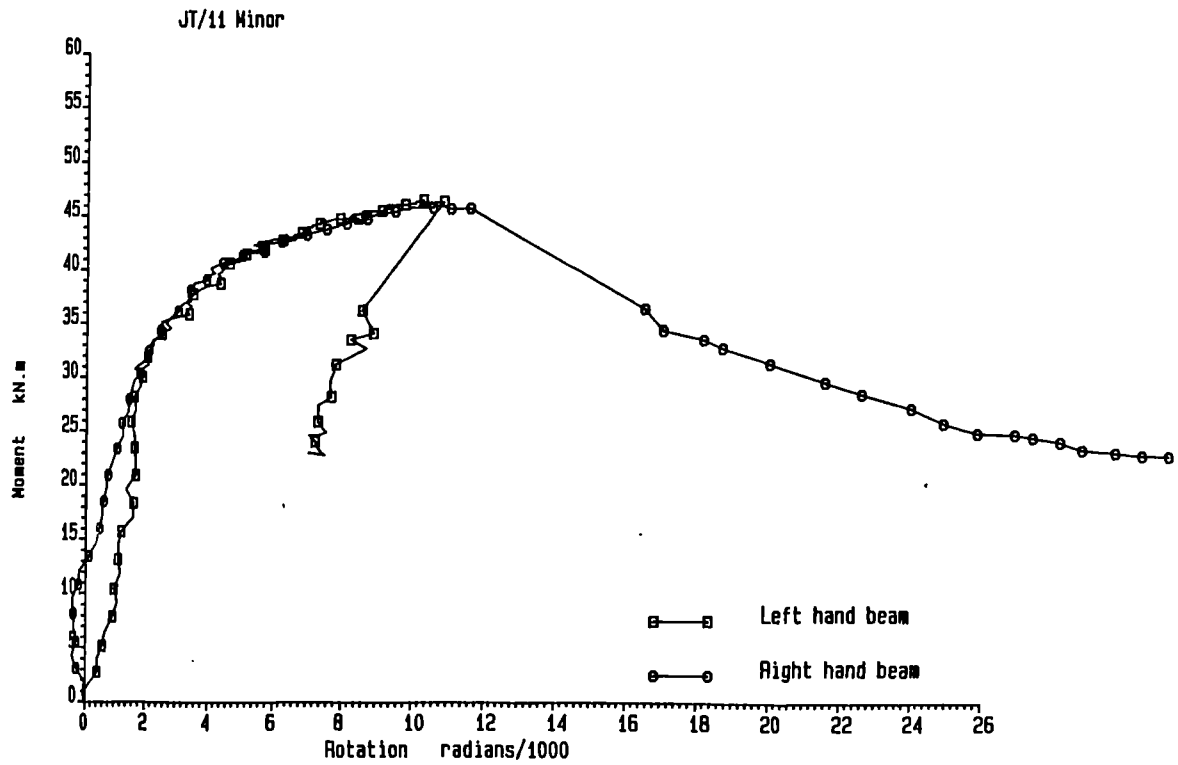


FIGURE 3.33 Experimental M- ϕ curve for flush end plate connection to column web (JT/11)

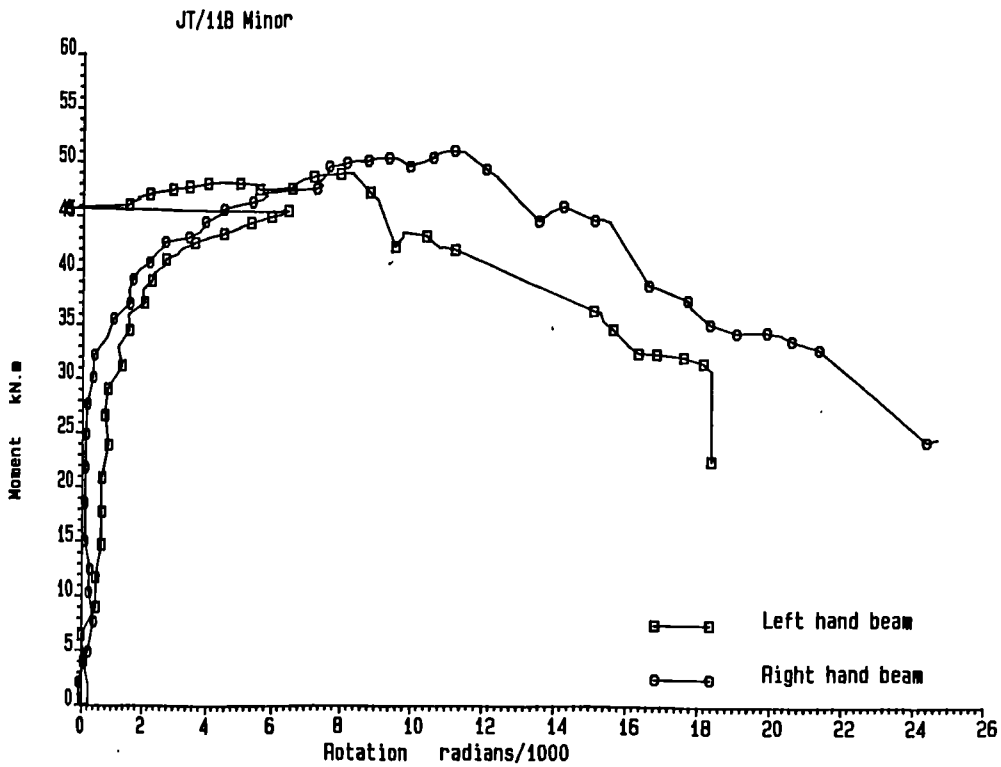


FIGURE 3.34 Experimental M- ϕ curve for flush end plate connection to column web (JT/11B)

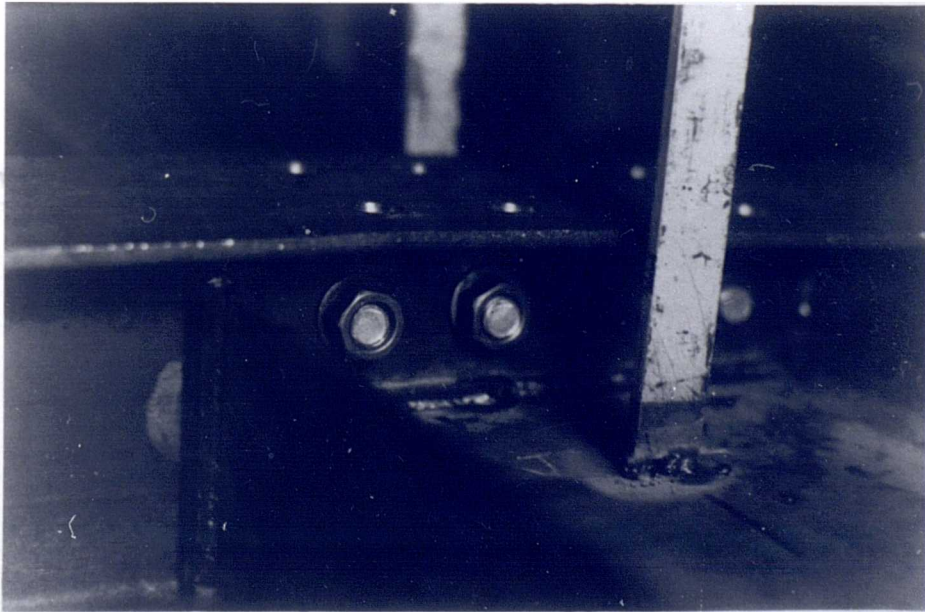
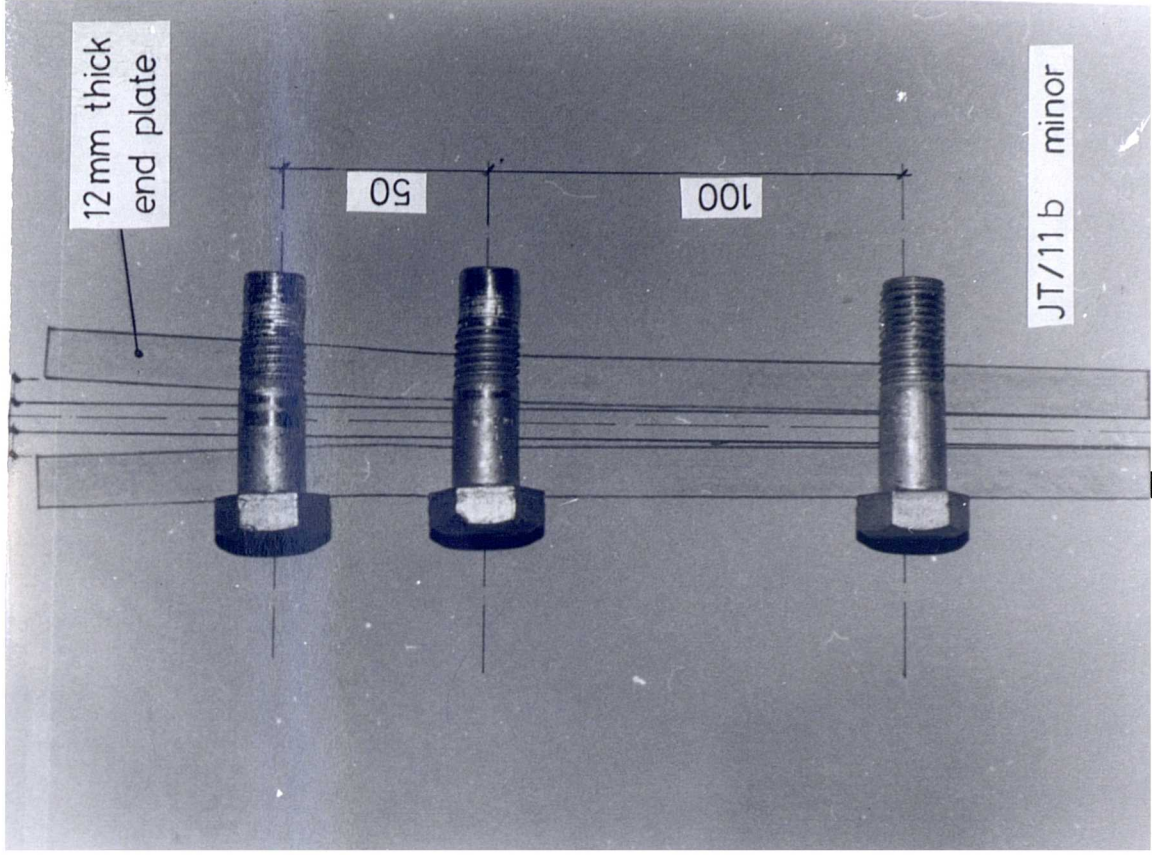


FIGURE 3.35 Test JT/11B - Failure of M16 grade 4.6 bolts

E 3.36 (right)

d b lts from test JT 11B

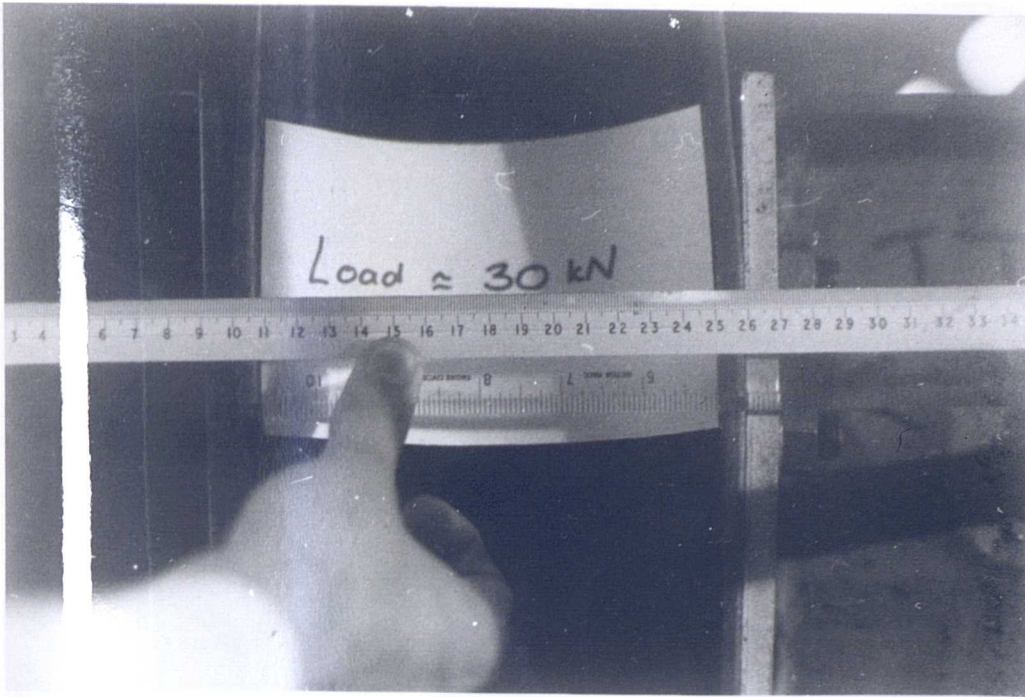


FIGURE 3.37 (above)

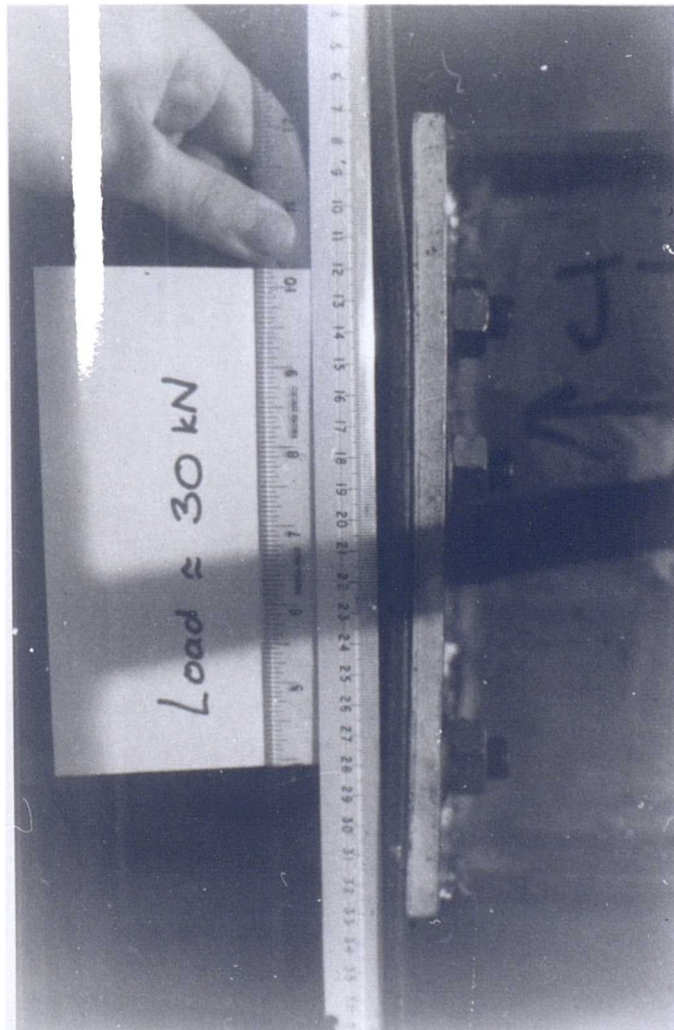


FIGURE 3.38 (left)

Deformation of column
flange produced by flush
end plate connection

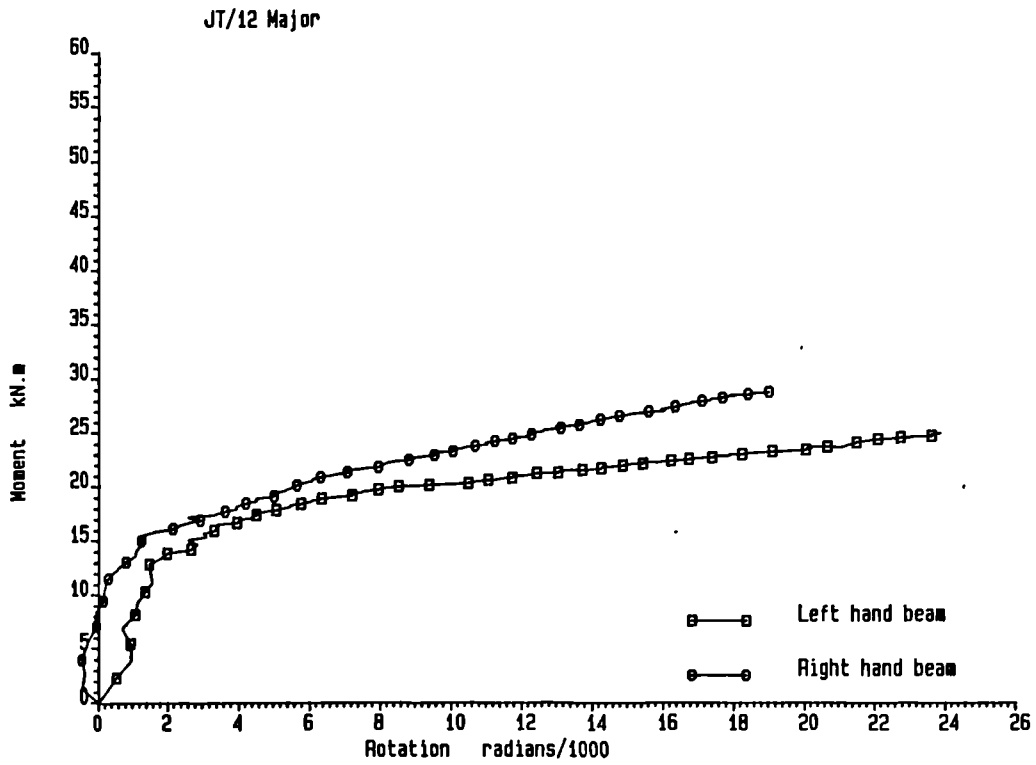


FIGURE 3.39 Experimental M- ϕ curve for flush end plate connection to unstiffened column flanges (JT/12)

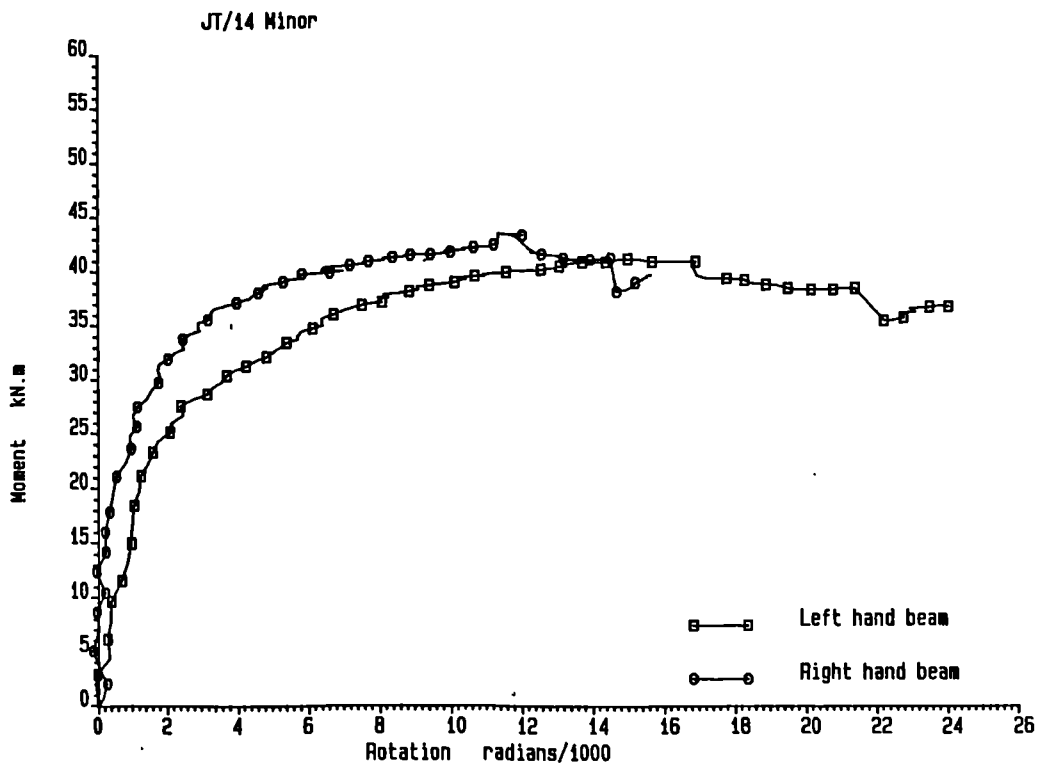


FIGURE 3.40 Experimental M- ϕ curve for header plate connection to JT/14

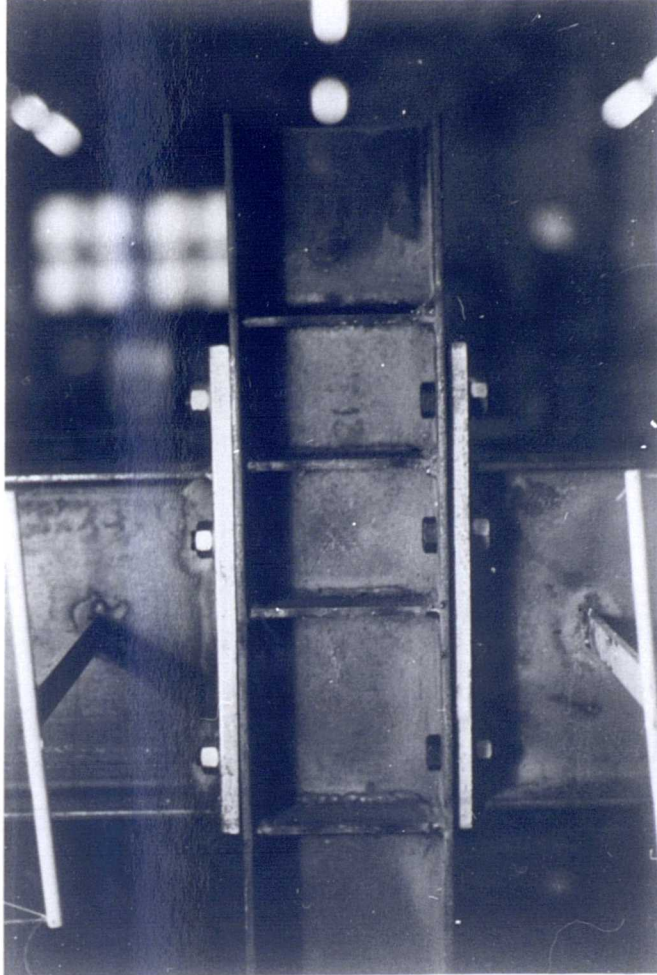


FIGURE 3.41 Extended end plate connection prior to testing

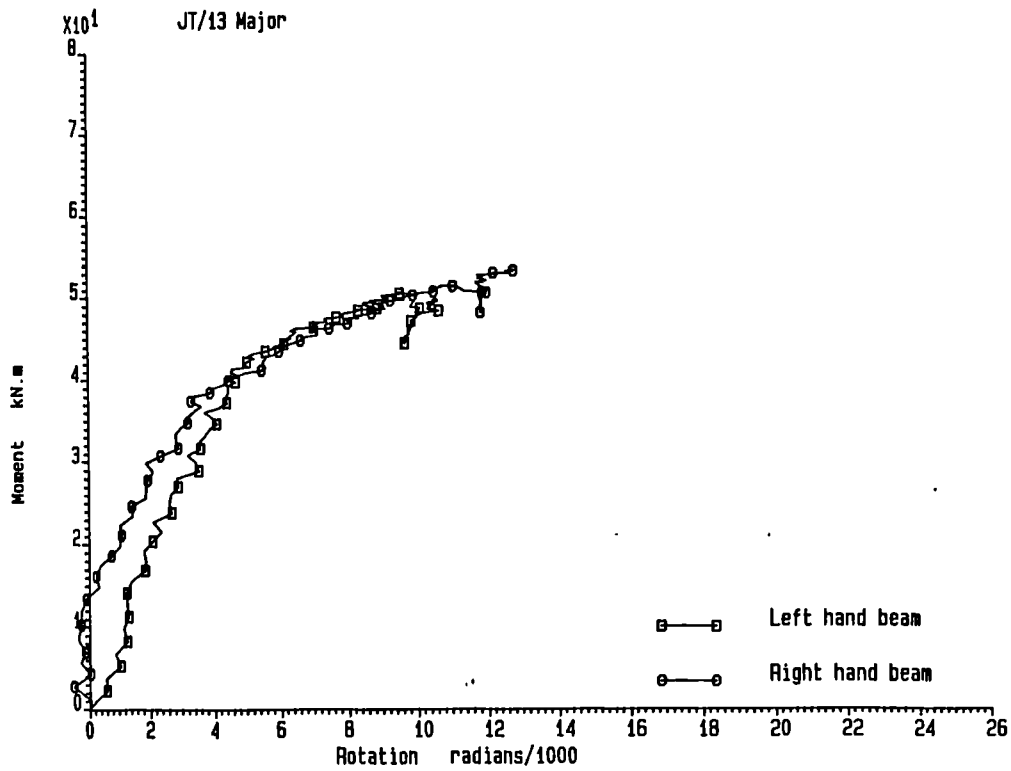


FIGURE 3.42 Experimental M- ϕ curve for extended end plate connection to stiffened column flanges (JT/13)

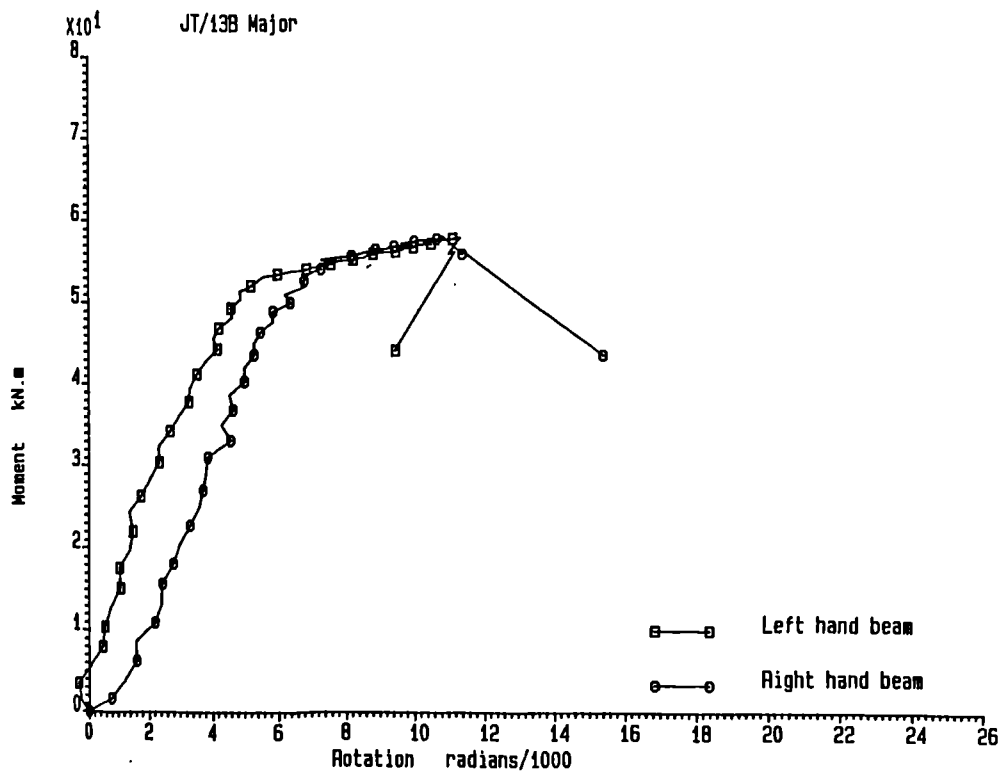


FIGURE 3.43 Experimental M- ϕ curve for extended end plate connection to stiffened column flanges (JT/13b)

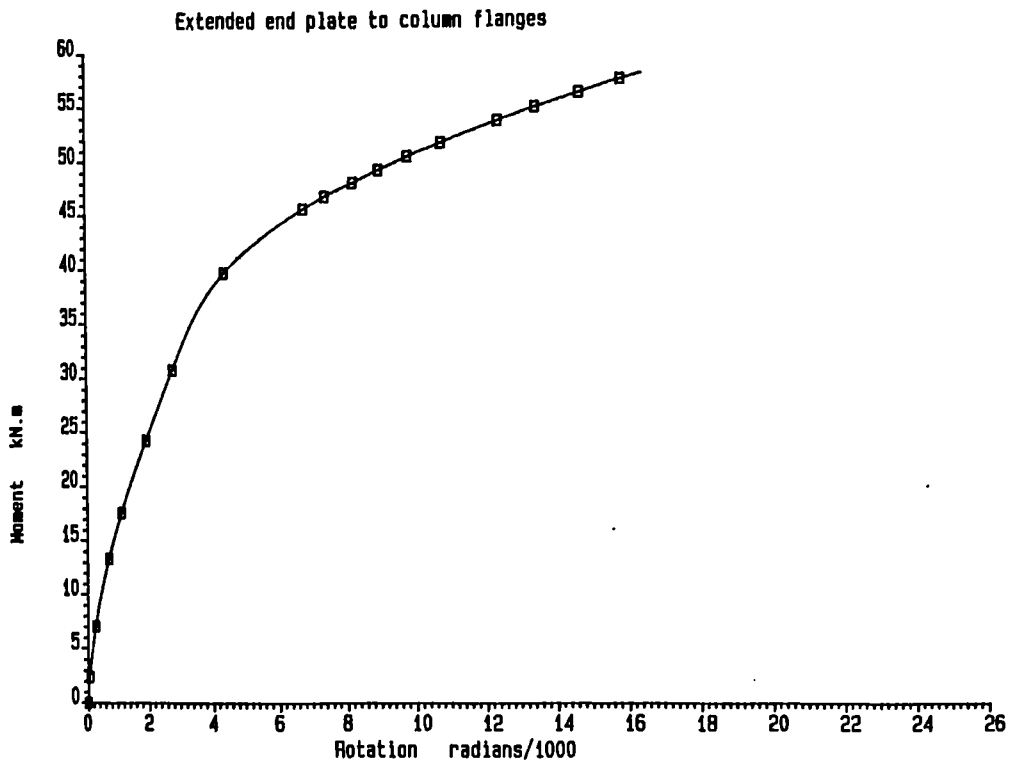


FIGURE 3.44 Typical M- ϕ curve for extended end plate connection to stiffened column flanges

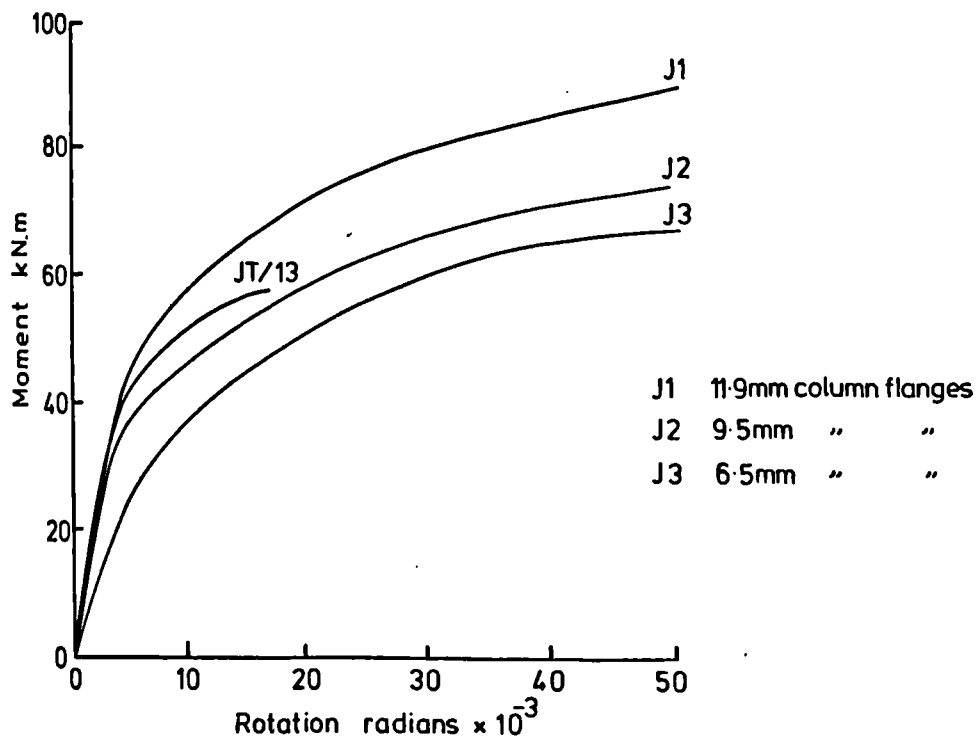


FIGURE 3.45 Comparison of extended end plate connection tests with similar connection tests by Packer and Morris

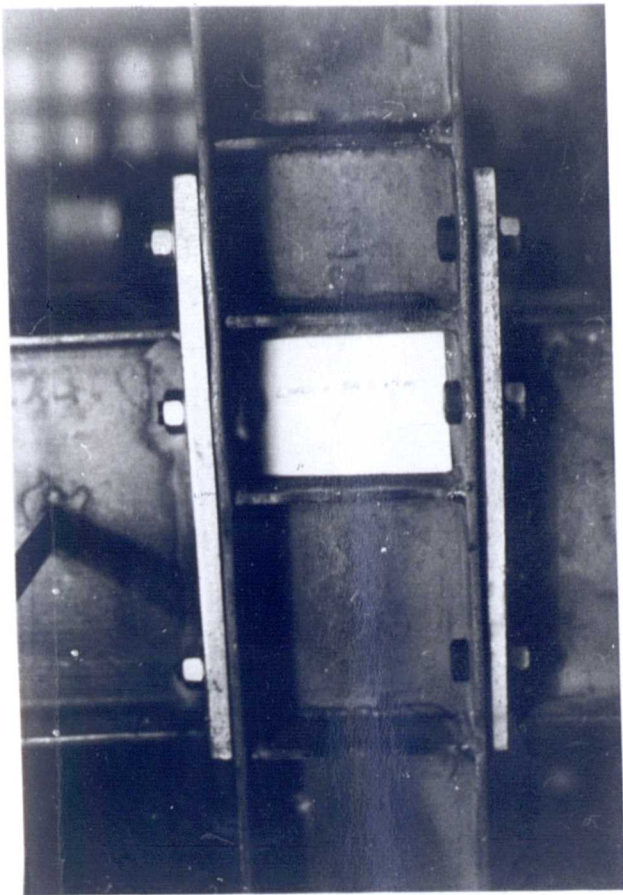


FIGURE 3.46

Deformation produced in extended end plates

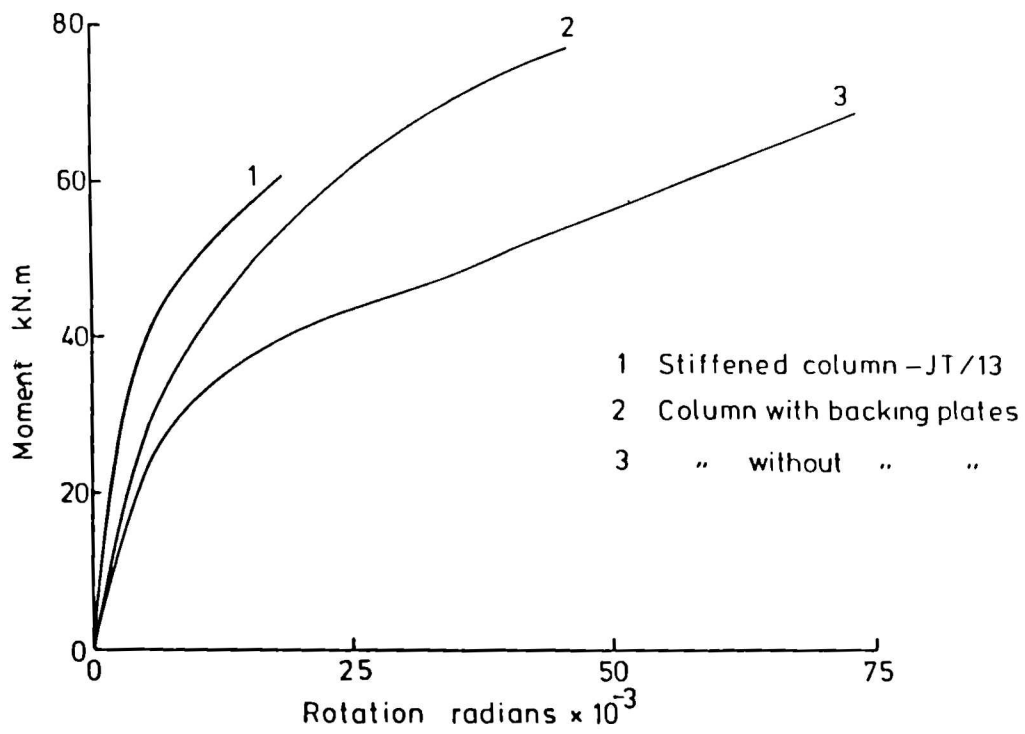


FIGURE 3.47 Comparison of extended end plate connection test with tests conducted at BRE incorporating backing plates

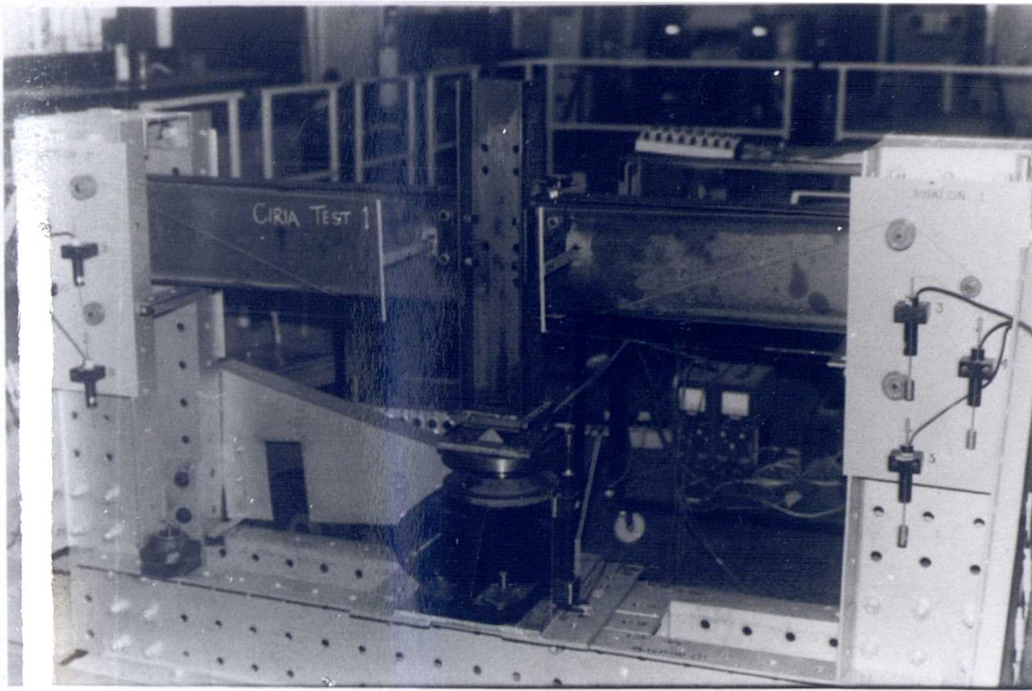


FIGURE 3.48 (above)

Web cleat lack of fit test
(CT/01)

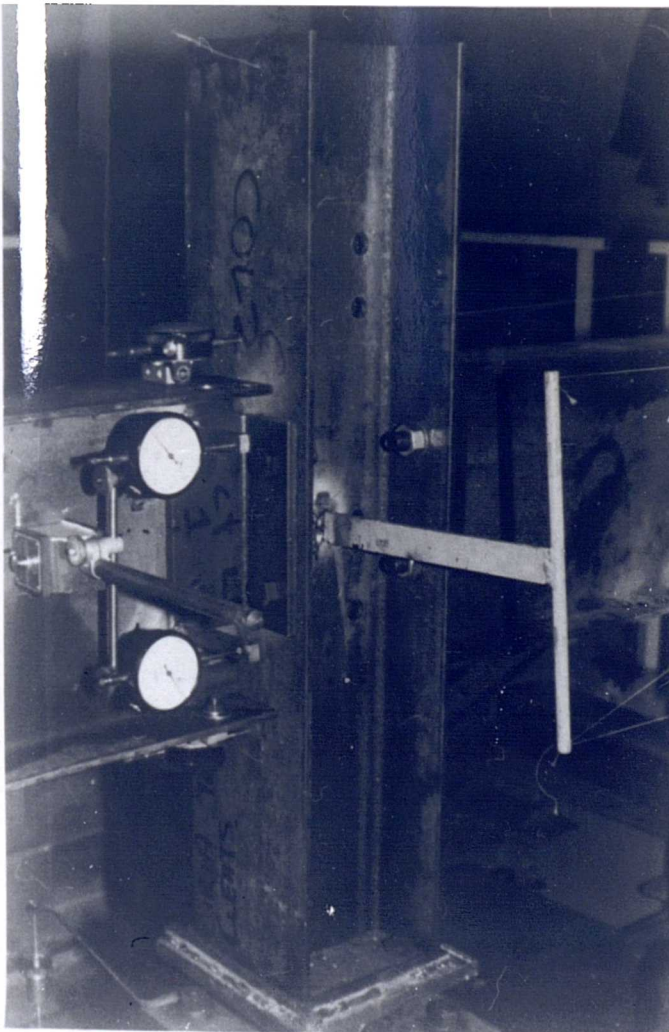


FIGURE 3.49 (left)

Additional instrumentation
on test CT/01

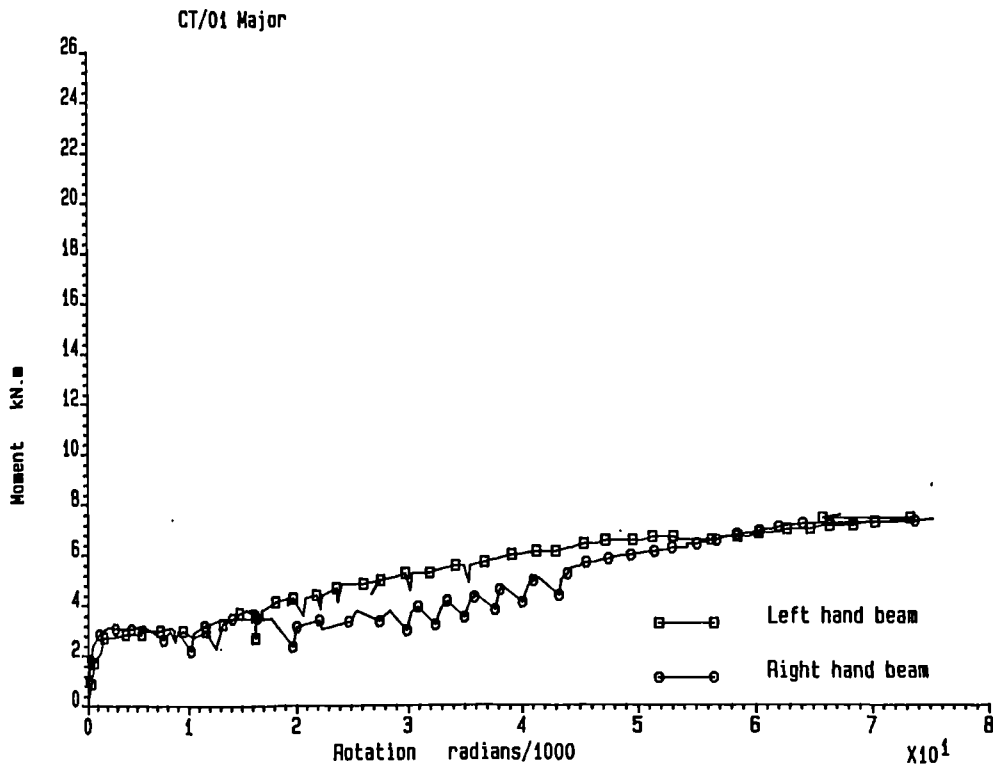


FIGURE 3.50 Experimental $M-\phi$ curve for web cleat connection with oversized holes through beam web (CT/01)

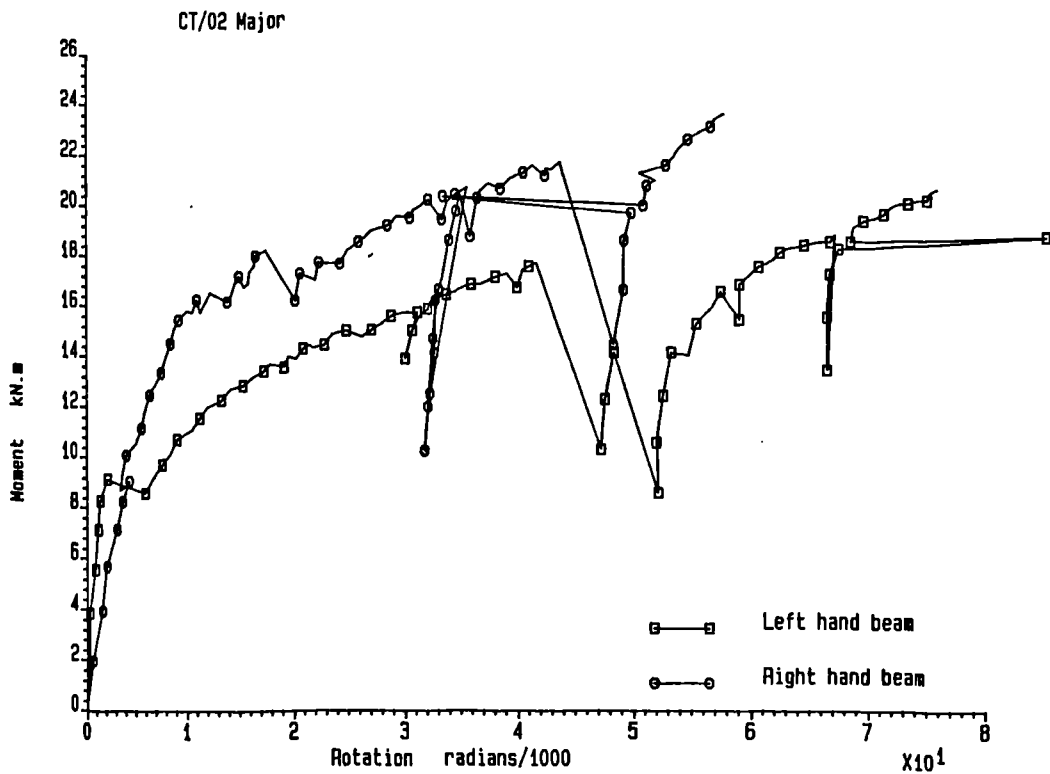


FIGURE 3.51 Experimental $M-\phi$ curve for flange cleat connection with holes in the beam flanges (CT/02)

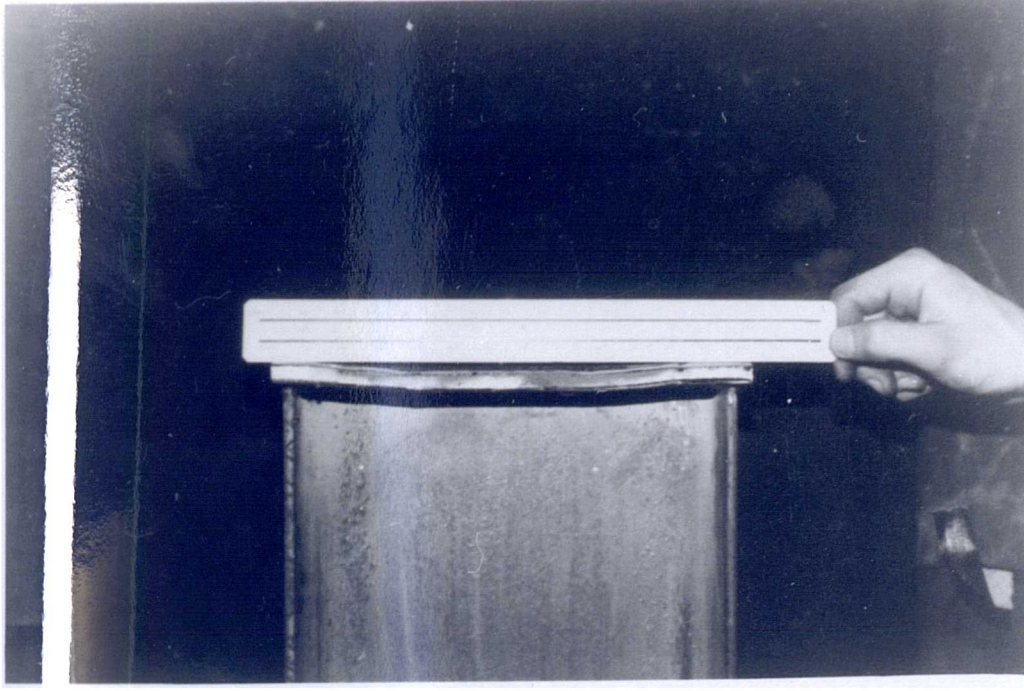
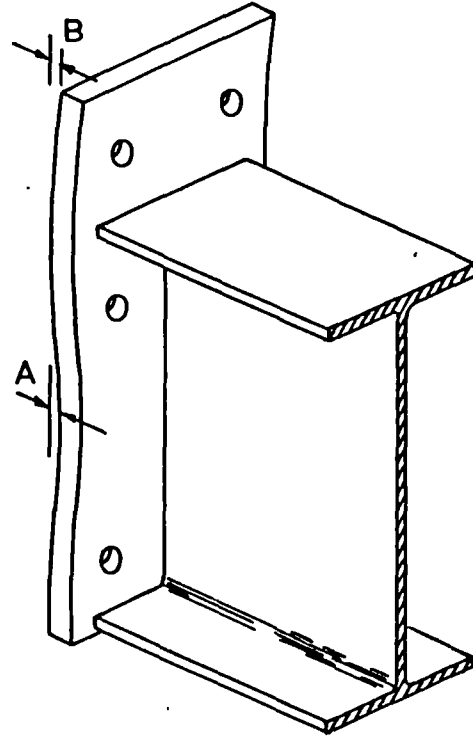
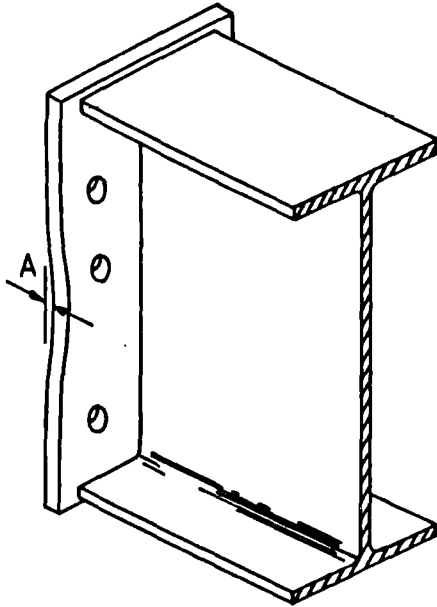


FIGURE 3.53 Deformed shape of deliberately distorted flush end plate (CT)



FIGURE 3.52 Test CT/02 in progress



TEST	A (mm)	B (mm)
CT/03	3	-
CT/04	2.5	5
CT/05	3	-
CT/06	2.5	5
CT/07	AS TEST CT/04	
CT/08	NOT DISTORTED	

FIGURE 3.54 Lack of fit introduced into end plates

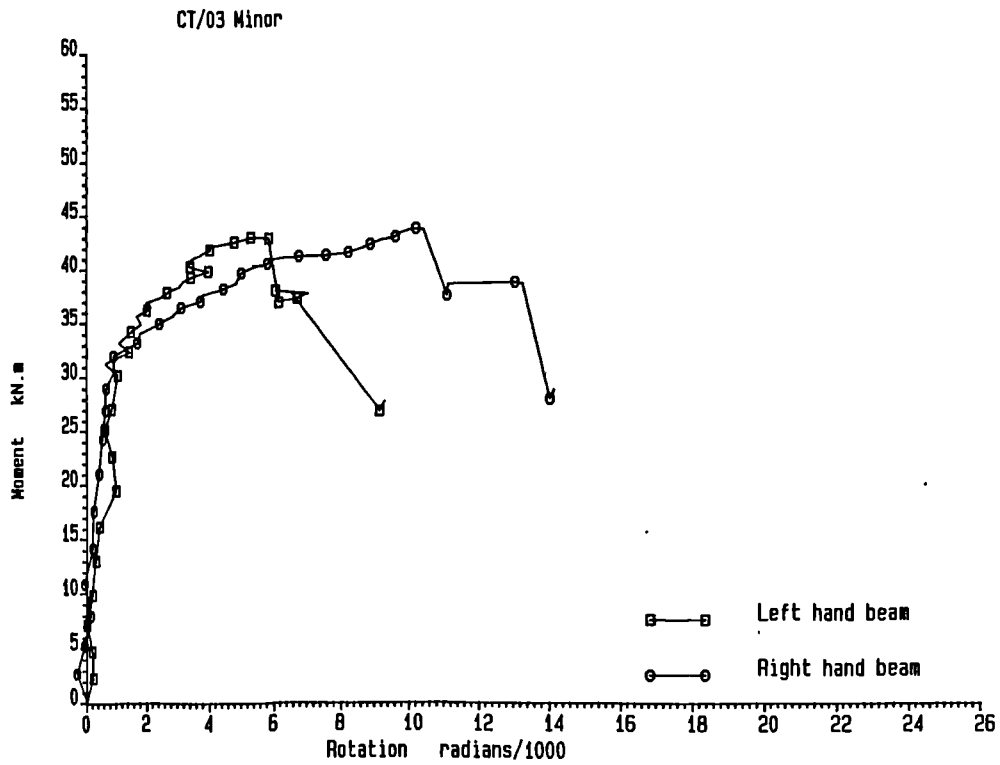


FIGURE 3.55 Experimental M- ϕ curve of distorted flush end plate connection (CT/03)

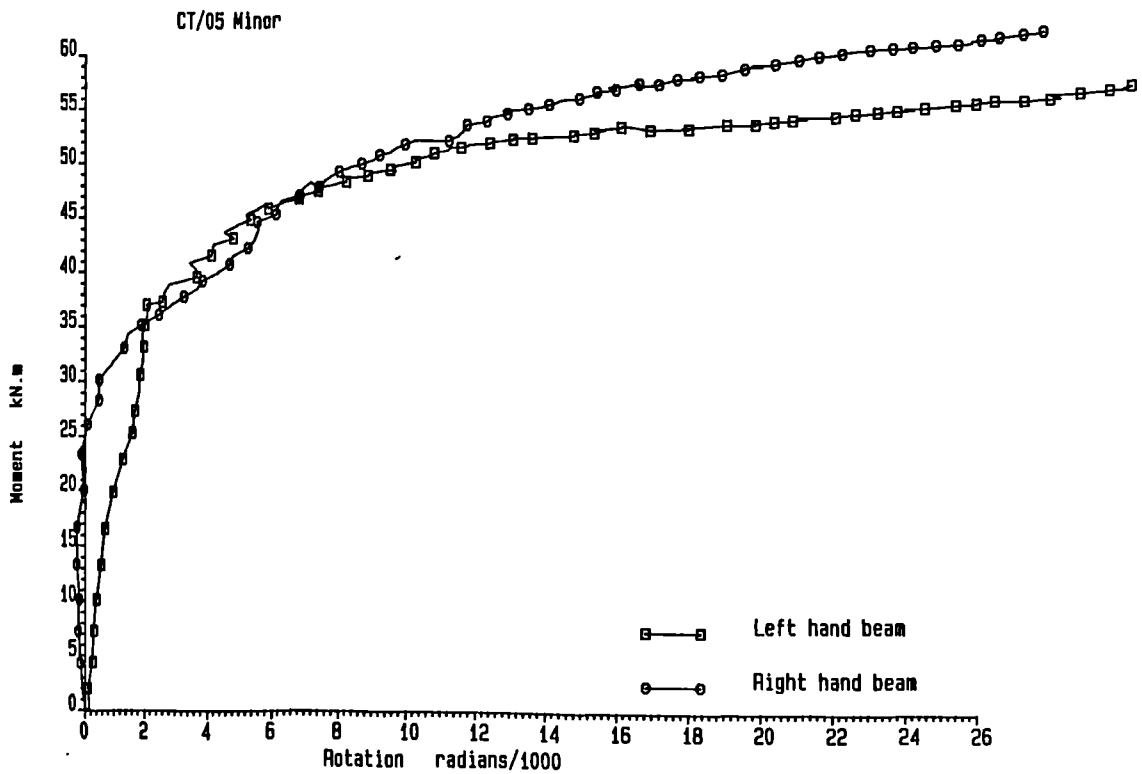


FIGURE 3.56 Experimental M- ϕ curve of distorted flush end plate connection with grade 8.8 bolts (CT/05)

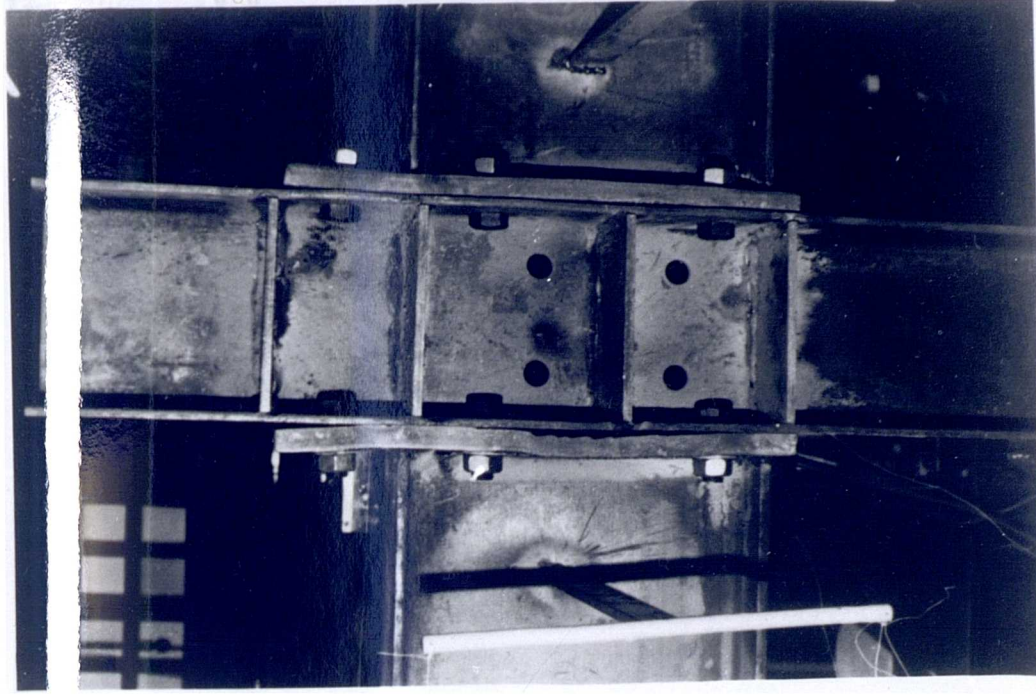


FIGURE 3.58 Deformation of column flanges produced by tightening grade 8.8 bolts (CT 04)

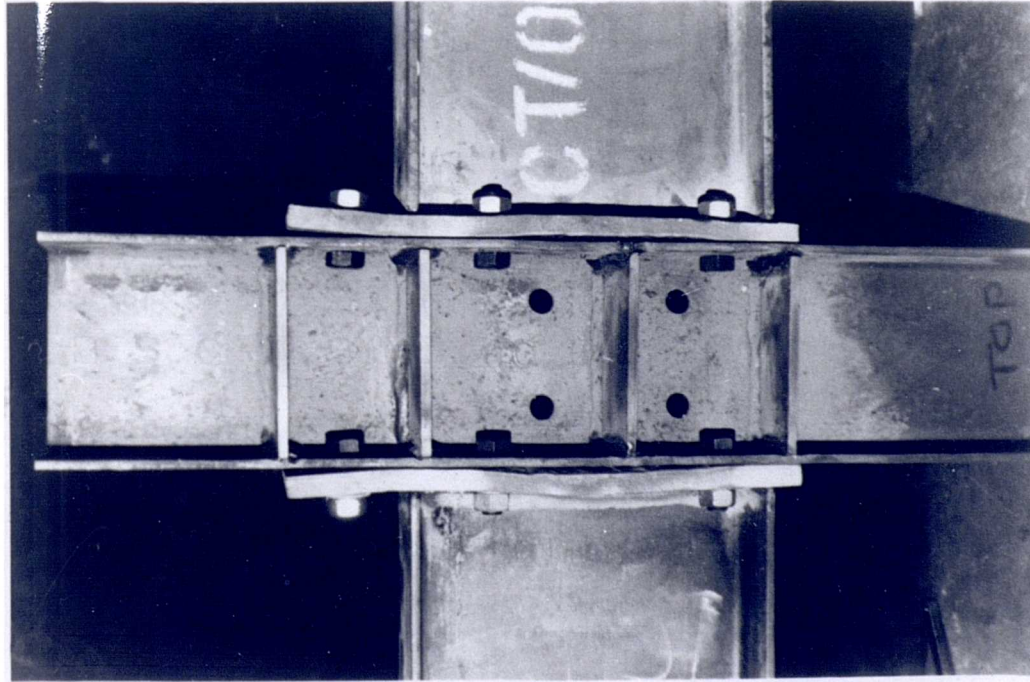


FIGURE 3.57 Extended end plate (CT/04)

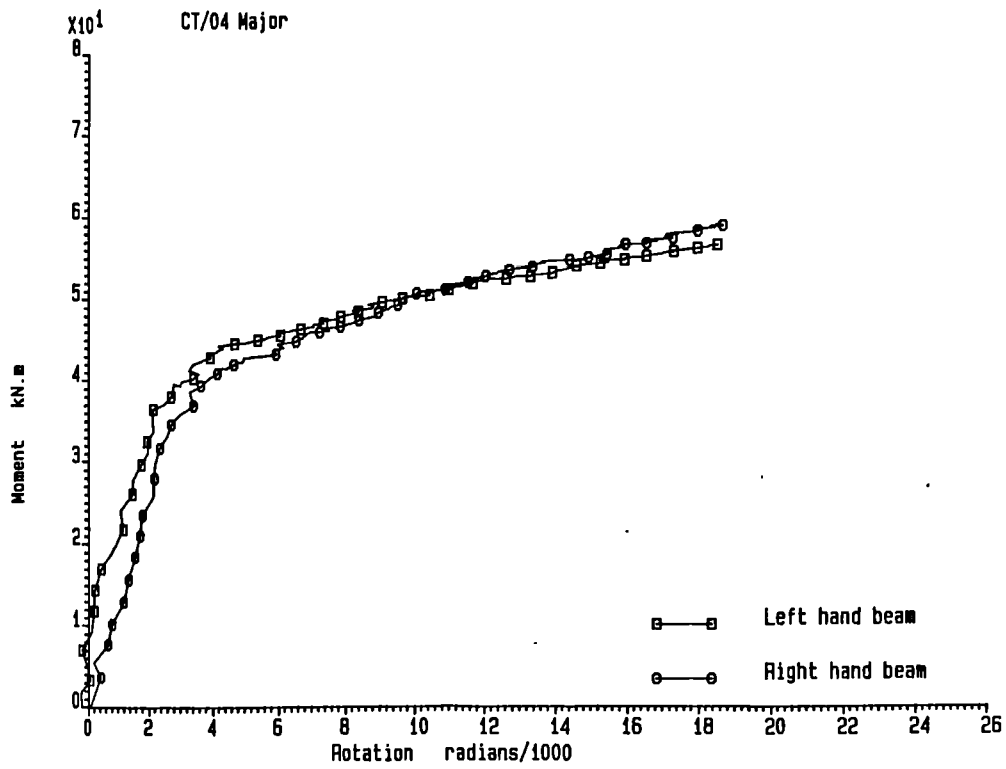


FIGURE 3.59 Experimental M- ϕ curve for extended end plate connection with deliberate lack of fit - grade 8.8 bolts (CT/04)

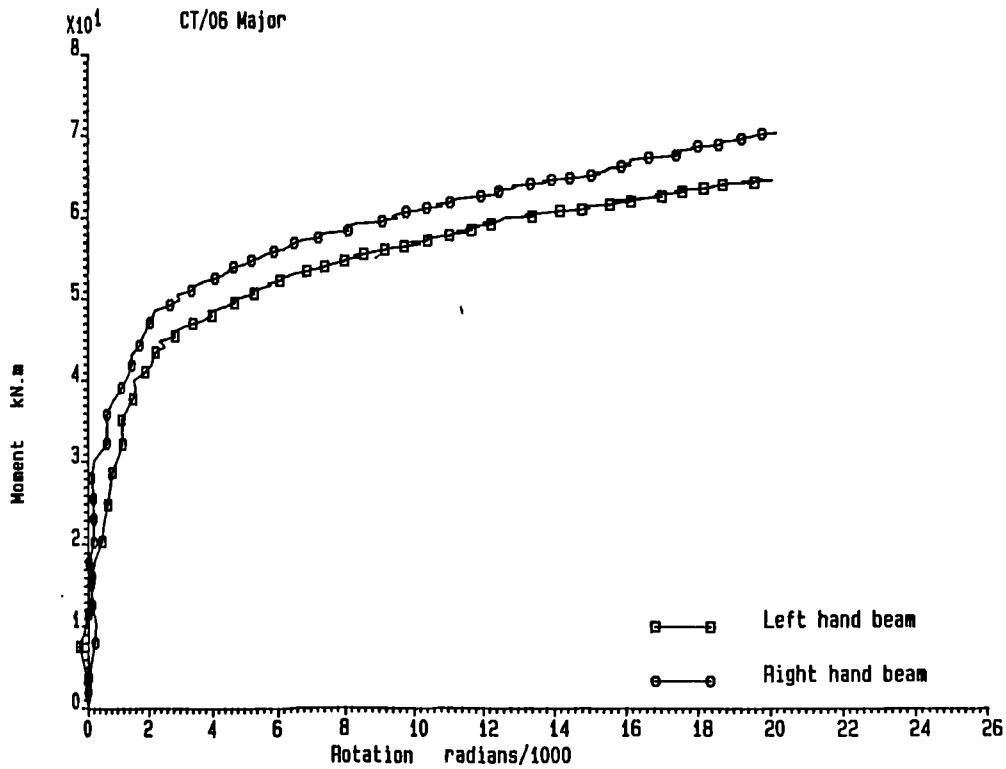


FIGURE 3.60 Experimental M- ϕ curve for distorted extended end plate connection with HSFG bolts (CT/06)

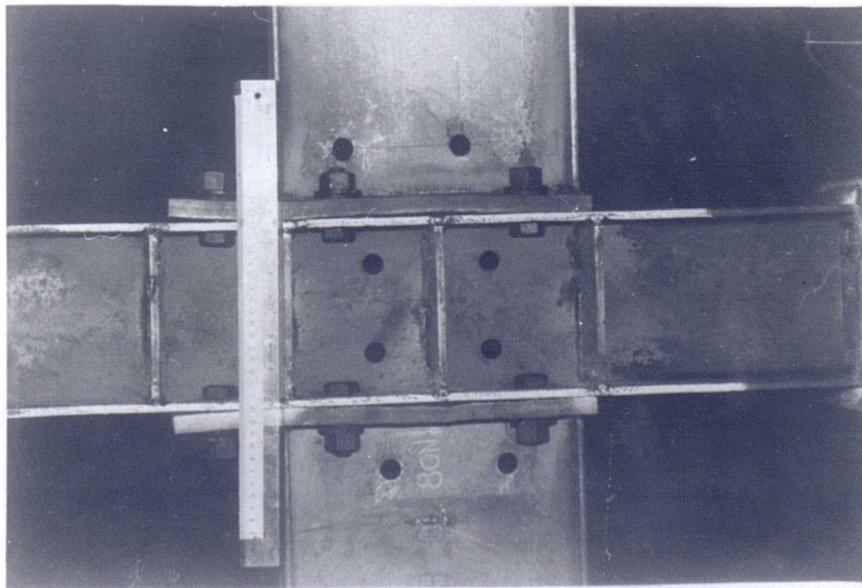


FIGURE 3.61 Distorted extended end plate test with HSFG bolts prior to pre-tensioning CT 6

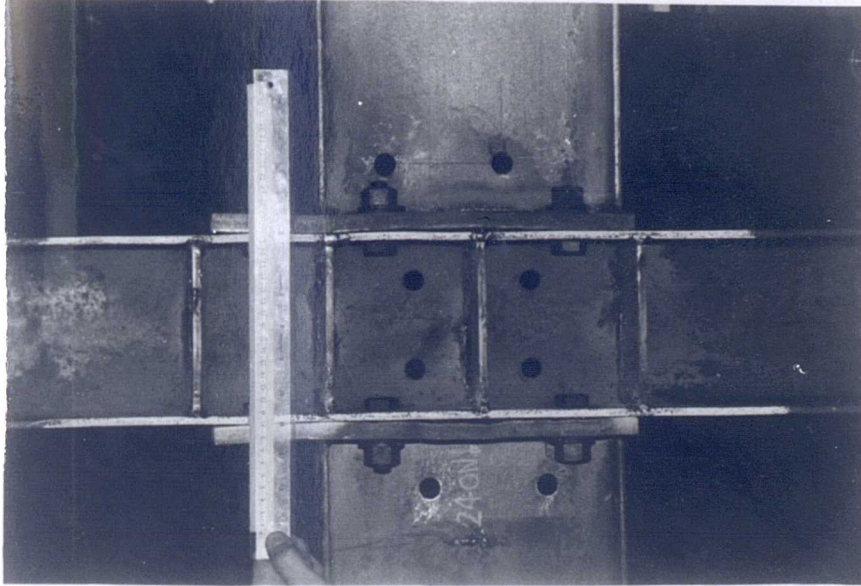


FIGURE 3.62 Distorted extended end connection with fully torqued HSFG bolts



FIGURE 3.63 Deformation of column flanges at end of test CT 06

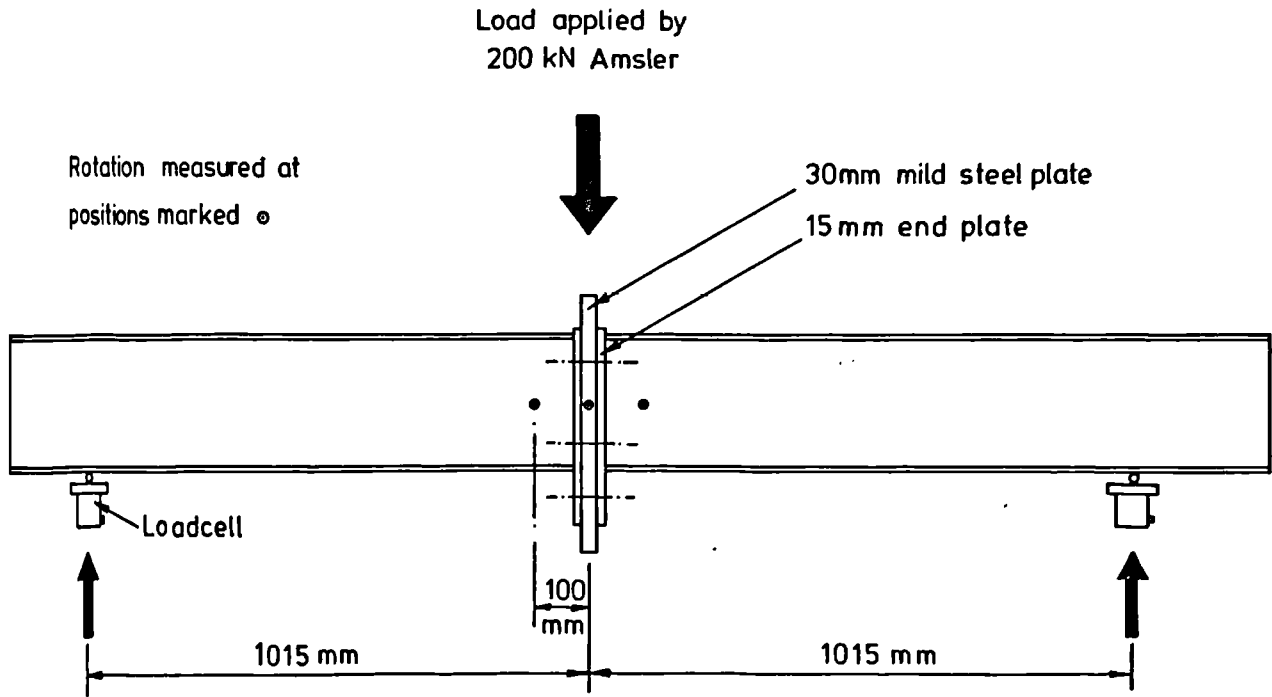


FIGURE 3.64 Test arrangement for tests CT/07 and CT/08

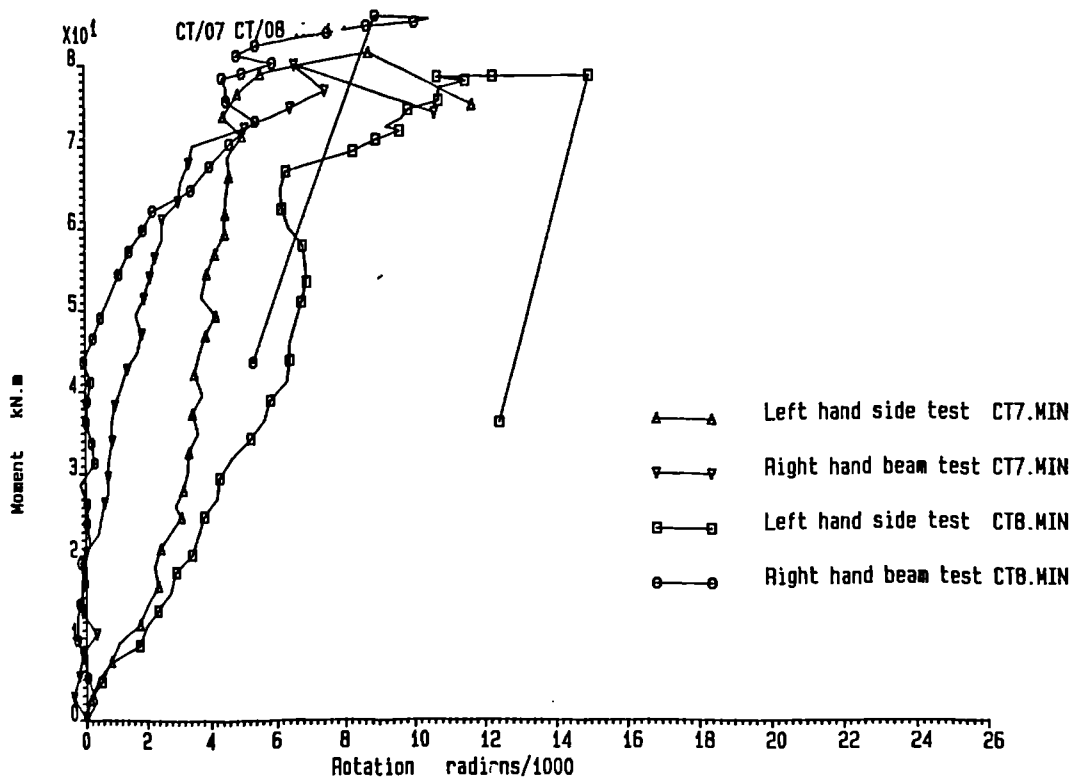


FIGURE 3.65 Experimental $M-\phi$ curves for extended end plates to the column web (CT/07 and CT/08)

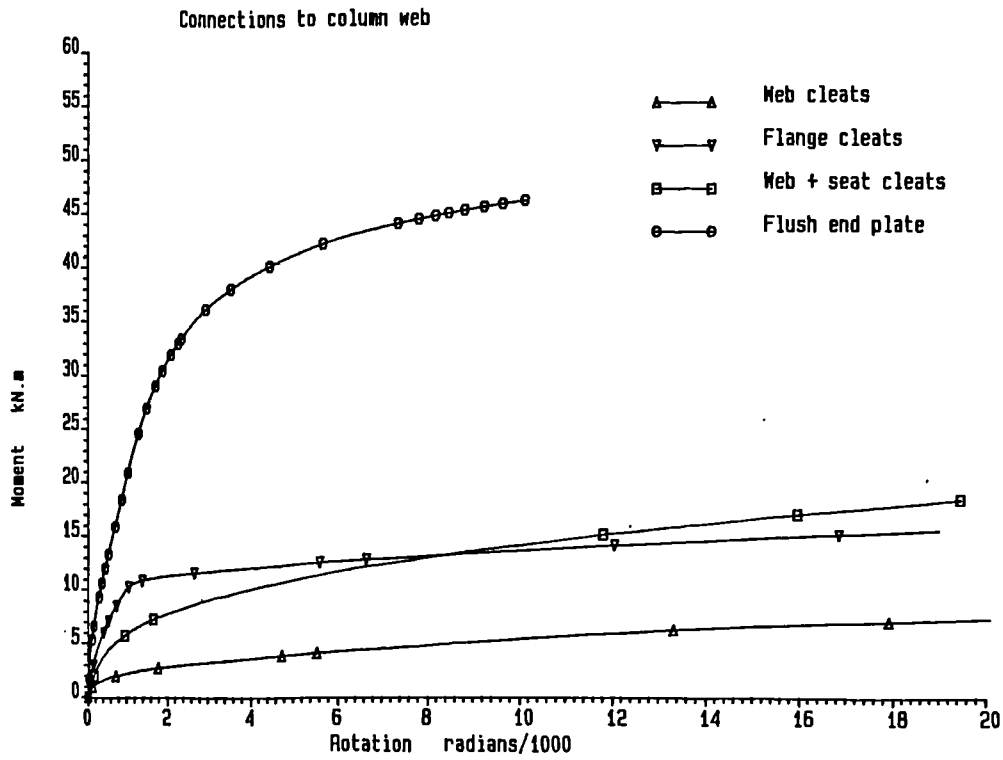


FIGURE 3.66 Typical $M-\phi$ curves for a range of connections to the column web

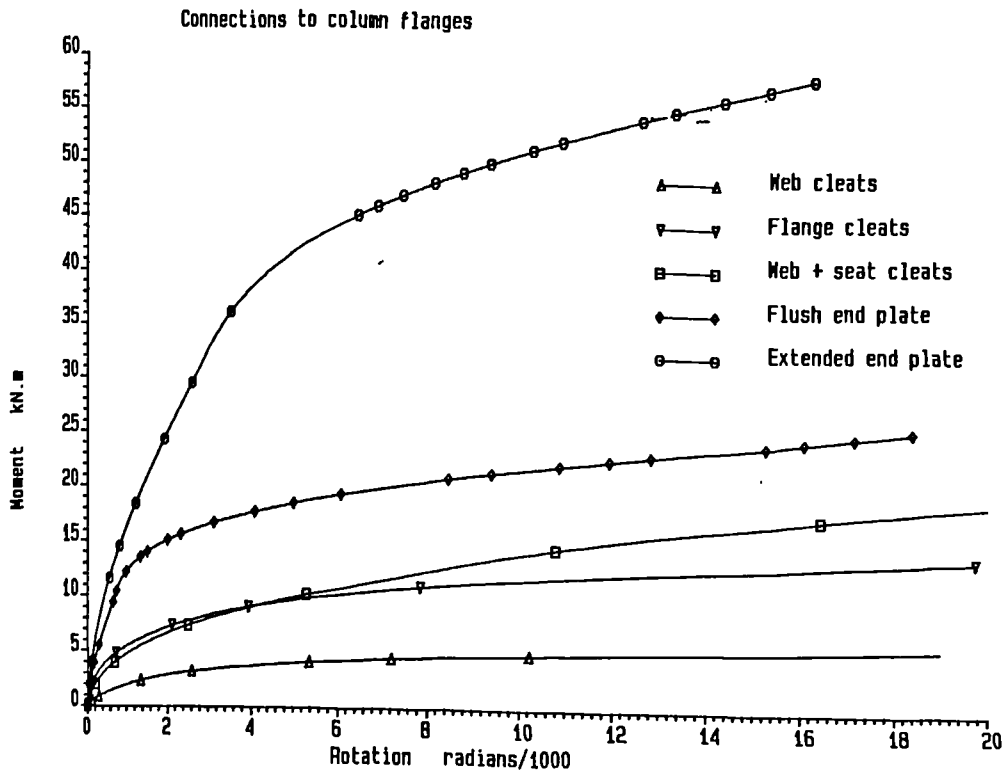


FIGURE 3.67 Typical $M-\phi$ curves for a range of connections to the column flanges

4.0 SUBASSEMBLAGE TESTS

4.1 Introduction

Chapter 1 of this report detailed the need for a series of tests to be conducted on columns restrained by a variety of bolted beam to column connections. The aim of the study was to provide firstly a limited number of experimental results to demonstrate the behaviour of columns in semi-rigid frames, secondly a series of checks against which an analysis program could be verified and finally test histories against which other theoretical approaches could be checked. In addition the subassemblage tests were to be used to assist in the evaluation of the results of the frame tests (which are discussed in the following chapter).

An I shaped subassemblage was selected as the most appropriate for investigation. A total of nine subassemblages and two 'pin-ended' columns were tested.

4.2 Test Apparatus and Instrumentation

'I' shaped subassemblages shown diagrammatically in figure 4.1 were tested in the horizontal position in the purpose built rig shown in figures 4.2 and 4.3. The self restraining rig was constructed from 305 × 102 RSC sections and securely bolted to a strong floor. Physical constraints and limits on loading capacity necessitated the adoption of a rather extreme test specimen shape which had a column 6.5m long and very short beams. In order to reduce the influence of the shortness of the beams special restraints were devised for the ends of the beams remote from the column. These restraints, shown in figures 4.4 and 4.5, permitted the beam to deflect freely along an axis parallel to the longitudinal axis of the column but prevented in-plane rotation. In this way the short beam

simulated a beam which was twice as long. A further advantage was that all load introduced to the subassemblage had to pass through the column and could not escape into the rig as might have been the case if a simpler beam end restraint i.e. full fixity, had been adopted. Out of plane action was prevented by restraints at three positions along the column length.

Load to the column was applied through a screw jack nominally rated at 500 kN. Load could also be applied through the beams at the head of the column using two hydraulic jacks driven by a single automatic pump. Four load cells were used to monitor the three applied loads and the reaction at the foot of the column.

Bending moments at 11 positions around the subassemblage were measured using groups of 10×3 mm foil strain gauges. The locations of the strain gauges are shown in figure 4.6 and table 4.1. Bending moments in the beams were measured directly by wiring four gauges into a full bridge circuit; secondary bending effects were cancelled. At the head and foot of the column a half bridge circuit was used to permit measurement of both the in-plane bending moment and the axial load in the column, and at the column centre four gauges were wired singly into separate bridges so that the state of axial load and in-plane and out-of-plane bending moments could be recorded. Deflections of the column were measured near to the restraint positions by 250mm travel linear voltage displacement transducers. Rotations of the column at its intersection with the upper and lower pairs of beams were measured by a system of three LVDT's. The method used was the same as that used in the joint tests and described in chapter 3.

Relative rotations of the beams to the column were calculated from the readings of two transducers mounted at the ends of a bar which in turn was held in place on the beam centreline by a magnetic base.

All the instrumentation was read by an automatic data logging system driven by a microcomputer. The equipment required three analogue to digital converters to handle the 40 channels of information. Data was stored on a floppy disk and later transferred to a PRIME computer for interpretation.

4.3 Test Procedure

All the test specimens were fabricated by the same technician using the facilities available in the department, except for the welding of the end plates in tests ST9 and 10 which was done by an experienced welder. After fabrication the cross section of each component was carefully measured. Strain gauging and the associated wiring was completed before the frame was assembled. The column was lightly nipped into position with the screw jack and the beam members were then carefully aligned before tightening up the connection bolts. A torque of 160 N.m was applied to all the bolts in order to achieve consistency both from test to test and also to ensure comparability with the previous joint test series. Transducers were then mounted around the test frame and the 'T' bars used in measuring the column rotation welded on. Checks were made on all the instrumentation and the strain gauges balanced, before application of any loads.

The data logging system was capable of displaying a plot of two channels as the test proceeded and could also give an instant readout of any single channel. To assist in the control of the test a

display of central deflection against the load recorded at the bottom of the column was utilised and the load applied by the screw jack was monitored continuously. The monitoring system permitted the following test procedure to be implemented.

The screw jack was backed off until the cap for the load cell could be moved slightly, indicating that no load was applied. A few scans of all channels were then taken to establish a zero condition. Load was then applied to the column by the screw jack until a value of 25 kN was displayed on the monitor. A few scans were taken during this stage. Next an increment of load was applied to the beams by hydraulic jacks fed from an automatic pump. Pump pressure was increased by use of a pressure release valve which gave reasonable control. The application of the hydraulic loads caused a slight drop in the load applied by the screw jack. The loading in this jack was increased until the monitor again showed 25 kN. At this point a scan of all the channels was recorded before incrementing the beam loads and repeating the procedure. Once the desired level of load had been applied the screw jack was used to gradually increase the load in the column to failure. The loads on the beams remained constant due to the hydraulic loading. Scans were taken at regular timed intervals. The trace on the monitor enabled the operators to detect the onset of failure and adjust the speed of the jack and the frequency of taking readings accordingly.

The above test procedure was typical however and some test variations were necessary. In the next section the tests conducted are reported and the method of testing for each discussed in detail.

4.4 Summary of Tests Conducted

All of the tests conducted used 152x152x23 serial size universal column sections and 254x102x22 universal beam sections in grade 43A steel. Table 4.2 summarises the tests conducted. The table contains a reference for the column and beam sections used in each test and the dimensions and material properties of each are given in Appendix C. From the residual stress patterns measured (see Appendix C), the marks in the mill scale and the initial straightness of all the columns (generally less than 2mm in 6500mm, L/3250) it appeared that all the columns used had been cold straightened.

In the design of columns the role played by simple connections, those designed to operate in shear, in restraining the column is either ignored or estimated by the selection of an effective length. Attention was therefore focused upon connections designed to carry shear loads, but which are known to possess some rotational stiffness and moment capacity, as these are of greatest interest in the context of multistorey steel construction. However, two tests incorporating end plate connections were also included to widen the range of results.

In the following subsections the tests will be discussed in detail. The test series was numbered in order of ascending connection stiffness (ie ST1 had no beams, ST10 incorporated extended end plates) but it is more appropriate to deal with the tests in chronological order as the test procedure was to some extent evolutionary.

4.4.1 Details of Test ST5

Preliminary tests were conducted on a column restrained by beams connected to the column flanges by top and seat cleats. The results

of these tests, which were conducted to check the loading arrangement and adequacy of the test rig, are not reported. A revision of the screw jack motor gearing was found to be necessary and the need for the addition of two tension members to tie the reactive abutments together was highlighted by these preliminary tests.

The first test to be conducted was ST5 which had top and seat cleat connections between the beam and column and was tested about its major axis. Minor axis buckling was prevented by 25mm diameter bars fastened above and below the column at three locations -see figure 4.7. Prior to assembling the test specimen in the rig the column had an initial bow at its centre of 0.5mm ($L/13000$). Loads were applied to the beams by hydraulic jacks, supplied by the same pump, at distances of 266 and 268 mm from the face of the column. The beam loads were applied in increments up to a maximum of around 125kN per beam. This level of load caused considerable local deformation of the column flanges (as figure 4.8 clearly shows). Having loaded the beams, axial load was then introduced to the column through the screw jack. Despite the slight eccentricity of load in the beams and the initial curvature the column failed by deflecting in the opposite direction at a peak load about 610kN. On completion of the test the column was examined and it was noted that failure had occurred by biaxial buckling of the length between the screw jack and first lateral restraint position. After carefully considering the test it was realised that the introduction of the beam loads had moved the column away from the screw jack, which located the column head, and had allowed the column to deflect vertically under its self-weight and the weight of the beams. Thus, when the axial load was applied by the screw jack, it was no

longer acting axially in the vertical plane and introduced a significant minor axis moment into the column. The results for this test are therefore not useful and not reported.

4.4.2 Details of Test ST6

In this second test flange cleats were again used to join the beams and column but the connections were made to the column web and the behaviour of the column bent about its minor axis investigated. The column had no measurable out-of-straightness. Experience from test ST5 suggested that it would be better to put some load into the column via the screw jack and locate it before applying loads to the beam. A load of 50kN was applied to the column in a series of increments and then the screw jack was stopped. Loads were then applied to the beams at equal distances from the face of the column web in several increments up to a maximum of approximately 40kN per beam. On completion of the beam loading phase the screw jack was switched on and the column loaded to failure with readings taken at regular intervals. A maximum load of 520kN was recorded. Figure 4.9 shows the plot of total load in the column against deflection measured by the transducer approximately at the column's midheight.

Readings of the load recorded by the loadcell at the head of the column showed that the application of the beam loads had reduced the preload in the column from 50kN to a minimum of 5kN. Although this did not present a problem in this test it was thought desirable to try to maintain a constant preload in the column and a slightly different loading sequence was devised for test ST7.

4.4.3 Details of Test ST7

ST7 was a minor axis test with flange cleat connections, as ST6, but load was applied to the righthand beam only at a distance of 325mm

from the column web. The column was initially straight. In this test the procedure described in section 4.3 was adopted. Briefly this entailed the application of a 25kN axial load into the column via the screw jack which was maintained by frequent adjustment as load was added to the beam in small increments up to a maximum of 42kN. The axial load in the column was then increased to cause failure. Figure 4.10 shows the total axial load against deflection trace for the test which followed the unloading of the column in the post buckling region. The stepped nature of the plot suggested that there was some friction in the apparatus. *It was most likely that the problem was due to the lateral restraints and these were modified for the subsequent tests.*

4.4.4 Details of Test ST3

Test ST3 was the first test in which improved lateral restraints were used. These are shown in figures 4.11 and 4.12. At the central position a pair of 80x60x6 RSA angles were positioned above and below the column. A mild steel plate was fastened to the underside of the top angle and the top of the lower angle to act as a wearing plate. Shoes made from 30 × 10mm mild steel plate were placed on the column at the restrained position. To allow for the shortening of the column the wearing plate was made larger than the shoe. The surface of the shoe was coated with grease to reduce friction. At the two remaining restraint positions 40 × 40mm mild steel bars were used; these were polished on the wearing side. Shoes similar to those at the central position were again used. Before the test was conducted each restraint position was checked to ensure that the shoes could move smoothly on the restraints.

The column had an initial bow of 2mm about its minor axis. Beams were fixed to the column web with double web cleats. Loads were applied to each beam at distances of 330 and 340mm from the column web, for the left and right hand beams respectively. This slight eccentricity of loading was introduced to capitalise on the initial bow at the centre of the column. The now standard procedure of introducing a small, constant axial load into the column before applying beam loads was again used. Failure of the column was caused by increasing the axial load to 435kN, which combined with the 41 and 44 kN beam loads gave a total axial load of 520kN. The load-deflection plot for this test is shown in Figure 4.13. The smooth nature of the curve suggests that the new restraints were performing satisfactorily.

4.4.5 Details of Test ST2

Test ST2 featured web cleat connections between the beams and column flanges. In order to fail the column about its major axis a load of 45kN was applied to the right-hand beam only to add to the effect of a 2.25mm initial bow in the column. The screw jack was run up to 623kN without failure of the column. On the monitor an almost linear trace was produced up to this point. Since the screw jack load was considerably in excess of its rating (500kN) it was decided that the beam load should be increased. In several increments the beam load was increased from 45kN to 110kN; the screw jack load decreased during this phase of the test. Next the screw jack was switched back on and the test run to failure.

Figure 4.14 shows the total load against deflection plot for the test.

An examination of the loadcell readings revealed that failure was encountered when the beam load was increased as the column was then unable to support additional axial loading. This is illustrated in the figure as a large increase in deflection from 7.5mm to 13mm, which took place towards the end of the beam loading phase.

Although this test was not ideal for computer analysis due to the complicated loading sequence it has been successfully modelled by an analysis program - see chapter 6.

4.4.6 Details of Test ST8

Seat and web cleats were used for the connection between the beams and column in this test. The column was tested about its minor axis. An initial out-of-straightness of less than 1mm was measured. In the previous test the strength of the column had caused problems due to the limited capacity of the screw jack. To reduce the failure loads, and also to ensure the column failed in a predetermined direction, an initial imperfection was put into the column after the specimen had been assembled in the rig, and instrumented as usual. A 25kN preload was applied axially to the column to locate it in position then a hand operated screw jack was inserted between the column and upright support at the central restraint position (see figure 4.2). A 12.5mm imperfection, measured using a dial gauge, was jacked transversely into the column. No measurement of the load applied at this location was taken. The load-deflection plot for this test, figure 4.15, clearly shows this operation. Loads up to 70kN were then applied to the beams approximately equidistant from the column. Application of an additional axial load of 384kN through the main screw jack caused a controlled failure, allowing several points in the unloading phase of the test to be recorded.

4.4.7 Details of Test ST4

ST5 incorporated flange cleat connections to a column bent about its major axis. That test had been useful in proving the apparatus and testing procedure, but had not produced particularly useful results. The later frame tests were to use flange cleat connections so a test on the major axis behaviour of a column restrained by this type of connection was desirable. It was anticipated that the level of loading would be quite high so loads applied to each beam, as in ST5, were used in test ST4. The previous test, ST8, had successfully shown that a more controlled and predictable test could be conducted if the column had a significant initial bow. Once again the initial out-of-straightness for the column was negligible so a similar procedure to that used in test ST8 was adopted and an imperfection of 6.25mm was introduced at the start of the test.

Figure 4.16 shows the total load deflection trace for the test. A total load of 762kN was sustained by the column. As the lateral deflections increased, increasing the moment at the centre, a local buckle formed which can be clearly seen in figure 4.17 and 4.18.

4.4.8 Details of Test ST9

The penultimate test was a minor axis test with flush end plates used to connect the beams to the column web. An initial bow of only 2mm was measured at the centre of the column. An axial load of 25kN was applied to the column before application of the first increment of beam loading. In this test an eccentricity of loading was introduced by applying equal beam loads at distances of 340mm and 425mm, measured from the web face, to the left and righthand beams respectively. An additional imperfection of 5mm (to make the total 7mm) was added at

this stage by the small hand jack. Beam loads were gradually increased to 85kN per beam, whilst maintaining the applied axial load at 25kN before increasing the axial load to initiate failure.

Figure 4.19 illustrates the load-deflection response of the test. The combination of eccentric loading and initial out-of-straightness resulted in a rounded response. Several readings were again taken in the post-buckled part of the test.

4.4.9 Details of test ST10

The influence of the restraint provided by the stiffest connection tested in the joint test series, the extended end plate, on the strength of a column bent about its major axis was investigated in test ST10. Beam loads of equal intensity were applied to the left and right-hand beams at distances of 260mm and 355mm from the column face respectively. The column was initially straight so an imperfection of 7.5mm was put into the column. By increasing the axial load, through the screw jack, the column was brought up to failure.

Figure 4.20 shows the total load against deflection plot for this test. At a load of approximately 620kN the slope of the plot changes and the column begins to deflect to the right. This continues till the total load approaches 700kN at which point the column deflects back to the left and moves towards failure. An examination of the loadcell readings revealed that the hydraulic jacks applying the beam loads had exceeded their travel and lost load. The right-hand beam load had decreased more rapidly than the left thereby relieving some of the moment on the column. Despite the loss of load to the beams the axial load from the screw jack alone was capable of

failing the column since it was able to capitalise on the deflection created by a combination of pushing the column over and the eccentric loading.

4.4.10 Details of Unrestrained Column Tests

As a lower bound to the range of connections a notionally pin-ended column, without any beams, was tested about the minor and major axes. The column in the first test conducted, ST1Y1, had an initial out-of-straightness of 1.0mm at the centre. After applying a load of 25kN to the column the centre was pushed out by 13mm. The column failed at a load of 390kN. This was considerably in excess of the theoretical buckling load (π^2EI/L^2) of 195kN, but well below the column squash load, 791kN, indicating that elastic buckling effects were dominant. A further test on the same specimen was conducted by removing the slight permanent set in the column and putting an imperfection of 6mm in the opposite direction. The column was again loaded to failure and sustained a load of 410kN. Clearly the loadcells at the ends of the column and the out-of-plane bracing provided some restraint.

Finally the same column was tested about its major axis. An initial curvature about the x-x axis of 4mm was increased to 7mm before loading the specimen to failure. A maximum load of 660kN was applied compared with a theoretical load of 611kN for buckling about the major axis.

A first impression of the results suggested that the apparatus was enhancing the strength of the columns by a very significant margin. However it should be recognised that tests on a truly pin-ended column are very difficult to conduct and require sophisticated bearings to simulate a pin at high load levels. (Compare the

tests of reference 4.1.) The purpose of the experimental study was to examine the influence of connection restraint on column performance so an examination of the relative magnitude of the restraint provided by the apparatus in tests ST1 was of interest.

Figure 4.21 shows the Euler curves for the column section buckling about its major and minor axes. Also shown on the figure are the test loads. The 'effective length', ie the length of a pin ended column which has a load carrying capacity equal to the real column, can be obtained as shown. Table 23 in BS 5950 (4.2) relates the effective length to the joint restraint characteristics, k , at the two extremities of the column, where k is defined in cl E.2.1 as

$$k = \frac{\text{Total column stiffness at joint}}{\text{Total stiffness of all members at joint}} \quad (1)$$

If it is assumed that the restraint provided by the loadcells may be modelled by beams of length L rigidly connected to the column at 6.5m centres, as shown in Figure 4.22, a qualitative assessment of the degree of restraint provided may be made.

For the major axis case the effective length required to give a failure load equal to the test load is 0.954. This corresponds to k values at the top and bottom of the column of 0.93 (from Table 23). By substitution into equation (1), the length of beam (254x102x220mm) required if rigidly connected to the column may be found as follows,

$$k = 0.93 = \frac{I_c/650}{2(0.5 \frac{I_B}{L}) + \frac{I_c}{650}} \quad (2)$$

which may be rearranged to give

$$L = \frac{0.93 I_B}{I_c \left(\frac{1}{650} - \frac{0.93}{650} \right)} = 196m \quad (3)$$

In the minor axis case the effective length required to give a failure load equal to the test load is 0.754, for which a joint restraint factor of 0.67 would be required., This implies a length of beam L given by

$$L = \frac{0.67I_g}{I_c \left(\frac{1}{650} - \frac{0.67}{650} \right)} = 94m \quad (4)$$

Compared with the lengths of beam used in the subassemblage tests, which were 1.5m but with the special end restraint representative of a 3m beam, it can be seen that the rigidity of the beams and connections are very much greater (see also section 4.5.3). Thus the modest restraint provided by the test apparatus would be unlikely to significantly influence the test results. The 'pin-end' column tests also illustrate the sensitivity of column strength to very modest degrees of restraint.

4.5 Discussion of Results

4.5.1 Behaviour of Connections

In order to examine the role of the connections in the performance of the subassemblage the bending moment and rotations of the four joints were recorded. Bending moments were measured at two positions on each beam, adjacent to the connection and at the remote end. Figure 4.1 and Table 4.1 give the exact locations of the gauges in each test. It was necessary to position the gauges some distance from the connection to avoid local strain distributions. However because the beam loads were applied relatively close to the connection (to permit the application of large loads without deforming the joints excessively) the gauges were located on a steep moment gradient. The analysis program, written to interpret the data, predicts the moment at the column flange or web face (for major and minor axis tests

respectively) by linear extrapolation of the moment gradient calculated from the moment under the beam load and that adjacent to the connection. This assumption would appear to be valid since in no test did the stresses in the beams approach yield. Rotations were measured using two LVDT's as described in section 4.2. The resolution of the transducers was approximately 0.04mm. When mounted on a bar of typically 400mm length changes in angle of 0.2×10^{-3} radians could be detected. Although this was sufficiently sensitive for the top connections in some tests the angular movements of the lower connections were so small until failure that interpretation of the moment-rotation curves was not possible.

4.5.1.1 Comparison of Joint Test and Subassemblage M- ϕ Response

Comparisons of the moment-rotation responses measured in three subassemblage tests, ST4, ST7, ST8 and ST6 with their corresponding joint tests are made in figures 4.23 - 4.26. The comparisons are between the raw data points from the subassemblage tests and the refined average joint test curves required by the analysis program discussed in chapter 6. Having in mind the differences in measuring techniques, the degree of control in loading and the number of test points recorded, the correspondence appears to be good. For all the connection types used in the subassemblage tests the moment-rotation curves are below those of the individual joint tests. This may be coincidence but it appears more likely that differences in the test arrangements, particularly the proximity of the beam load to the joint, and the measurement of the bending moment has imparted bias into the results. Be that as it may the comparisons show that there are no fundamental differences in the behaviour of the joints when tested as isolated components or as part of a larger frame.

4.5.1.2 Joint Action During Column Failure

Test ST6 most clearly shows the behaviour of the top connections as the column failed. Figure 4.26 plots the moment-rotation curves for the top two connections. This test incorporated flange cleat connections between the beams and column flanges and had equal loads applied to the beams. Both connections performed in a similar way during the beam loading phase of the test, rotating to approximately 14×10^{-3} radians and sustaining a moment in the region of 8 kN.m. As the column was loaded axially, with the beam loads remaining reasonably constant, little further rotation of the connections took place. When the column began to fail by buckling towards the left the rotation of the column head in a clockwise direction caused the left hand connection to open further and conversely closed the right hand connection. Thus the left-hand connection can be seen to rotate further in the last stages of the test and to continue to follow the loading $M-\phi$ response, whereas the right-hand connection unloaded. Clearly the restraint offered to the column is mainly from the unloading connection, as the loading joint follows the $M-\phi$ curve with little stiffness. Interestingly, since the loads on the beams were not shed by the hydraulic system the decrease in moment on the right-hand connection was balanced by an increase in moment in the centre. The opposite was true of the left-hand beam with the span moment decreasing as the joint moment increased.

This pattern of behaviour was also demonstrated by the Bergquist tests^(4.3) and has been verified analytically by Rifai^(4.4) and Poggi^(4.5).

4.5.2 Effective Restraint Provided by Connections

Figure 4.27 compares the test results with strengths predicted by BS 5950 (4.2). In making this comparison no allowance has been made for any end restraint effects when determining the design values i.e. the full column length has been used as its effective length when calculating the column strength component of the interaction. Since the experimental results plot so far above the design values - above even the axially loaded column strength in every case - some considerable measure of end restraint must have been transmitted by the semi-rigid action of the "simple" connections employed, a fact that was also evident from inspection of the column deformations at failure where clear evidence of the presence of points of inflection within the column length was observed. A method of incorporating the effect of semi-rigid connection restraint into column strength calculations has been described by Bjorhovde (4.6). The method uses the initial tangent stiffness of the connection, C , as illustrated in figure 4.28 in conjunction with the stiffness of the beam to which the connections are attached to determine an effective end restraint factor, C^* . In reference 4.4 the derivation assumes beams to be bent in single curvature with equal and opposite end rotations. However in BS 5950 the charts presented in Appendix E to calculate the effective lengths of columns in rigid frames assume that the remote end of the beam is fixed. Therefore it is more appropriate to consider the effective restraint of a connection attached to a beam whose remote end is fixed. In this case the effective end restraint factor C^* is defined in ref. 4.7 as

$$C^* = \frac{4EI_b/L_b}{1 + (4EI_b)/L_b C} \quad (5)$$

In order to simplify this expression define β , the connection-to-beam factor as

$$\beta = \frac{C}{EI_b/L_b} \quad (6)$$

and the effective connection-to-beam factor, β^*

$$\beta^* = \frac{C^*}{EI_b/L_b} \quad (7)$$

or from eqn. (5)

$$\beta^* = \frac{4}{1 + 4EI_b/L_b C} \quad (8)$$

Multiply the numerator and denominator of eqn.(4) by $\frac{C}{EI_b/L_b}$, to obtain

$$\beta^* = \frac{4\beta}{\beta + 4} \quad (9)$$

Re-arranging eqn.(3) gives

$$C^* = \beta^* \times \frac{EI_b}{L_b} \quad (10)$$

Notice that as β tends towards infinity, i.e. the connection becomes much stiffer than the beam, the value of β^* tends towards a value of 4, and C^* becomes equal to $4EI_b/L_b$, which is the correct solution for a column rigidly attached to a beam whose far end is also fixed. But in the code beam stiffness is defined only as I/L , in other words the 4 is taken into account in figure 23 of BS 5950 , therefore β^* should be redefined as

$$\beta^* = \frac{\beta}{\beta + 4} \quad (11)$$

so that in the limiting condition of β tending towards infinity β^* becomes equal to 1 and $C^* = \frac{EI_b}{L_b}$.

Having calculated the effective connection restraint, C^* , from eqn. (6), the elastic distribution factors, k , at the top and bottom of the column may be calculated from the expression

$$k = \frac{\text{total column stiffness at joints}}{\text{total stiffness of all members at joints}} \quad (\text{BS 5950 cl. E.2.1})$$

The effective length ratio L_E/L for the column may be determined from figure 23 in BS 5950. However cl. E.4.1 of BS 5950 states that for a sway prevented rectilinear frame the critical buckling mode of failure puts the beams in single curvature and therefore in order to use figure 23 the beam stiffness must be halved. Hence the effective restraint factor C^* (given in eqn. (6)) must also be halved.

Referring again to figure 4.28 a connection which is continuing to load reduces in stiffness and its effectiveness as a restraint diminishes. However, an unloading connection regains its original stiffness, a fact confirmed from the connection tests in which unloading stiffnesses were measured. Therefore in the subassemblage tests only one connection at the top of the column has been considered as providing an effective restraint along with both connections at the bottom of the column (since neither beam was loaded and rotations were small). Tables 4.3 and 4.4 present the results of calculations to include the effect of the semi-rigid connections in determining column effective lengths and thus in predicting failure loads.

When these revised column strengths are used as the basis for plotting the test results, the points denoted by solid squares and circles are re-positioned much closer to the design expression. Because of the proportions of the components in the particular subassemblages tested - specifically the stiffness of the beams, connections and the column - the magnitude of this correction is quite

different for the major and minor axis tests but is not very sensitive to changes in connection type, see Table 4.4. Thus the original underestimates of some 200% in the case of the minor axis tests and approximately 70% for the major axis tests are both reduced to more modest figures. Note that all results still plot comfortably above the design interaction despite the very low column effective length factors being used. It is believed that this is due to relaxation in column end moments as failure is approached. This has been observed in the parallel theoretical study (4.8, 4.9).

To check that the influence of the restraint provided by the connections on the column's strength was not peculiar to the particular frame geometry tested the effect of the restraint provided by web cleat connections on a 3.6m column with beams spanning 5m was considered. Effective length factors of 0.56 and 0.66 for the column bent about its minor and major axis were calculated. These values are larger than those obtained in the subassemblage tests but they show that by using the same design procedure significant reductions in effective length in non-sway frames of representative geometry are possible. The degree of restraint provided by the connections is dependent on the relative stiffness of the beam to column connection, the beams and the column. The effect of restraint provided to the minor axis tests was in all cases greater than that in the major axis tests because of the increased flexibility of the column when bent about its weak axis.

The wisdom of using the initial stiffness of the very non-linear moment rotation curves of semi-rigid connections in analysing the be-

haviour of end restrained columns has been discussed in several papers (4.6). In comparing the results of this test series with a simple analysis method the correspondence is good. However, with the computational power that the wide availability of desk top computers has made available the use of more accurate representations of the moment-rotation relationship in analysis and design is now possible. This is discussed more fully in chapter 7.

References

- 4.1 Estuar, F.R. and Tau, L.
'Testing of pinned-end steel columns'
Test Methods for Compression Members, ASTM STP 419, American Society of Testing Materials, 1967, p. 80.
- 4.2 British Standard
'Structural use of steelwork in building'
Part 1, Code of Practice for Design in Simple and Continuous Construction: Hot Rolled Sections, BS 5950, Part 1 : 1985.
- 4.3 Bergquist, D.J.
'Tests on columns restrained by beams with simple connections'
CESRL Thesis No. 77-1, University of Texas, January 1977.
- 4.4 Rifai, A.M., Nethercot, D.A. and Kirby, P.A.
'Stability of column subassemblages with semi-rigid connections'
Proceedings, Second Regional Colloquium on 'Stability of Steel Structures', Budapest, September 1986.
- 4.5 Poggi, C. and Zandonini, R.
'Behaviour of strength of steel frames with semi-rigid connections'
Flexibility and Steel Frames, ed. W.f. Chen, ASCE, 1985, p. 57-76.
- 4.6 Bjorhovde, R.
'Effect of end restraint on column strength practical applications'
American Institute of Steel Construction, Engineering Journal, Vol. 21, No. 1, 1st Quarter, 1984, p. 1-13.
- 4.7 Nethercot, D.A. and Chen, W.F.
'Effects of connections on columns'
To be published.
- 4.8 Nethercot, D.A., Kirby, P.A. and Rifai, A.M.
'Design of columns in PR construction - Analytical studies'
Structures Congress, ASCE, New Orleans, September, 1986 (to be published in Canadian Journal of Civil Engineering, 1987).
- 4.9 Rifai, A.M.
'Behaviour of columns in sub-frames with semi-rigid connections'
Ph.D. Thesis, University of Sheffield, 1987.

DIMENSIONS IN MM									
TEST	A	B	C	D	E	F	G	H	J
ST2	-	346	125	1115	541	3250	6025	140	251
ST3	333	343	125	1185	490	3250	5990	60	250
ST4	338	353	125	1115	547	3250	5950	100	204
ST5	343	344	1225	1115	542	3250	5972	100	196
ST6	335	335	125	1185	550	3250	5950	65	210
ST7	-	328	125	1185	550	3250	5950	65	217
ST8	342	348	125	1185	550	3250	5950	65	217
ST9	343	428	125	1185	500	3250	5995	40	247
ST10	336	431	125	1115	520	3250	4880	100	220

TABLE 4.1 Strain gauge positions

TEST NUMBER	DATE TESTED	DESCRIPTION OF CONNECTION	COLUMN AXIS	EQUAL/UNEQUAL BEAM LOAD
ST1Y	19/2/86	No beams	Minor	Not Applicable
ST1X	19/2/86	No beams	Major	Not applicable
ST2	6/2/86	Web cleats	Major	Unequal
ST3	3/2/86	Web cleats	Minor	Equal
ST4	14/2/86	Flange cleats	Major	Equal
ST5	16/2/86	Flange cleats	Major	Equal
ST6	20/1/86	Flange cleats	Minor	Equal
ST7	24/1/86	Flange cleats	Minor	Unequal
ST8	11/2/86	Web and seat cleats	Minor	Equal
ST9	21/2/86	Flush end plate	Minor	Unequal
ST10	25/2/86	Extended end plate	Major	Unequal

TABLE 4.2 Subassemblage test series

TEST	CONNECTION TYPE	C	β	β^*	C*	K _{top}	K _{bottom}	k L _E /L
3	Web Cleats (Minor)	11100	5.6811	0.5868	1149	0.197	0.109	0.54
4	Flange cleats (Major)	7000	3.5618	0.4710	922	0.489	0.324	0.64
6	Flange Cleats (Minor)	29500	15.0644	0.7902	1548	0.154	0.083	0.53
7	Flange Cleats (Major)	20300	10.2771	0.7198	1410	0.166	0.091	0.53
8	Web and Seat (Minor)	11700	5.9792	0.5992	1174	0.194	0.107	0.54
9	Flush End Plate (Minor)	72550	37.028	0.9025	1768	0.137	0.074	0.53
10	Extended End Plate (Major)	46750	23.8613	0.8564	1678	0.345	0.208	0.59

where

C = initial tangent stiffness

$$\beta = \frac{C}{EI_b/L_b}$$

$$\beta^* = \frac{\beta}{\beta + 4}$$

$$C^* = \beta^* \times \frac{EI_b}{L_b}$$

$$K_{top} = \frac{EI_c/L_c}{EI_c/L_c + 0.5 \times C^*}$$

$$K_{bottom} = \frac{EI_c/L_c}{EI_c/L_c + 0.5 \times 2 \times C^*}$$

TABLE 4.3 Calculation of effective length factor k

TEST	P _y (N/mm ²)	AREA (mm ²)	TEST LOAD (kN)	M _p (kN.m)	M (kN.m)	M/M _p	λ (k = 1.0)	P _c STRESS (N/mm ²)	DESIGN LOAD (kN)	TEST DESIGN	k L _e /L	λ	P _c STRESS (N/mm ²)	DESIGN LOAD (kN)	TEST DESIGN
3	265	2914	520	20.51	4.36	0.212	164.8	57.7	168.1	3.09	0.54	89.0	141.0	410.9	1.26
4	273	2983	760	50.10	11.95	0.238	92.3	155.2	463.1	1.64	0.64	59.1	221.1	659.5	1.15
6	288	2874	520	22.19	3.23	0.146	164.4	59.1	170.0	3.06	0.53	87.1	151.9	436.6	1.19
7	278	2824	526	20.79	6.62	0.318	165.3	58.1	164.1	3.20	0.53	87.6	1146.9	414.8	1.27
8	279	2837	518	20.81	7.75	0.372	166.2	57.6	163.4	3.17	0.54	89.7	142.9	405.4	1.28
9	271	2927	486	20.00	9.87	0.494	166.7	56.91	166.6	3.02	0.53	88.4	145.0	424.4	1.14
10	272	2845	743	47.33	26.8	0.566	92.74	154.08	438.37	1.69	0.59	54.7	226.9	645.5	1.15

TABLE 4.4 Comparison of test and design loads

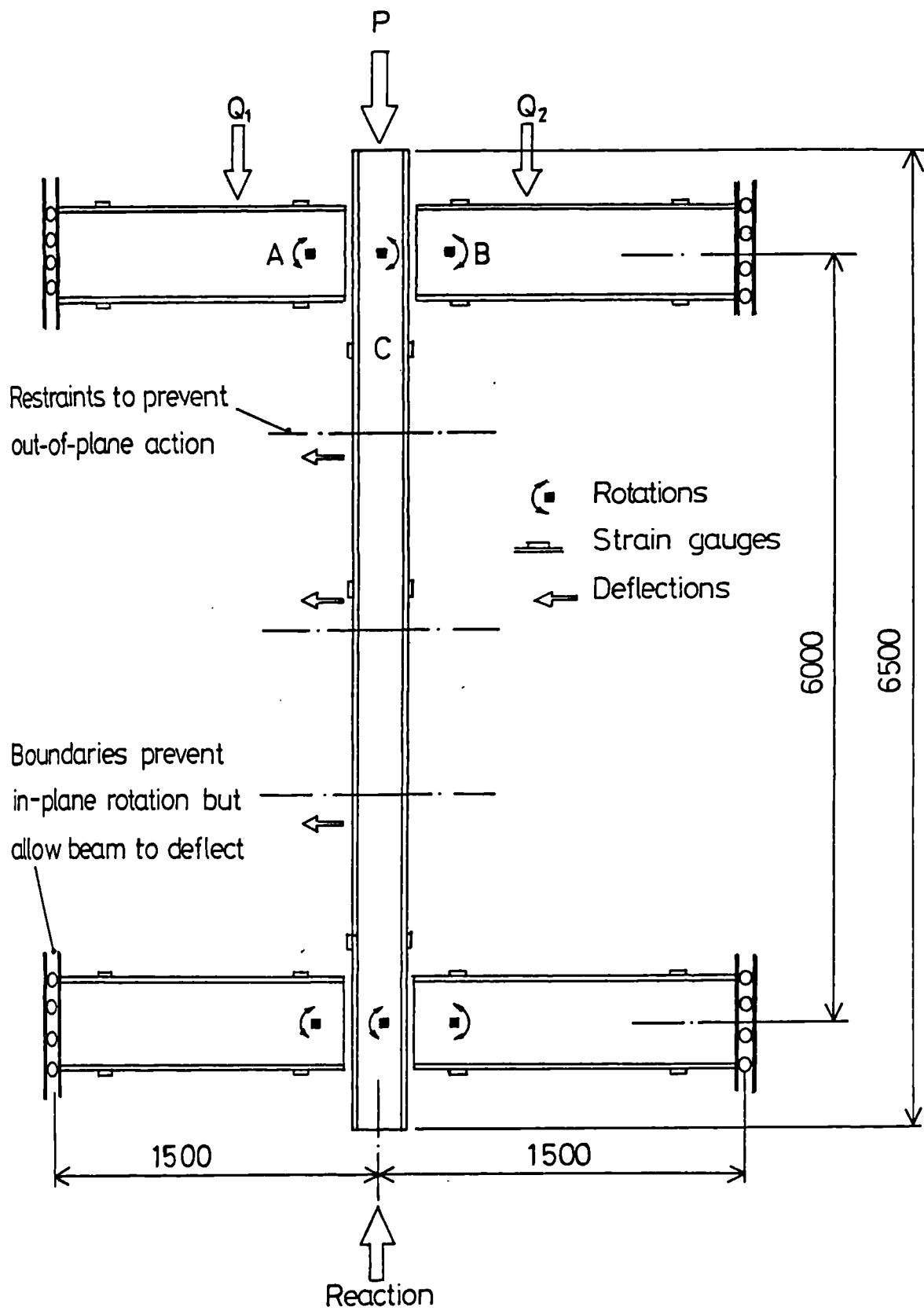


FIGURE 4.1 'I' shaped subassemblages

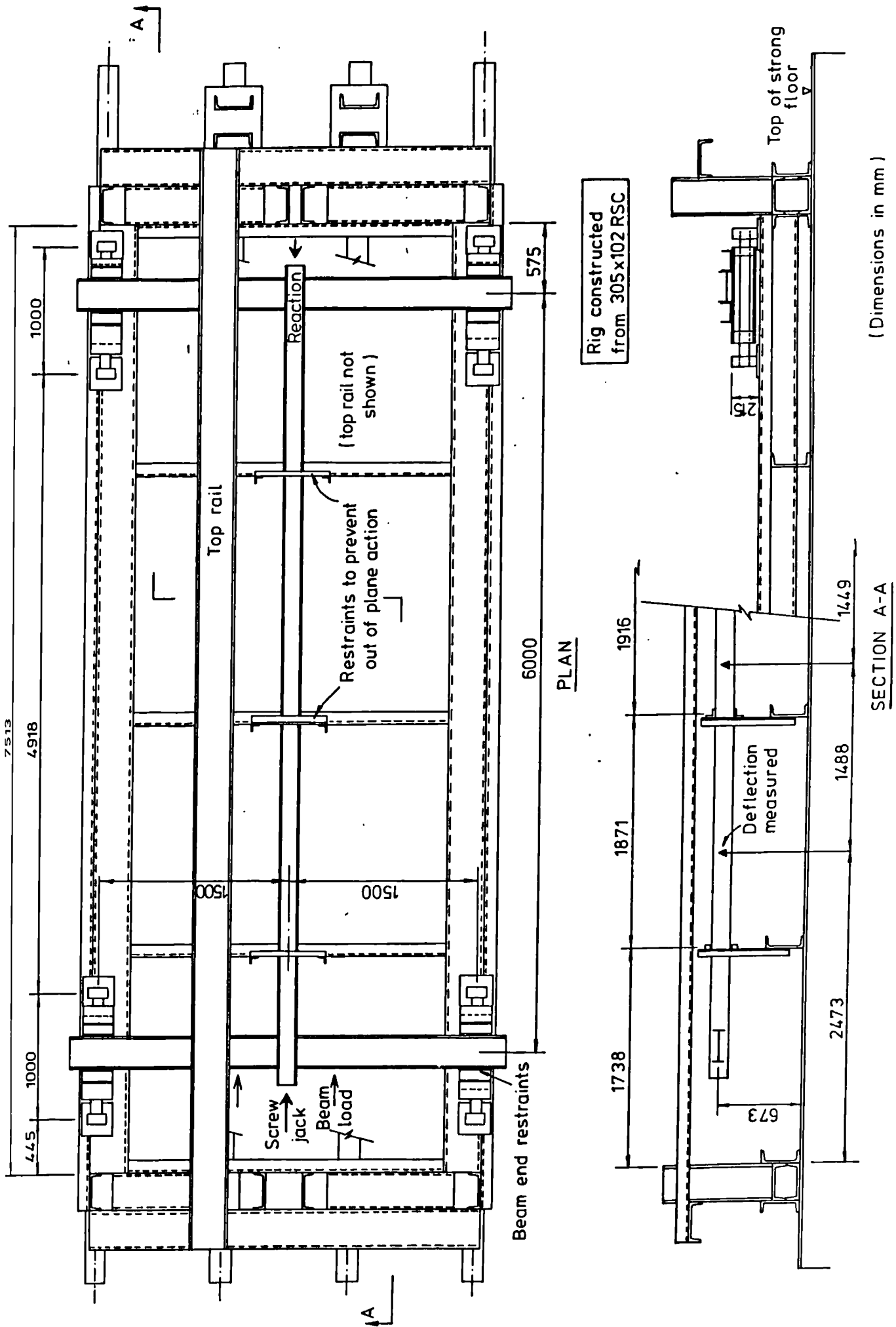


FIGURE 4.2 Subassemblage test rig

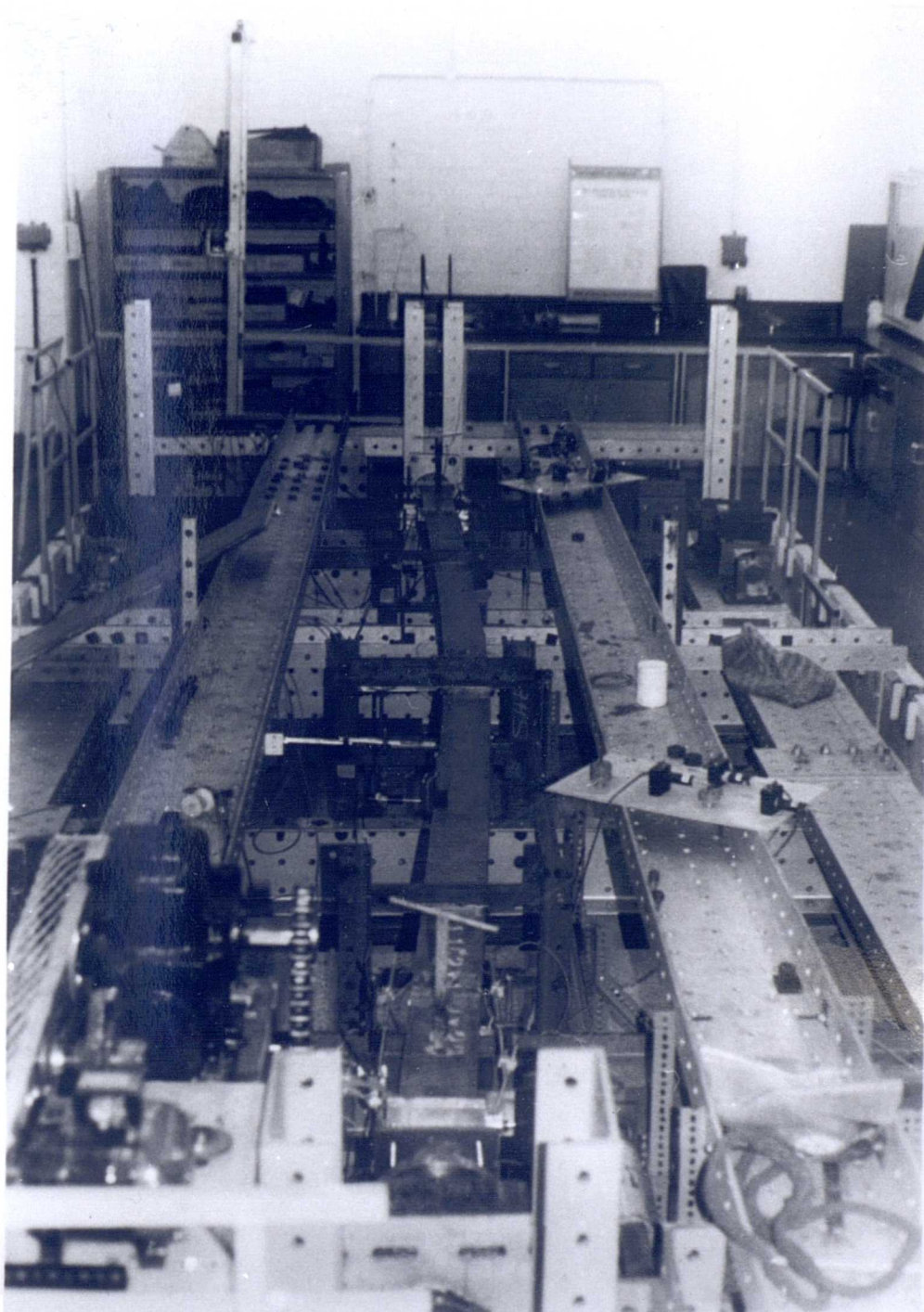
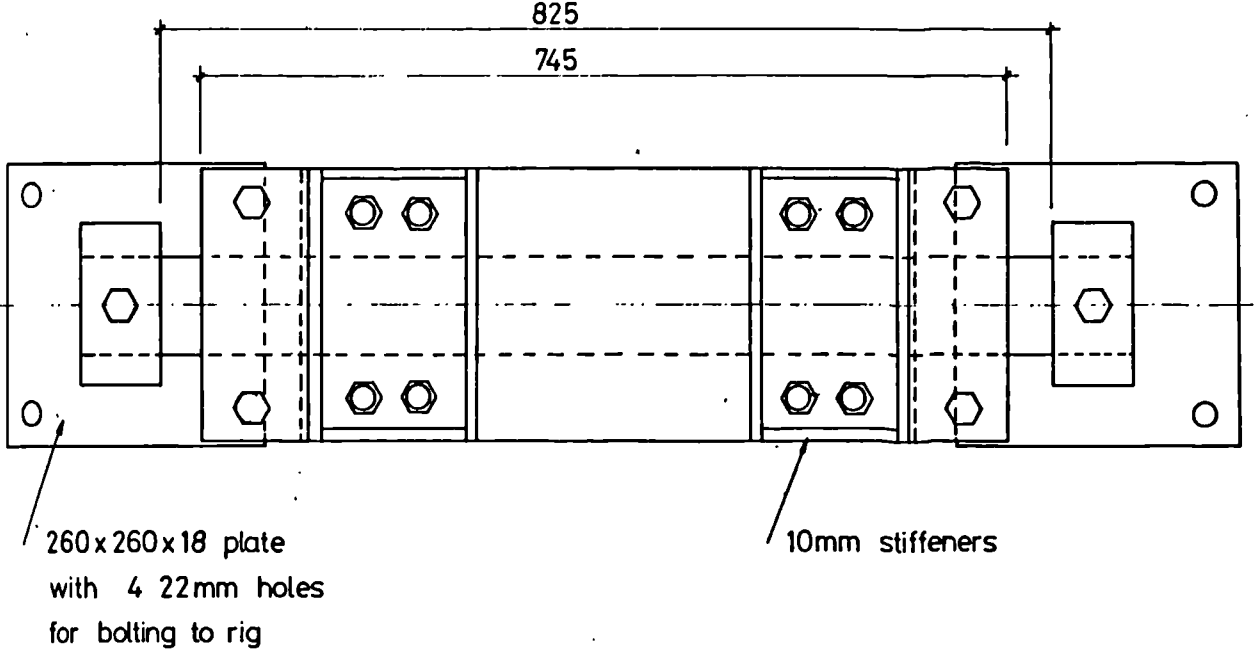
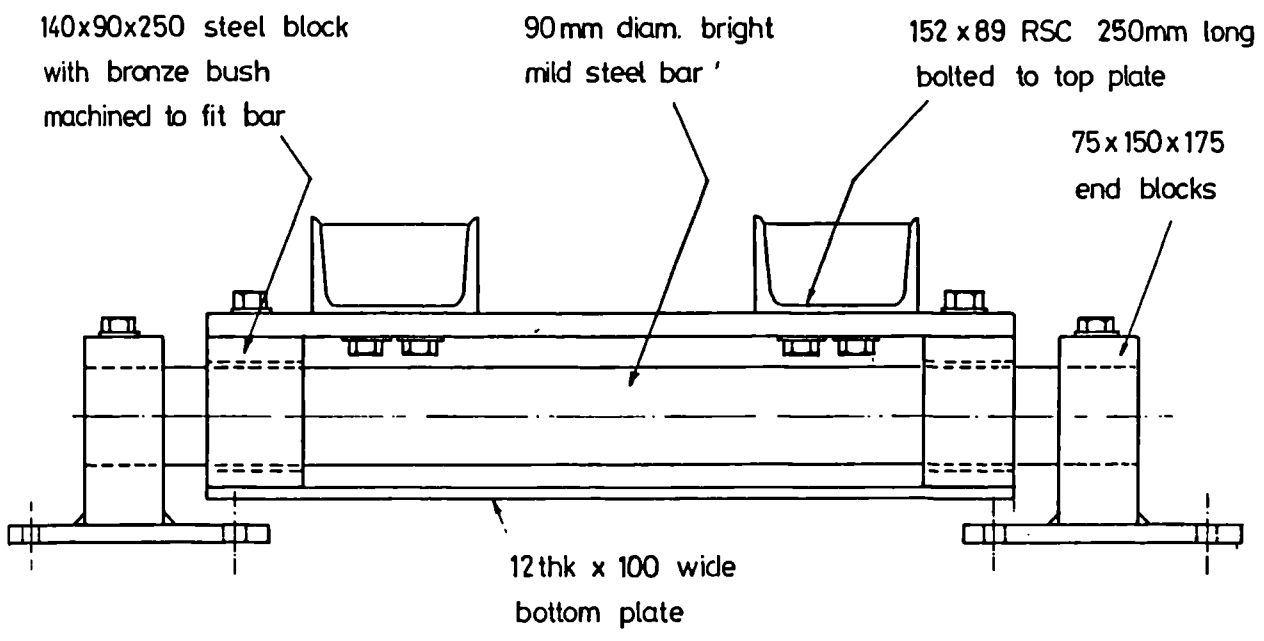


FIGURE 4.3 Test specimen under load



P L A N



E L E V A T I O N

FIGURE 4.4 Beam end restraints to prevent in-plane rotation

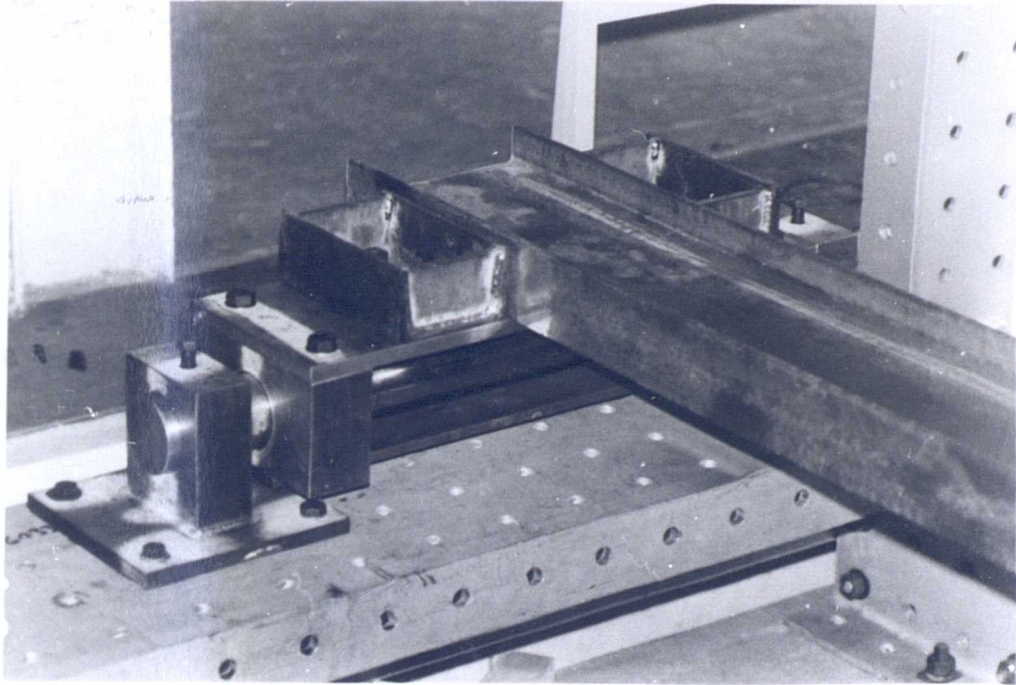


FIGURE 4.5 Beam end restraints

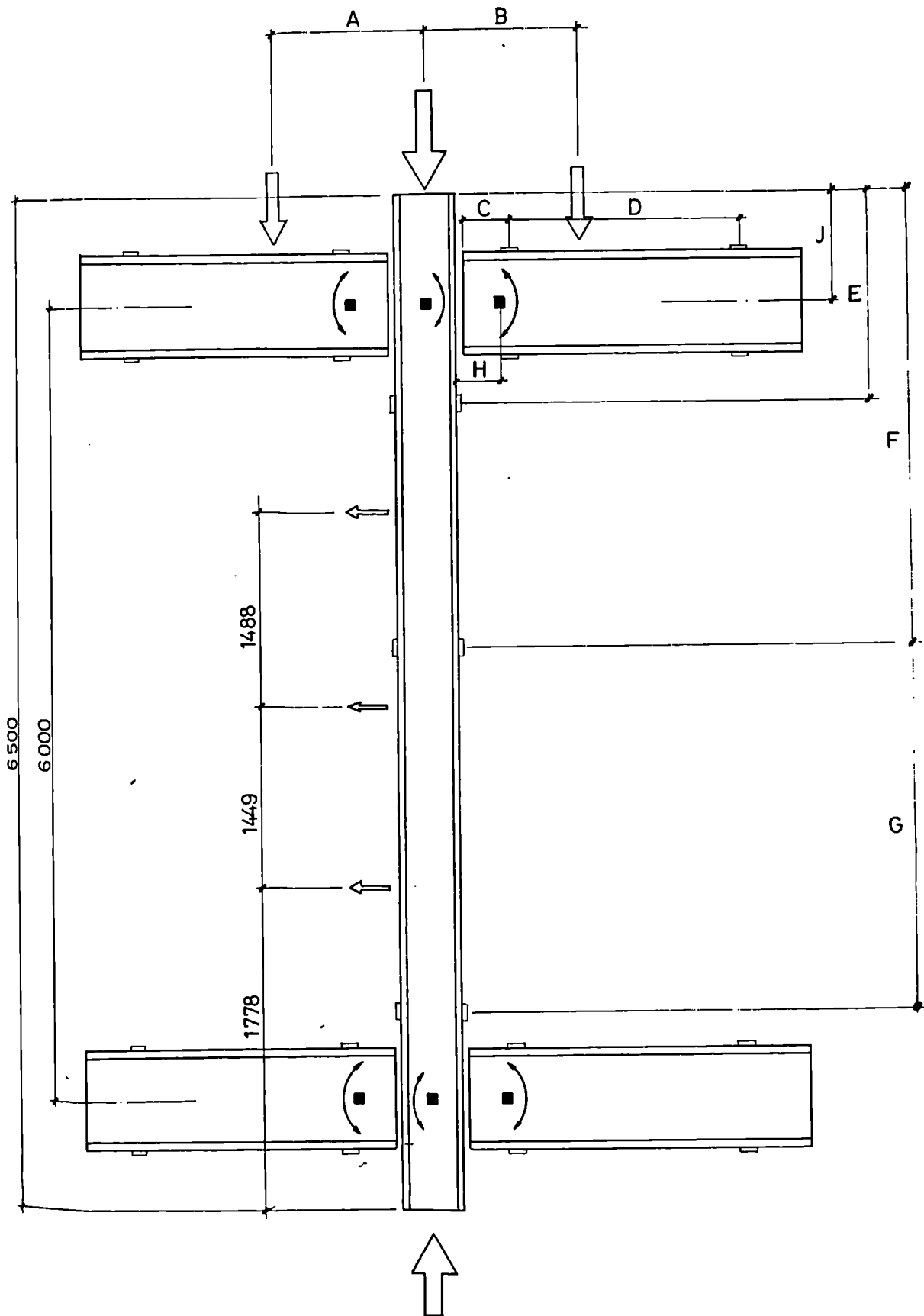


FIGURE 4.6 Location of strain gauges

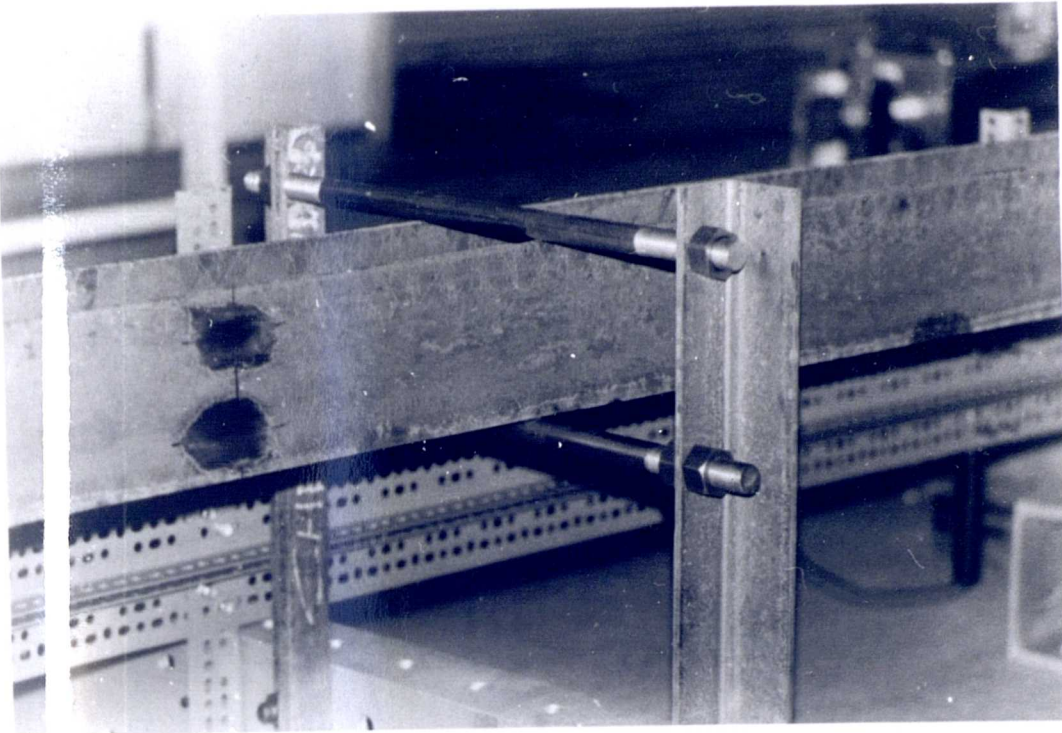


FIGURE 4.7 (above)
Restraints to prevent
out-of-plane action

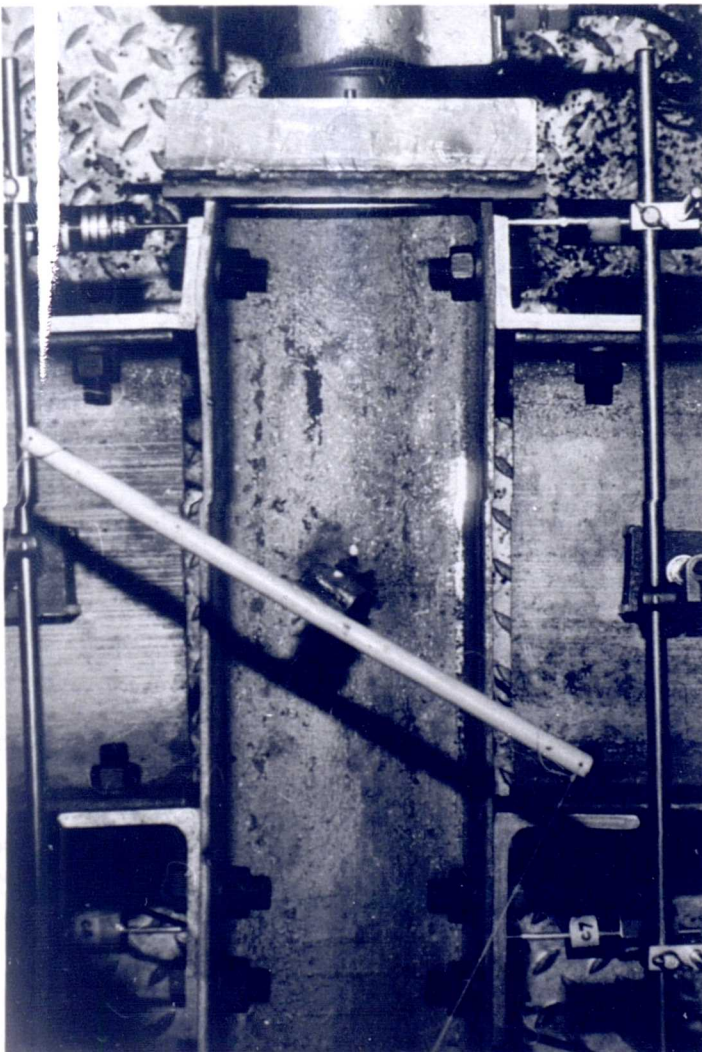


FIGURE 4.8 (left)
Local deformation
produced by flange
cleats - ST5

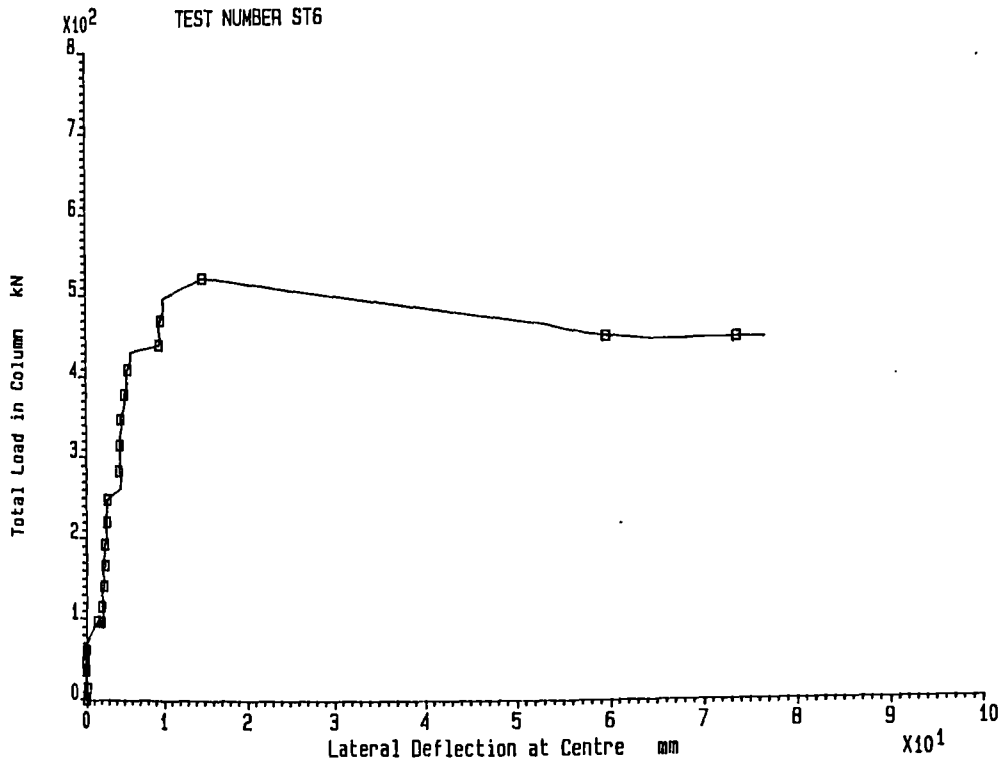


FIGURE 4.9 Total axial load v. central displacement - ST6

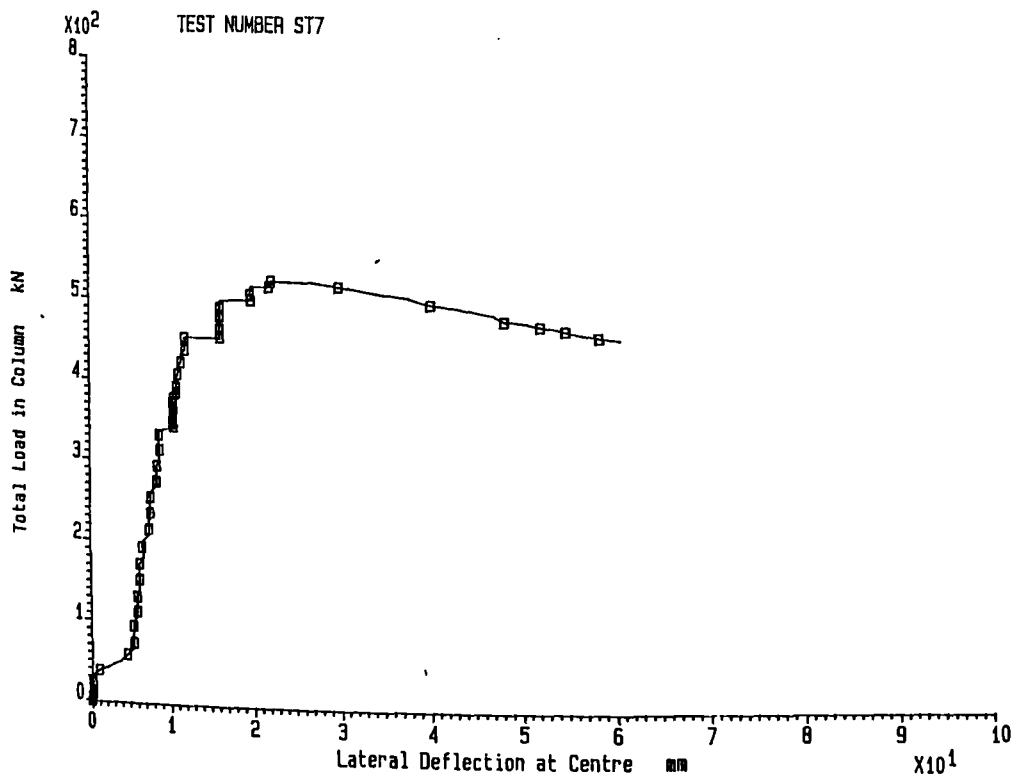


FIGURE 4.10 Total axial load v. central displacement - ST7

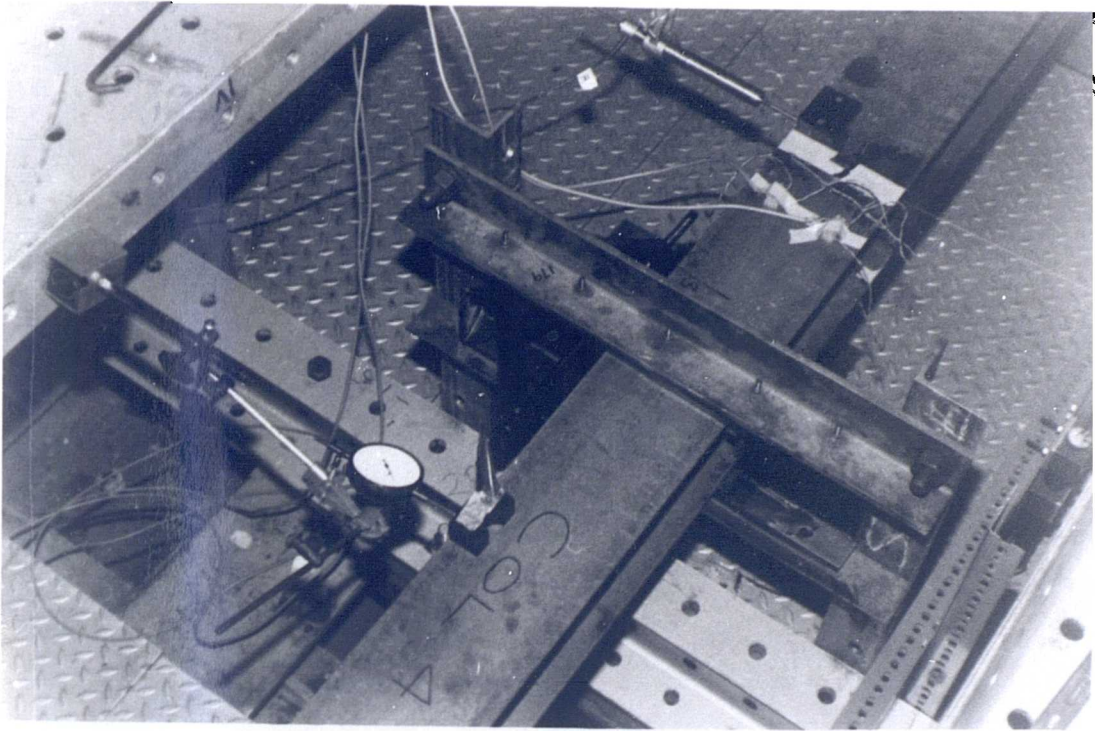


FIGURE 4.11 Improved restraints at mid-height

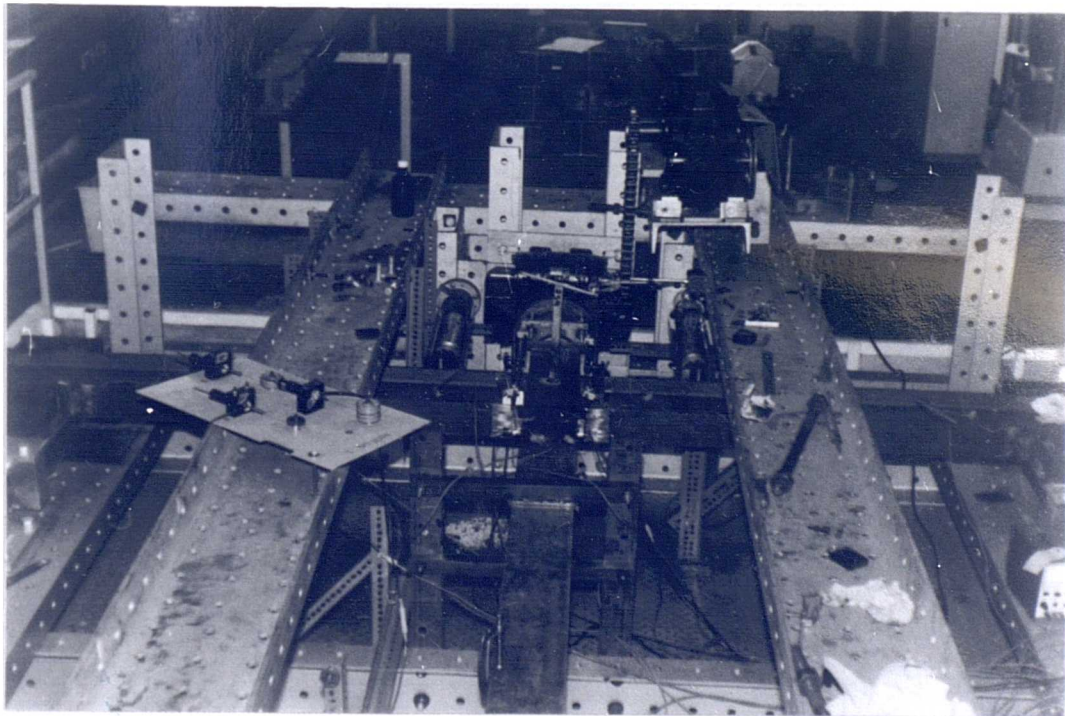


FIGURE 4.12 Improved restraints at third points

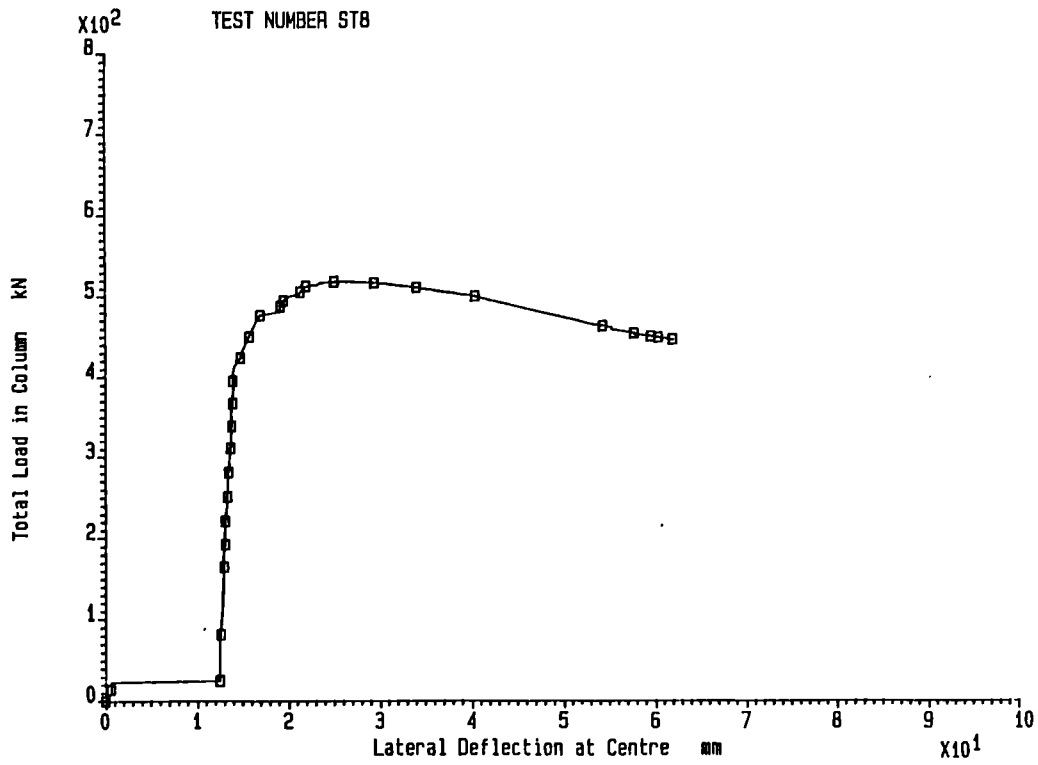


FIGURE 4.15 Total axial load v. central deflection - ST8

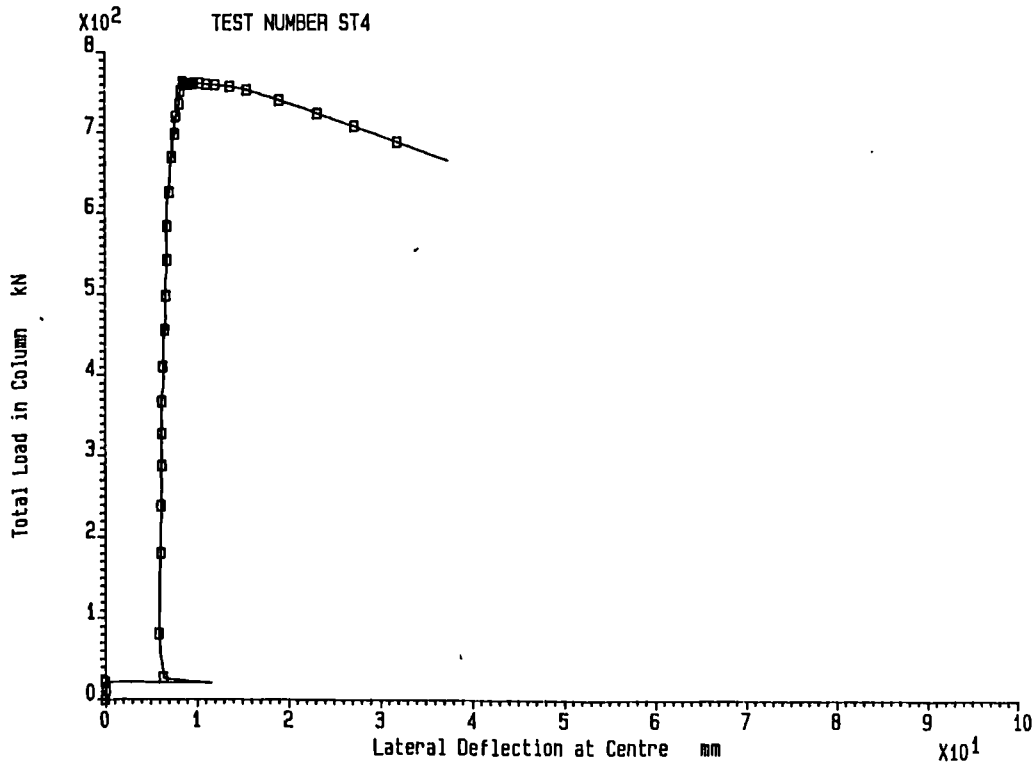
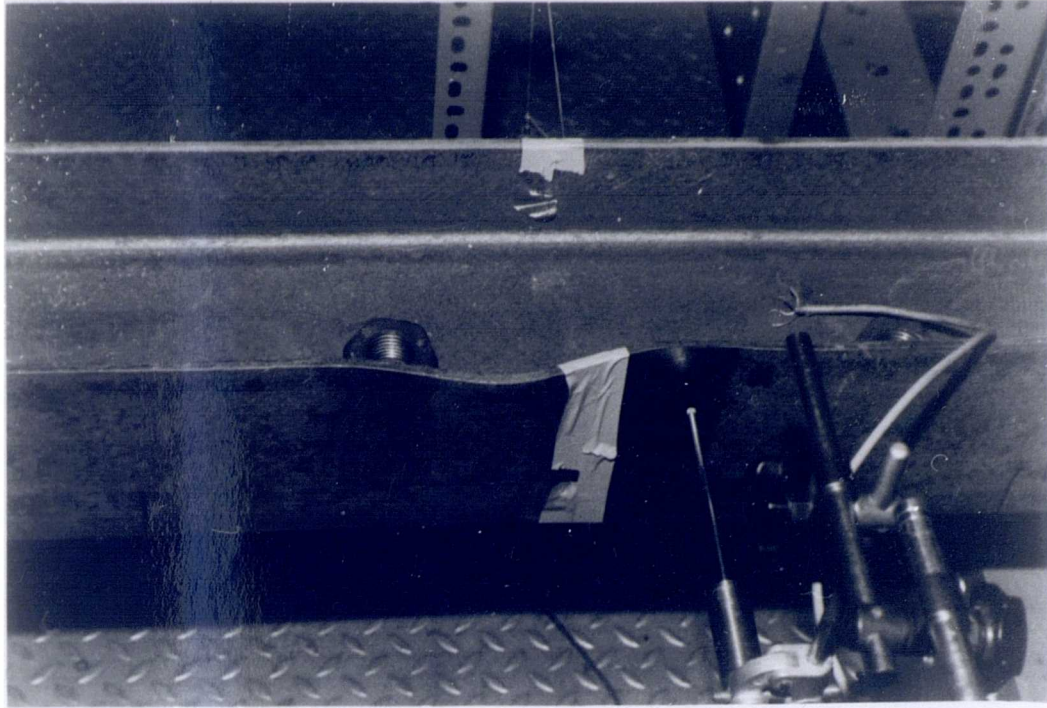
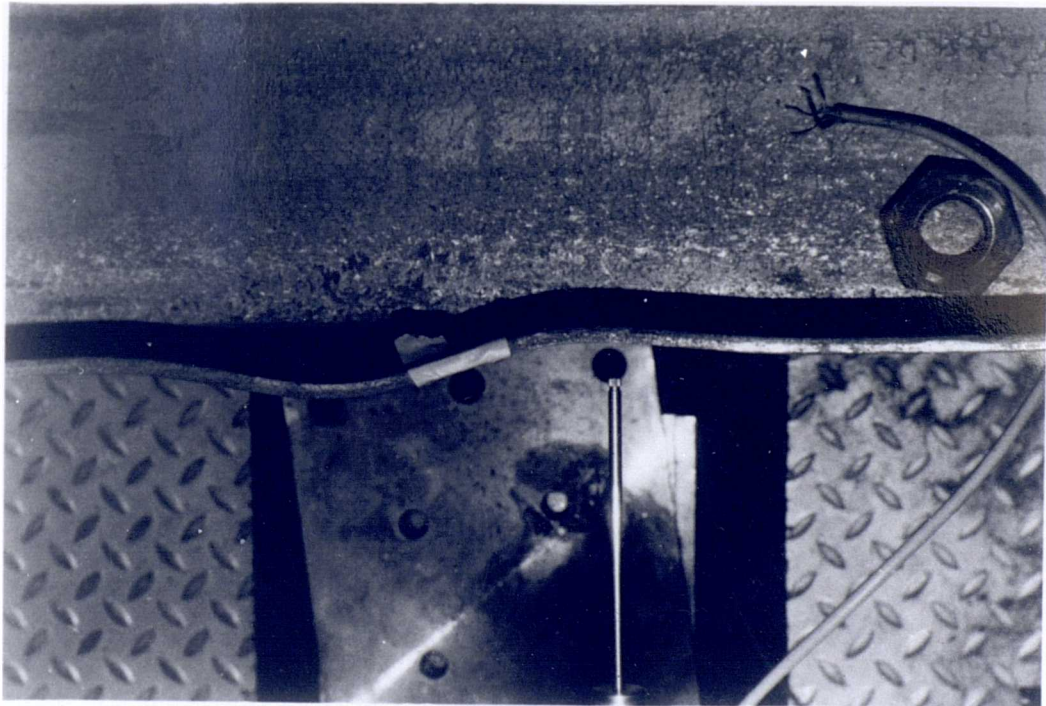


FIGURE 4.16 Total axial load v. central deflection - ST4



IGU 4.17 Local buckling of column flange - ST4



E 4.1 Local buckling of column flange - ST4

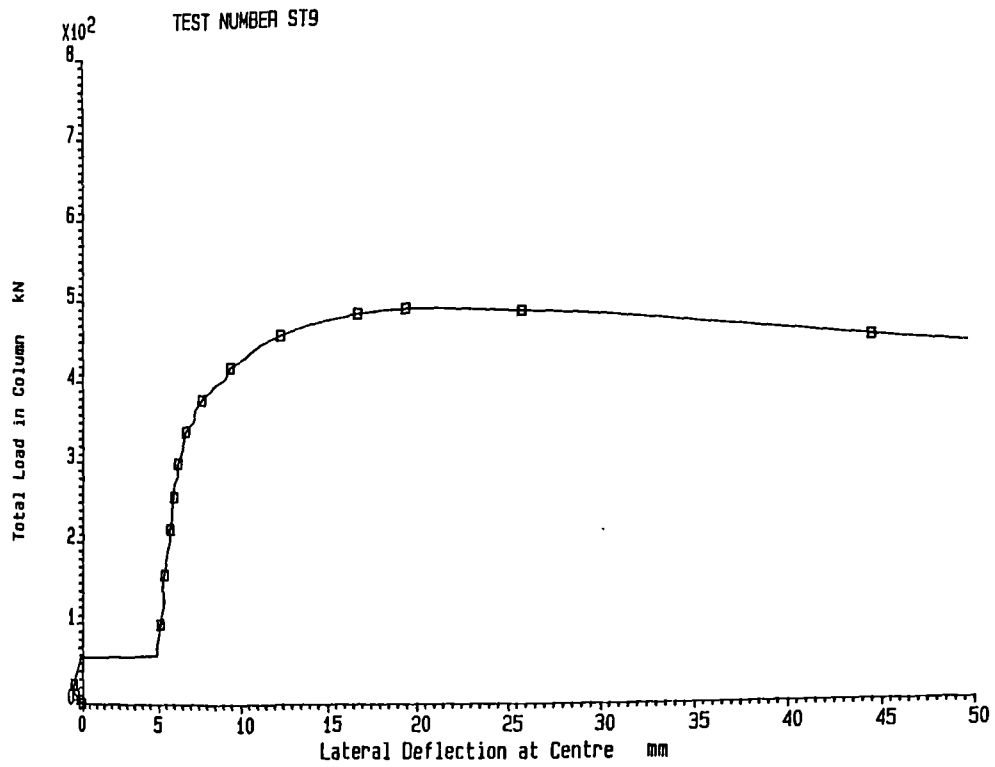


FIGURE 4.19 Total axial load v. central deflection - ST9

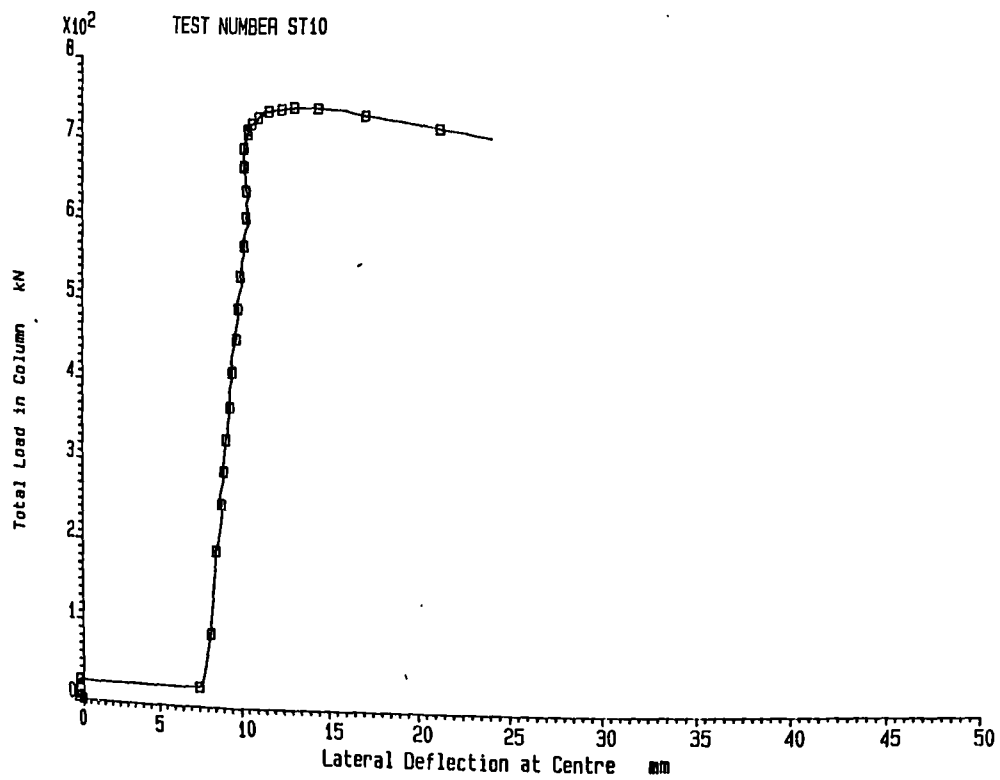


FIGURE 4.20 Total axial load v. central deflection - ST10

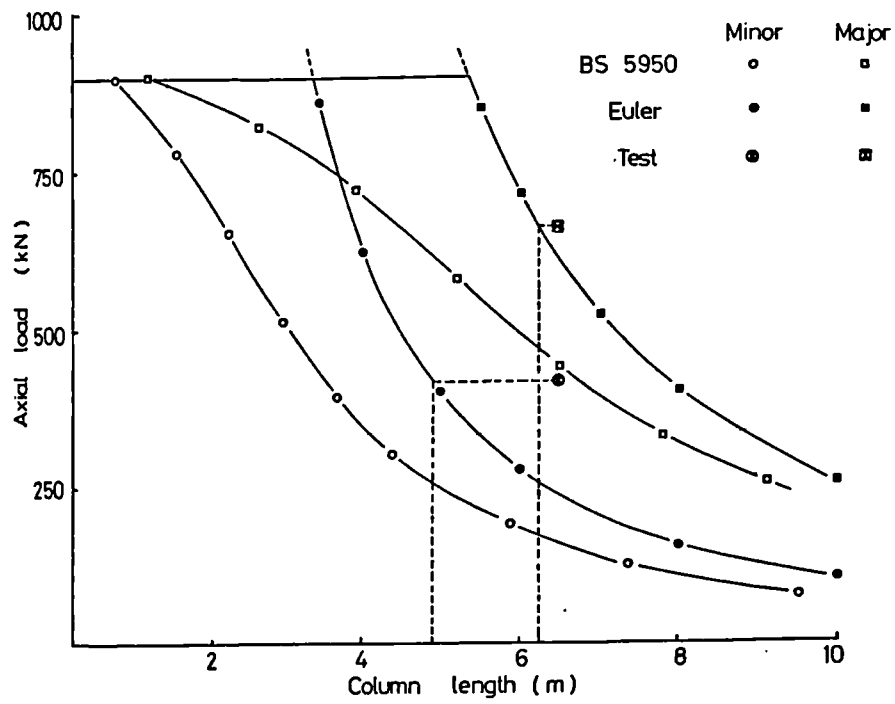
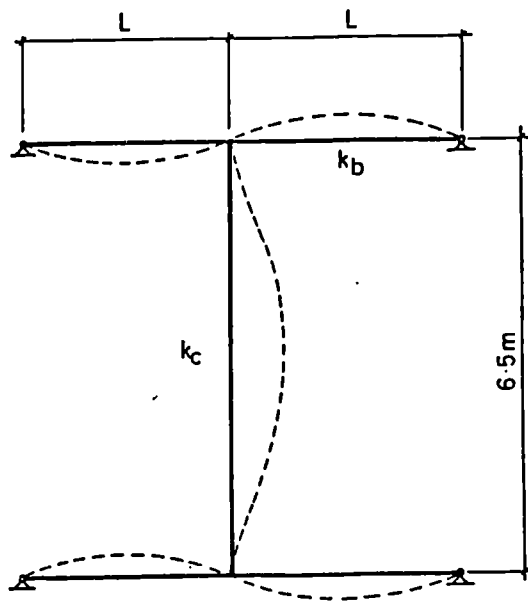


FIGURE 4.21 Effective length of pin-end column tests - ST1



$$k_c = I_c / 6.5$$

$$k_b = 0.5 I_b / L \quad (\text{BS 5950 E.4.1.})$$

$$k_{\text{top}} = k_c / 2k_b = k_{\text{bottom}}$$

FIGURE 4.22 Model for estimating degree of restraint in test ST1

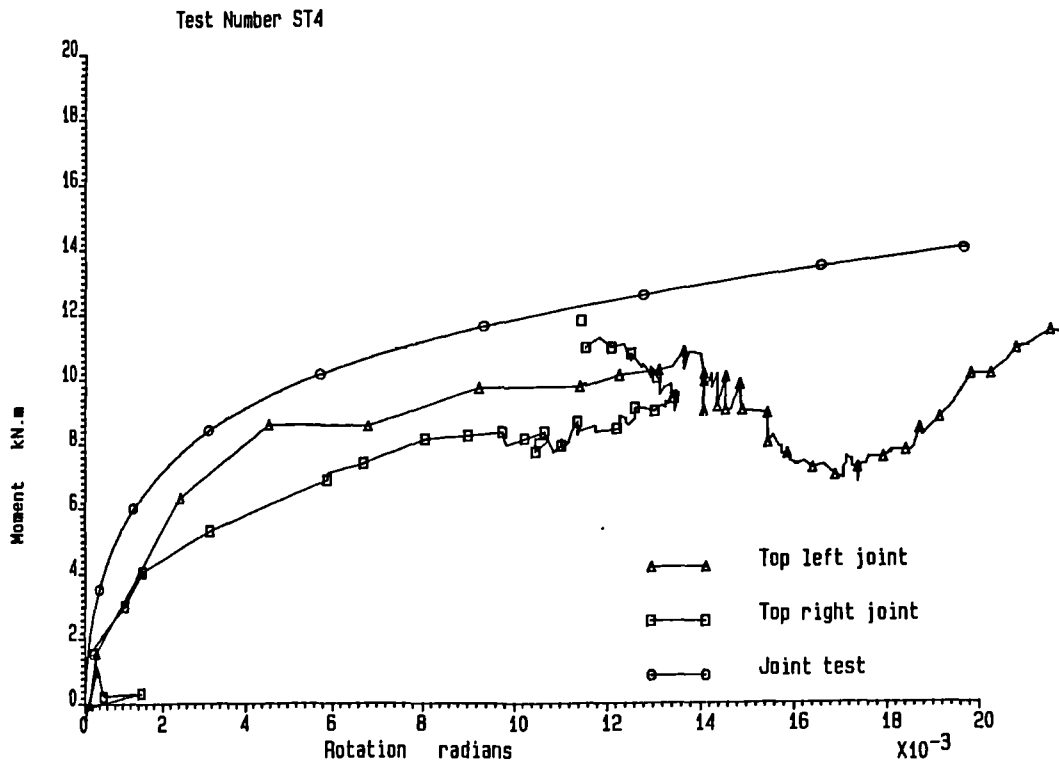


FIGURE 4.23 Comparison of moment-rotation curves from joint test and subassemblage test ST4

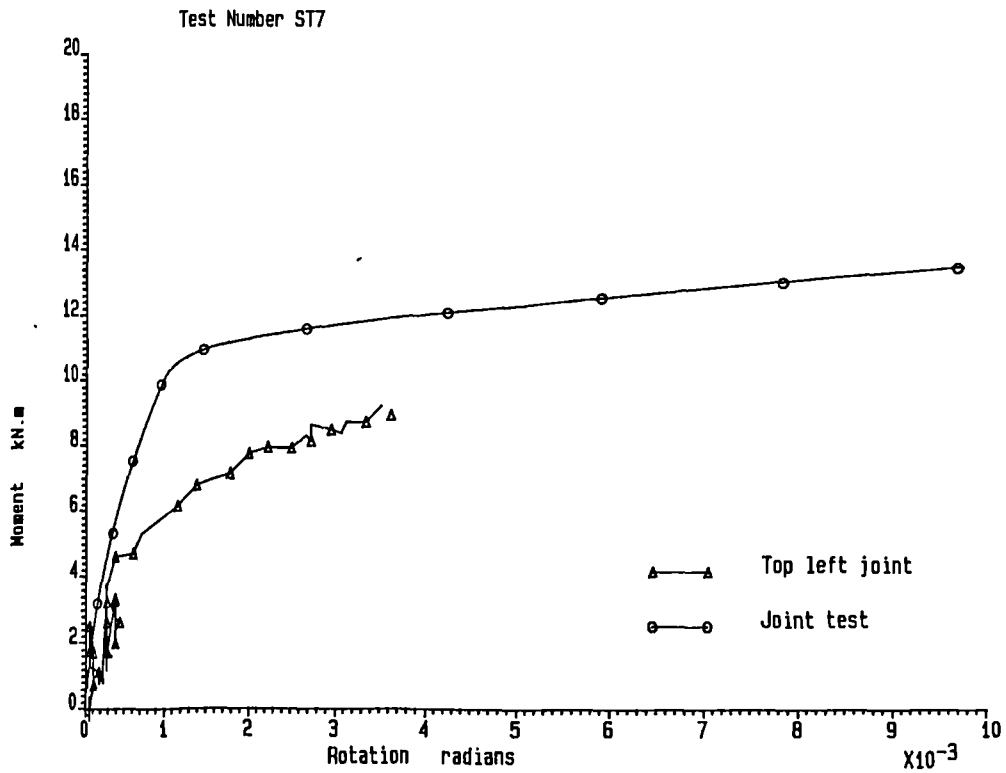


FIGURE 4.24 Comparison of moment-rotation curves from joint test and subassemblage test ST7

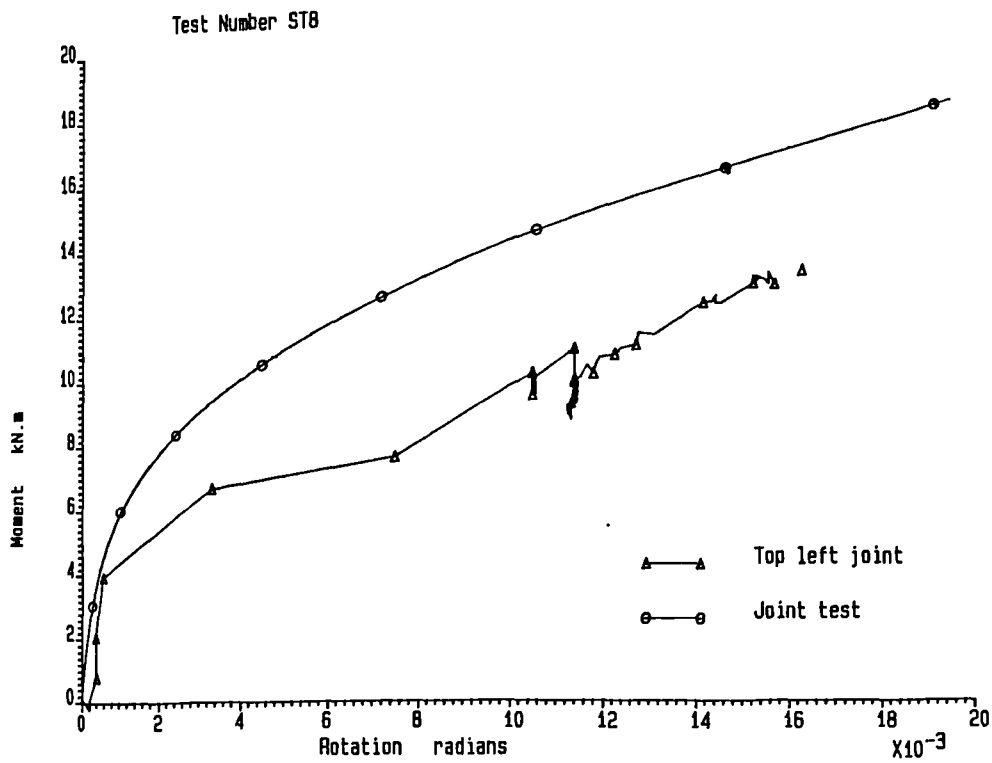


FIGURE 4.25 Comparison of moment-rotation curves from joint test and subassemblage test ST8

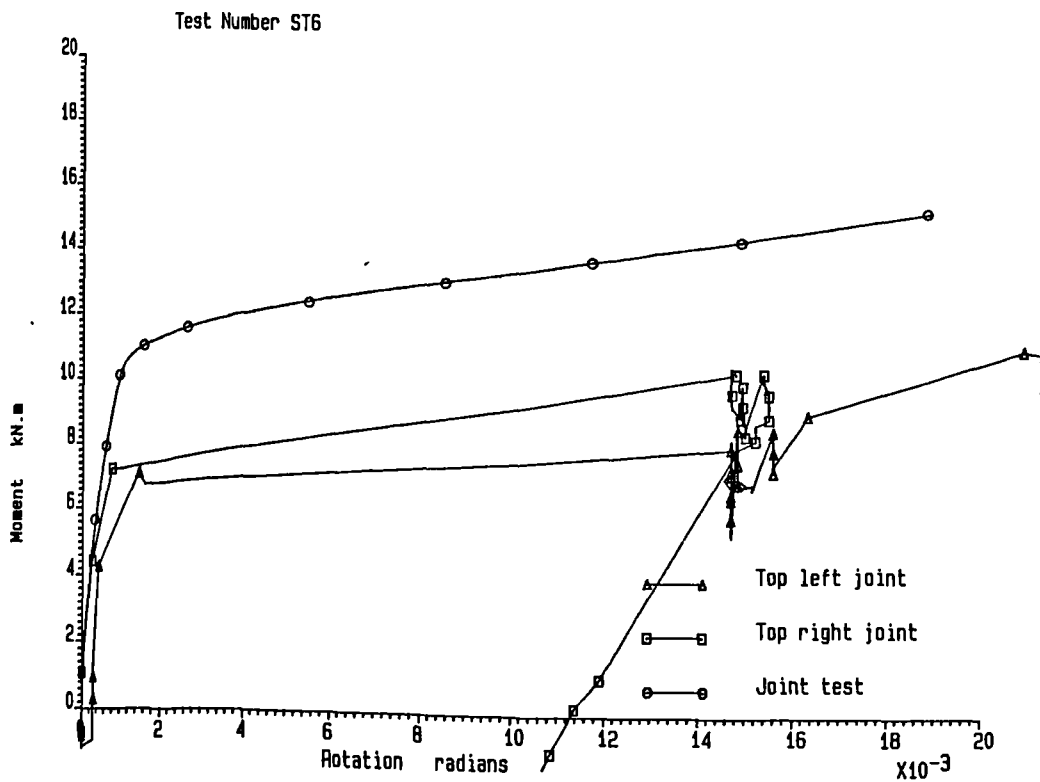


FIGURE 4.26 Comparison of moment-rotation curves from joint test and subassemblage test ST6

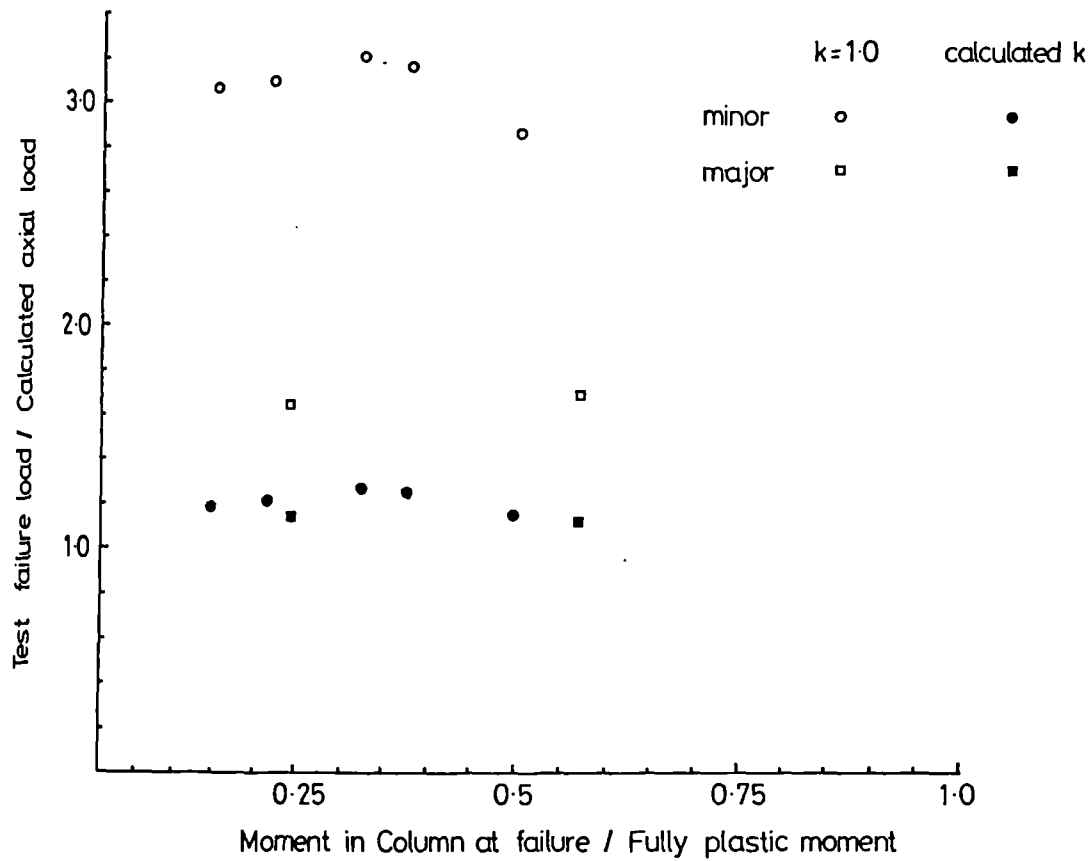


FIGURE 4.27 Moment and axial load interaction for test results

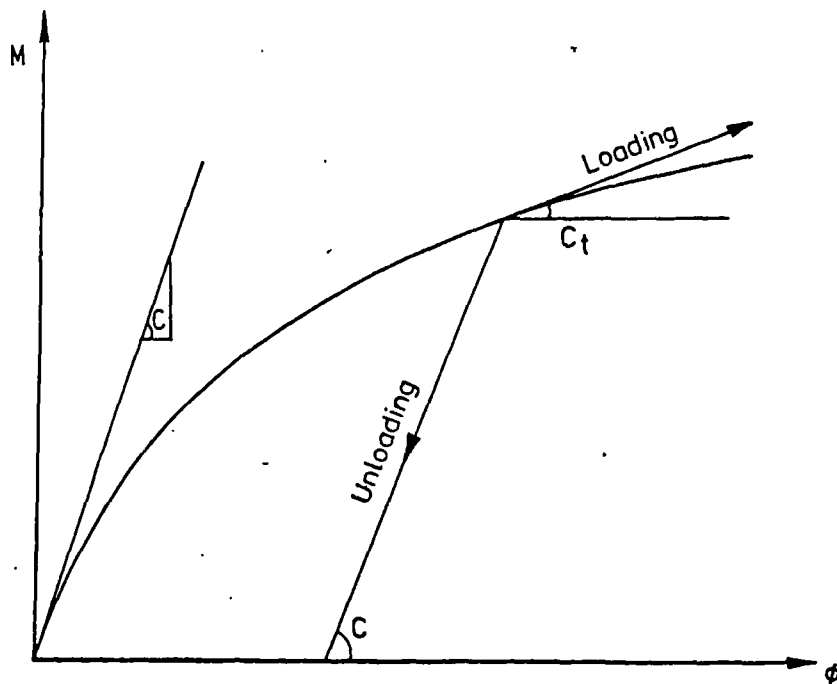


FIGURE 4.28 Typical moment-rotation response of a semi-rigid connection

5.0 FULL SCALE FRAME TESTS

5.1 Introduction

The final phase of the experimental testing programme examined the response of two full scale, flexibly connected, no sway frames loaded up to failure. Both frames were tested at the Building Research Establishment, Garston, Watford, using a facility developed there for testing full scale plane steel frames. The tests contributed towards a collaborative effort by BRE, Hatfield Polytechnic and Sheffield University to study the influence of semi-rigid bolted connections on frame behaviour. In total five frames were tested (two each by Sheffield University and Hatfield Polytechnic and the fifth by BRE) which covered the spectrum of connection stiffness, from extended end plates to flange cleats. The contents of this chapter deal only with the two frame tests for which Sheffield University were responsible though the reader is referred to publications covering the related tests.

5.2 Frames Selected for Study

It was intended that the frame tests be viewed as a logical extension of the work conducted on joints and subassemblages, and therefore the same sections, namely 254×102×22UB and 152×152×23UC, were used for both frames. As the principal aim of the work was to examine the effect of the inherent, but usually neglected, stiffness of 'simple' connections the flange cleat type of connection was selected. This type of connection is frequently used in steel frame construction, often because of the usefulness of the seat cleat during erection, and, as was demonstrated in chapter 3, it has a 'typical semi-rigid' moment-rotation response. A further requirement of the frame tests was that of realism so that convincing experimental

evidence of the capacity of flexibility connected frames could be presented. A bay width of nominally 5m was chosen as being reasonably representative and suitable for the beam section used. The storey height was 3.6m; a figure again selected as representative of current office building practice. The maximum frame size which could be tested in the laboratory was three storeys high and two bays wide. Frame designs for a three storey, two bay wide structure with beams framing into the column flange in test 1, and into the column web in test 2 were performed to BS 5950 and BS 449 (see Appendix B). The calculations were used to determine the level of beam loading which the chosen section would sustain at the ultimate condition and to estimate the 'design' capacity of the columns. Both frames were tested in-plane and with no sway ie out-of-plane buckling and lateral displacement of the frame was prevented by bracing.

5.3 Fabrication and Material Properties

Fabrication of the two frames was carried out by the workshop at BRE. Normal fabrication tolerances were adhered to. Prior to fabrication the sections were measured at several locations. Tensile tests were conducted from off-cuts of all sections used in the frames prior to testing to give a good indication of the expected test loads. The details of the sections used are contained in Appendix C. Residual stress measurements and stub column tests were conducted on lengths of column cut from the test specimens after completion of testing (see Appendix C).

5.4 Test Arrangement

Figures 5.1 and 5.2 show test frames 1 and 2 in place ready for testing. The frames were erected adjacent to the laboratory wall so that the balconies could be used as a bracing system. Nine structural

Tee sections were bolted to the balconies and aligned with bracing positions on the frame. Articulated bracing bars were fixed to the beams and columns at the positions shown in figure 5.3. Movement in the vertical direction was unhindered but out-of-plane displacements were restrained. In order to prevent sway displacements the nodes of the left-hand column (as viewed in figure 5.1) were braced to the adjacent balcony. The columns had a fixed base detail with heavy base plates bolted to the laboratory floor through the existing grid of holes spaced at 381mm centres. Figure 5.4 illustrates the nomenclature used for describing the frames when viewed from the balcony behind.

5.4.1 Loading System

Each beam was loaded independently by the system illustrated in figure 5.5. The arrangement, comprising of longitudinal and transverse RHS spreader beams, allowed loads from two steel cables to be transferred to the test beam at its quarter and three-quarter points. Each load spreading arrangement had a design capacity of 600 kN. The steel cables passed through the laboratory floor and were tensioned by two hydraulic rams reacting against the underside of the floor. A pair of hydraulic rams was controlled by a single servo-control valve. In order to achieve good control the rams, which were nominally identical, were driven at the same hydraulic pressure by splitting the supply into two branches after the oil had left the servo-valve. Two load cells with identical load-strain characteristics were used, one for each cable, and were connected together to provide an average feedback signal. A description of the complete servo-controlled hydraulic system is given by Jennings et al (5.1).

A similar loading system was used to apply axial loads to the columns. Figure 5.6 shows the detail at the head of the column. Two 1000kN rams were used to load each column. McAlloy bars, instead of steel cables, were used to apply loads to the RHS spreader. Control of the system was again achieved by control of a servo-valve, but the feedback signal was supplied by a displacement transducer mounted to the head of the column. Control by displacement rather than load was considered much safer in the inelastic range near failure.

Application of loads to the frame was achieved remotely via an LSI 11/73 minicomputer and digital to analogue converter. The software permitted the operator to load any number of beams and columns to a specified level. Safeguards, for example responding to the prompt, 'Are you sure?', a display of the loading requested for each beam and column, and the need to select a specific key to apply loads to the structure helped to minimise the possibility of 'accidents'.

5.4.2 Instrumentation

The primary requirements of the instrumentation were to measure the applied loads, the distribution of forces around the frame, the deflected shape of the structure and the moment-rotation response of the connections. These requirements were met by the instrumentation illustrated in figure 5.7.

The distribution of forces around the frame was measured using strain gauges located at three sections in each column storey, and four sections along each beam. Four gauges at each section permitted the components of axial strain, bending strains about both major and

minor axes, and torsional warping strains to be identified at that section. A linear strain distribution between gauges was assumed. Gauge positions for the frames are shown in figure 5.8.

Column and beam rotations at the connections were measured using a rotation device similar to that described by Yarimci (5.2). Figures 5.9 and 5.10 show the device. Rotation of the beam (or column) causes the thin metal strip to bend as the weight remains vertical. The relationship between rotation and the resistance of gauges mounted on the strip is linear. A total of 21 of these devices was used. Rotation of the column at the base was measured by an electro level, shown in figure 5.11. The device is quite delicate and subject to vibration and therefore when reading the output a total of 50 readings was taken and averaged in order to 'damp' the device.

Displacements of the beams and columns were measured relative to their ends. A light aluminium rig was bolted to each column storey and each beam (see figures 5.11 and 5.12). Deflections of the column or beam relative to the rig were recorded by LVDT's. For a no-sway frame the connection displacements are negligible and so the measurement system was suitable for the type of test conducted. An advantage of the system was that an additional independent instrument supporting frame was not required and left the frame free of visual obstructions.

In addition to the primary instrumentation strain gauges were also fixed to the bracing bars restraining the beams and columns, and to the holding down bolts in test frame 2. This information may be regarded as supplementary to the main investigation but was recorded with little inconvenience and it was thought to be sensible to take advantage of the test and record as much potentially useful data as was practically possible.

5.4.3 Data Acquisition System

The data logging system used to record all the test data consisted of three Solartron Orion data loggers each connected via an IEEE interface to an LSI 11/73 mini computer with a 10 mega-byte Winchester hard disk and an 8-inch floppy disk drive. The system could log and transfer as many as 1000 channels to hard disk in under 10 seconds, thereby taking a set of readings at an instant of time which is useful in the elastic plastic range. During the tests around 400 channels were used and the first 370 channels, which included the loads, strain gauges and displacement transducers, were recorded in 37 seconds. The rotation gauges were recorded last and took longer to record because the average of 50 readings was taken over a 25 second period. A total time of 120 seconds was required from start to finish for a single scan. Information recorded by the data logger was immediately transferred to a hard disk. The mini computer accessed this information and permitted the user to examine the current forces and bending moments in any member of the frame or to trace the history of a number of channels through the tests. This facility was extremely useful during the execution of a test particularly near failure. Detailed information on the data acquisition system and interrogation procedures may be found in Jennings et al (5.1).

At the completion of a test the information was transferred to an 8 inch floppy disk. For use in Sheffield the information was transferred first to a 5 $\frac{1}{4}$ inch floppy disk and then onto the PRIME computer. A suite of programs, similar to that developed at BRE, was written to interrogate the raw data on the PRIME computer in Sheffield (and also in Milan).

5.5 Test Procedure

The frames were erected and checked for alignment. Adjustment of the bracing bars allowed the frame to be pulled into position. A survey of the frame geometry was then taken and recorded. Figures 5.13 and 5.14 show the initial set up of both frames. All bolts in the connections were tightened to 160 N.m (compare chapter 3 and 4). With the frame in its test position all the instrumentation was checked. First the location of every strain gauge was ascertained and correspondence between the data logging system and interrogation programs verified. Next each displacement transducer was inspected and its calibration figure confirmed by placing a block of known dimensions between the transducer shaft and the test frame. A consistent sign convention was adopted, namely, vertical downward deflections and horizontal movement to the right (as viewed from the balcony behind the test frame) were defined as positive. A check on all the rotation gauges was made to ensure that they functioned and conformed to a convention of positive rotation defined as clockwise (when viewed from the balcony).

Preliminary testing was undertaken to check the loading apparatus and the measuring system. Each beam was loaded to a maximum of 20kN and the distribution of forces through the beam and adjacent columns was examined. The columns were loaded to a maximum of 50kN and the load at the level of each set of gauges was checked. This test enabled any discrepancies between the applied load and that recorded in the column to be identified. Particular attention was paid to those gauges on the column near the beam and column connection in frame 1 because of the possibility of local deformation of the column flanges causing spurious gauge readings. A short length of column and

beam had been tested in Sheffield to examine the extent of flange bending and the required distance of the gauges from the connection to ensure no interference occurred. A distance of 250mm above the holes for the upper cleat and 250mm below the lowest row of holes for the seat cleat had proved satisfactory. Similarly in the frame test the gauges at these locations appeared to be unaffected by secondary bending.

During preliminary testing of frame 1 the upper storey of the left hand column was damaged by overloading. This accident occurred as the column loading apparatus was being commissioned. A feedback signal to the servo-valve was not connected and on application of load the rams applied full load in an attempt to equalise the input signal and free ranging feedback signal. This resulted in severe damage to the column head and top floor beam, but fortunately the damage was not extensive and did not harm anyone. An investigation into the accident was undertaken by BRE and precautions to ensure it could not be repeated were taken. In order to proceed with the testing schedule with the minimum of disruption it was decided that the upper storey column and beam should be removed and the remaining asymmetric frame be tested.

Data files of tests on the frame were assigned names of the form
SUFxy.DAT

where x refers to the frame, either 1 or 2

and y refers to the test number, e.g. 1 was the preliminary test,

and SUF is an acronym of Sheffield University Frame

5.6 Test Frame 1

5.6.1 Loading History

Test frame 1, which featured columns bent about their major axis, was tested to failure under a combination of beam loading and column loading applied to the two three storey columns. After taking initial readings loads were applied to the five beams in small increments, and a scan was taken after each load step. The beam in the fifth position was loaded to a level corresponding to unfactored dead loads (see also Appendix B) and remained constant at this load as the remaining four beams were loaded to factored dead and imposed load. Table 5.1 summarises the load levels applied to the beams. After the beam loads had been applied the connections around the frame were inspected for signs of distress. During the beam loading phase a few audible slips occurred in the connections, but none were dramatic or unduly affected the structure. On completion of loading the beam, loads were applied to columns 2 and 3. Displacement, rather than load, was employed to control the hydraulic system used to apply axial deformation to the columns. In the first phase of column loading both columns were loaded to around 250kN in five increments. Column 3 was then kept constant as column 2 was brought up to failure in a further six increments. Having failed column 2, column 3 was similarly loaded to failure, although more increments were required due to the lower load passed into this outer column from the beams.

After failing both columns the axial deformation applied to each was released and the beam loads reduced to 53kN/beam before taking all load off the structure.

Table 5.2 gives the complete loading history for the test frame and displays the load applied to each beam and column for each scan recorded.

5.6.2 Action of Connections

A survey of the joints after loading the beams revealed some distortion, particularly in the connections to the interior column at the first and second floor levels. The beam appeared to have moved in towards the column flange by approximately 1mm at the bottom flange and had caused some distortion of the top cleat and column flanges - see figure 5.15. Connections to the outer columns were generally less distressed.

Figures 5.16 to 5.24 show the moment-rotation curves for joints C and E-L. The rotation device at D developed a fault during the test and no useable data was recorded.

A close examination of these figures illustrates the influence that the connections have on the performance of the frame. The initial phase of the curves is due to the increase of beam loads, and generally the joints behaved in a similar way, except joints I and J which were subjected to smaller moments due to the reduced load applied to their associated beam. Next the columns were axially shortened. Figure 5.25 shows the deflected shape of the frame at runs 12, 17 and 22, corresponding to completion of beam loading, equal loading of both columns and the deformed shape after failure of the central column. Considering the history of joint I, as the central column rotated anti-clockwise during loading the connection was subjected to an increasing rotation (i.e. further opening in the same direction as that due to beam loading), and this is evident as a collection of points at around 8×10^{-3} radians. The connection

immediately below I, K by contrast, was forced to close as the column at the first floor level rotated in a clockwise direction - this is clear in figure 5.23 as a reduction in moment as the connection closes and unloads. The adjacent connection F, continued to rotate in the same direction as that produced by beam loading, although an unexpected reduction in moment as rotation increased was recorded.

Turning attention to the external three storey column and connections H, J and L, a similar pattern of opening and closing connections can be seen. Figure 5.26 shows the deflected shape of the frame at runs 12, 17 and 36 (completion of beam loading, equal loading of both columns and failure of the external column). Starting with connection H, shown in figure 5.20, as columns were loaded the deformed shape produced reduced connection rotation i.e. the change in relative angle between the beam and column was in the opposite direction to that produced by beam loading. Further loading of the central column and later the external column produced further unloading of the connection. The unloading of this connection forced G, at the opposite end of the beam to attempt to accept more moment and hence an increase in rotation - compare with figure 5.19. The behaviour of joint J is difficult to interpret, but points towards the end of the test during which time the external column was brought up to failure appeared on an increasing moment path. This is in accord with the expected behaviour since the column rotated in a clockwise direction which would produce rotation in the connection in the same sense as the initial beam loading. The connection at L behaved predictably, as shown in figure 5.24. Firstly as the central column was brought to failure the connection continued to increase in rotation - this was due to the action of joint K which reduced its

moment. However when the external column was subsequently loaded to failure the connection at L unloaded as the rotation of the column decreased the connection rotation. A corresponding increase of moment caused by connection K during this phase can be seen in figure 5.24.

5.6.3 Effect of Connection Restraint on Beam Moments

Figures 5.27 to 5.31 show the change in moment at the four strain gauged sections along each beam as load was applied to the structure. In all cases the connections at each end of the beam attracted a modest moment, leading to a decrease in moment at the two loading points below the free bending moment. The moments measured at the beam connections were located 150mm from the beam end in a region of steep moment gradient; the measured moments are shown in figures 5.27 to 5.31. (The moments presented in the moment-rotation figures are those at the beam end and were extrapolated from the measured values).

As the beams were loaded the connections attracted moment in a non-linear fashion, and consequently the load and moment relationship was not linear. The distribution of moments to the beam ends and centre as the beam loading was increased is illustrated by figure 5.32 which displays the superimposed bending moment distributions for beam number 3 during the beam loading phase of the test. At a load level corresponding to the ultimate design load for the beam the connections sustained a moment of approximately 20% of the free bending moment in the centre segment of the beam.

Failure of the columns required either further rotation or relaxation of the connections with a consequent shift of moment towards the beam centre. This is evident on the load against moment diagrams (figures 5.27 to 5.31) as an increase in moment under loading

positions with no increase in applied loading (and was explained in section 5.6.2) and is also apparent in the load-deflection behaviour of the beams - see figures 5.33 to 5.37. At the end of the beam loading phase deflections of 25mm at the midspan were typical for the four fully loaded beams. This compares favourably with the deflection expected for a simply supported beam which may be readily calculated as 33mm and demonstrates the benefit of connection restraint in reducing beam deflections.

5.6.4 Bending Moment Distribution around the Frame

The semi-rigid nature of the connections obviously influences the distribution of moments around the frame. Figure 5.38 illustrates the distribution of bending moments at two load levels; run number 6 which corresponds to 53kN on each beam (dead load only) and run number 12, at which full ultimate loading was applied. Table 5.3 gives the numeric data for the distributions shown in figure 5.38. The moments attracted by the semi-rigid connections are transferred into the columns. The apparent out-of-balance at the beam-column intersections is due to the additional moment induced at the column centreline by the eccentricity of the beam end reaction. In figure 5.39 the moments at each beam and column intersection are shown along with the notational eccentricity of the beam end reaction which would be required to satisfy equilibrium. Eccentricities range between 58 and 102mm. These values compare very well with the half-depth of the column section, i.e. 76mm.

5.6.5 Effect of Connection Restraint on Column Capacity

The internal column and three storey external column were loaded by additional axial load after completing beam loading. Consider first the internal column (comprising of column lengths designated 4,

5 and 6, the last being the lowest lift) the load deflection plots for the three sections of this column are shown in figures 5.40 to 5.42. In the upper two lifts a discontinuity in the behaviour is clear at the end of beam loading and commencement of axial loading. The transition is less marked in the behaviour of the lowest lift. Beam loads produced the largest deflections in the top storey column, since the column sustained a large moment from the single beam connected at its head. The central lift deflected less due to the reduced moments introduced at the second and first floor levels. At the ground to first floor level very little deflection occurred during the beam loading phase because of the balanced loads introduced at the first floor level and the stiffness of the column base. As axial load was applied the deflections of columns 4 and 5 increased slightly, but the deflection in column 6 increased steadily. Failure occurred when the column was unable to sustain a steady axial load at an applied axial deformation - the peak value recorded was 482kN, resulting in a total load of 746kN in the lowest lift. Figure 5.44 and table 5.4 display the bending moment distribution throughout the frame at this level of loading.

A close inspection of the strain gauge readings suggests that failure was imminent in both the upper and ground to first floor lift, but the top storey appeared to be the cause of failure to carry increased loading. The failure of the top lift was peculiar to the experimental arrangement since the severity of the bending produced in the column was due in part to the absence of a column length above the third storey level coupled with the application of a high axial load, which in reality would be difficult to achieve without the presence of

upper column lifts. However the test illustrates that severe moments, considerably in excess of those based on a notional 100mm eccentricity, can be introduced into columns in asymmetric frames.

A comparison of the test load in each column lift compared with the maximum axial load predicted by the interaction equation in BS 5950 clause 4.8.3.3 is presented in table 5.5. In order to make a fair comparison calculations based on the assumed parameters (section properties, yield stress, effective length, moment distribution) have been supplemented by similar calculations based on the experimental data. Note also that the section's moment capacity has not been reduced from its fully plastic value even though the section is actually semi-compact. An assumed effective length factor of 1.0 for all columns above first floor level and 0.85 for the ground to first floor was chosen from the guidance provided by Table 24 in BS 5950 (or Appendix D in BS 449). Base rotations recorded during the test revealed that the bases were almost fixed, with a maximum rotation of only 2.9×10^{-3} radians (0.16°). Thus the assumption of a fixed base appears to be reasonable. The calculated effective lengths were based on the method suggested by Bjorhovde (5.4), which was explained in chapter 4.

The first point of note is that the calculations based on assumed values of material properties and section size underestimate the load capacity in all columns except number 4. Variations in section sizes and material properties clearly influence the column strength but the designer can do no more than use the suggested, expected figures. A more useful comparison may be made by using the measured section and material properties. In column 4 the influence of the actual moments present in the column compared with the assumed

values is clear in case 2 and case 4 - the former underestimates the moments in the column and consequently overpredicts the axial capacity at 652kN, the latter limits the axial load to 598kN due to local capacity. This reflects what happened in the test where severe moments produced at the head of the column caused a failure predominantly governed by material strength and not overall column behaviour.

Turning attention to column 6 cases 2 and 5 which predict column capacity at 803 and 801kN. This illustrates the 'trade off' between two compensating assumptions; in case 2 the moments have been underestimated since no moment would be assumed to be transmitted at the first floor level, but the effective length of the column has been slightly underestimated also, and the two assumptions have led to a reasonable prediction of axial capacity very similar to that of case 5, which uses the experimentally recorded values of moment induced in the column and a more considered value for the effective length factor.

Having failed the internal column loads were then applied to the external three storey column. Figure 5.45 and table 5.6 show in graphic and numeric detail the distribution of moments around the frame at maximum load in the external column resulting in a deformed shape as depicted in figure 5.26. Again the moments transmitted to the column at the third storey level were large and caused appreciable deformation in the column as noted from the load-deflection plot in figure 5.43. An examination of the strain gauges indicates that failure occurred in the lowest lift at an axial load of between 769 and 835kN. (Some doubt of the accuracy of the column load measuring system has been raised by the calibrations conducted at the end of the tests. However in this case the loads predicted by the strain gauges

appear to be high, which suggests that the rather high value of E measured in the stub column test may be in error - see Appendix C.) The prediction of cases 2, 4 and 5 are all reasonably close to 769kN.

5.7 Test Frame 2

5.7.1 Loading History

The second test frame was a three storey, two bay symmetrical frame with beams framed into the column webs. Loads were applied to the beams in eleven increments as summarised in table 5.1. Loading of beam 5 was restricted to 53kN, corresponding to unfactored dead load; the other beams were loaded to ultimate design values. Next the three columns were loaded by axial deformation in three increments of 1.0mm and the resulting applied load recorded. Column 1 (i.e. the left hand external column) was then brought up to failure by successively incrementing the axial deformation in 1.0mm and, near failure, 0.5mm steps. Similarly column 2, the internal column, was failed by gradually increasing the axial load. The test was concluded by removing the applied axial loads and finally the beam loads. In table 5.7 the load applied to each part of the structure at each scan during the test is documented.

Throughout test 2 the lateral movement of joint C was monitored using a theodolite. This was undertaken to verify that the frame was effectively braced. A maximum displacement of only 1mm was observed.

5.7.2 Action of Connections

The moment-rotation curves for the dozen joints in the frame are presented in figures 5.46 to 5.57. The action of the connections, and their role in contributing to the frame's stability, may be discussed with reference to these figures.

During beam loading all the connections loaded up reasonably smoothly (except A which was rather erratic). The difference in performance of connections to the external columns (A, C, E, H, J, L) and those to the internal columns (B, D, F, G, I, K) is quite apparent. Those connected to the internal column were able to sustain quite large moments, 15 to 20kN.m, particularly where the loading on adjacent spans was equal (compare joints B/G, F/K with D/I). However those to the external column behaved more flexibly due both to the absence of a connection on the opposite side and column flexibility and moments in the range 10-15kN.m were typical.

Consider next the behaviour of the connections to the left hand external column as the test proceeded. Figure 5.58 shows the deformed shape of the frame at the completion of beam loading, commencement of loading to the external column only, and after failure. Beam loading produced considerable deformation of the top lift and addition of an axial load caused further lateral deflection. This produced rotation in connections A and E in a direction opposite to that experienced previously and a reduction in moment can be seen in figures 5.46 and 5.50. In joint C further positive rotation was experienced as the column deformed and the moment-rotation curve continued to follow a loading path (figure 5.48). A sympathetic action in the connections B, D and F at the opposite ends of beams 1 to 3 is evident in figures 5.47, 5.49 and 5.51. The behaviour of connections A and B is confused by a slip which occurred between scans 15 and 16 which caused connection B to lose moment, but thereafter as the column was further loaded it attempted to pick up more moment, in contrast to A which continued

to unload. However comparisons of the figures for connections C and D, and E and F very clearly show one connection loading thus forcing its companion to lose moment, and vice-versa.

The internal column was next brought up to failure in several increments of displacement. Figure 5.59 shows the deformed shape of the structure at scans 12, 27 and 36 (i.e. end of beam loading, failure of column 1 and failure of the internal column). The deformations produced during the earlier loading sequences were amplified as the column was loaded axially causing the response of connections D and F to continue further - see figures 5.49 and 5.50. The connections on the adjacent side of the column behaved oppositely. This is best illustrated by comparing the response of connection D and I, and F and K. As D unloaded, I continued to load. As F loaded, K began to unload.

Finally the column applied axial loads were released, causing reloading of some connections and further unloading in others, followed by removal of beam loads.

5.7.3 Effect of Connection Restraint on Beam Moments

The relationship between applied load and resulting moment at four locations for each beam is shown in figures 5.60 to 5.65. As load was applied to the beams the connections attracted some moment. Moments were attracted to the joints most readily early in the loading, when the joint stiffness was greatest. The distribution of moment in beam 3 is shown in figure 5.66, which superimposes the changing bending moment diagrams as the beam was loaded. At a load level corresponding to the ultimate design load for the beam the connections sustained

moments in the range 15-25% of the free bending moment dependent on the stiffness of the column and the presence of an equal load on an adjacent span.

Loading of the left and central column required a response from the connections, some underwent further rotation whilst others relaxed producing a shift of moment towards the beam centre. This is most clearly shown in figures 5.60 to 5.62 for beams 1 to 3, which were affected by failure of both columns, whereas beams 4 to 6 (figures 5.63 to 5.65), were affected mainly by the failure of the central column. For beams 1 to 3 the moment under the loading points increased significantly, but for beams 4 to 6 the change in moment was less pronounced since only the left hand connections were actively involved in restraining the internal column (see particularly beam 6).

Beam deflections were reduced by the connection restraint up to ultimate design loads - see figures 5.67 to 5.72. Relative central deflections of around 27mm were recorded at this stage, which is significantly better than the 33mm which is suggested by simple hand calculation. At the serviceability limit state the change in deflection between dead load and dead and live load is around 7mm; a simply supported beam would deflect by 7.7mm. During column loading, when the connections were engaged in restraining the column, beam deflections naturally increased, typically to around 35 to 40mm.

5.7.4 Bending Moment Distribution around the Frame

Figure 5.73 is the bending moment distribution around the frame at load levels corresponding to dead load on all six beams, and secondly at ultimate design load on five of the beams. Table 5.8 gives the numeric data for the above two distributions. The top lifts of the two external columns were subjected to quite high moments (12.8kN.m) which

caused considerable deflection. At the second and first floor levels slightly higher moments were transmitted to the column, but with less detriment because it was shared between the upper and lower column lengths. It would appear that the connections at the top of the two external columns, A and H, were prevented from transferring larger moments by the columns' flexibility, which illustrates that frame behaviour is dependent on the interaction of all components and cannot be completely understood simply by consideration of the individual elements in isolation. The presence of a connection on each side of the internal column reduced the moment transferred to the column and allowed larger moments to be developed in both connections. At the second floor level the modest load on beam 5 restricted the moment induced in connection I and also D, the right hand end of the adjacent beam.

A check of the state of equilibrium at each beam to column intersection is made in figure 5.74. In all cases the out-of-balance is small, less than 1.5kN.m, and where appropriate this out-of-balance has been converted to an equivalent eccentricity through which the beam end reaction would be required to act. Eccentricities ranging from 7 to 29mm were calculated.

5.7.5 Effect of Connection Restraint on Column Capacity

After applying full design loads to the beams all three columns were simultaneously loaded axially. The hydraulic loading gear was displacement controlled and small deflection increments (about 1.0mm) were applied to the columns until an axial load of approximately 150kN was generated in each. The left hand external column was selected as the first to be loaded to failure whilst the load (or more correctly the applied displacement) in the remaining two columns was held

constant. Table 5.7 presents the full loading history. This first column resisted axial deformation until the applied load reached a recorded value of 451kN (scan 27). Figure 5.58, figure 5.76 and table 5.9 show the deflected shape and bending moment distribution at this stage in the test from which it is clear that failure occurred in the top lift due to a combination of excessive bending produced by the beam loading and the effect of the applied axial load. Figures 5.76 to 5.78 show the load-deflection response of each column lift, which confirm the point of failure.

A comparison of the experimental column capacities with design values is made in table 5.10. In calculating the axial load capacity the interaction equation used in BS 5950 clause 4.8.3.3. have been used (the less conservative of the 'simple' and more 'exact' method is tabulated). The moment capacity about the minor axis has been taken as the product of the plastic section modulus and yield stress, rather than the elastic section modulus and yield stress which is suggested for a semi-compact section, on the basis that moments in excess of the first yield value were recorded and also that the classification of sections bent about their minor axis producing a stress gradient through the compression flange are not expressly covered in Table 7 of BS 5950. The most striking feature of the comparison is that the predicted capacities are substantially lower than the test results, particularly where the measured moments at failure are used. This suggests that the interaction equation is not accurate in this case, though it is conservative. This point is addressed in chapter 7.

The internal column was next brought up to failure in several small increments of displacement resulting in the loading shown in Table 5.9. Figures 5.59 and 5.79 and table.5.11 show the deflected

shape and bending moment distribution at scan 36. The largest deformations occurred at the centre of the first to second floor level column due to the out-of-balance beam loads at level 2. Figures 5.80 and 5.81 are the load-deflection plots for columns 5 and 6 - both appear to be flattening out suggesting failure was imminent in both. A close examination of the strain gauges in the centre of column 5 revealed that some major axis instability had occurred.

The results of the comparison of test results and design predictions made in table 5.10 once again illustrates that the interaction equation is very conservative. For this reason it is difficult to quantify the improvement in response of the columns due to the semi-rigid nature of the connections. The calculations show the likely improvements (compare the results of case 2 and 3 and case 4 and 5) of including the effect of inherent joint stiffness and associated beam flexibility into the determination of effective lengths. Section 5.7.2 explained the action of the joints throughout the test and demonstrated how they influence the performance of the columns in the frame.

5.8 Conclusions

Experiments on two three-storey, two-bay bare steel frames with flange cleat beam to column connections have been described and the results reported. The tests illustrated that the rotational stiffness of the simple connections influenced the distribution of moments around the frame, reduced beam deflections and enhanced column capacities. Moments transmitted by the connections were considerably greater than assumed values obtained from the beam end reaction acting at a nominal 100mm eccentricity. The moment transferred to the column was found to be dependent on the balance of stiffness of the connec-

tion, beam and column. During failure of the column connections on either side rotated in the same direction causing unloading of one and continued loading of the other. The unloading connection has the greater stiffness and hence restrains the column more than the adjacent, loading connection.

Criticism of the experiments may be directed towards the loading arrangement at the head of the columns and the measurement of the load applied. Rotation of the column head caused the applied load to be eccentric. In view of the size of the sections necessary to apply loads to the column head it is difficult to conceive of an arrangement which would have overcome this problem and yet remained stable and safe. It may have been prudent to have applied lower loads to the third floor beams and hence reduce the rotation at the column head. Strain gauged bars were used to record the loads in the McAlloy bars which applied load to the columns rather than commercial loadcells. With the benefit of hindsight the bars appear to lack accuracy and repeatability - a fact confirmed by recalibration after the tests.

Comparison of the column failure loads with those predicted by BS 5950 showed reasonable correlation for the major axis test, but the minor axis column capacities were considerably underestimated.

In the next chapter the results of the two frame tests are compared with the predictions of a finite element frame analysis program.

References

- 5.1 Jennings, D.A., Moore, D.B. and Sims, P.A.C.
'Instrumenting and testing bolted steel frame structures'
Proceedings, Determination of Dangerous Stress Levels and Safe
Operation Conditions, Edinburgh, August 1986.
- 5.2 Yarimci, E., Yura, J.A. and Lu, L.W.
'Rotation gauge for structural research'
Experimental Mechanics, November 1968, p. 525-526.
- 5.3 Moore, D.B. and Sims, P.A.C.
'Tests on full-scale steel frames with semi-rigid connections'
Proceedings, Steel Structures - Recent Research Advances, Budva,
September 1986.
- 5.4 Bjorhovde, R.
'Effect of end restraint on column strength - practical applica-
tions'
AISC, Engineering Journal, First Quarter, 1984, p. 1-13.

TOTAL LOAD PER BEAM (KN)	COMMENTS
10.0	
20.0	
30.0	
40.0	
53.0	unfactored dead load only (1.0D.L.)
60.0	
74.2	factored dead load only (1.4D.L.)
79.5	unfactored dead + imposed load (1.0D.L.+1.0L.L)
90.0	
100.7	factored dead + unfactored imposed (1.4D.L.+1.0L.L)
116.6	factored dead + factored imposed (1.4D.L.+1.6L.L)

TABLE 5.1 Load increments for application of beam loading

Test SUF12 Major Axis Frame

Scan	Total Load per Beam (kN)					Column Load (kN)	
	beam 2	beam 3	beam 4	beam 5	beam 6	col. 2	col. 3
1	0.00	0.00	0.00	0.00	0.00	0.00	0.00
2	8.72	8.01	8.78	8.82	8.81	0.00	0.00
3	18.88	18.09	19.08	19.50	19.60	0.00	0.00
4	29.02	28.21	29.29	30.17	30.35	0.00	0.00
5	39.18	38.39	39.52	40.86	40.89	0.00	0.00
6	52.36	51.60	52.77	54.71	54.37	0.00	0.00
7	59.51	58.76	59.93	54.69	61.63	0.00	0.00
8	73.93	73.24	74.46	54.68	76.36	0.00	0.00
9	79.31	78.64	79.84	54.70	81.81	0.00	0.00
10	90.02	89.36	90.61	54.69	92.70	0.00	0.00
11	100.73	100.02	101.34	54.68	103.52	0.00	0.00
12	117.03	116.21	117.70	54.71	119.98	0.00	0.00
13	117.12	116.12	117.57	54.68	119.75	41.40	41.92
14	117.12	116.10	117.58	54.68	119.75	97.84	98.00
15	117.13	116.09	117.58	54.69	119.76	155.90	153.65
16	117.15	116.08	117.61	54.71	119.76	229.79	207.36
17	117.15	116.09	117.56	54.69	119.75	297.25	259.78
18	117.17	116.14	117.52	54.69	119.75	367.23	252.12
19	117.16	116.15	117.55	54.67	119.74	444.58	252.31
20	117.19	116.16	117.59	54.71	119.77	461.38	247.43
21	117.20	116.17	117.57	54.71	119.77	471.94	244.84
22	117.18	116.15	117.54	54.69	119.76	482.63	242.96
23	117.18	116.14	117.51	54.68	119.76	415.35	246.39
24	117.16	116.14	117.54	54.66	119.74	412.72	305.87
25	117.16	116.15	117.52	54.67	119.74	414.10	369.41
26	117.16	116.15	117.53	54.67	119.75	415.06	422.12
27	117.15	116.15	117.55	54.66	119.73	413.75	474.30
28	117.14	116.16	117.52	54.66	119.73	412.00	506.55
29	117.12	116.15	117.60	54.64	119.72	408.18	531.92
30	117.11	116.14	117.63	54.64	119.72	407.51	548.62
31	117.11	116.16	117.67	54.65	119.74	406.78	563.28
32	117.10	116.15	117.62	54.64	119.72	409.45	575.99
33	117.11	116.17	117.60	54.65	119.73	409.37	589.31
34	117.12	116.18	117.59	54.66	119.75	409.05	601.94
35	117.12	116.18	117.56	54.66	119.74	408.15	613.82
36	117.11	116.18	117.55	54.65	119.74	407.75	622.88
37	117.10	116.17	117.58	54.64	119.73	406.38	608.29
38	117.13	116.23	117.44	54.64	119.75	86.57	416.59
39	117.13	116.25	117.58	54.64	119.72	-3.93	1.31
40	52.60	51.66	52.54	54.62	54.14	-4.37	0.49
41	0.42	0.13	5.14	-0.10	1.28	5.83	0.23

TABLE 5.2 Loading history of test frame 1

COLUMN	Mmt AT TOP (kN.m)	Mmt AT MIDDLE (kN.m)	Mmt AT BOTTOM (kN.m)
2	11.0	1.92	-7.18
3	6.32	0.71	-3.42
4	10.39	3.87	-2.73
5	-5.26	-2.38	0.91
6	3.34	1.40	-0.33
7	-11.65	-1.92	-7.70
8	-7.99	-0.04	8.00
9	-4.96	-1.23	1.84

BEAM	LEFT END (kN.m)	LEFT LOAD (kN.m)	RIGHT LOAD (kN.m)	RIGHT END (kN.m)
2	-8.06	21.81	20.12	-11.24
3	-10.41	20.37	21.49	-7.64
4	-8.79	22.39	21.61	-9.03
5	-9.00	21.90	19.95	-12.95
6	-10.35	21.16	20.72	-10.52

TABLE 5.3 Distribution of moments at beam loads of 53kN and 116kN (runs 6 and 12) - frame 1

TABLE 5.3 continued

COLUMN	Mmt AT TOP (kN.m)	Mmt AT MIDDLE (kN.m)	Mmt AT BOTTOM (kN.m)
2	21.21	5.50	-10.43
3	11.65	0.21	-8.07
4	18.27	7.66	-3.32
5	-13.08	-4.38	5.36
6	5.01	2.16	-0.61
7	-19.62	-4.93	9.58
8	-6.67	1.76	10.18
9	-11.00	-2.84	4.12

BEAM	LEFT END (kN.m)	LEFT LOAD (kN.m)	RIGHT LOAD (kN.m)	RIGHT END (kN.m)
2	-15.51	60.88	59.69	-17.68
3	-16.57	60.72	59.60	-14.75
4	-14.93	63.19	63.58	-14.90
5	-10.29	20.77	19.18	-13.56
6	-14.89	64.00	61.71	-16.50

COLUMN	Mmt AT TOP (kN.m)	Mmt AT MIDDLE (kN.m)	Mmt AT BOTTOM (kN.m)
2	17.28	3.18	-11.14
3	9.96	0.83	-5.66
4	17.17	8.82	-6.48
5	-11.89	-6.85	4.43
6	1.38	3.67	1.15
7	-16.51	-4.82	7.85
8	-6.23	0.42	8.05
9	-14.57	-2.88	7.62

BEAM	LEFT END (kN.m)	LEFT LOAD (kN.m)	RIGHT LOAD (kN.m)	RIGHT END (kN.m)
2	-11.46	63.62	63.68	-12.18
3	-15.57	62.37	61.53	-11.87
4	-11.14	65.57	65.81	-9.56
5	-10.58	20.95	20.75	-11.22
6	-10.15	65.99	63.02	-17.34

TABLE 5.4 Distribution of moments at failure of internal column - frame 1

COLUMN	EFFECTIVE LENGTHS (m)	COLUMN CAPACITY BASED ON BS5950 INTERACTION EQUATION (Cl. 4.8.3.3) VALUES IN kN					TEST LOADS (kN)		
		ASSUMED	CALCULATED	CASE 1	CASE 2	CASE 3	CASE 4	CASE 5	STRAIN GAUGES
4	3.60	3.00	578.0	651.8	691.9	598.3*	598.3*	535.2	541.4
5	3.60	3.16	633.6	707.2	739.8	671.5	694.6*	639.8	627.6
6	2.95	2.69	723.8	803.2	820.8	783.8	801.0	783.8	745.6
7	3.60	3.20	603.8	691.4	719.4	691.3	708.1*	728.2	681.7
8	3.60	3.37	665.3	752.7	770.6	679.1	695.2	764.8	709.0
9	2.95	2.69	689.4	781.8	798.4	764.4	780.7	834.7	769.9

CASE 1 assumed moments, assumed section and material properties, assumed effective length
 CASE 2 assumed moments, measured section and material properties, assumed effective length
 CASE 3 assumed moments, measured section and material properties, assumed effective length
 CASE 4 measured moments, measured section and material properties, calculated effective length
 CASE 5 measured moments, measured section and material properties, assumed effective length

Values marked * are limited by local capacity

TABLE 5.5 Comparison of test and design loads for columns in test frame 1

COLUMN	Mmt AT TOP (kN.m)	Mmt AT MIDDLE (kN.m)	Mmt AT BOTTOM (kN.m)
2	18.35	2.84	-12.90
3	8.09	0.77	-4.23
4	21.05	10.16	-6.30
5	-9.74	-7.40	0.76
6	1.56	4.13	2.38
7	-11.85	-5.40	9.10
8	-4.11	4.95	12.50
9	1.03	1.67	5.12

BEAM	LEFT END (kN.m)	LEFT LOAD (kN.m)	RIGHT LOAD (kN.m)	RIGHT END (kN.m)
2	-12.56	63.57	64.05	-11.92
3	-15.49	62.43	61.30	-12.59
4	-15.35	65.50	66.07	-2.00
5	-12.06	20.09	21.04	-10.36
6	-14.65	65.86	64.67	-7.52

TABLE 5.6 Distribution of moments at failure of external column - frame 1

Test SUF22 Minor axis frame

Scan	Total Load per Beam (kN)						Column Load (kN)		
	beam 1	beam 2	beam 3	beam 4	beam 5	beam 6	col. 1	col. 2	col. 3
1	0.00	0.00	0.00	0.00	0.00	0.00	0.00	0.00	0.00
2	9.33	8.53	8.60	8.63	8.91	8.58	0.00	0.00	0.00
3	19.91	18.70	18.74	18.81	19.62	19.11	0.00	0.00	0.00
4	30.47	28.88	28.91	29.04	30.32	29.69	0.00	0.00	0.00
5	41.02	39.05	39.07	39.26	41.01	40.09	0.00	0.00	0.00
6	54.66	52.26	52.26	52.51	54.87	53.53	0.00	0.00	0.00
7	62.08	59.49	59.49	59.75	54.93	60.81	0.00	0.00	0.00
8	77.00	73.97	73.94	74.27	54.90	75.45	0.00	0.00	0.00
9	82.50	79.37	79.36	79.63	54.90	80.87	0.00	0.00	0.00
10	93.58	90.10	90.05	90.46	54.89	91.74	0.00	0.00	0.00
11	104.58	100.85	100.69	101.28	54.89	102.57	0.00	0.00	0.00
12	121.31	117.13	116.81	117.61	54.88	118.93	0.00	0.00	0.00
13	121.28	117.24	116.77	117.62	54.86	118.60	36.30	14.47	49.66
14	121.27	117.23	116.78	117.65	54.86	118.60	85.24	46.33	99.96
15	121.23	117.21	116.77	117.60	54.82	118.57	132.76	82.87	153.13
16	121.25	117.22	116.82	117.60	54.84	118.59	176.03	135.05	145.20
17	121.25	117.24	116.85	117.61	54.85	118.60	225.51	134.98	143.67
18	121.26	117.25	116.85	117.61	54.84	118.59	272.50	134.76	144.67
19	121.25	117.25	116.87	117.61	54.84	118.58	315.18	135.70	149.84
20	121.27	117.27	116.87	117.63	54.86	118.61	335.66	136.79	150.89
21	121.25	117.25	116.84	117.61	54.84	118.59	355.54	138.32	147.63
22	121.27	117.27	116.83	117.62	54.86	118.61	376.03	138.09	144.99
23	121.27	117.28	116.85	117.63	54.86	118.61	393.76	138.77	144.12
24	121.27	117.28	116.86	117.63	54.86	118.60	412.68	140.78	142.37
25	121.28	117.27	116.91	117.63	54.86	118.58	417.87	143.33	139.75
26	121.28	117.28	116.93	117.64	54.87	118.58	436.98	143.22	137.74
27	121.28	117.26	116.90	117.60	54.85	118.55	450.75	143.87	135.97
28	121.25	117.24	116.88	117.61	54.84	118.56	433.47	199.81	142.10
29	121.26	117.25	116.83	117.59	54.84	118.56	429.99	251.95	140.40
30	121.25	117.24	116.83	117.58	54.84	118.56	427.06	277.83	138.74
31	121.29	117.26	116.88	117.59	54.87	118.57	424.69	302.25	137.67
32	121.28	117.25	116.93	117.58	54.88	118.56	424.03	326.16	136.64
33	121.28	117.25	116.96	117.58	54.88	118.56	422.94	349.31	135.38
34	121.26	117.23	116.95	117.56	54.87	118.53	421.86	371.32	135.19
35	121.26	117.22	116.93	117.56	54.86	118.52	420.17	394.14	135.14
36	121.26	117.23	116.88	117.57	54.87	118.53	418.39	411.90	134.56
37	121.25	117.22	116.90	117.57	54.88	118.54	365.70	404.36	137.53
38	121.27	117.18	117.08	117.62	54.87	118.51	-11.82	85.32	161.26
39	121.27	117.18	117.03	117.55	54.87	118.49	-12.26	3.69	0.15
40	82.25	79.60	79.28	79.82	54.86	80.38	-12.42	3.46	-6.72
41	54.40	52.66	52.34	52.78	54.87	53.20	-12.53	19.26	-6.81
42	-0.16	-0.12	-0.16	-0.16	-0.15	0.30	-12.63	40.13	27.71

TABLE 5.7 Loading history of test frame 2

COLUMN	Mmt AT TOP (kN.m)	Mmt AT MIDDLE (kN.m)	Mmt AT BOTTOM (kN.m)
1	5.99	0.50	-4.86
2	3.86	-0.28	-4.20
3	4.30	0.59	-2.12
4	-0.90	0.03	0.79
5	-0.25	-0.62	-0.55
6	1.32	0.27	-0.19
7	-6.30	-0.62	4.90
8	-4.69	0.22	4.88

BEAM	LEFT END (kN.m)	LEFT LOAD (kN.m)	RIGHT LOAD (kN.m)	RIGHT END (kN.m)
1	-6.03	25.46	21.88	-13.00
2	-7.98	22.89	21.14	-11.78
3	-7.87	23.92	21.51	-11.90
4	-12.15	23.08	26.42	-6.29
5	-11.18	24.10	25.51	-8.85
6	-13.96	21.14	24.45	-8.27

TABLE 5.8 Distribution of moments at beam loads of 53kN and 116kN (runs 6 and 12) - frame 2

TABLE 5.8 continued

COLUMN	Mmt AT TOP (kN.m)	Mmt AT MIDDLE (kN.m)	Mmt AT BOTTOM (kN.m)
1	12.05	1.53	-8.91
2	5.44	-0.77	-6.19
3	9.79	0.92	-5.73
4	-0.64	0.39	1.61
5	-2.15	-1.50	0.36
6	3.33	0.54	-1.17
7	-12.82	-3.15	6.85
8	-4.19	1.62	6.65
9	-7.75	-2.04	3.95

BEAM	LEFT END (kN.m)	LEFT LOAD (kN.m)	RIGHT LOAD (kN.m)	RIGHT END (kN.m)
1	-12.23	69.73	64.89	-21.67
2	-14.13	67.94	69.69	-16.64
3	-15.51	67.75	65.20	-19.74
4	-21.04	68.55	68.77	-12.58
5	-12.76	22.45	24.12	-10.35
6	-22.78	67.66	67.87	-13.53

COLUMN	Mmt AT TOP (kN.m)	Mmt AT MIDDLE (kN.m)	Mmt AT BOTTOM (kN.m)
1	15.57	9.80	-14.81
2	4.65	-5.95	-3.42
3	11.14	-0.43	-7.88
4	0.55	0.54	0.23
5	-2.18	-5.83	2.94
6	4.03	0.42	-0.94
7	-12.65	-5.60	5.97
8	-5.18	2.00	7.54
9	-7.76	-2.78	4.55

BEAM	LEFT END (kN.m)	LEFT LOAD (kN.m)	RIGHT LOAD (kN.m)	RIGHT END (kN.m)
1	3.83	72.29	68.58	-22.59
2	-14.78	68.69	70.65	-17.04
3	-9.96	69.99	67.08	-21.00
4	-22.40	70.18	69.45	-9.41
5	-13.75	21.86	24.26	-9.92
6	-22.39	68.48	68.37	-13.60

TABLE 5.9 Distribution of moments at failure of external column - frame 2

COLUMN	EFFECTIVE LENGTHS (m)		COLUMN CAPACITY BASED ON BS5950 INTERACTION EQUATION (cl. 4.8.3.3) VALUES IN kN					TEST LOADS (m)		APPLIED LOADS (kN)
	ASSUMED	CALCULATED	CASE 1	CASE 2	CASE 3	CASE 4	CASE 5	STRAIN GAUGES	ε	
1	3.60	2.93	340.3	378.1	478.3	307.5	342.5*	501.6		511.4
2	3.60	3.12	362.1	390.2	464.6	377.8	449.9	546.1		570.1
3	2.95	2.52	452.4	493.4	569.4	419.8	484.5	626.5		628.5
4	3.60	2.39	368.9	393.8	592.9	398.6	600.1	521.1		531.4
5	3.60	2.55	368.9	393.8	564.9	346.2	496.6	615.8		617.5
6	2.95	2.41	479.4	513.8	611.1	459.4	546.3	813.4		735.2

CASE 1 assumed moments, assumed section and material properties, assumed effective length
 CASE 2 assumed moments, measured section and material properties, assumed effective length
 CASE 3 assumed moments, measured section and material properties, assumed effective length
 CASE 4 measured moments, measured section and material properties, calculated effective length
 CASE 5 measured moments, measured section and material properties, assumed effective length

Values marked * are limited by local capacity cl. 4.8.3.2

TABLE 5.10 Comparison of test and design loads for columns in test frame 2

COLUMN	Mmt AT TOP (kN.m)	Mmt AT MIDDLE (kN.m)	Mmt AT BOTTOM (kN.m)
1	17.64	10.63	-16.83
2	3.35	-6.83	-2.11
3	12.54	-0.29	-8.80
4	0.74	0.89	0.39
5	-0.31	-10.47	6.59
6	3.73	-1.52	1.17
7	-12.43	-6.16	4.97
8	-7.20	1.63	8.93
9	-6.56	-2.55	3.86

BEAM	LEFT END (kN.m)	LEFT LOAD (kN.m)	RIGHT LOAD (kN.m)	RIGHT END (kN.m)
1	2.80	71.79	69.20	-20.51
2	-15.00	69.22	72.04	-12.64
3	-9.62	70.19	67.78	-21.40
4	-19.71	70.47	69.38	-8.65
5	-13.43	21.90	23.73	-10.81
6	-18.31	69.10	68.54	-13.81

TABLE 5.11 Distribution of moments at failure of internal column - frame 2

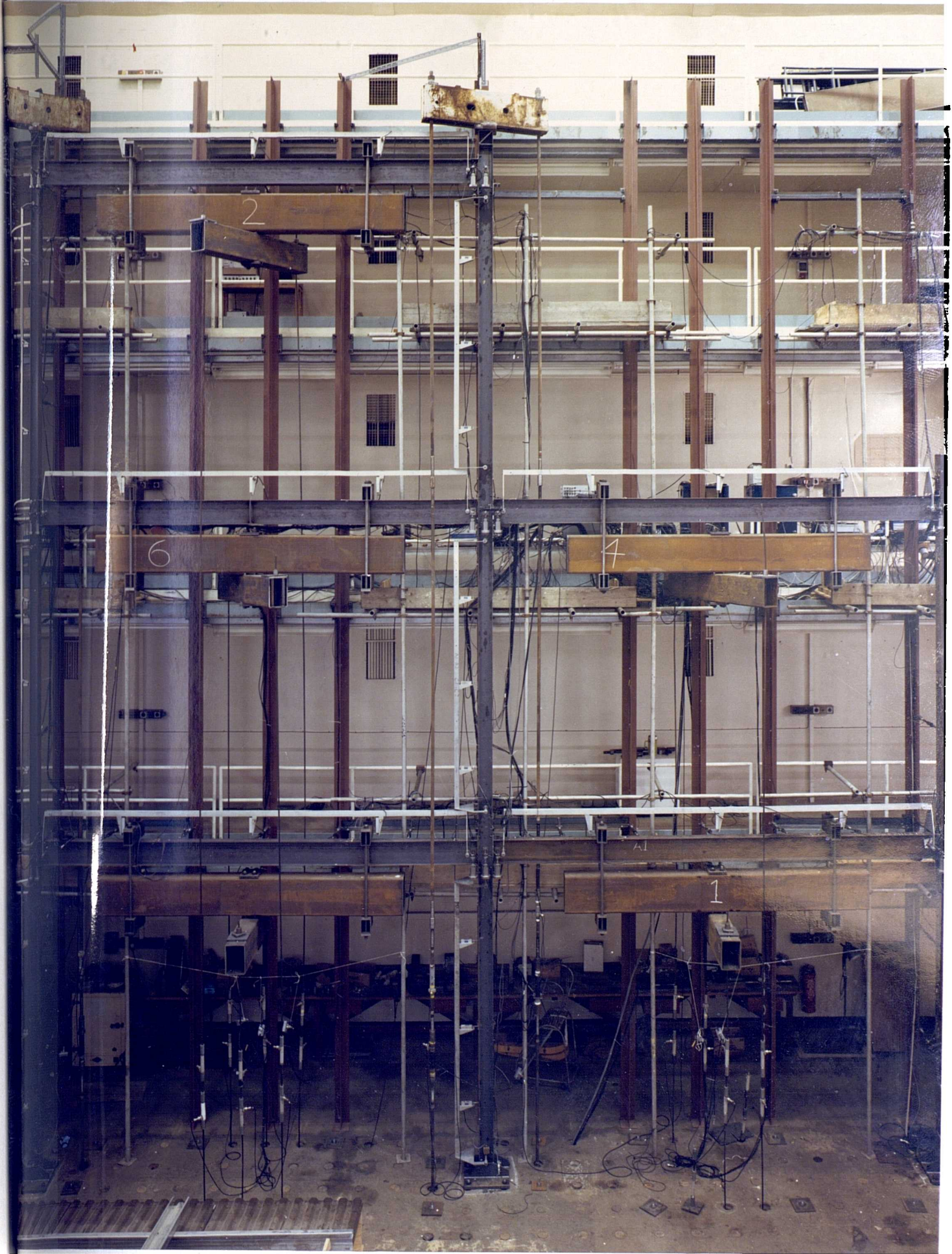
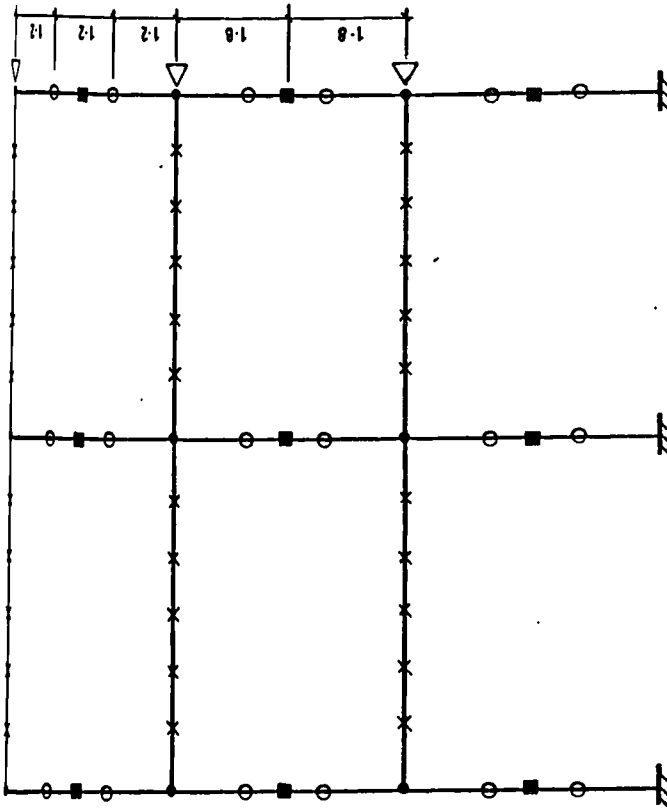


FIGURE 5.1 Frame 1 before testing (major axis)



beams laterally restrained at 812mm c/c X

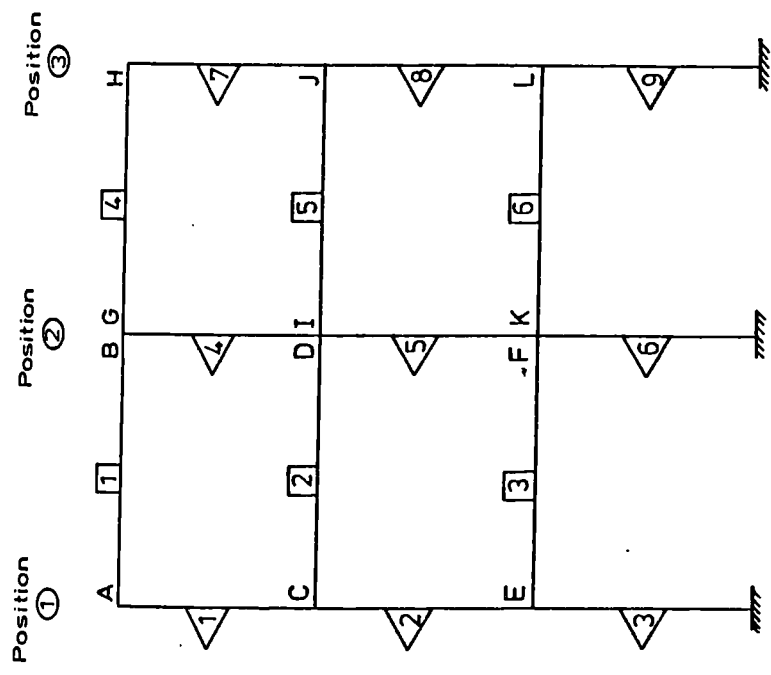
frames restrained laterally at nodes •

major axis columns - minor axis buckling prevented at ○

minor axis columns - major axis buckling prevented at ■

sway bracing ◁

FIGURE 5.3 Out-of-plane action bracing locations



⊗ Column position

⊠ Beam number

◁ Column number

View from balcony

FIGURE 5.4 Frame nomenclature

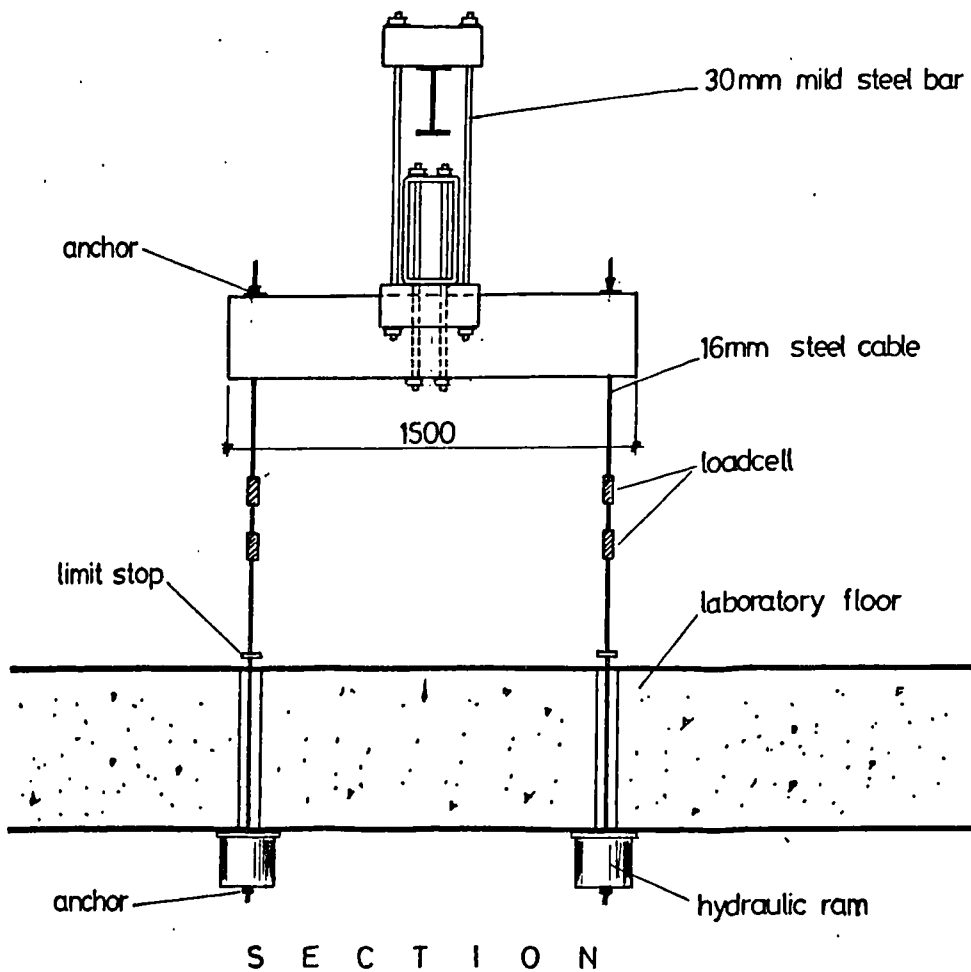
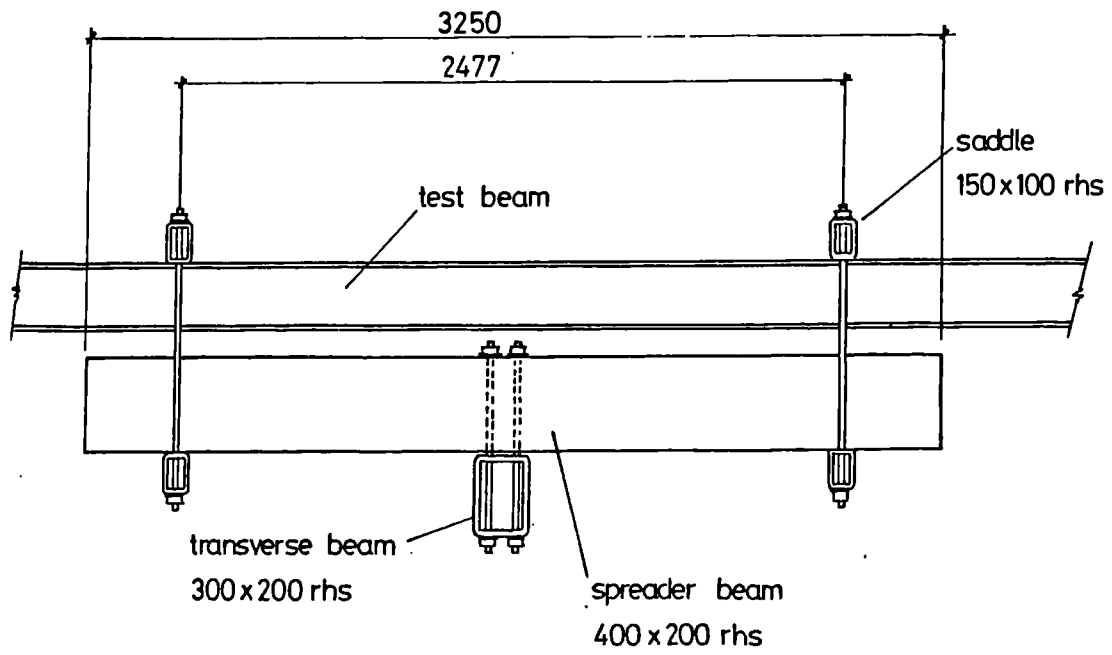


FIGURE 5.5 Hydraulic beam loading arrangement

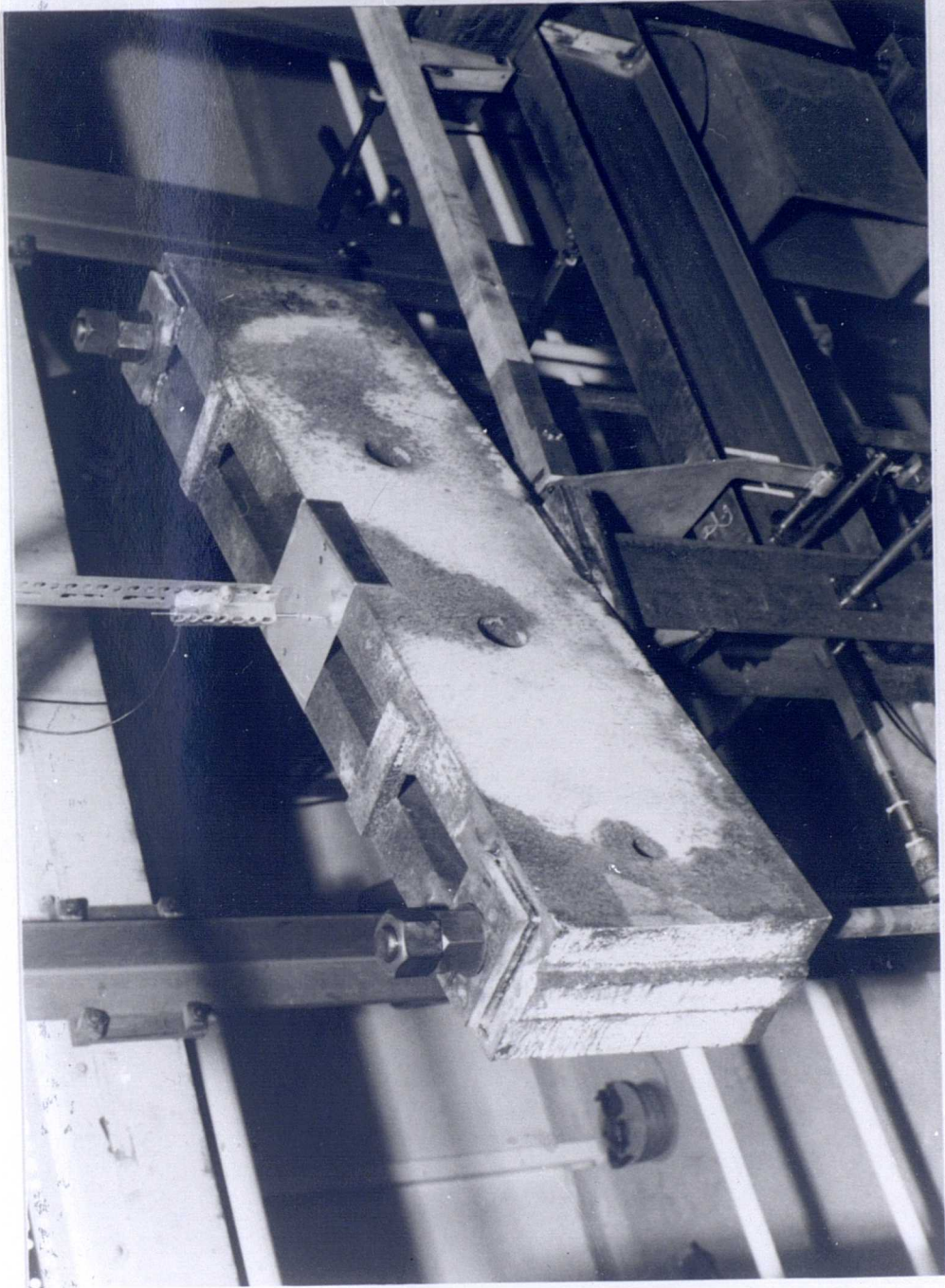
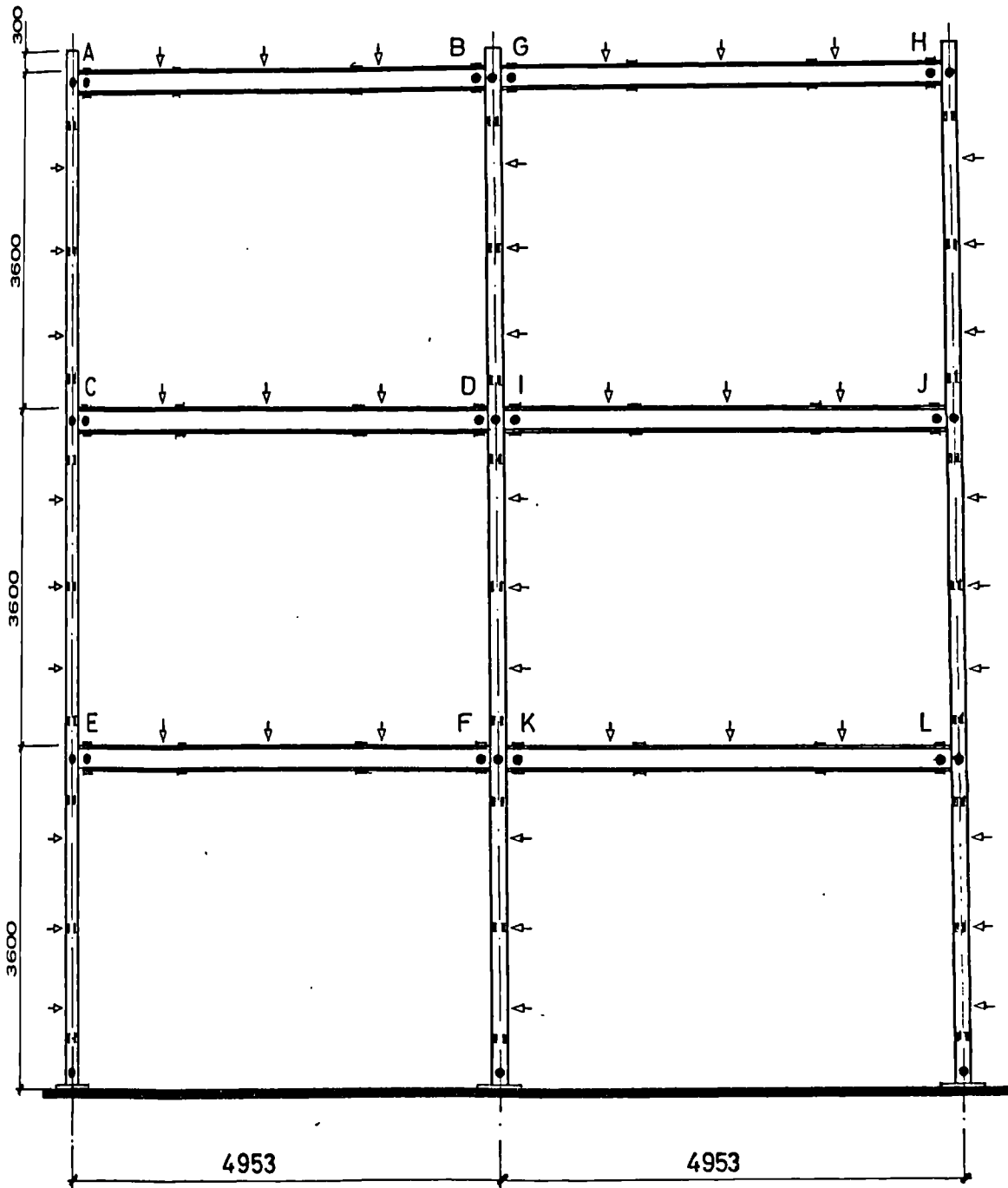


FIGURE 5.6 C lumn head loading arrangement



- ↓ Beam / column displacements 45
- ⇄ strain gauges 204
- rotation devices 24
- beam restraint bars gauged 30
- column bracing bars gauged 18
- force in holding down bolts 12

FIGURE 5.7 Frame instrumentation

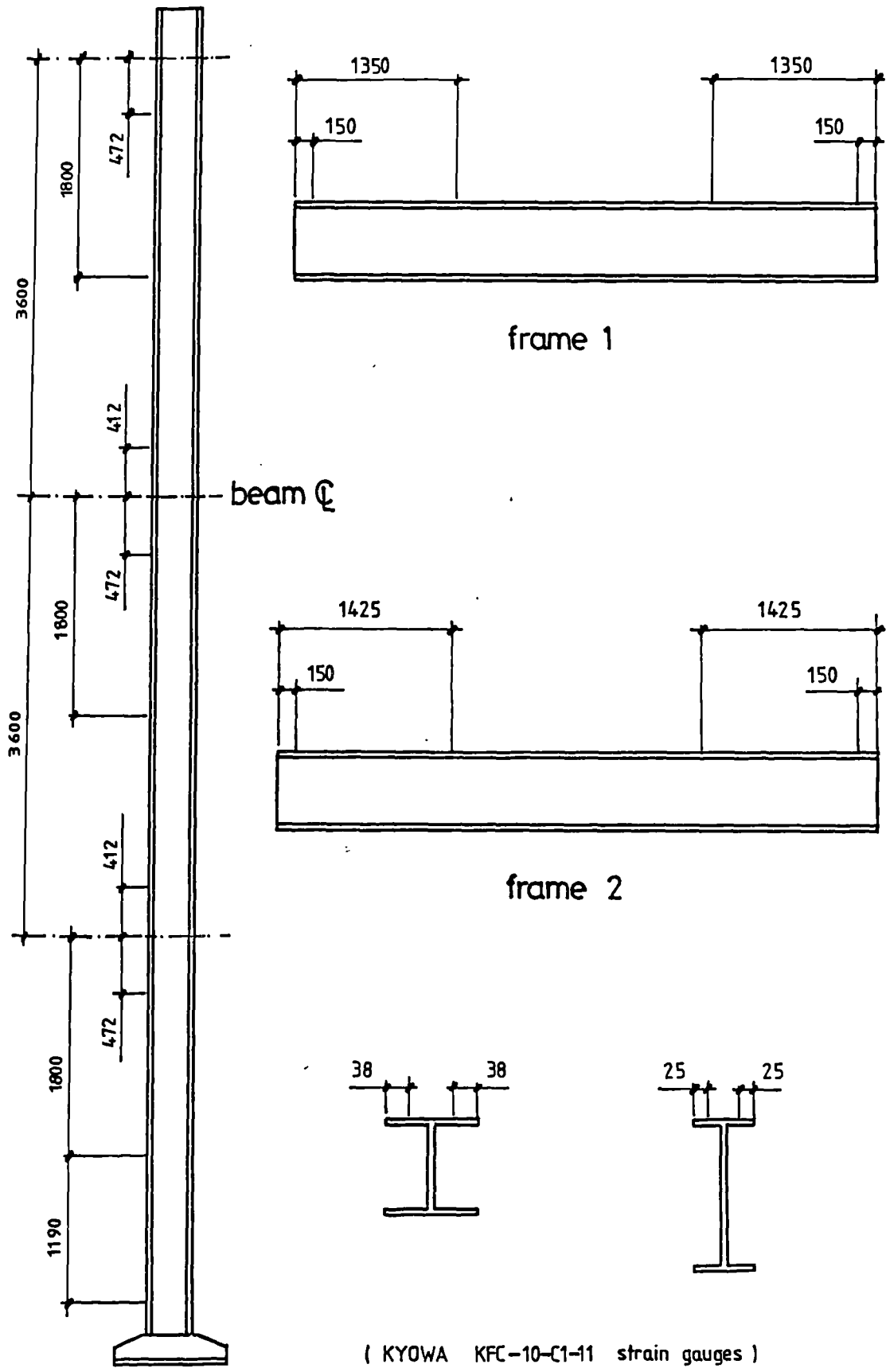
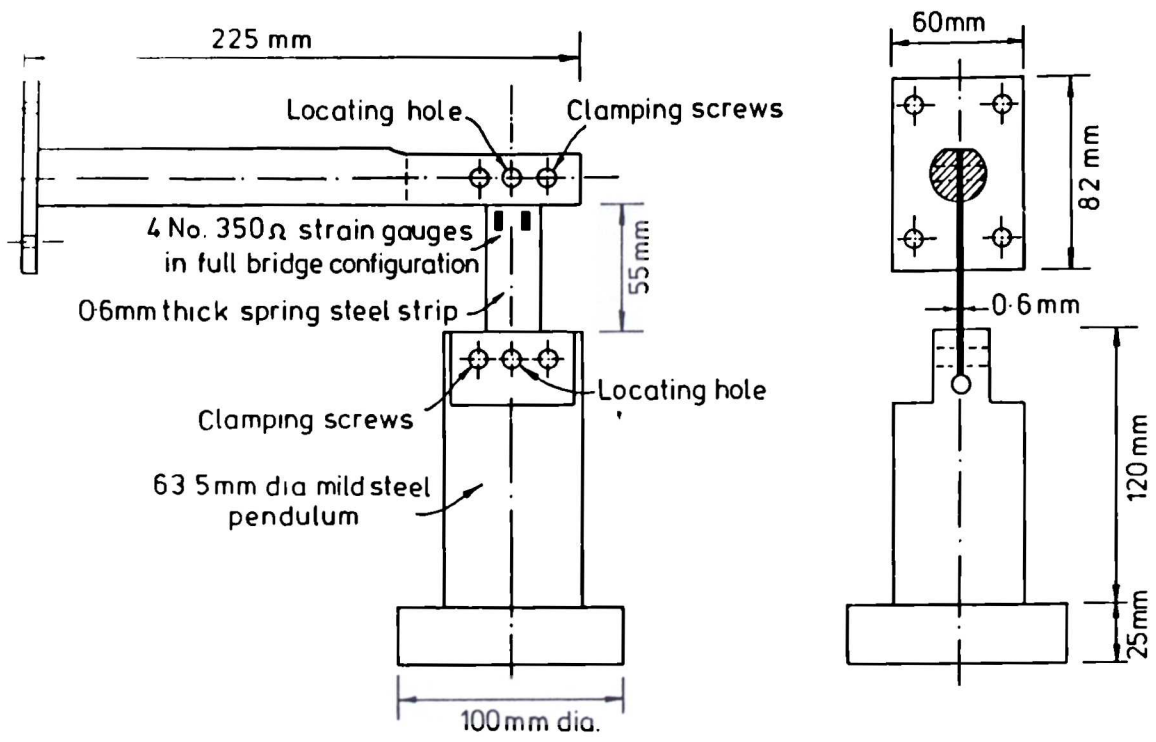


FIGURE 5.8 Strain gauge positions



ROTATION DEVICE

FIGURE 5.9 Illustration of rotation device

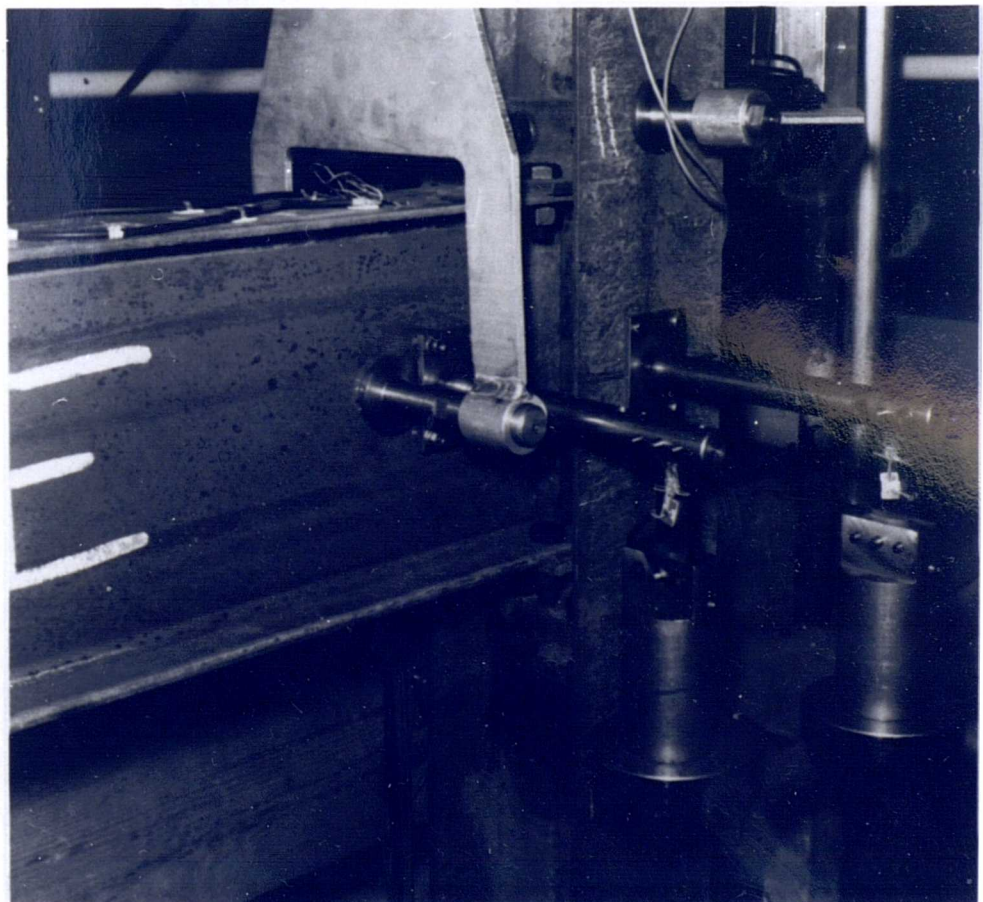


FIGURE 5.10 Beam and column rotation devices in position

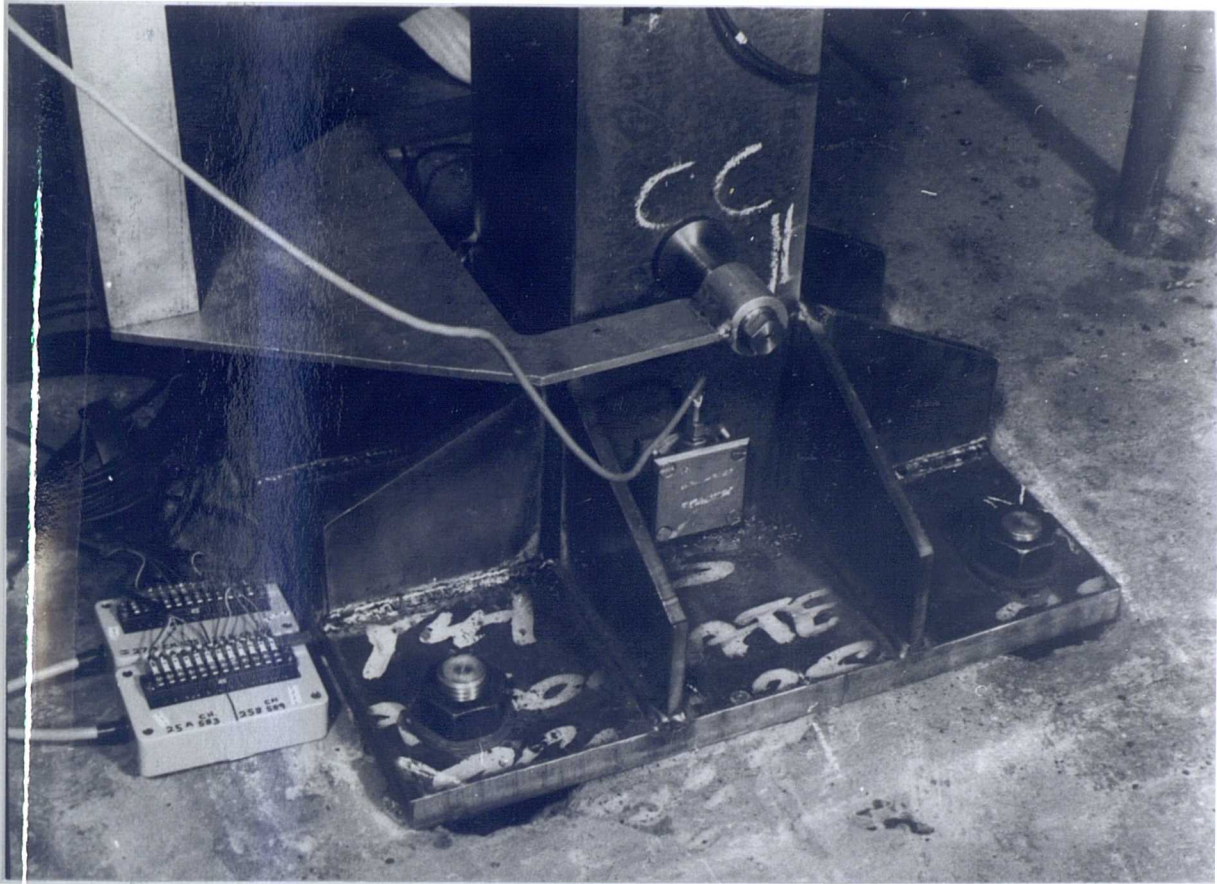


FIGURE 5.11 Rotation measurement at column base

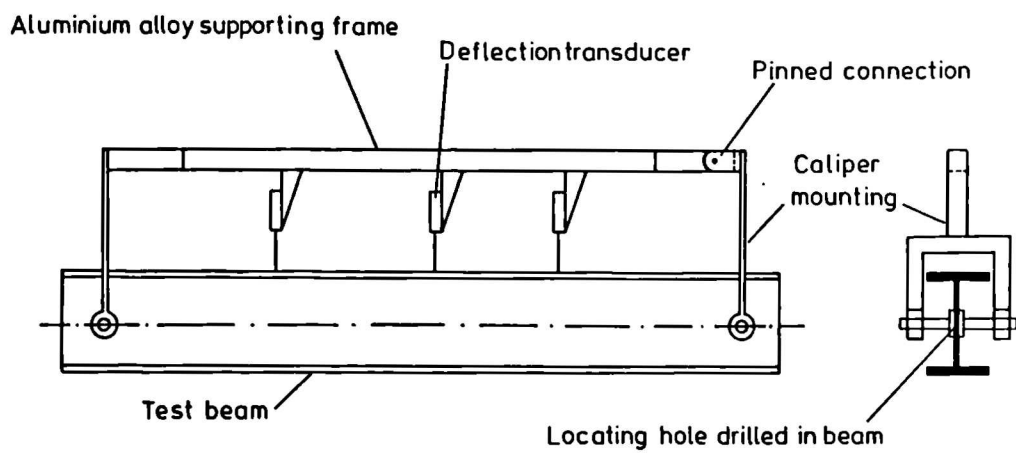
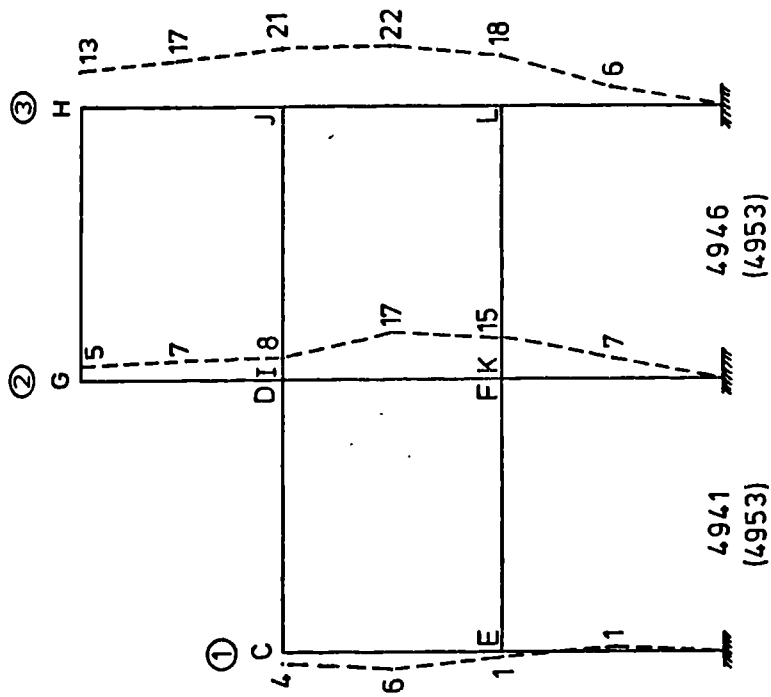


FIGURE 5.12 Displacement measurement system

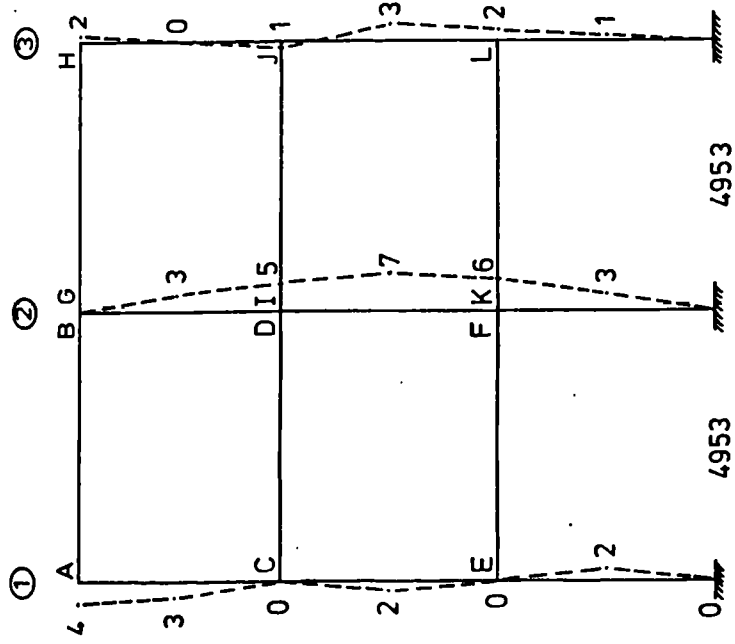
FRAME 1



(Dimensions in mm)

View from balcony

FRAME 2



(Dimensions in mm)

View from balcony

FIGURE 5.13 Initial shape of frame 1

FIGURE 5.14 Initial shape of frame 2

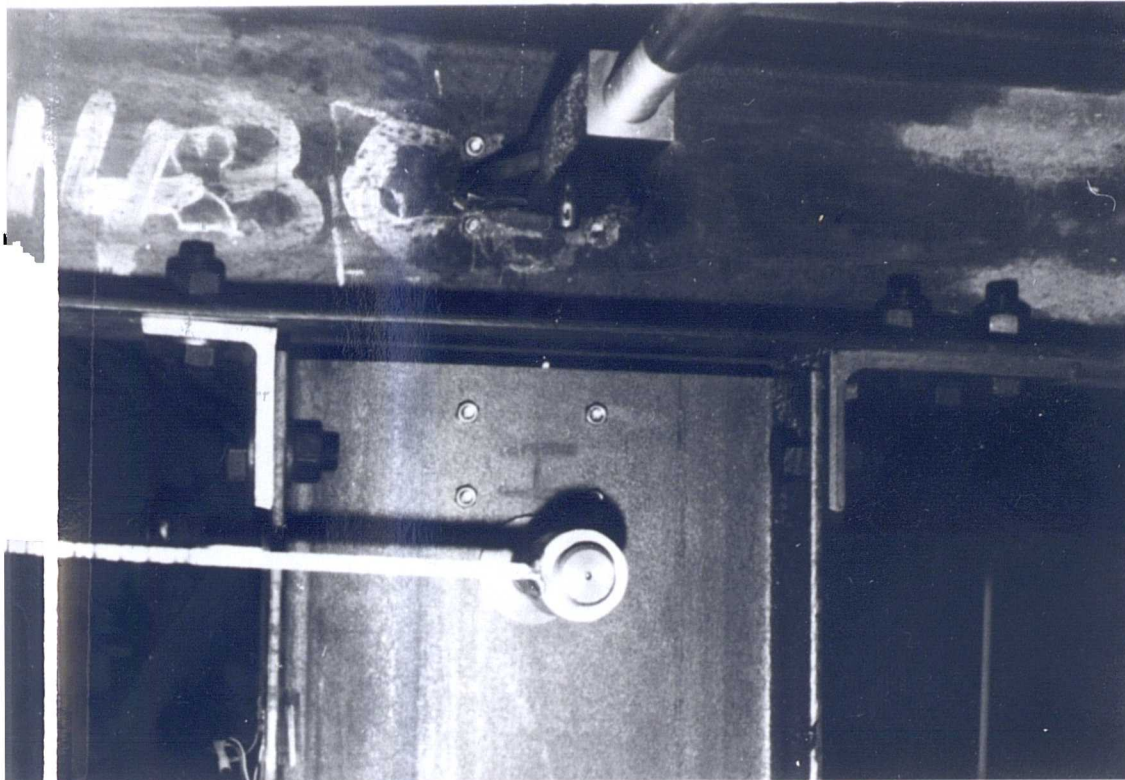


FIGURE 5.15 Distortion of connection due to beam loading

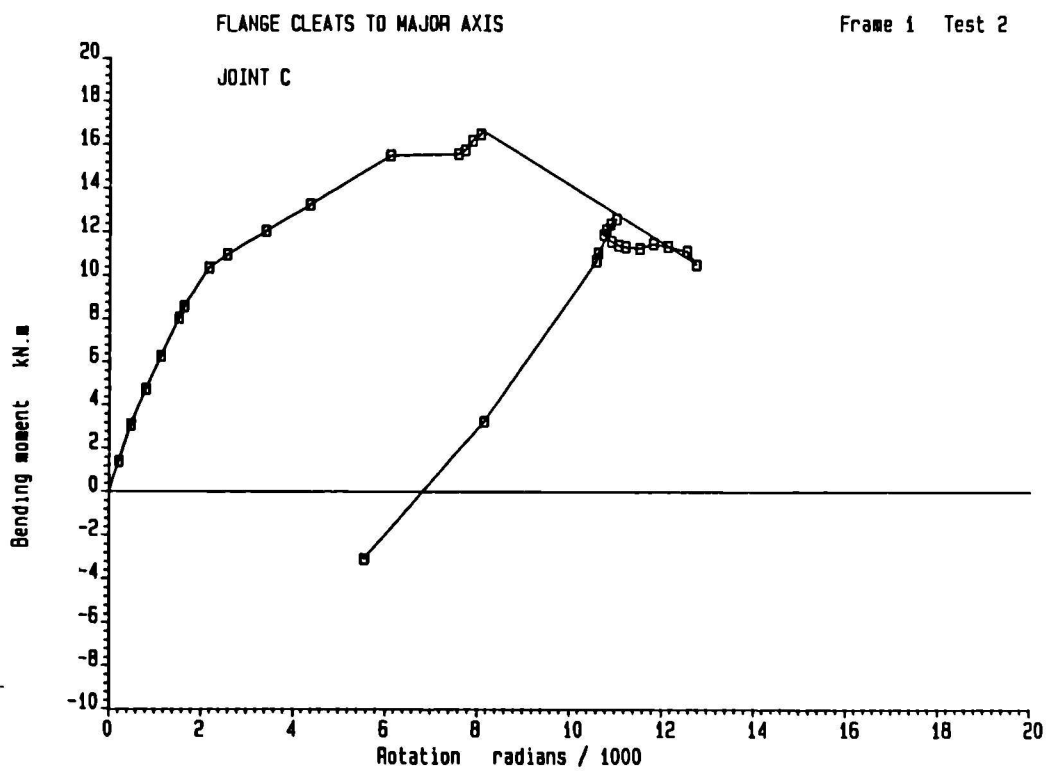


FIGURE 5.16 Moment-rotation curve for joint C

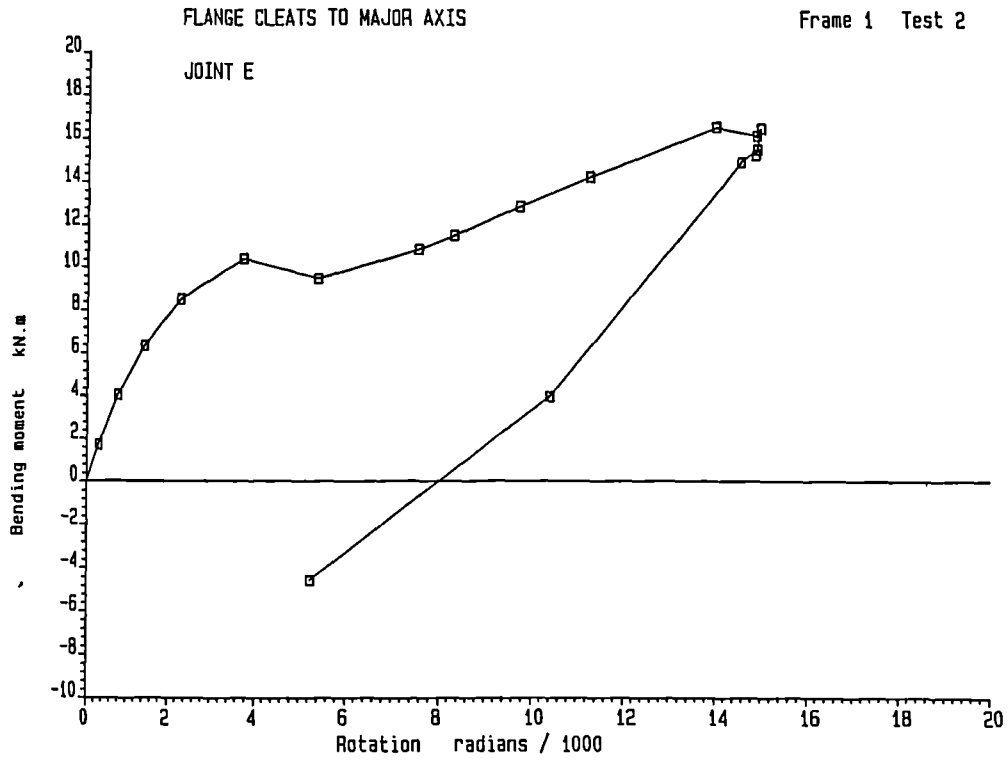


FIGURE 5.17 Moment-rotation curve for joint E

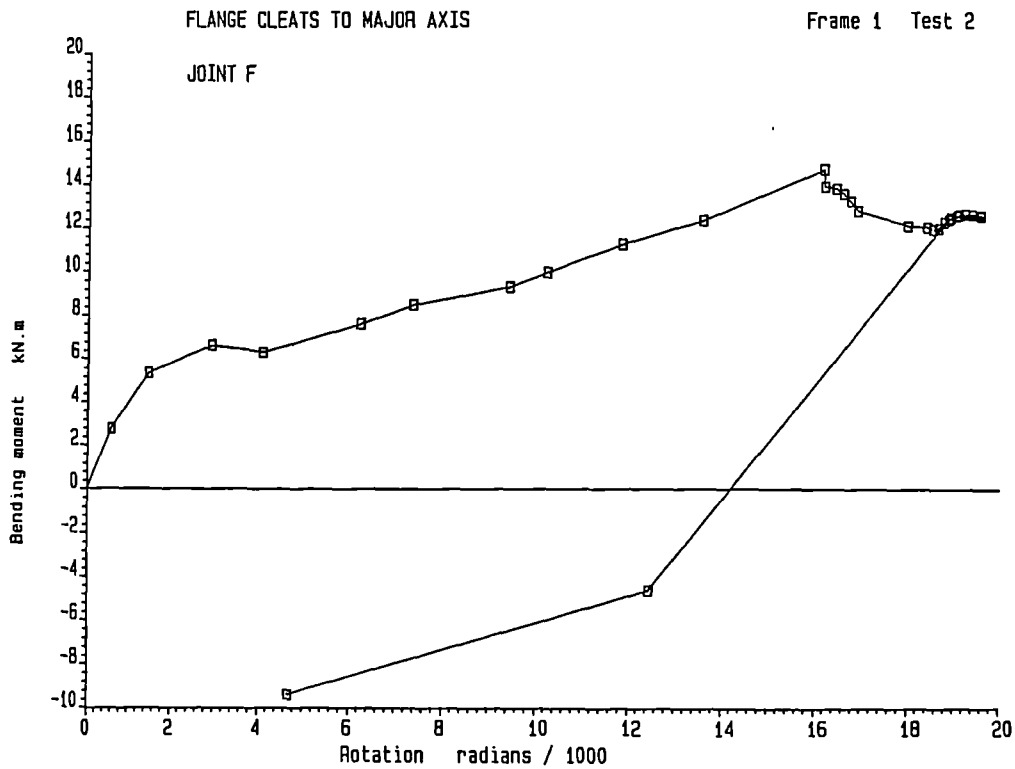


FIGURE 5.18 Moment-rotation curve for joint F

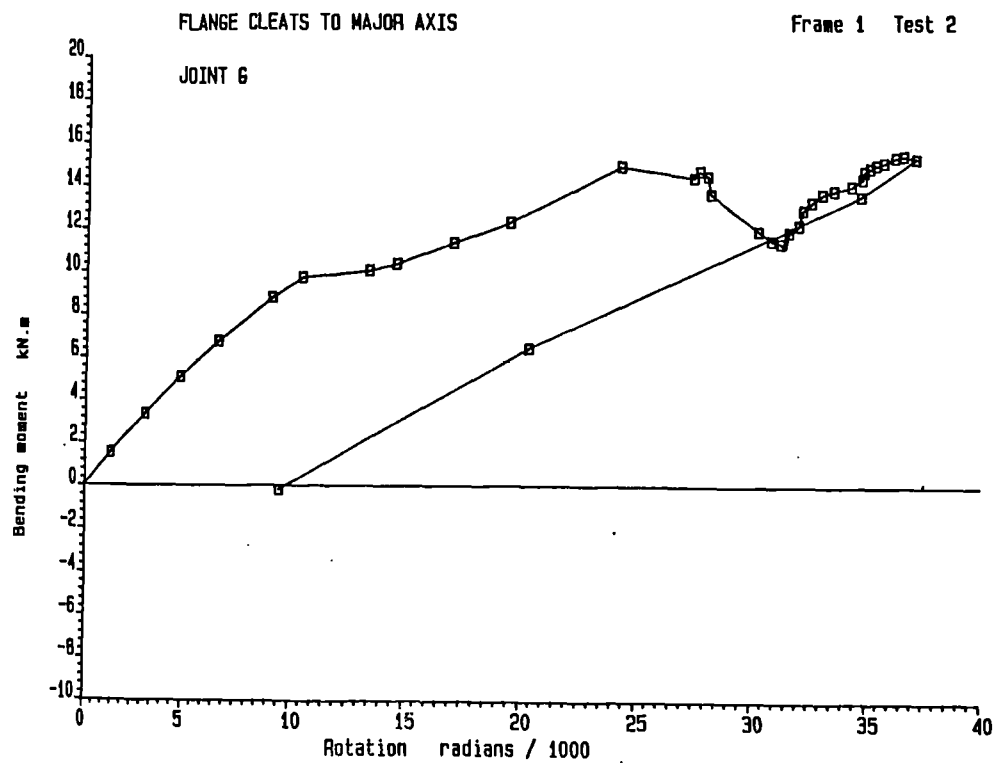


FIGURE 5.19 Moment-rotation curve for joint G

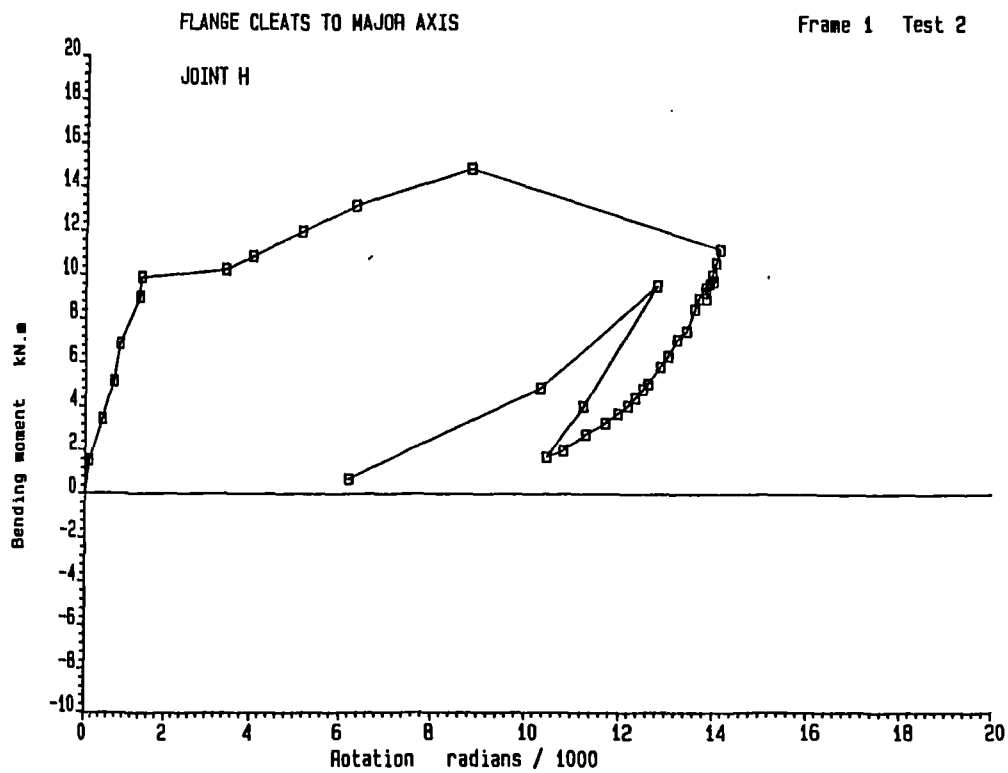


FIGURE 5.20 Moment-rotation curve for joint H

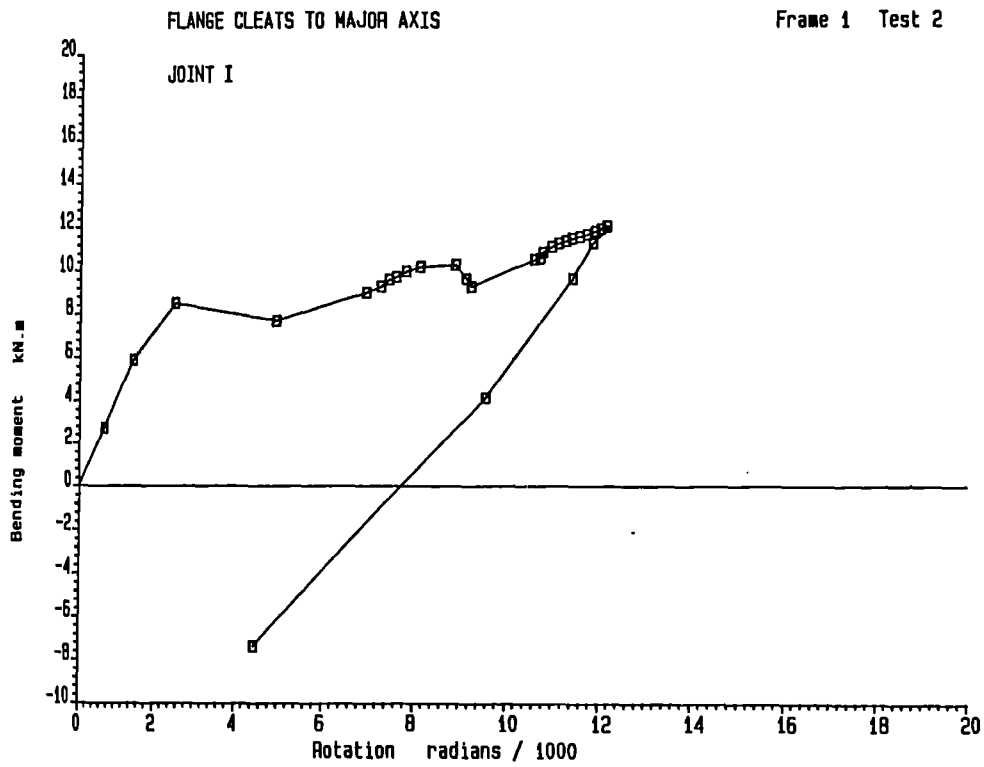


FIGURE 5.21 Moment-rotation curve for joint I

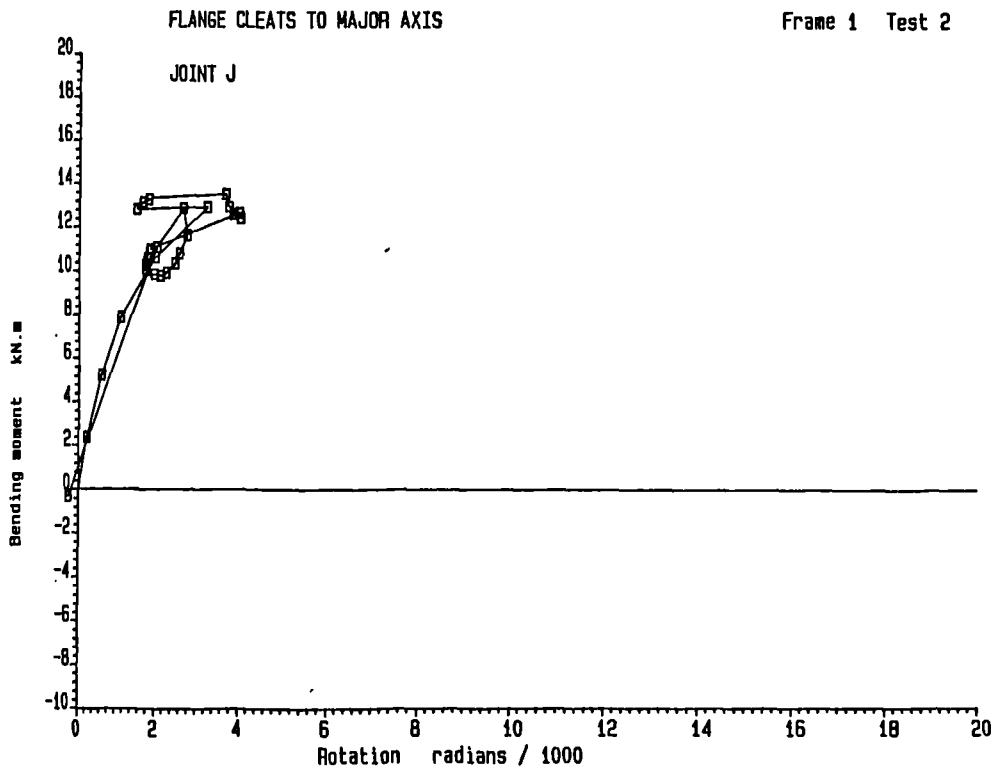


FIGURE 5.22 Moment-rotation curve for joint J

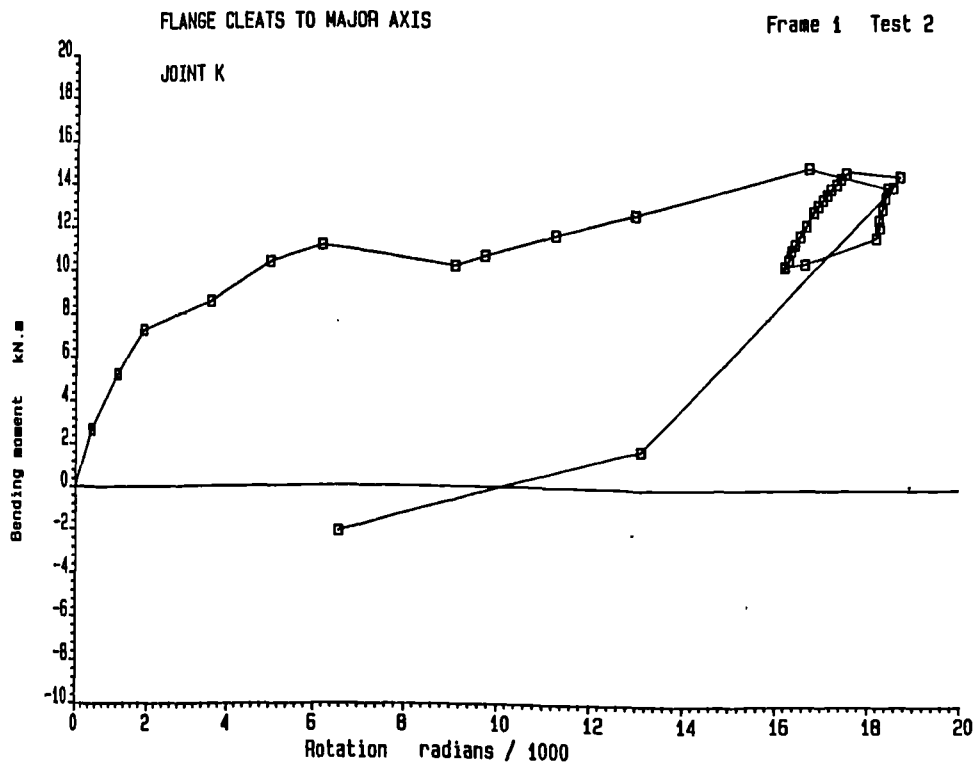


FIGURE 5.23 Moment-rotation curve for joint K

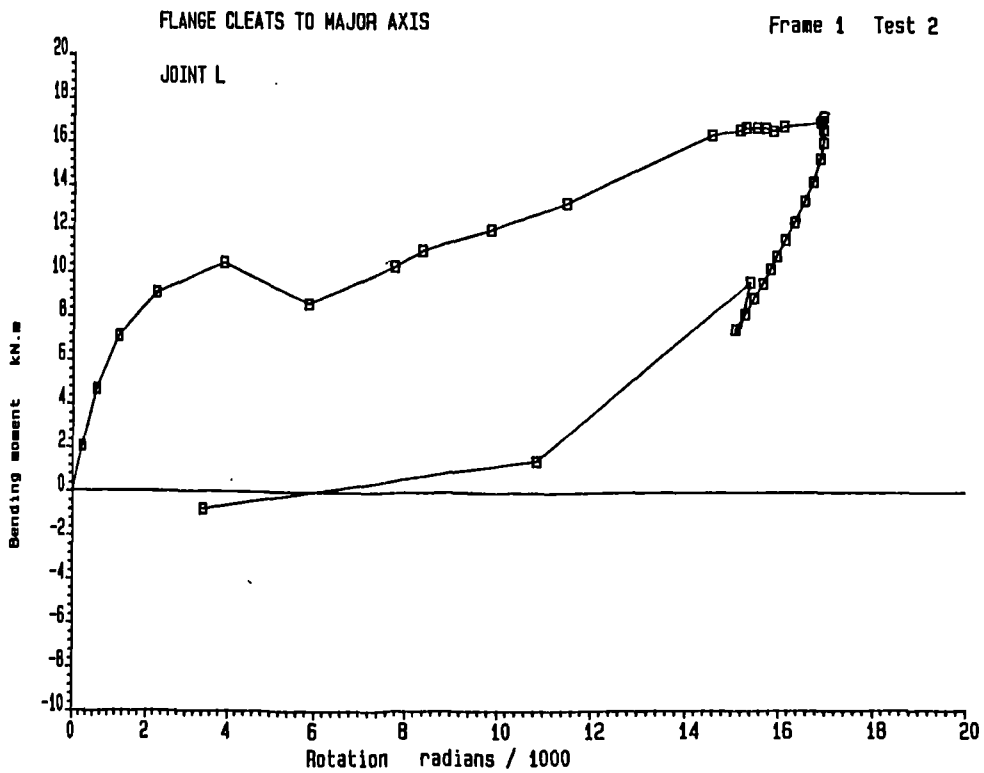
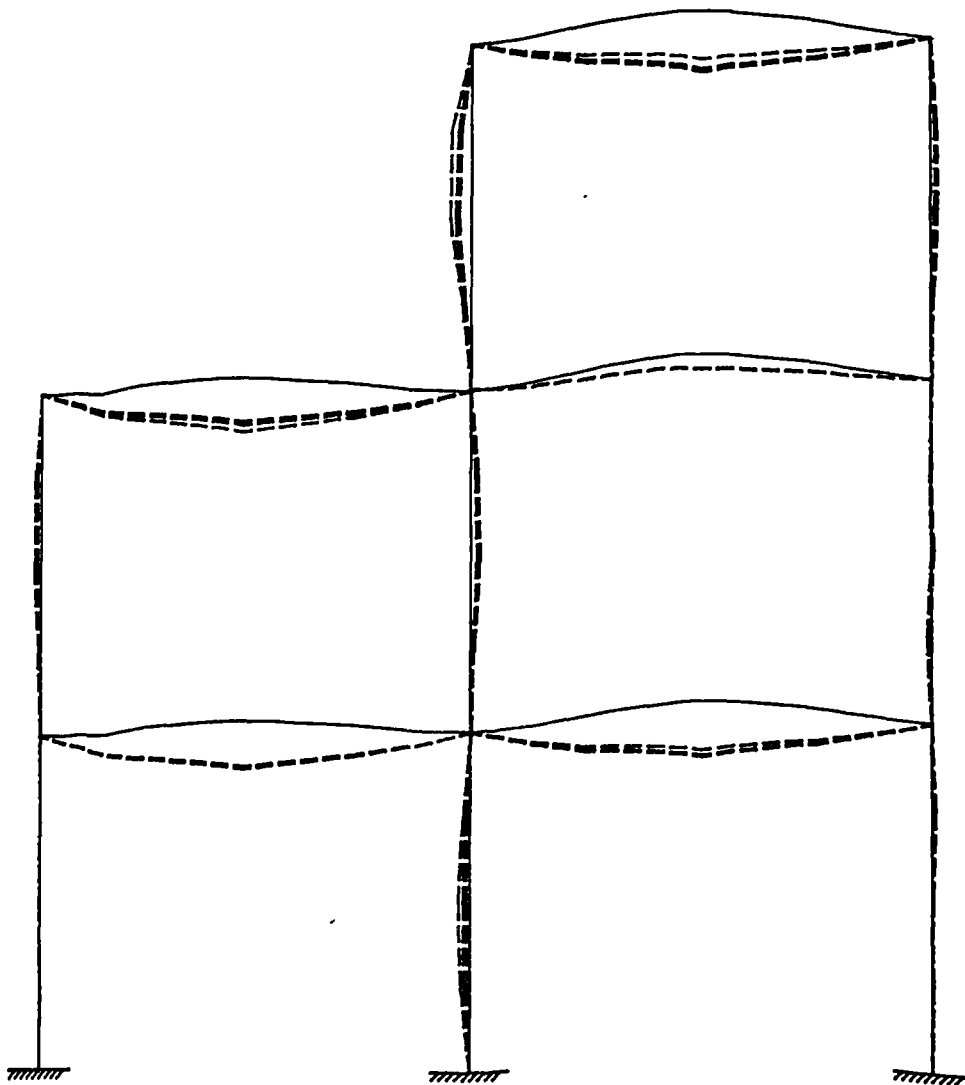


FIGURE 5.24 Moment-rotation curve for joint L

MAJOR AXIS FRAME

DEFLECTED SHAPE OF FRAME



Horizontal deflections scale : 0.50 mm/mm

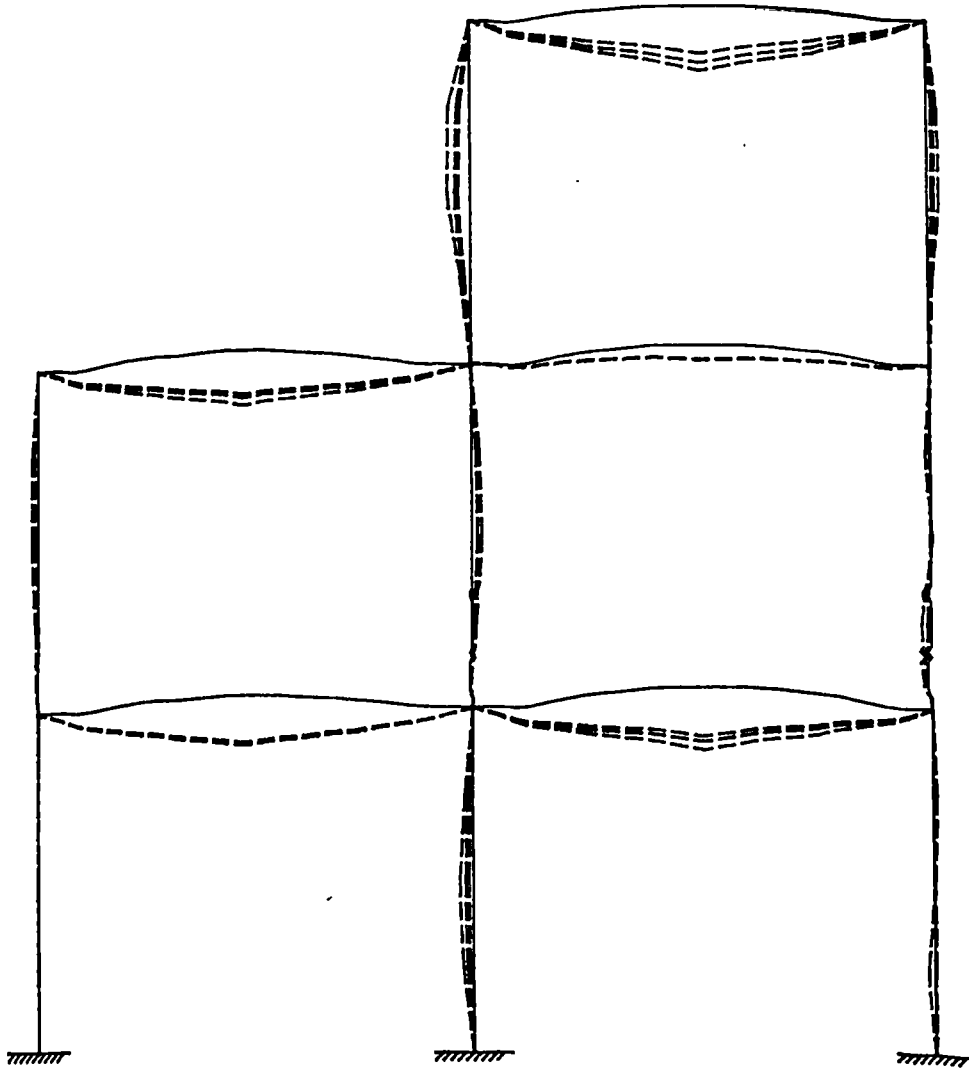
Vertical deflections scale : 0.25 mm/mm Frame 1 Test 2

Run Numbers Plotted : 12 17 22

FIGURE 5.25 Deflected shape of frame 1 at runs 12, 17 and 22

MAJOR AXIS FRAME

DEFLECTED SHAPE OF FRAME



Horizontal deflections scale : 0.50 mm/mm

Vertical deflections scale : 0.25 mm/mm Frame 1 Test 2

Run Numbers Plotted : 12 17 36

FIGURE 5.26 Deflected shape of frame 1 at runs 12, 17 and 36

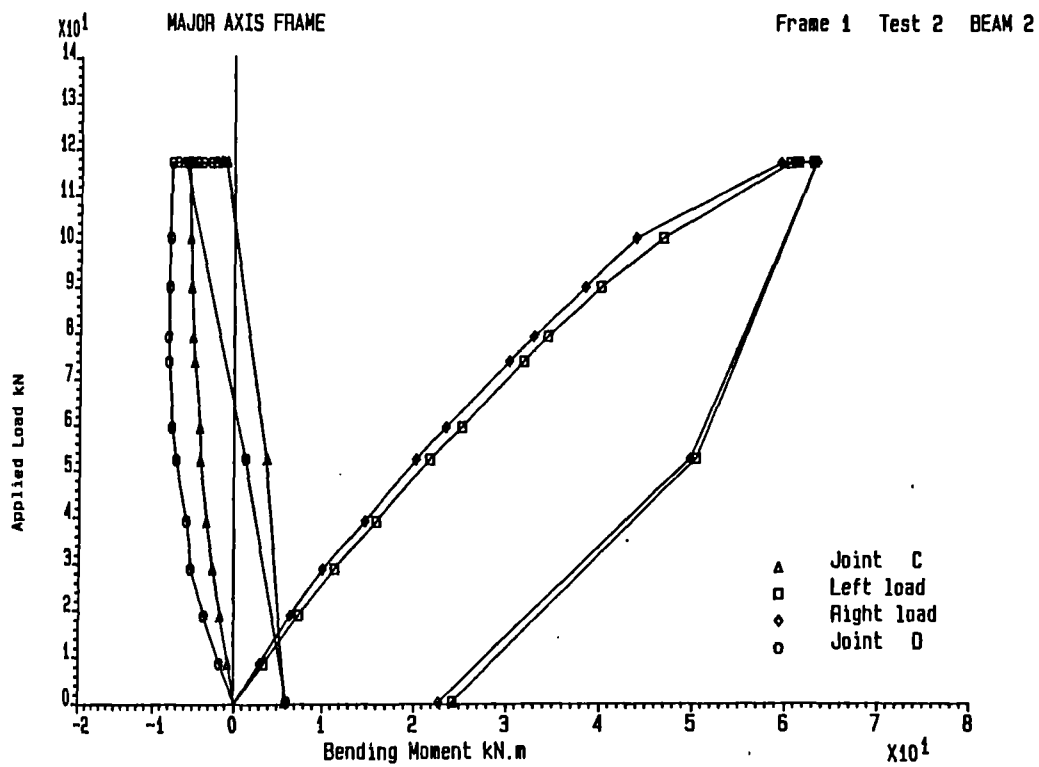


FIGURE 5.27 Applied beam load against bending moment for beam 2

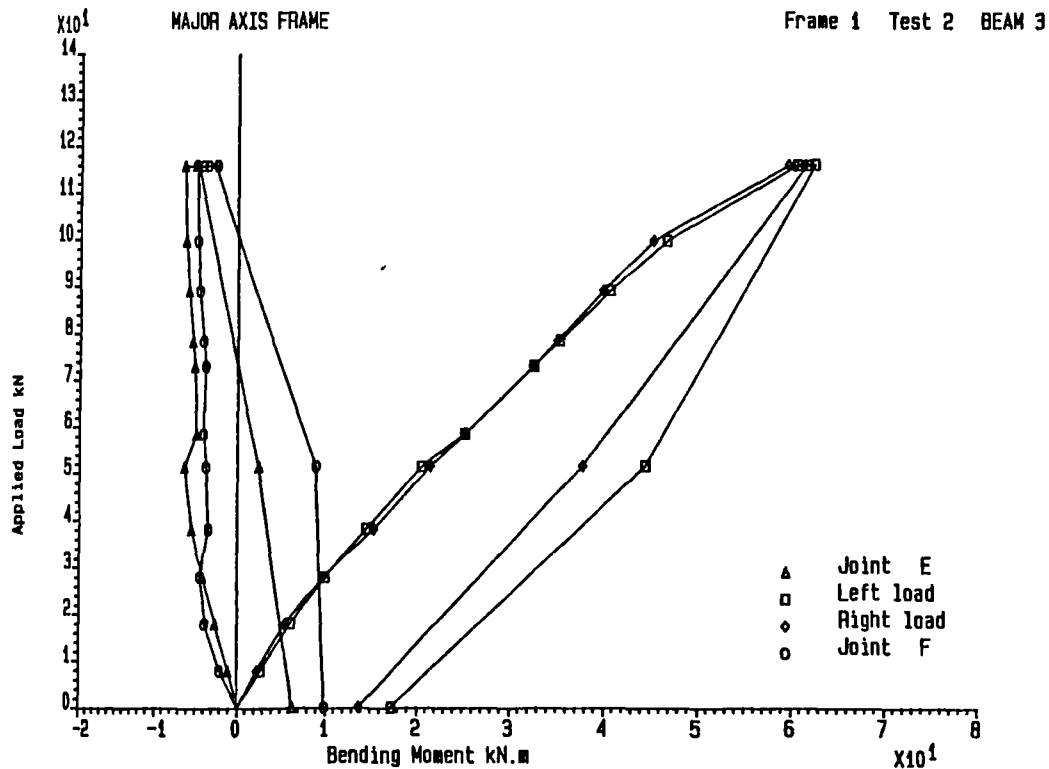


FIGURE 5.28 Applied beam load against bending moment for beam 3

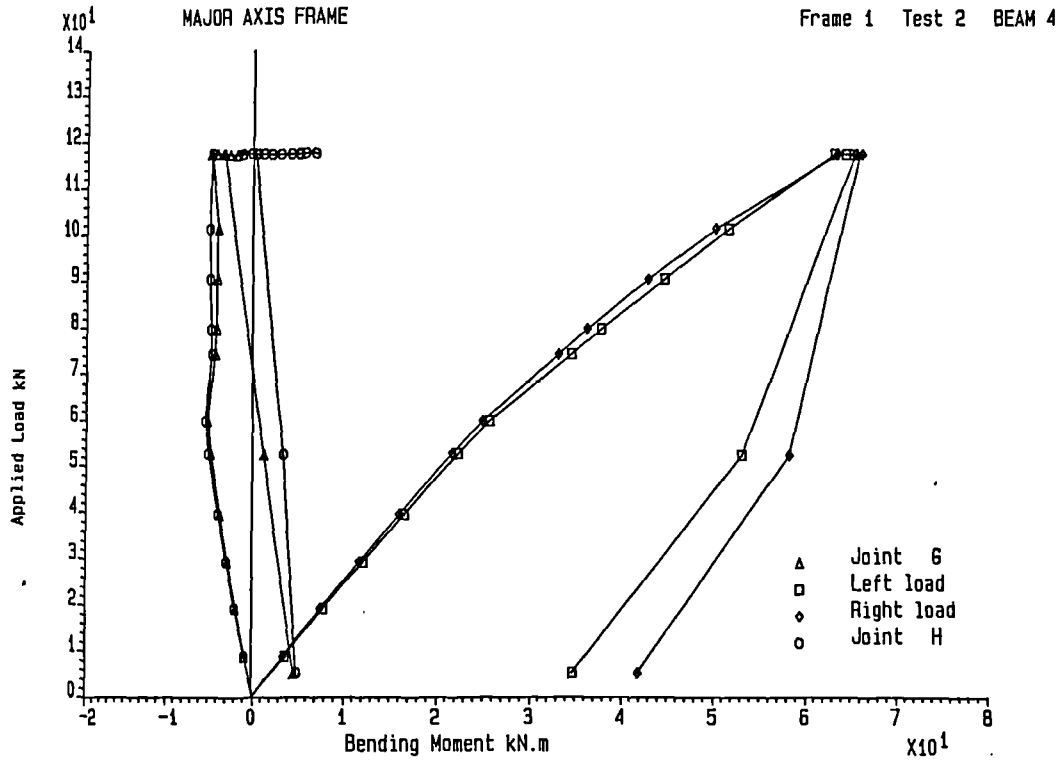


FIGURE 5.29 Applied beam load against bending moment for beam 4

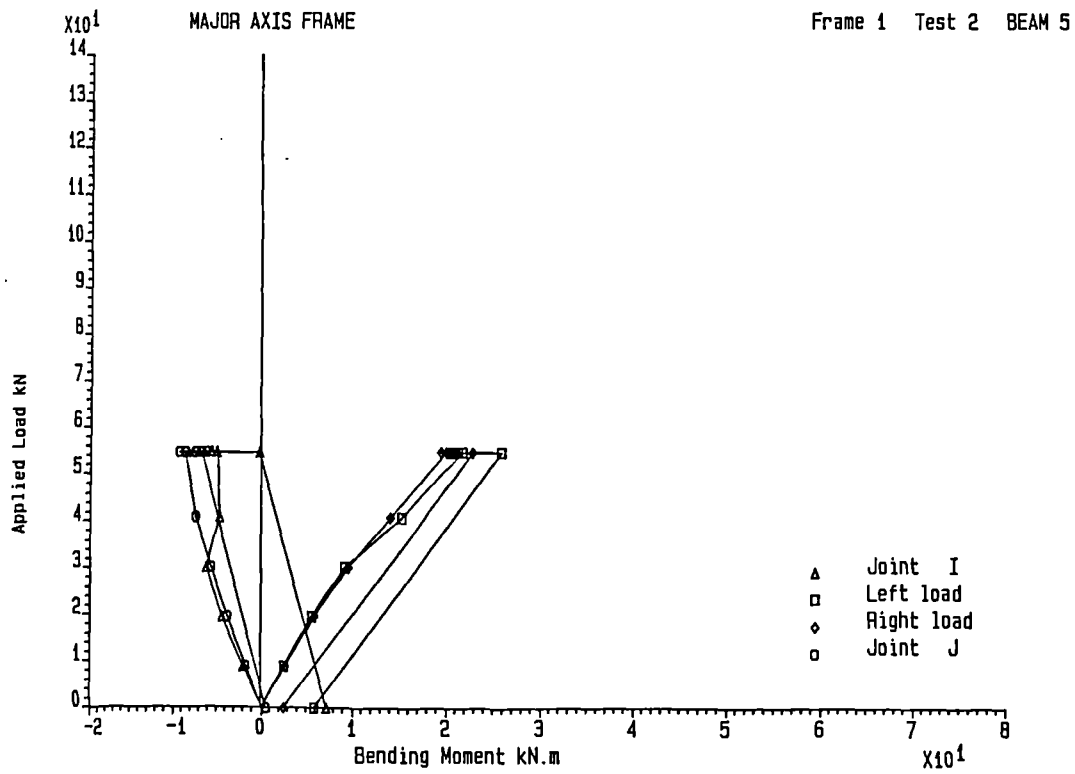


FIGURE 5.30 Applied beam load against bending moment for beam 5

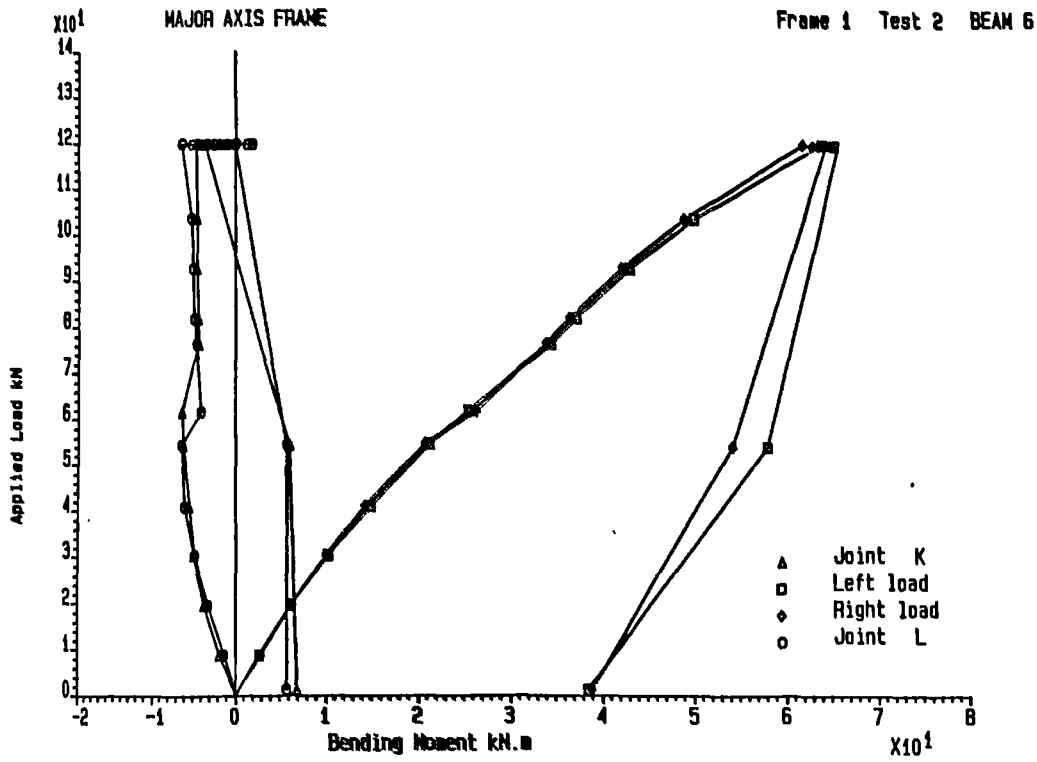
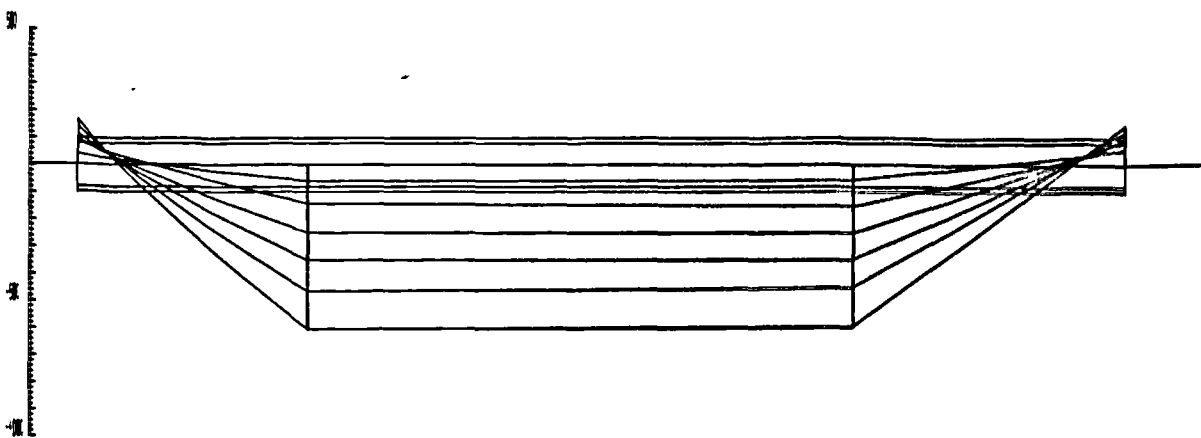


FIGURE 5.31 Applied beam load against bending moment for beam 6

Bending Moment kN.m Frame 1 Test 2BEAM 3

Run Number Plotted : 3 5 7 9 11 12



SUPERIMPOSED BENDING MOMENTS

FIGURE 5.32 Bending moment distribution in beam 3 as beam loads are applied

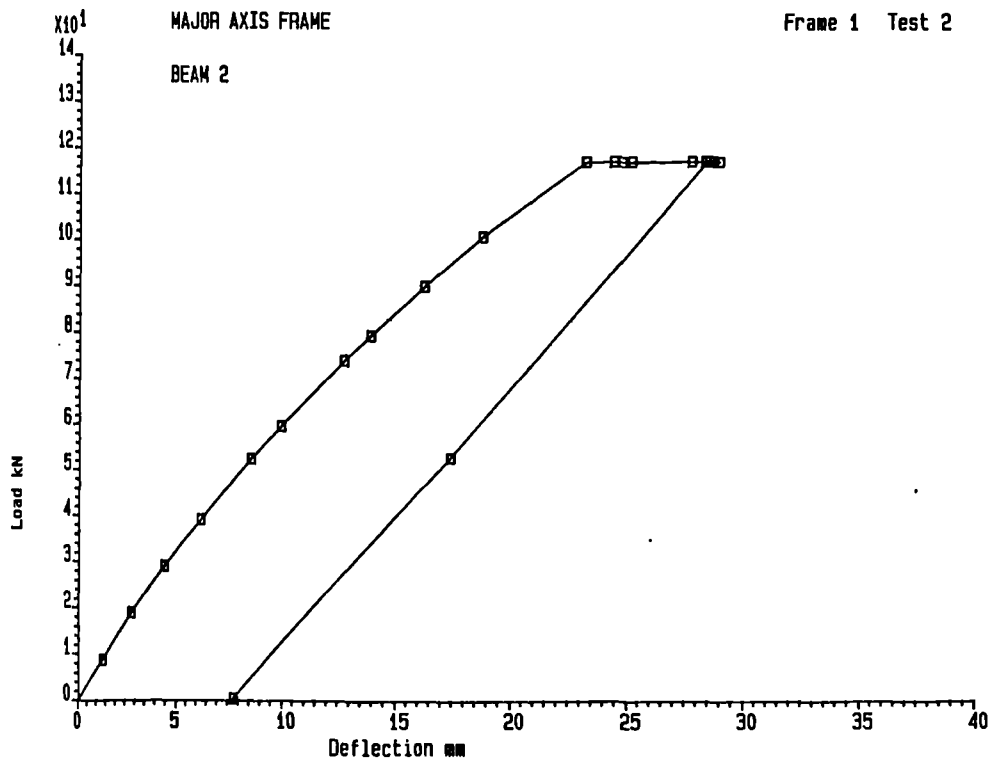


FIGURE 5.33 Applied beam load against central deflection for beam 2

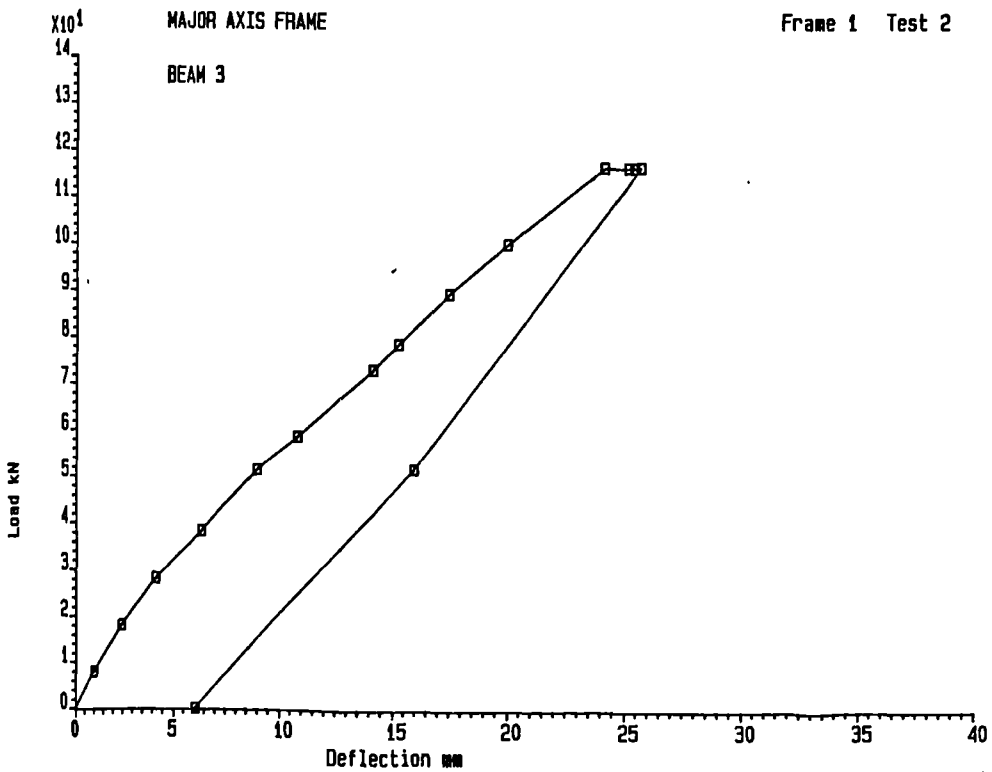


FIGURE 5.34 Applied beam load against central deflection for beam 3

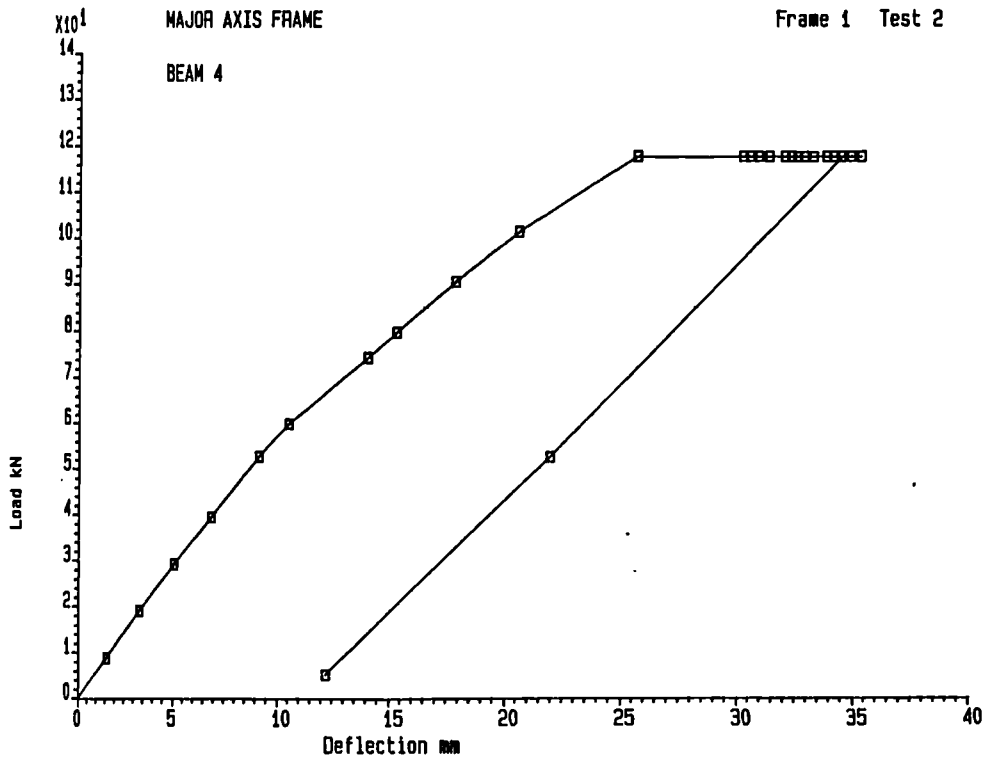


FIGURE 5.35 Applied beam load against central deflection for beam 4

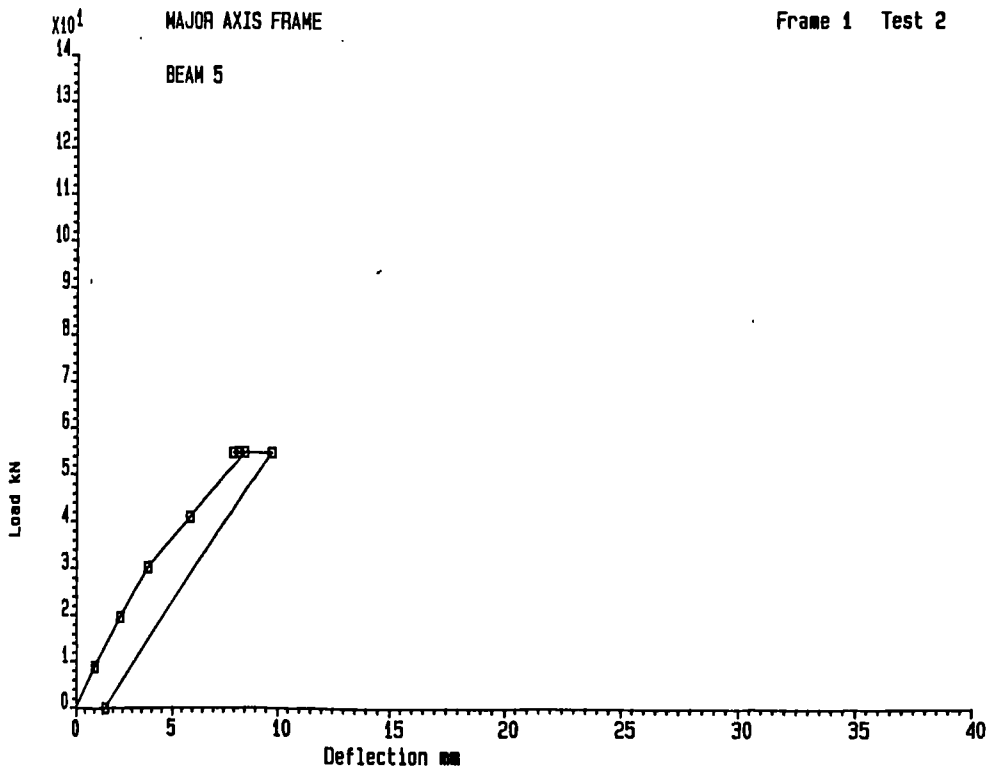


FIGURE 5.36 Applied beam load against central deflection for beam 5

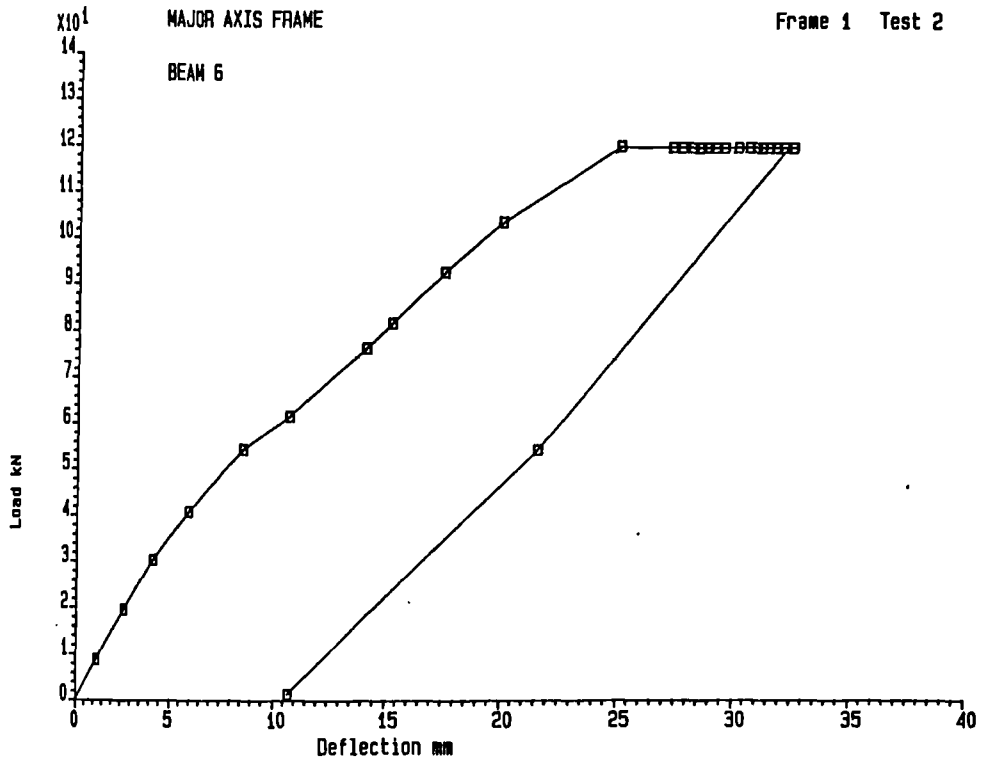
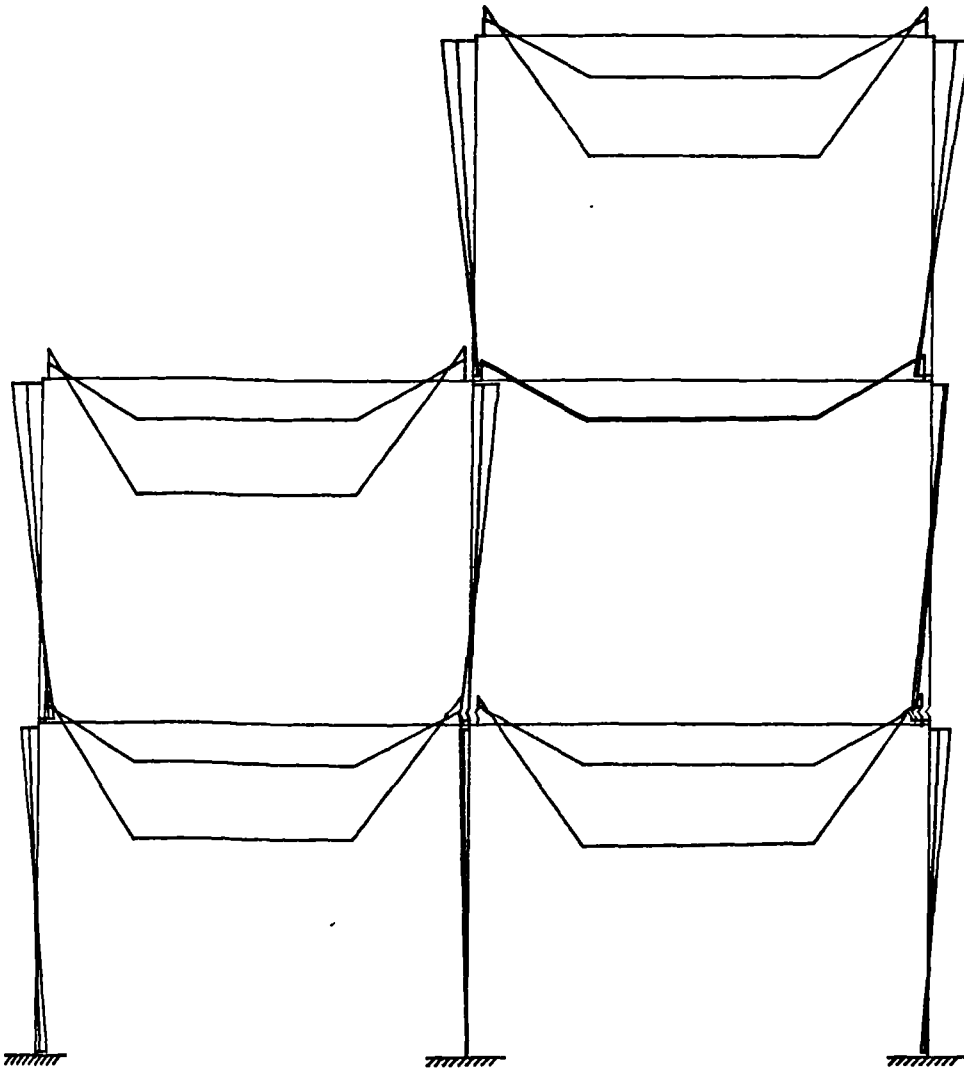


FIGURE 5.37 Applied beam load against central deflection for beam 6

MAJOR AXIS FRAME
BENDING MOMENT DIAGRAM
MAJOR AXIS COLUMN MOMENTS PLOTTED



Scale : 0.25mm/kN-m

Frame 1 Test 2

Run Numbers Plotted : 6 12

FIGURE 5.38 Moment distribution around frame 1 at runs 6 and 12

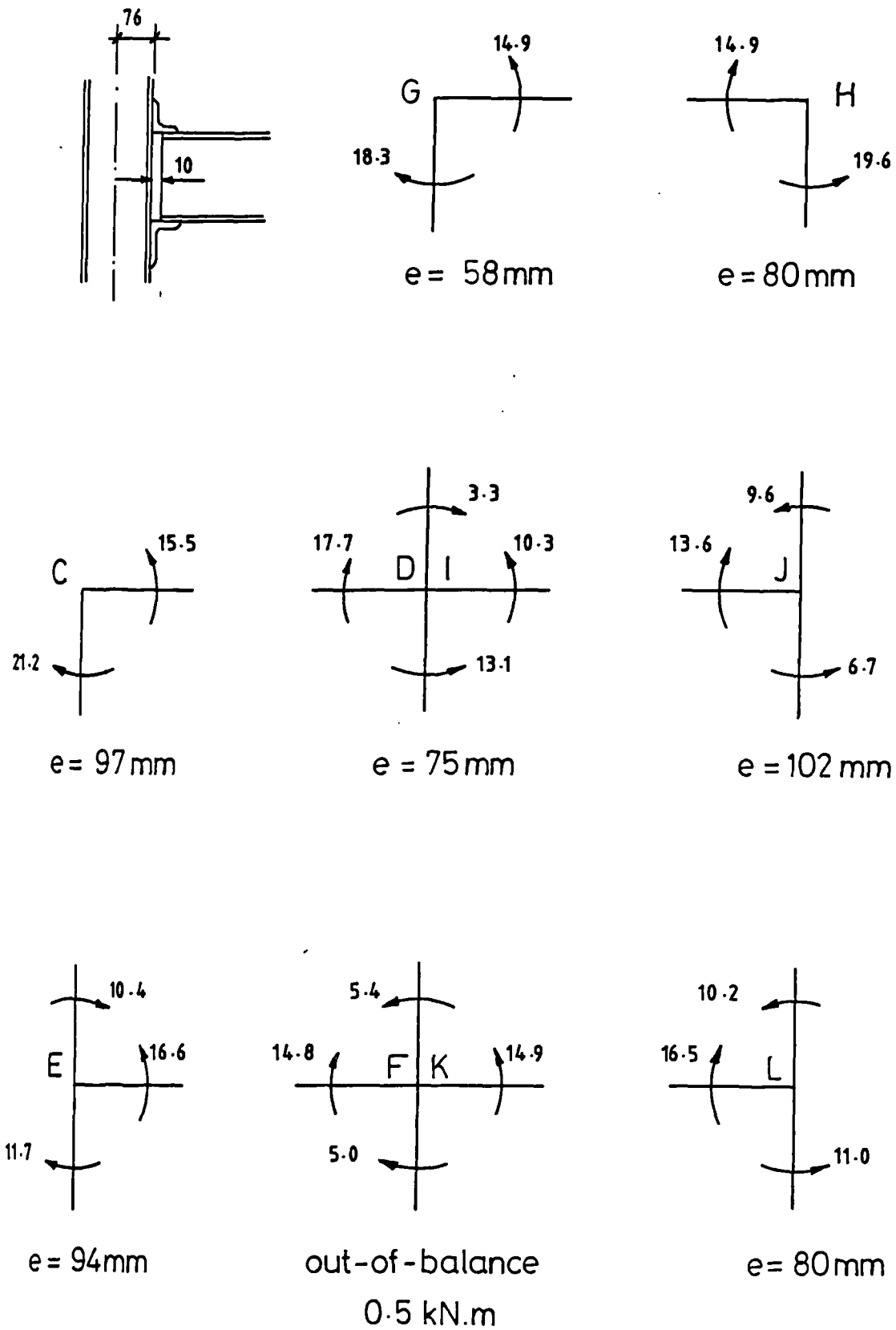


FIGURE 5.39 Moment equilibrium at joints in frame 1 at end of beam loading

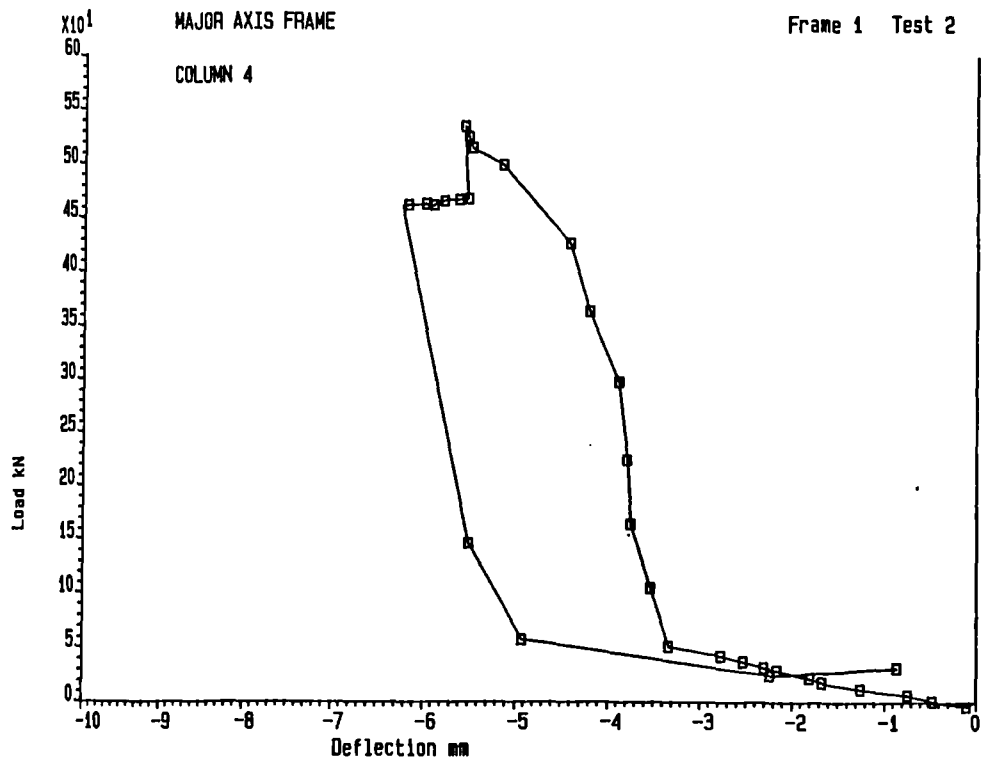


FIGURE 5.40 Total load in column against central deflection - column 4

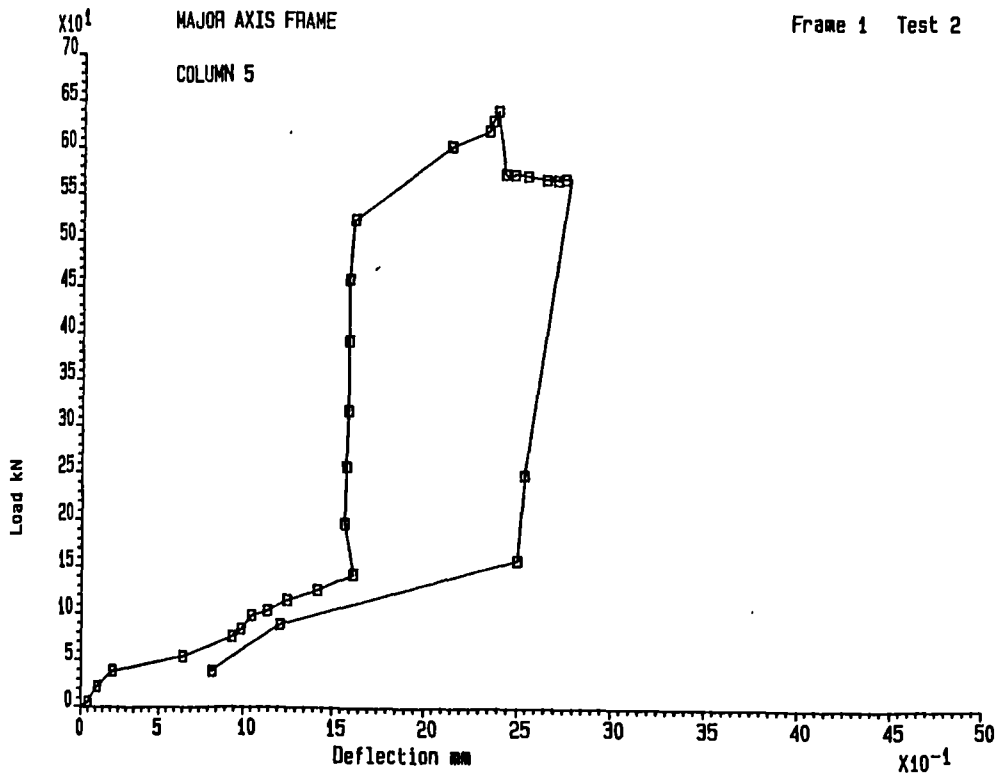


FIGURE 5.41 Total load in column against central deflection - column 5

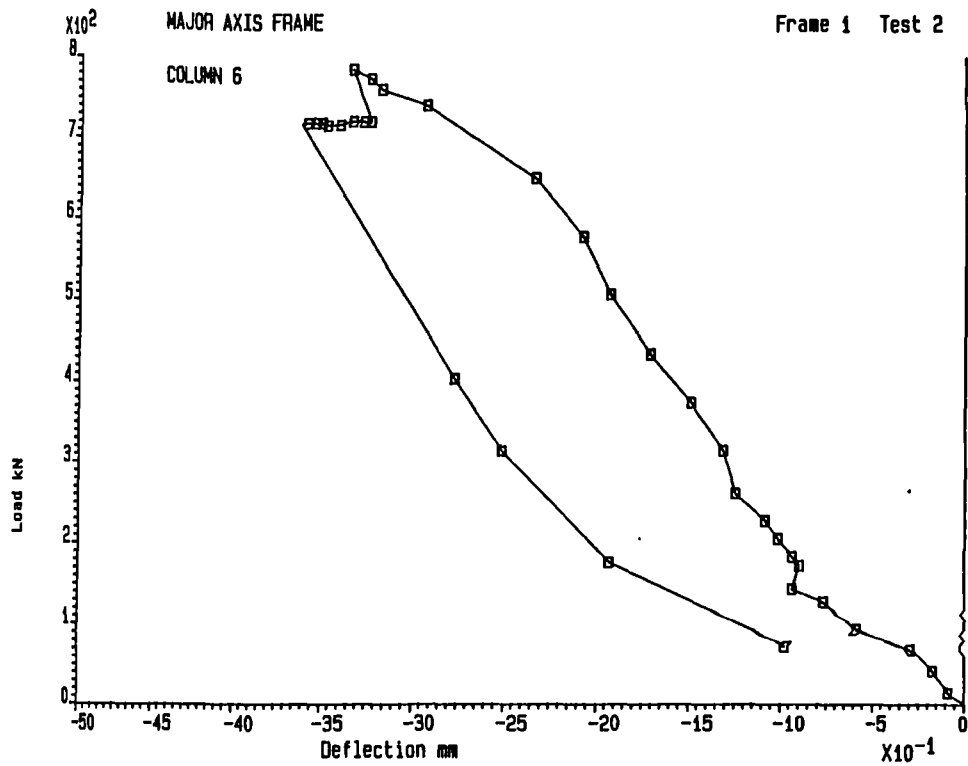


FIGURE 5.42 Total load in column against central deflection - column 6

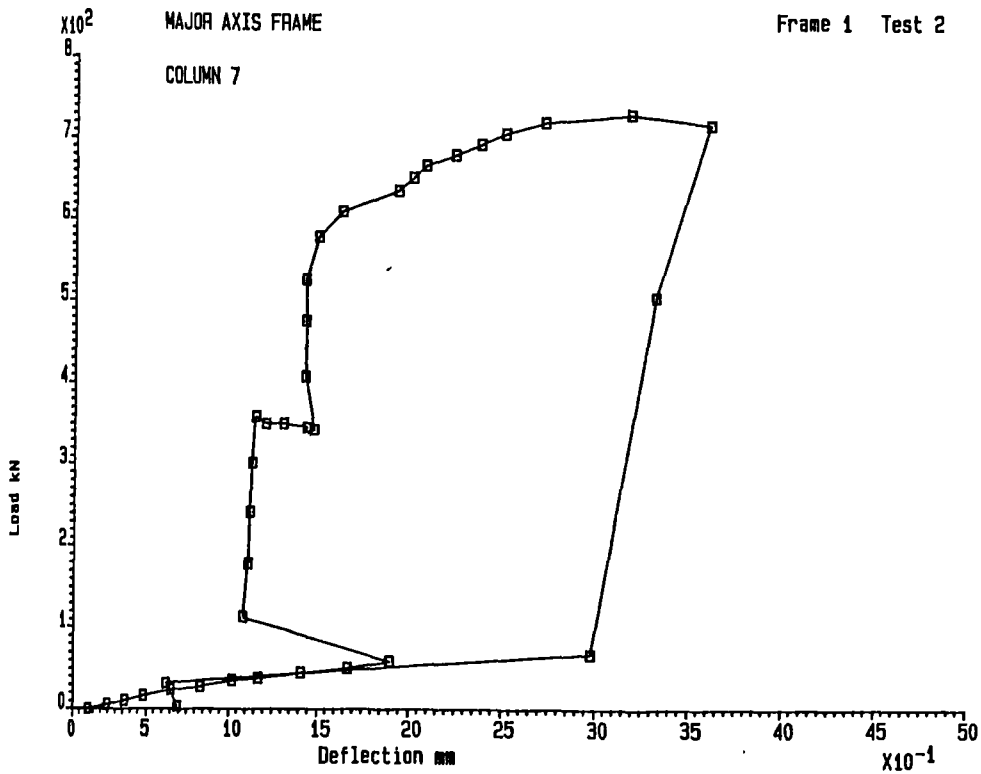
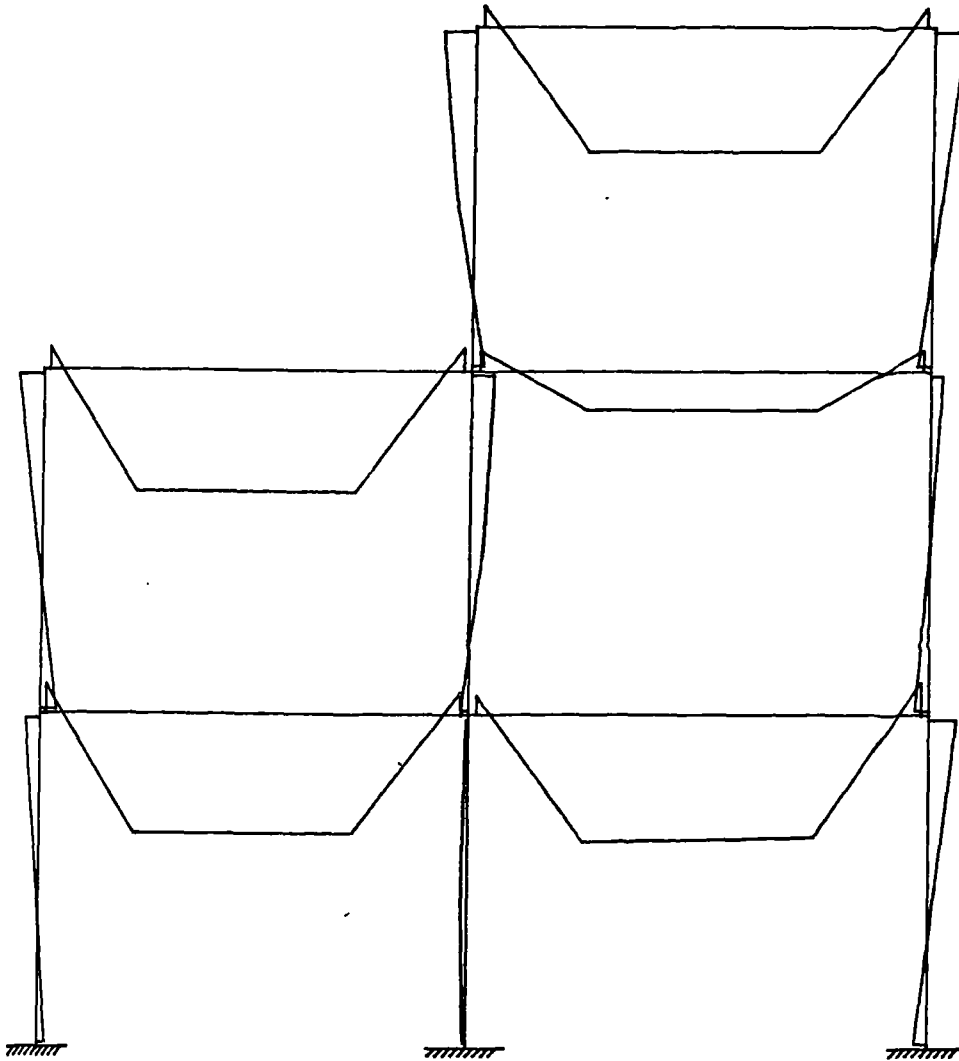


FIGURE 5.43 Total load in column against central deflection - column 7

MAJOR AXIS FRAME

BENDING MOMENT DIAGRAM

MAJOR AXIS COLUMN MOMENTS PLOTTED



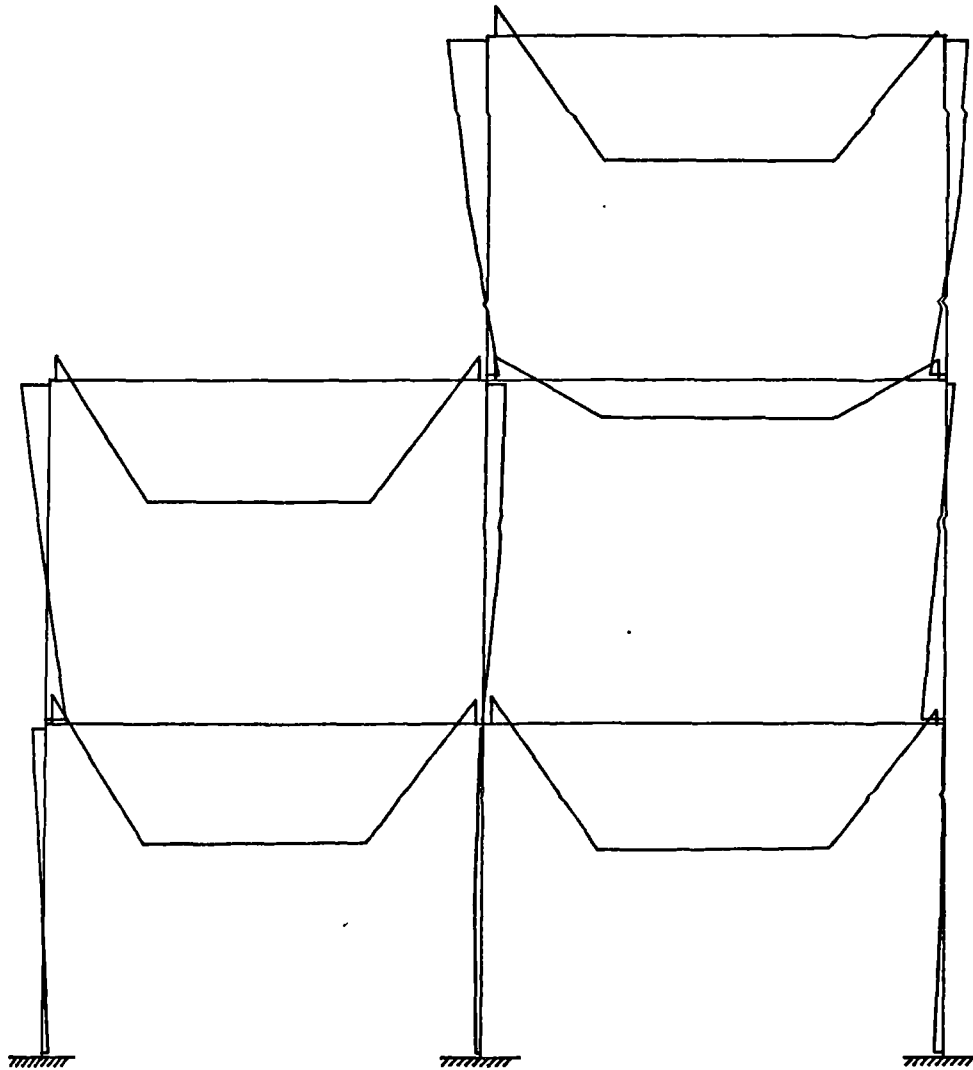
Scale : 0.25mm/kN-m

Frame 1 Test 2

Run Numbers Plotted : 22

FIGURE 5.44 Moment distribution around frame 1 at failure of central column

MAJOR AXIS FRAME
BENDING MOMENT DIAGRAM
MAJOR AXIS COLUMN MOMENTS PLOTTED



Scale : 0.25mm/kN-m

Frame 1 Test 2

Run Numbers Plotted : 36

FIGURE 5.45 Moment distribution around frame 2 at failure of external column

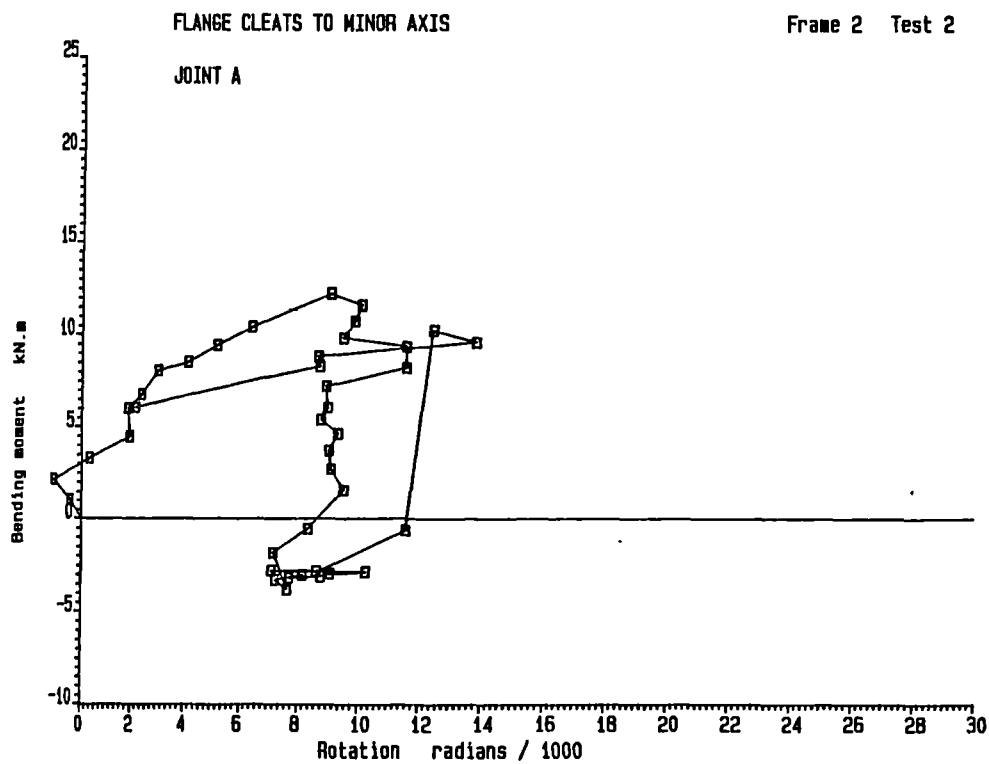


FIGURE 5.46 Moment-rotation curve for joint A

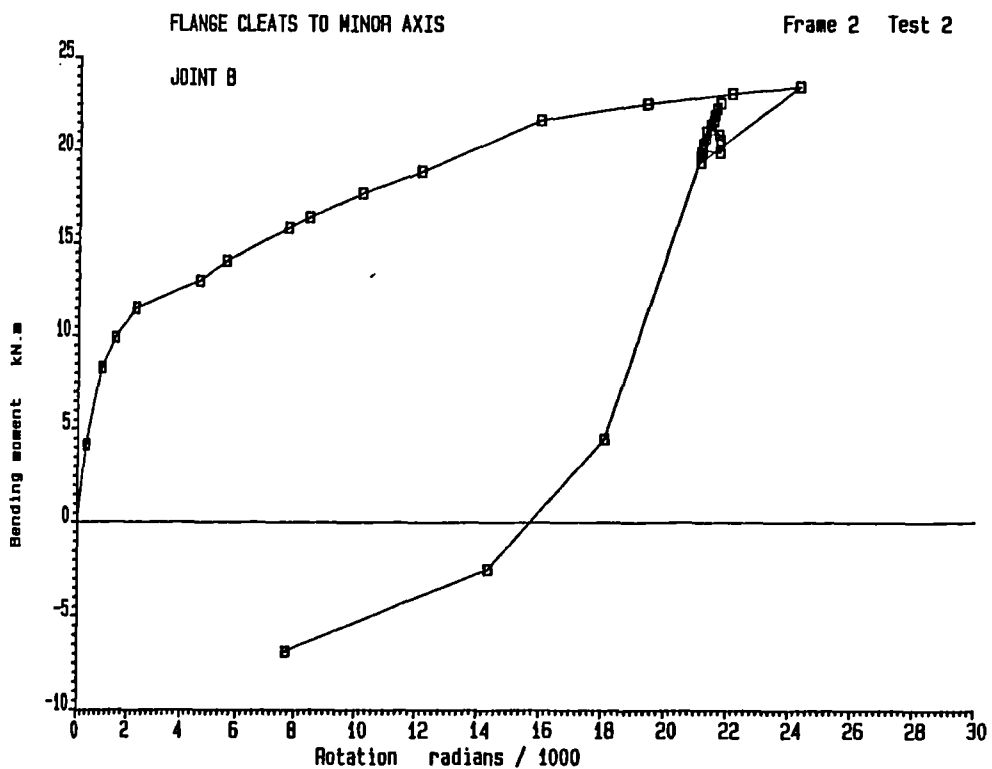


FIGURE 5.47 Moment-rotation curve for joint B

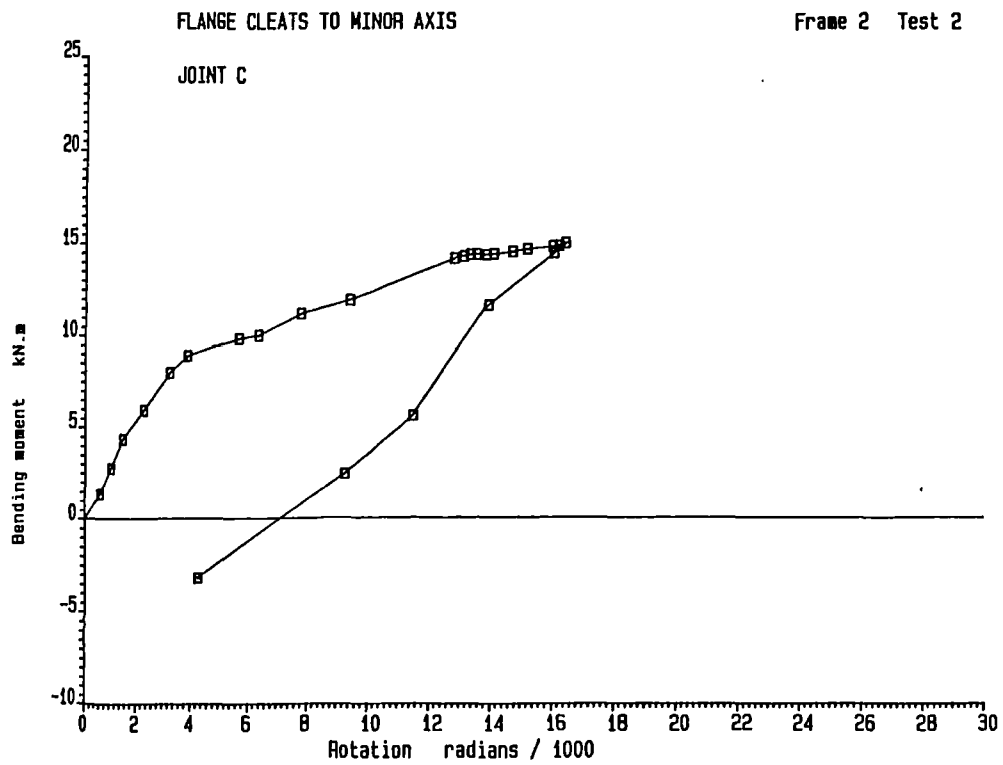


FIGURE 5.48 Moment-rotation curve for joint C

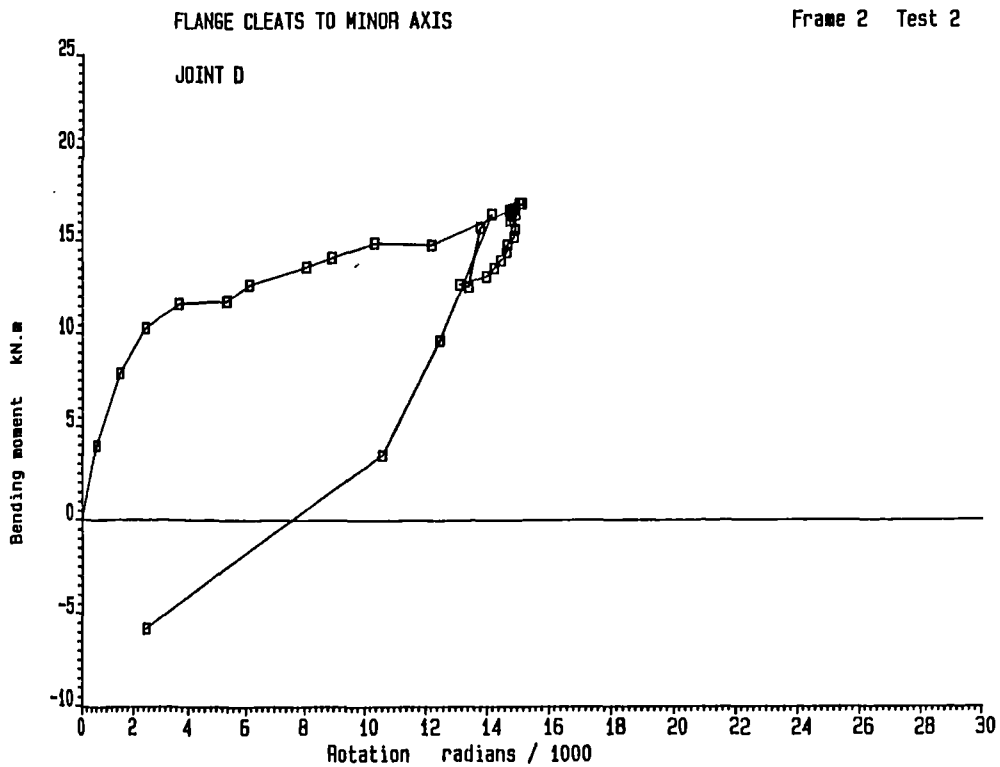


FIGURE 5.49 Moment-rotation curve for joint D

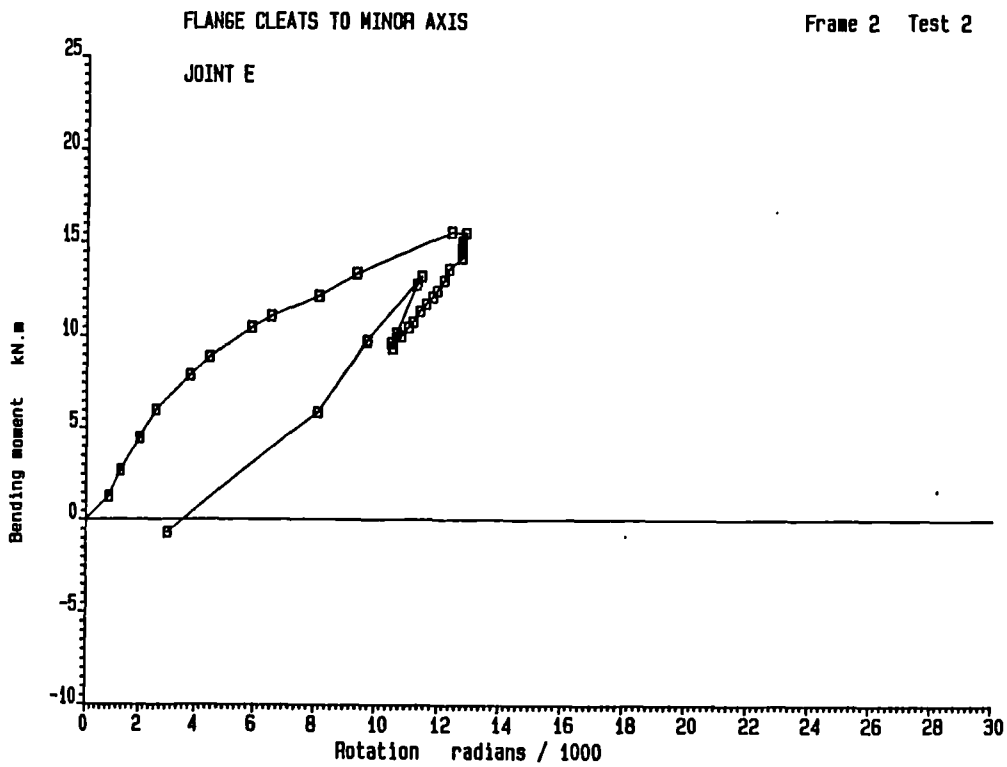


FIGURE 5.50 Moment-rotation curve for joint E

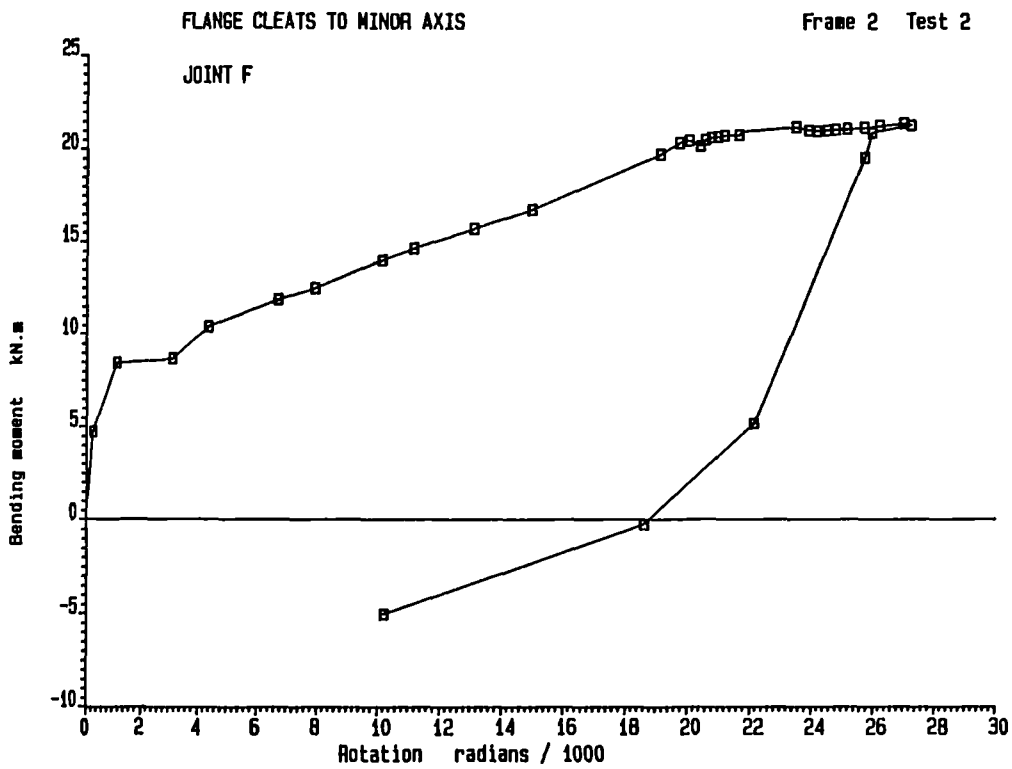


FIGURE 5.51 Moment-rotation curve for joint F

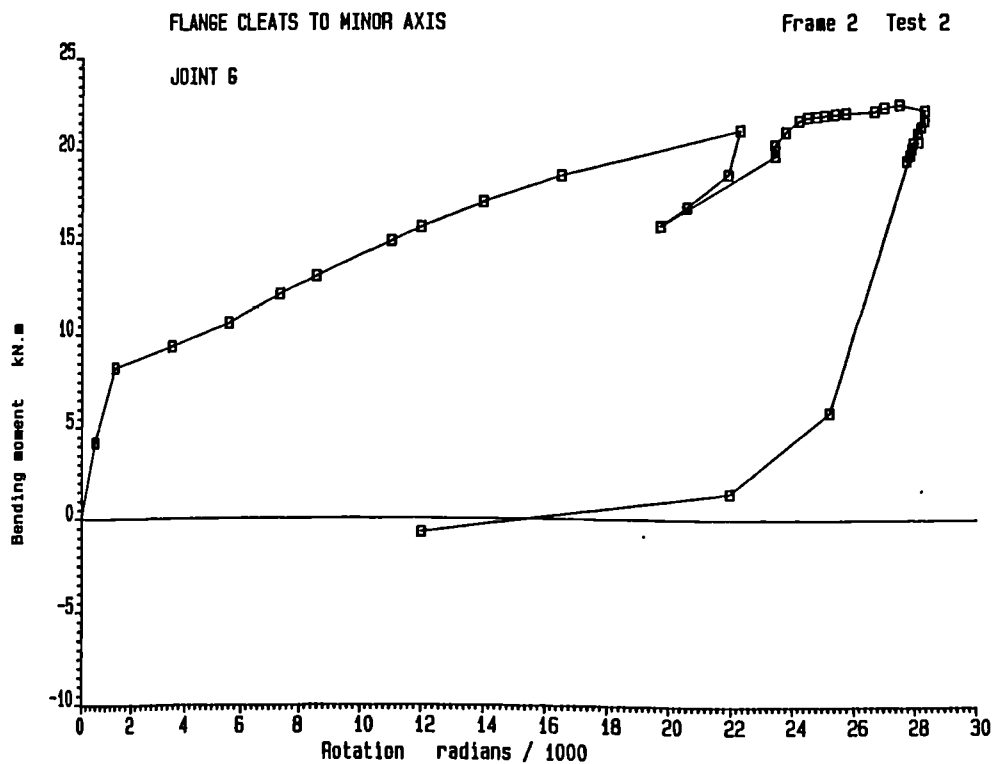


FIGURE 5.52 Moment-rotation curve for joint G

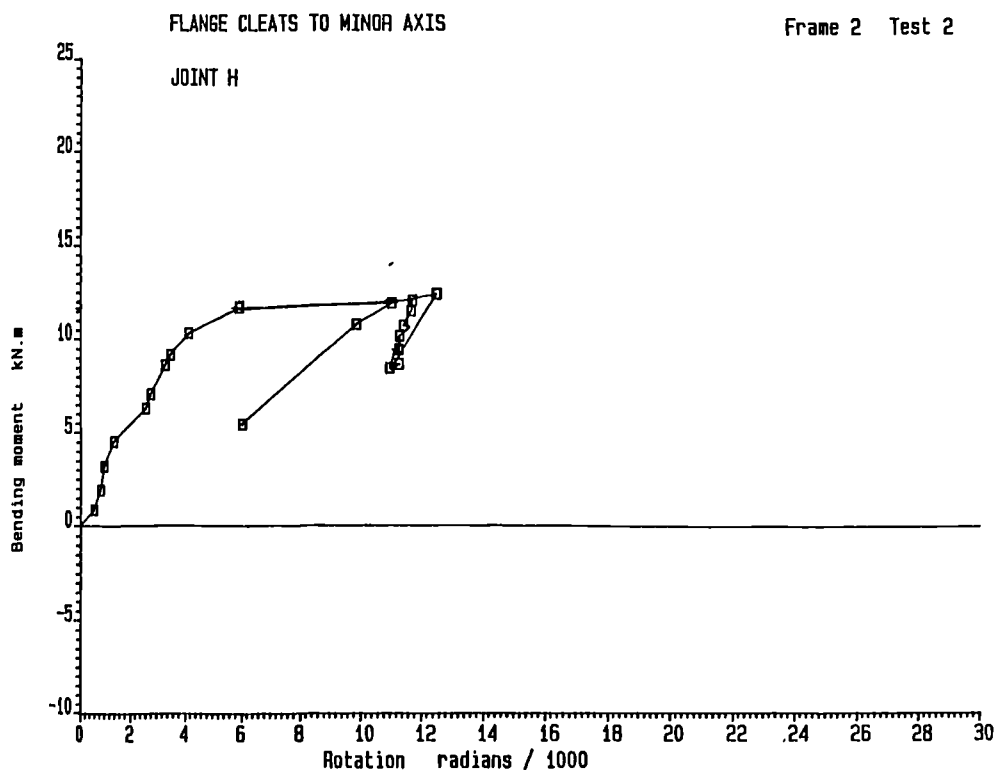


FIGURE 5.53 Moment-rotation curve for joint H

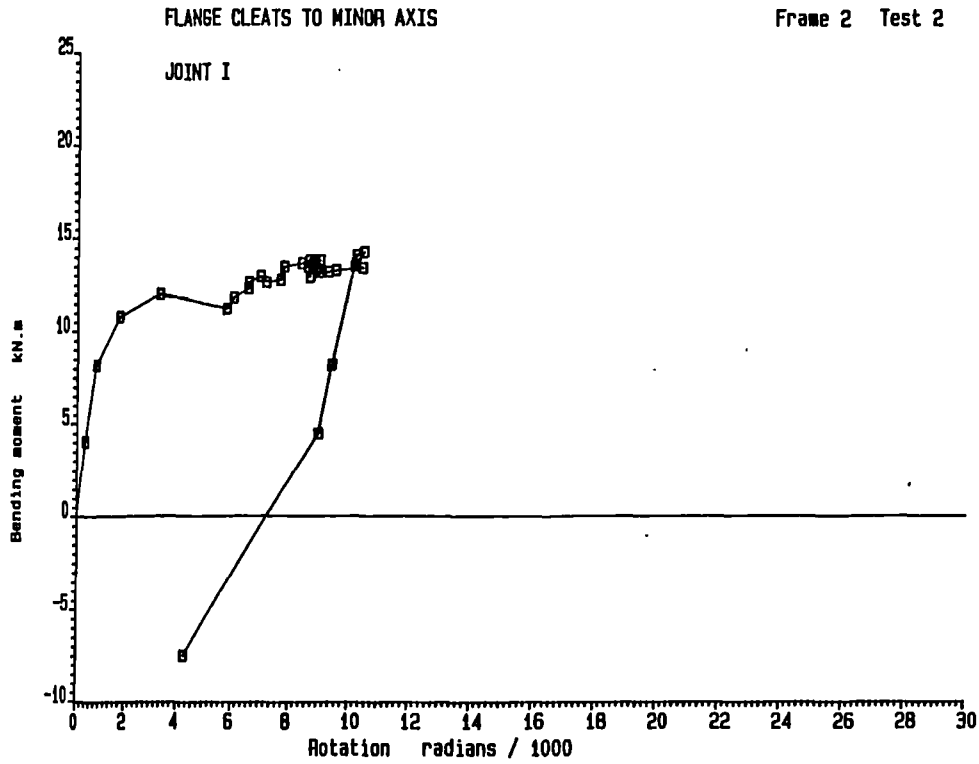


FIGURE 5.54 Moment-rotation curve for joint I

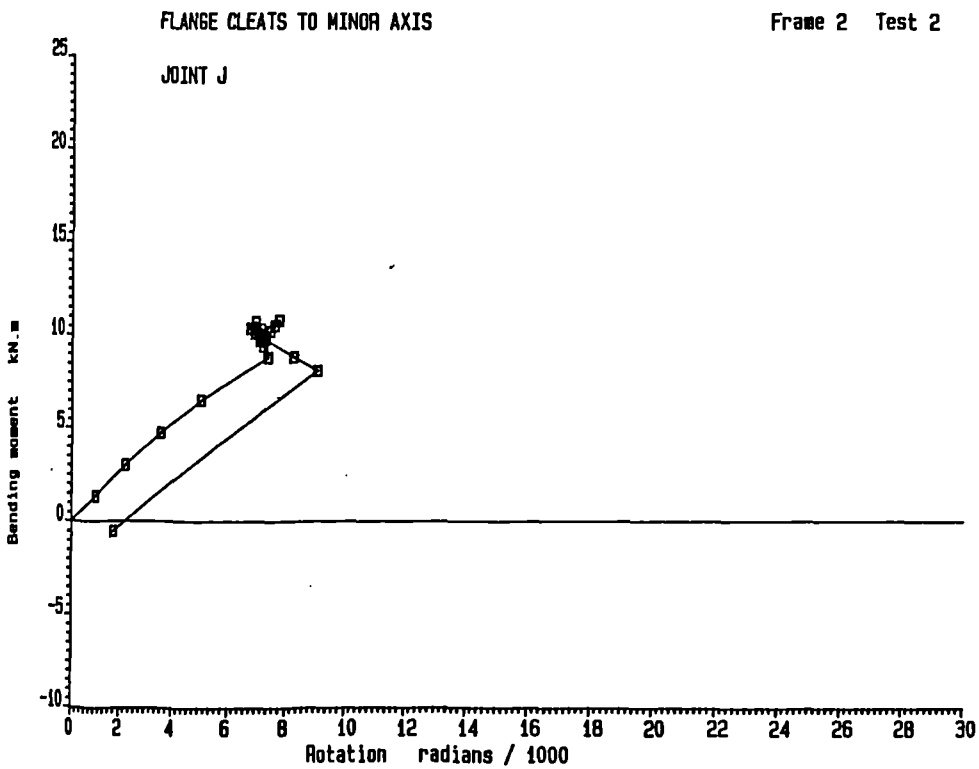


FIGURE 5.55 Moment-rotation curve for joint J

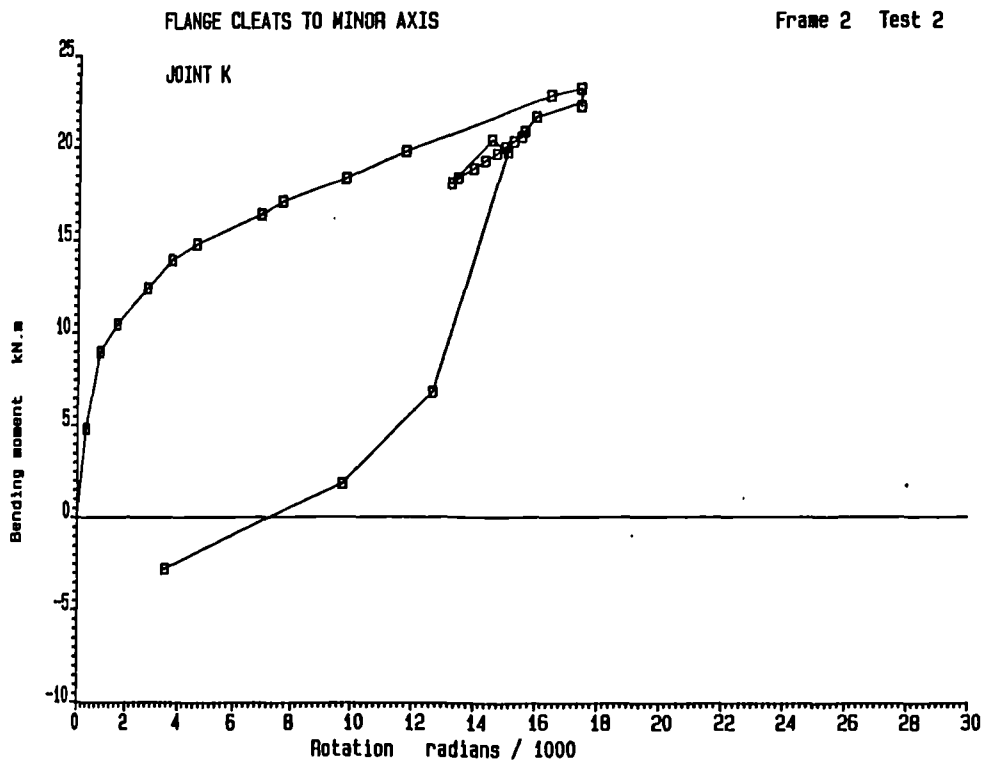


FIGURE 5.56 Moment-rotation curve for joint K

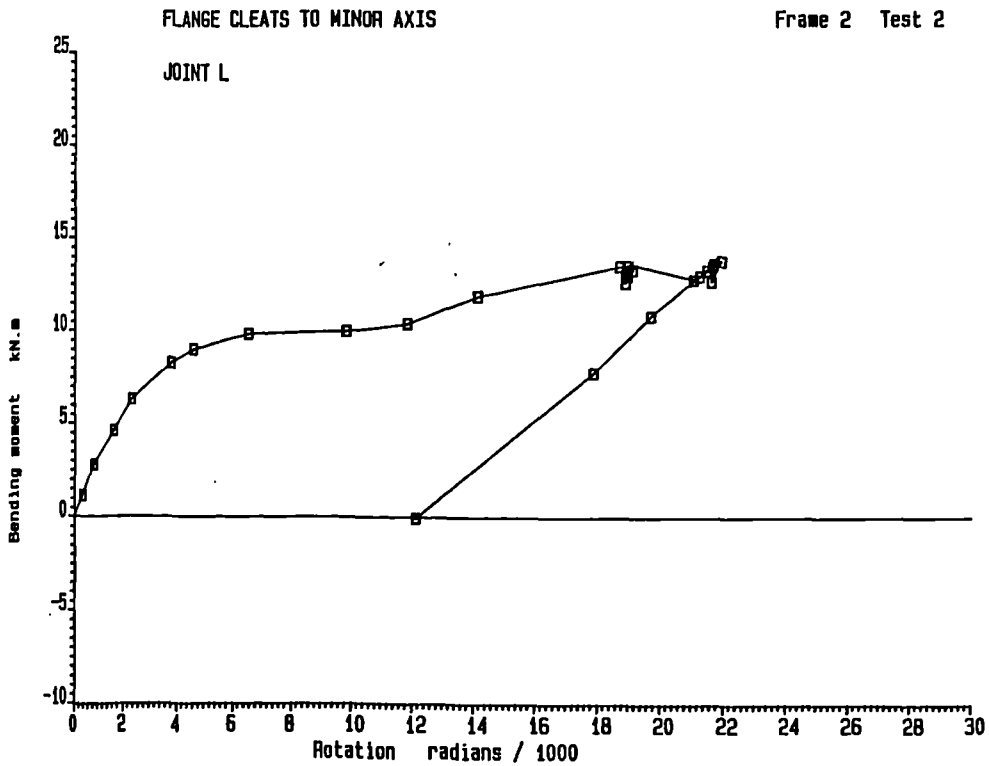
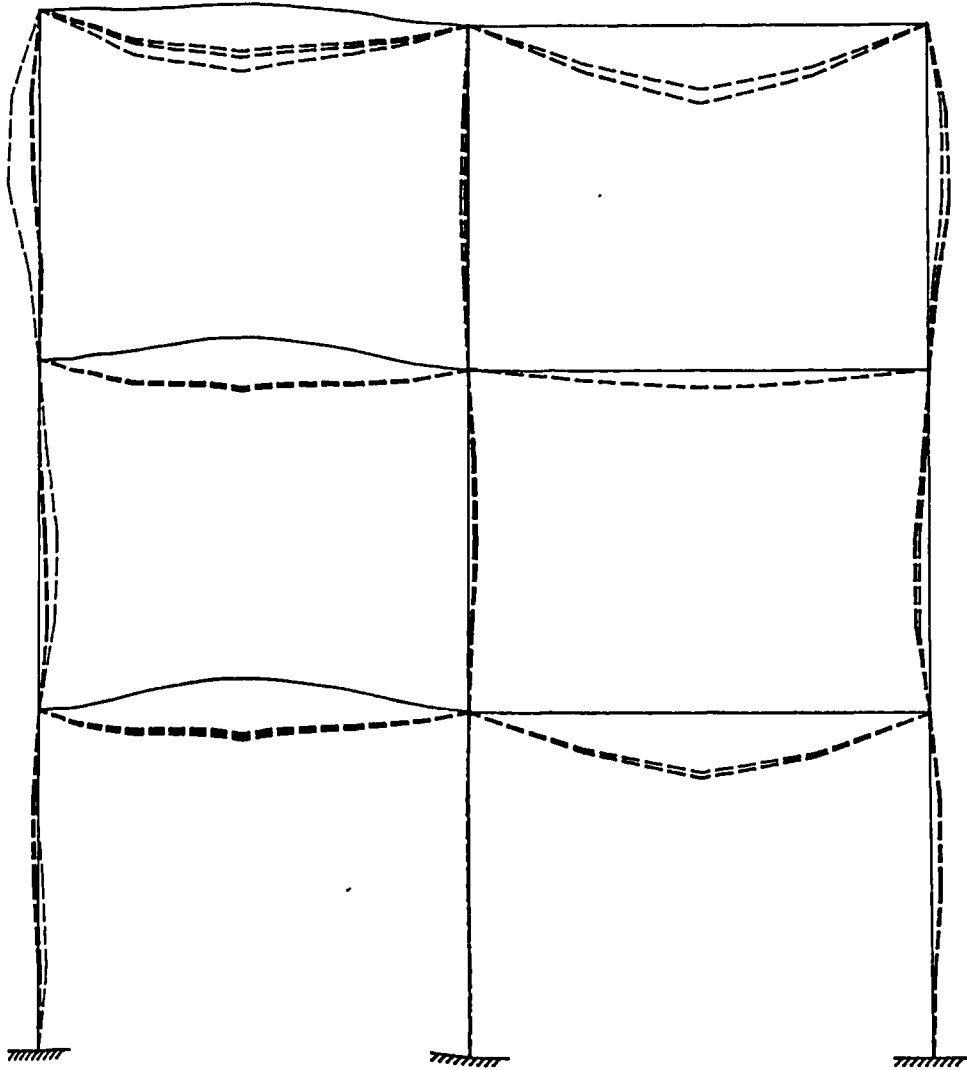


FIGURE 5.57 Moment-rotation curve for joint L

MINOR AXIS FRAME

DEFLECTED SHAPE OF FRAME



Horizontal deflections scale : 0.50 mm/mm

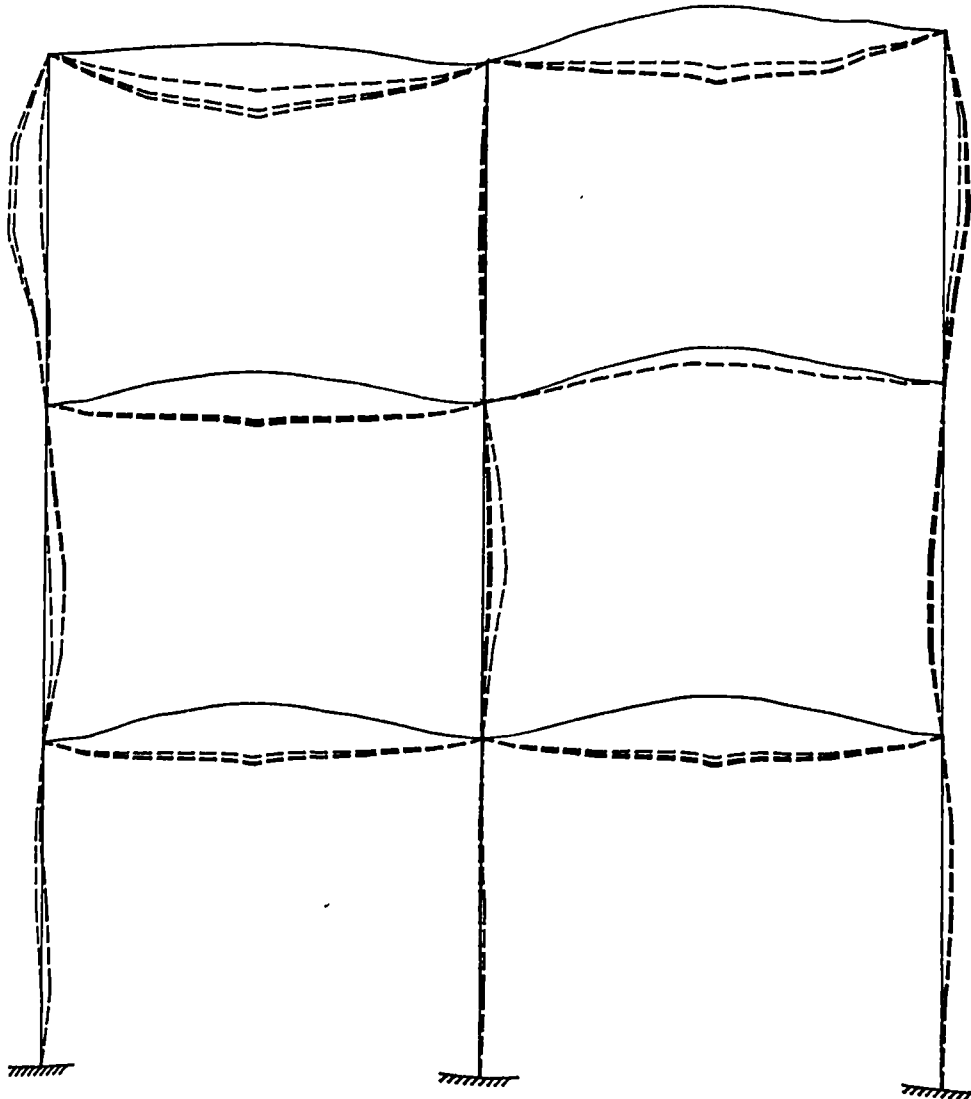
Vertical deflections scale : 0.25 mm/mm Frame 2 Test 2

Run Numbers Plotted : 12 16 27

FIGURE 5.58 Deflected shape of frame 2 at runs 12, 16 and 27

MINOR AXIS FRAME

DEFLECTED SHAPE OF FRAME



Horizontal deflections scale : 0.50 mm/mm

Vertical deflections scale : 0.25 mm/mm Frame 2 Test 2

Run Numbers Plotted : 12 27 36

FIGURE 5.59 Deflected shape of frame 2 at runs 12, 27 and 36

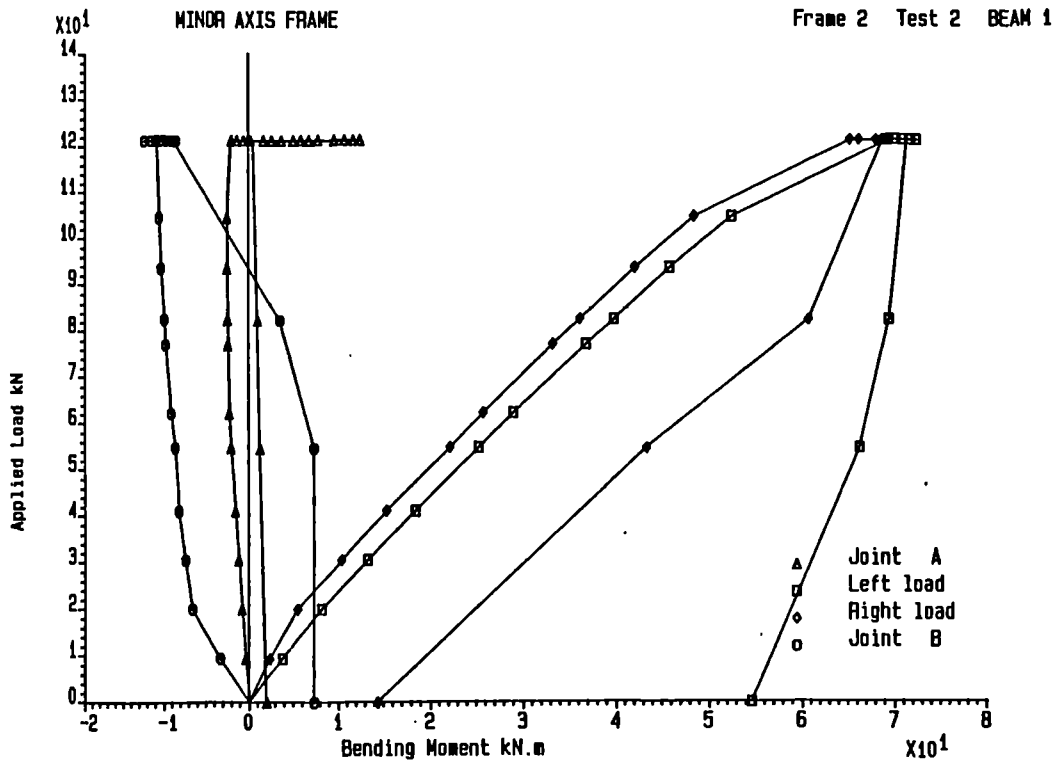


FIGURE 5.60 Applied beam load against bending moment for beam 1

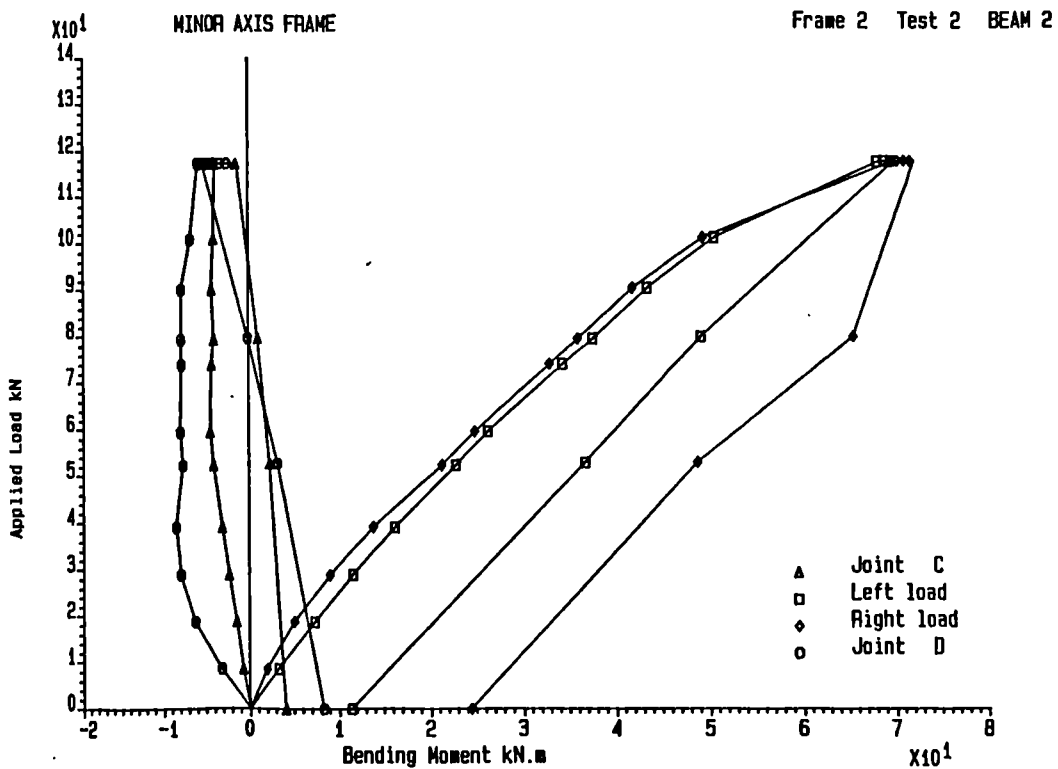


FIGURE 5.61 Applied beam load against bending moment for beam 2

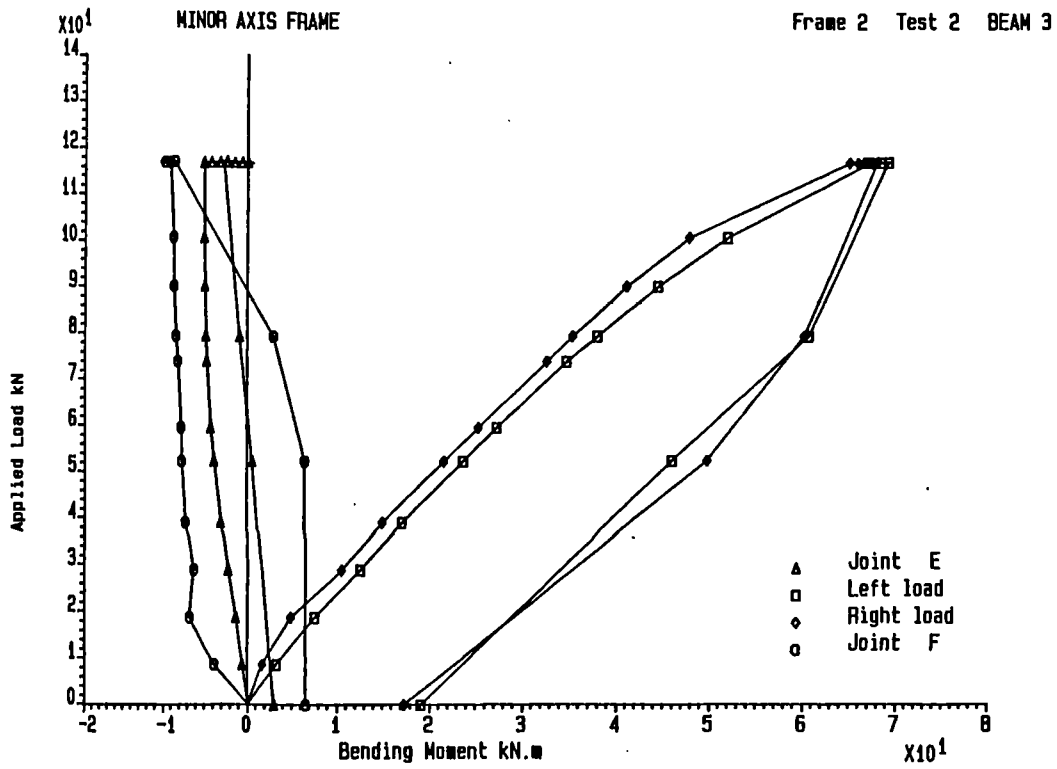


FIGURE 5.62 Applied beam load against bending moment for beam 3

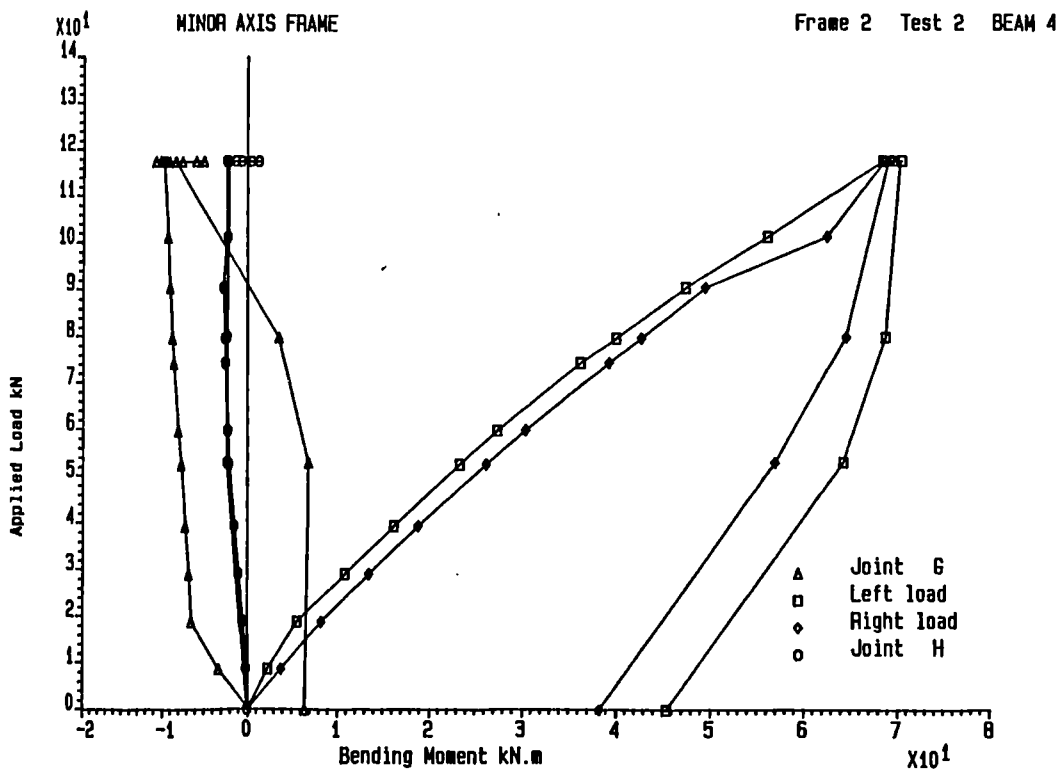


FIGURE 5.63 Applied beam load against bending moment for beam 4

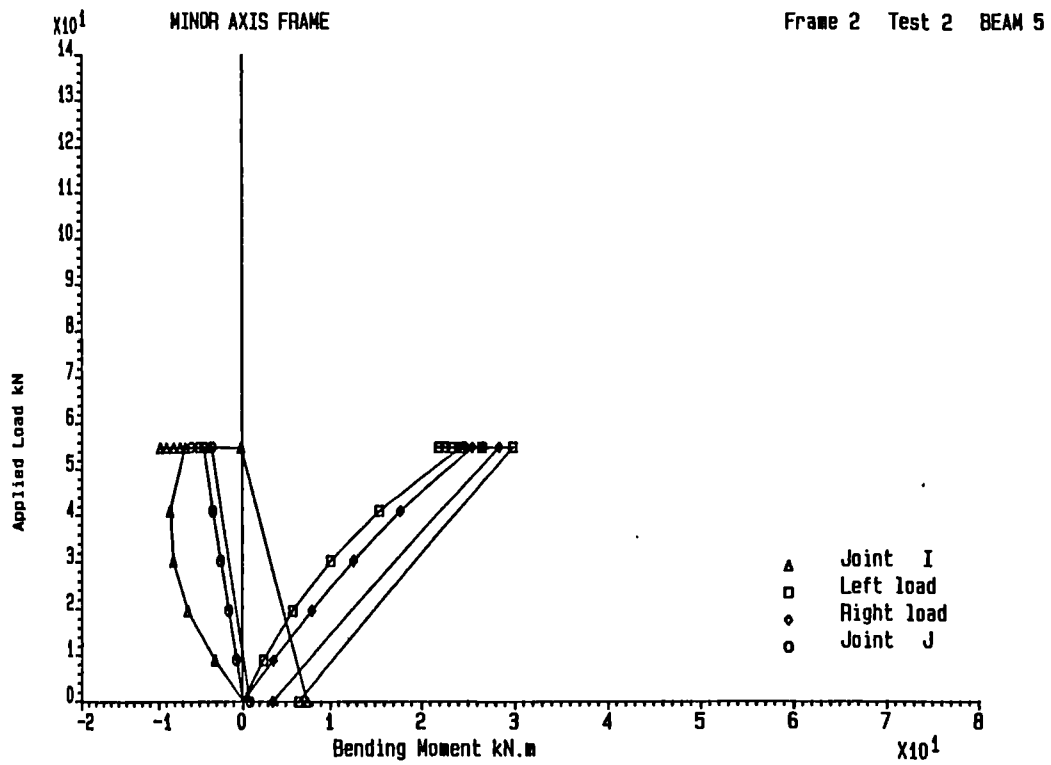


FIGURE 5.64 Applied beam load against bending moment for beam 5

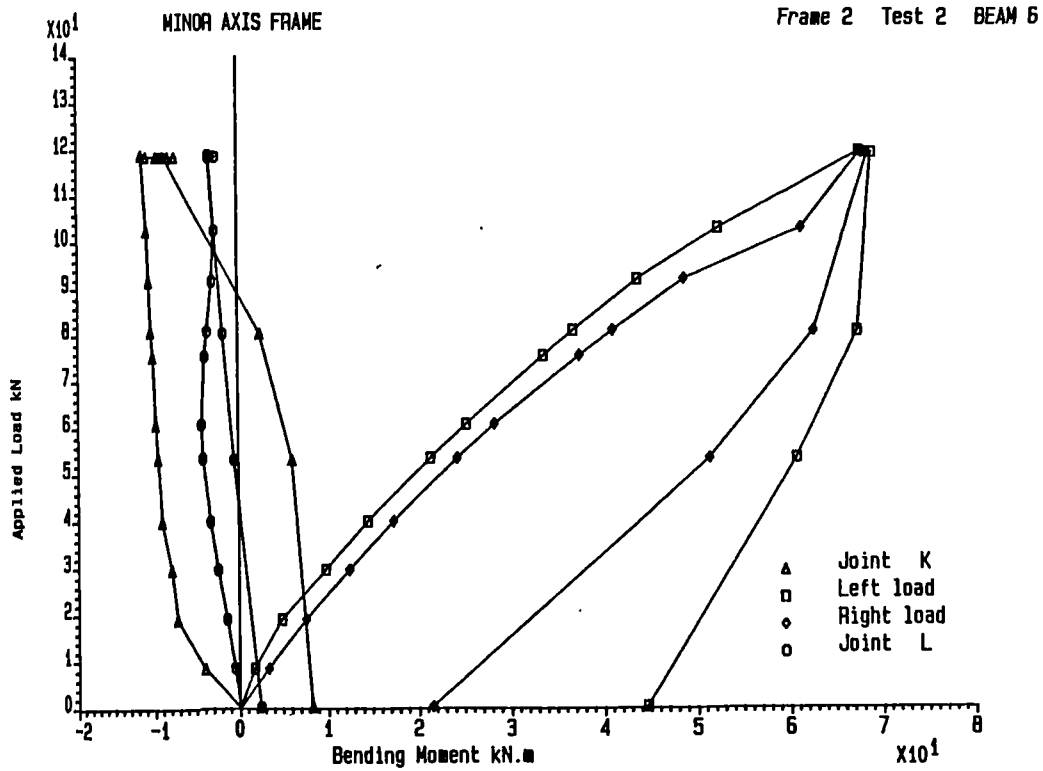


FIGURE 5.65 Applied beam load against bending moment for beam 6

Bending Moment kN.m

Frame 2 Test 2BEAM 3

Run Number Plotted : 3 5 7 9 11 12

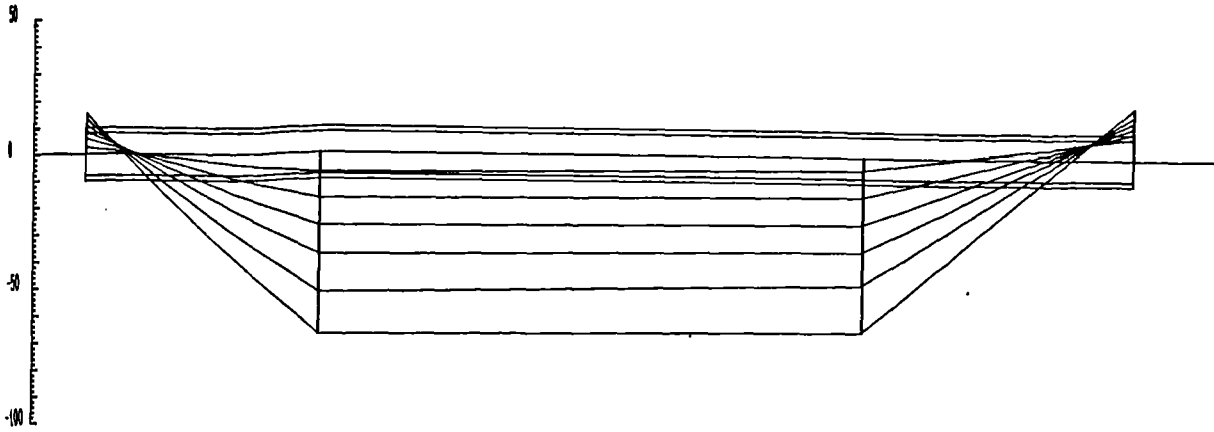


FIGURE 5.66 Bending moment distribution in beam 3 as beam loads are applied

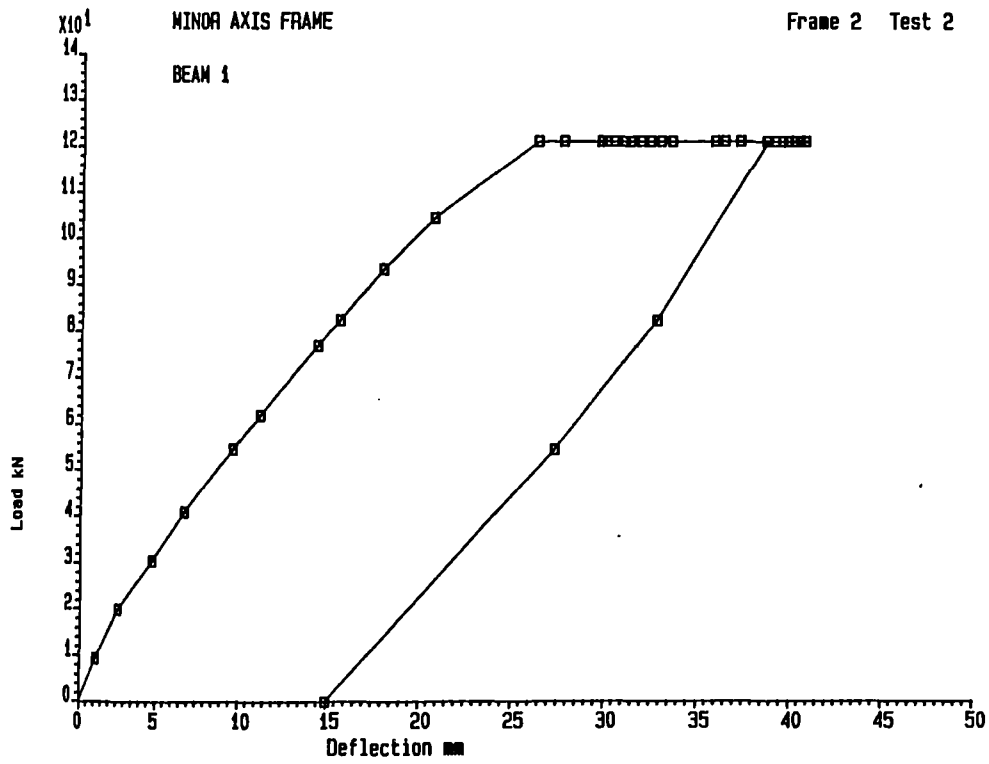


FIGURE 5.67 Applied load against central deflection for beam 1

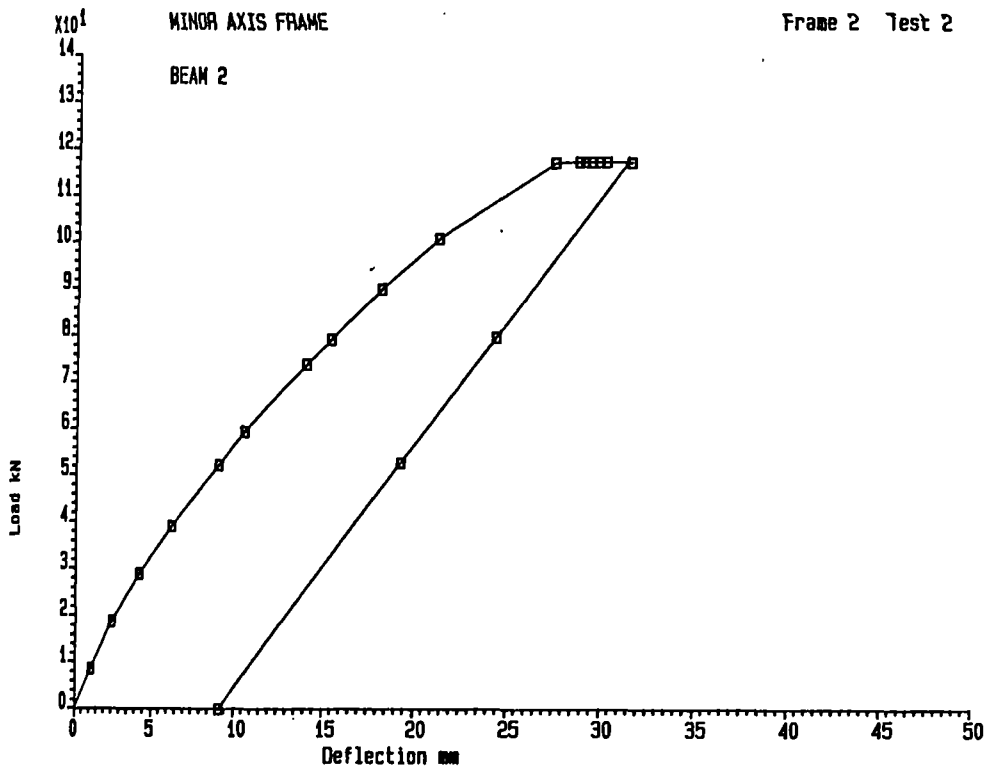


FIGURE 5.68 Applied load against central deflection for beam 2

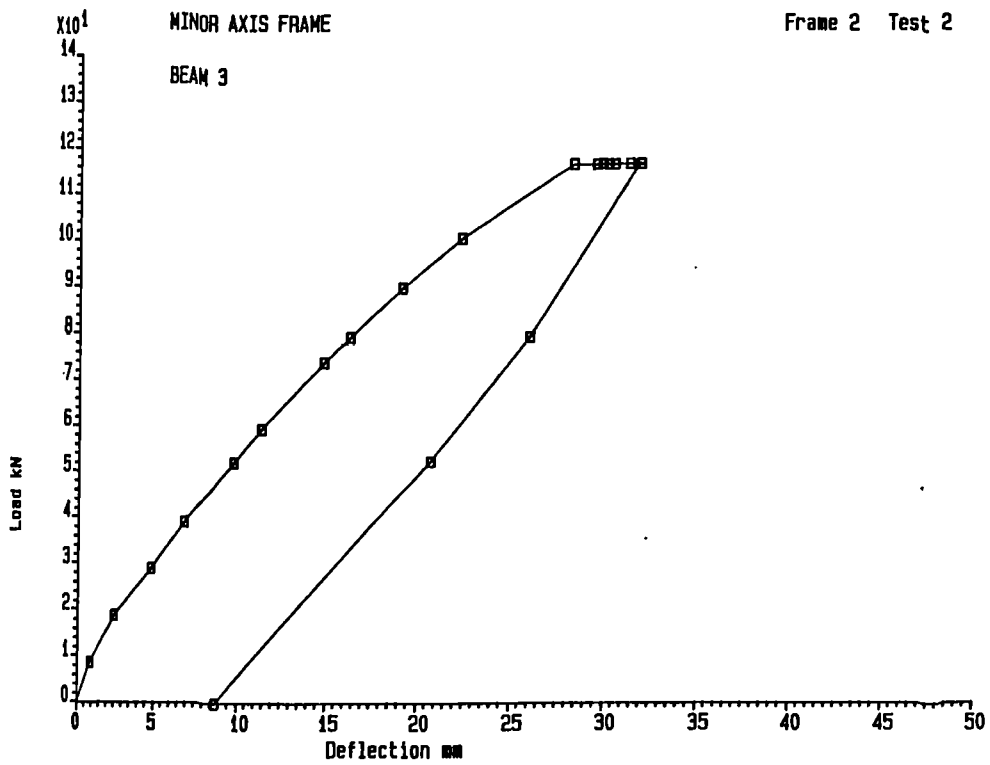


FIGURE 5.69 Applied load against central deflection for beam 3

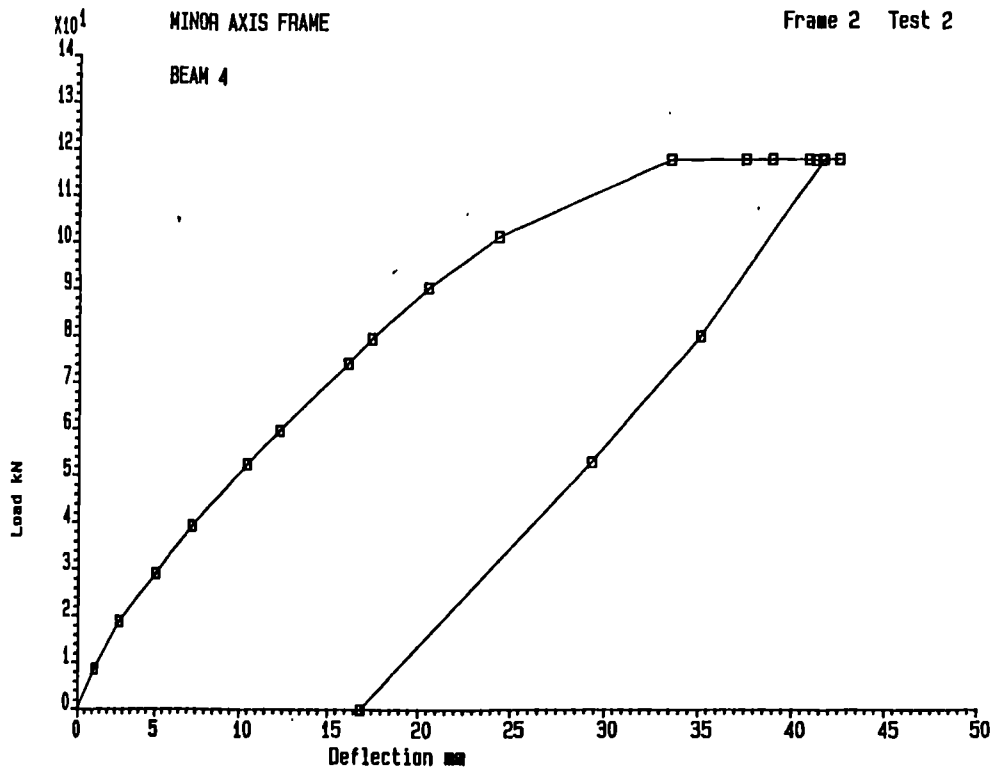


FIGURE 5.70 Applied load against central deflection for beam 4

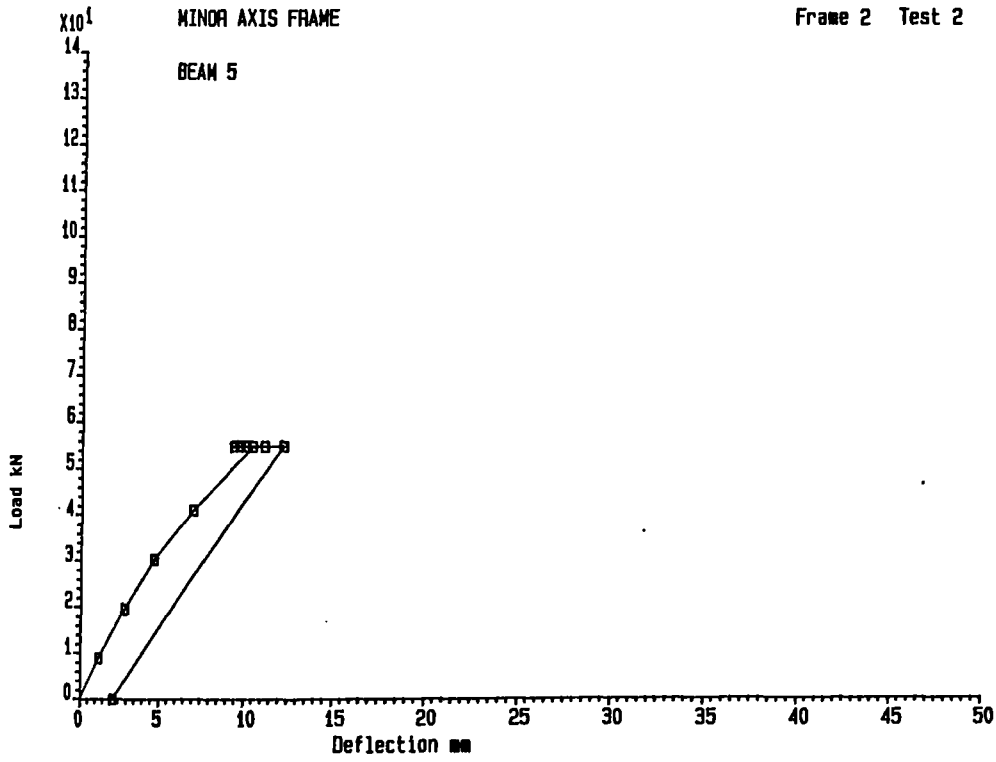


FIGURE 5.71 Applied load against central deflection for beam 5

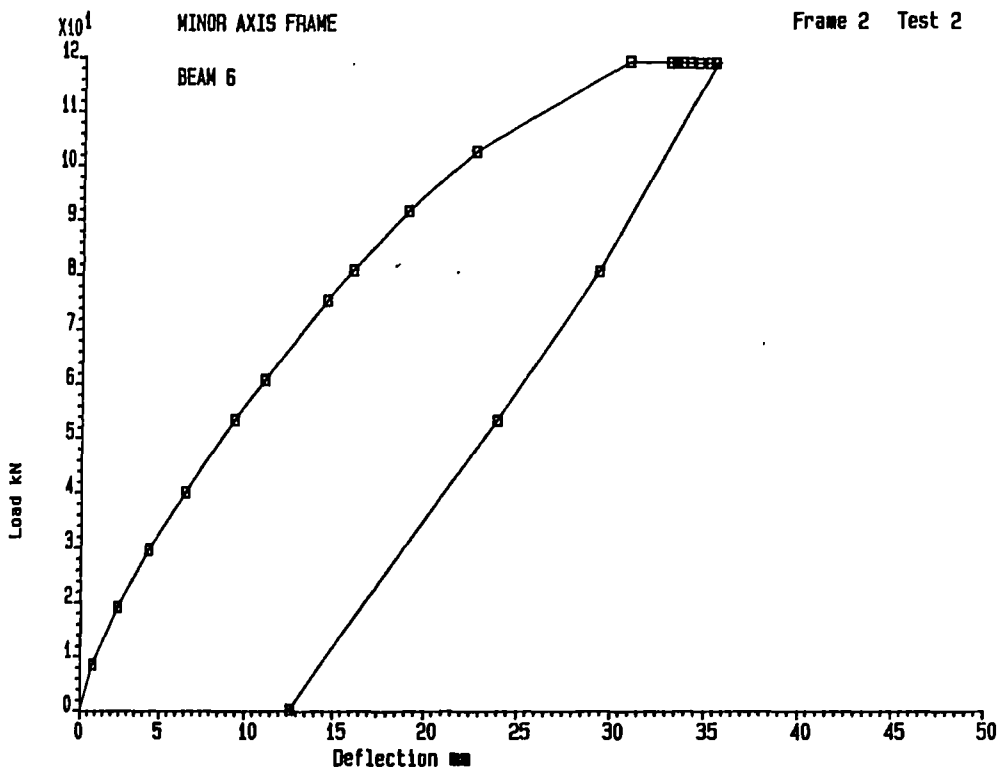
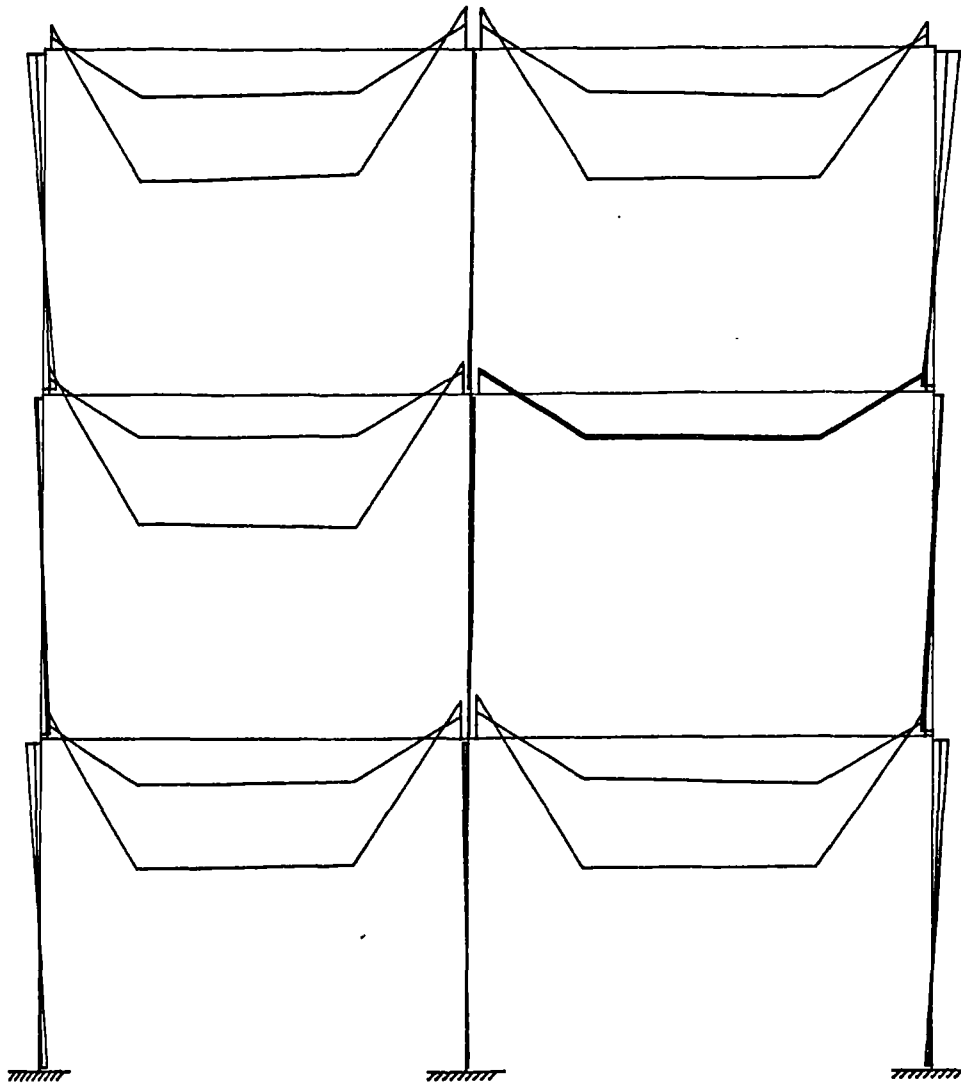


FIGURE 5.72 Applied load against central deflection for beam 6

MINOR AXIS FRAME

BENDING MOMENT DIAGRAM

MINOR AXIS COLUMN MOMENTS PLOTTED



Scale : 0.25mm/kN-m

Frame 2 Test 2

Run Numbers Plotted : 6 12

FIGURE 5.73 Moment distribution around frame 2 at runs 6 and 12

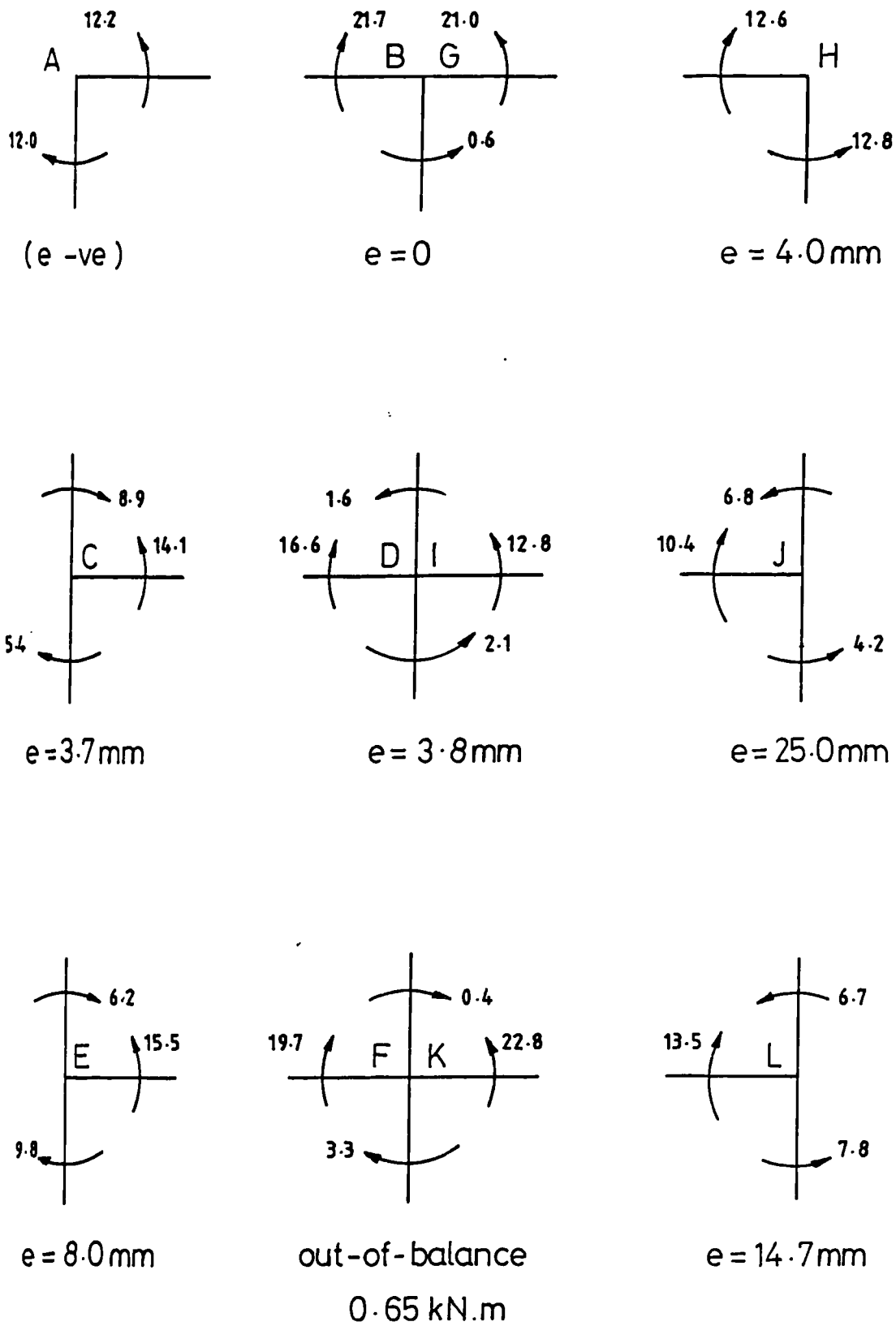
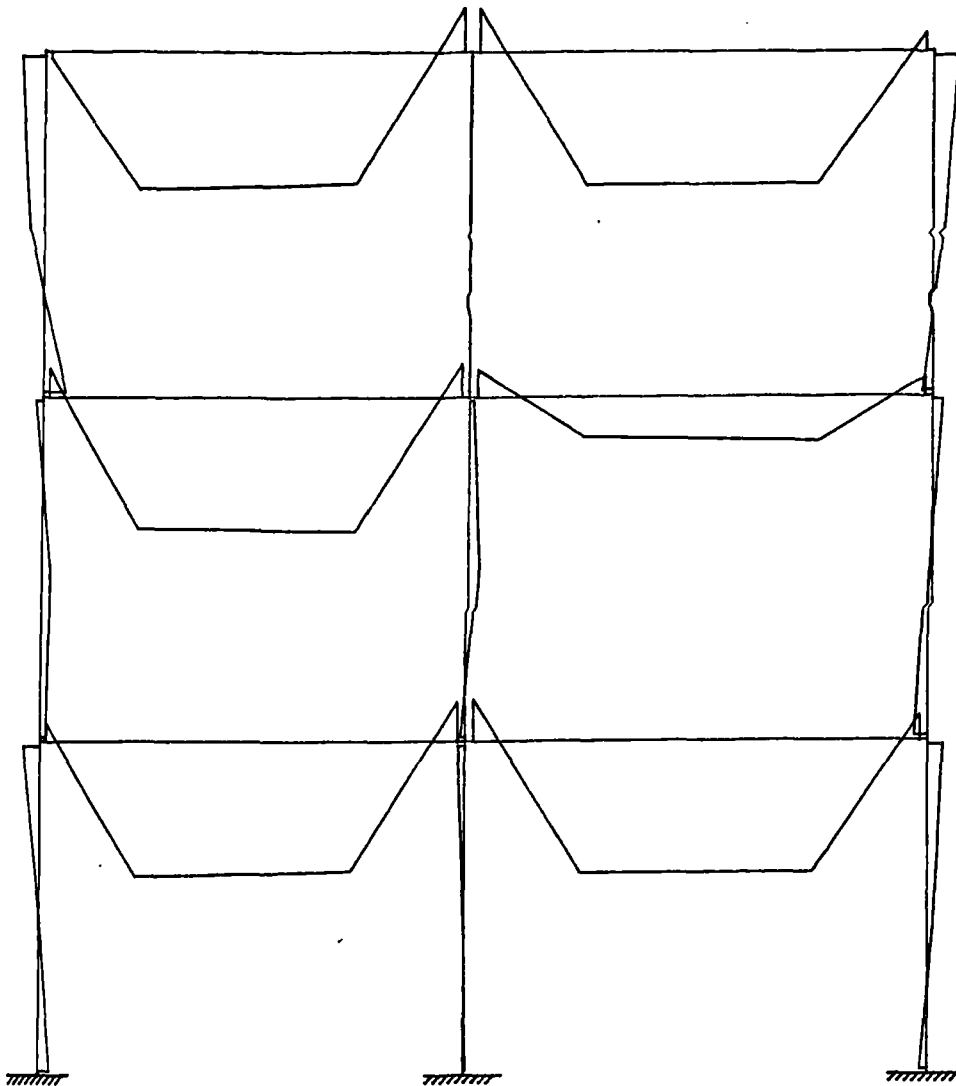


FIGURE 5.74 Moment equilibrium at joints in frame 2 at end of beam loading

MINOR AXIS FRAME

BENDING MOMENT DIAGRAM

MINOR AXIS COLUMN MOMENTS PLOTTED



Scale : 0.25mm/kN-m

Frame 2 Test 2

Run Numbers Plotted : 27

FIGURE 5.75 Moment distribution around frame 2 at failure of column in position 1

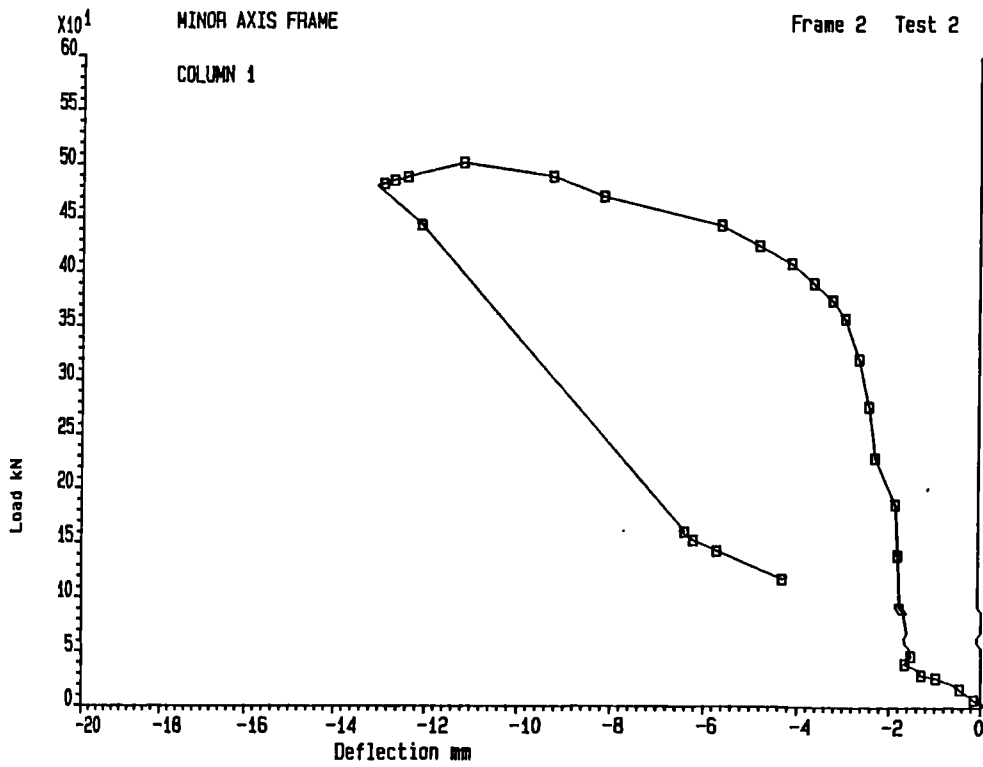


FIGURE 5.76 Total load in column against central deflection - column 1

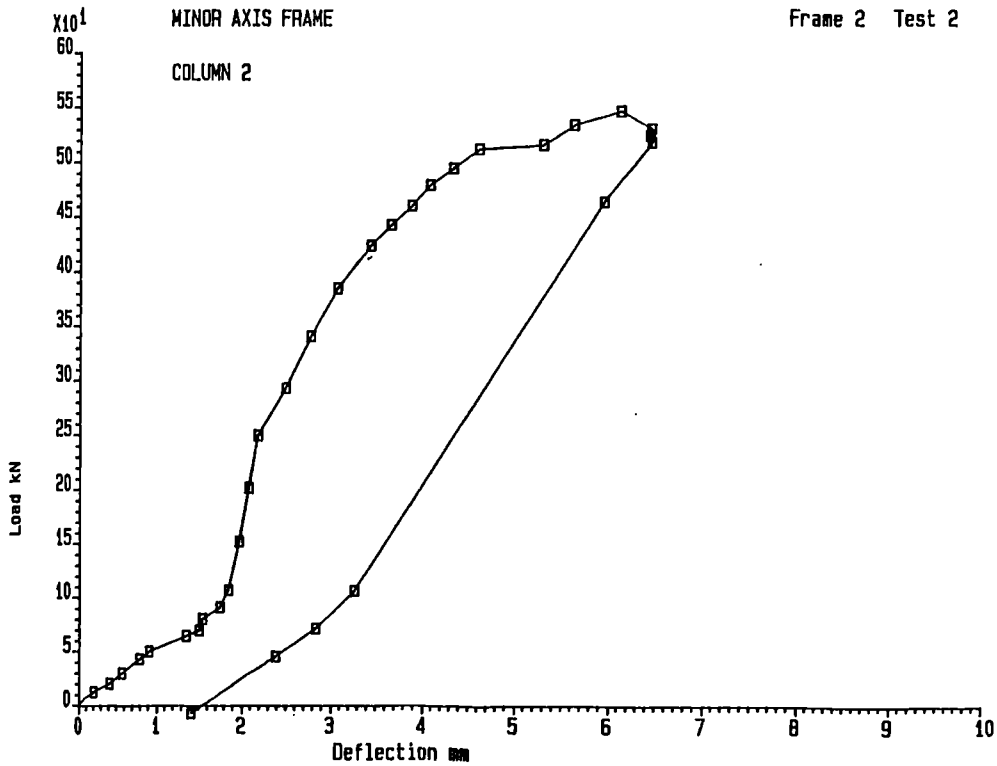


FIGURE 5.77 Total load in column against central deflection - column 2

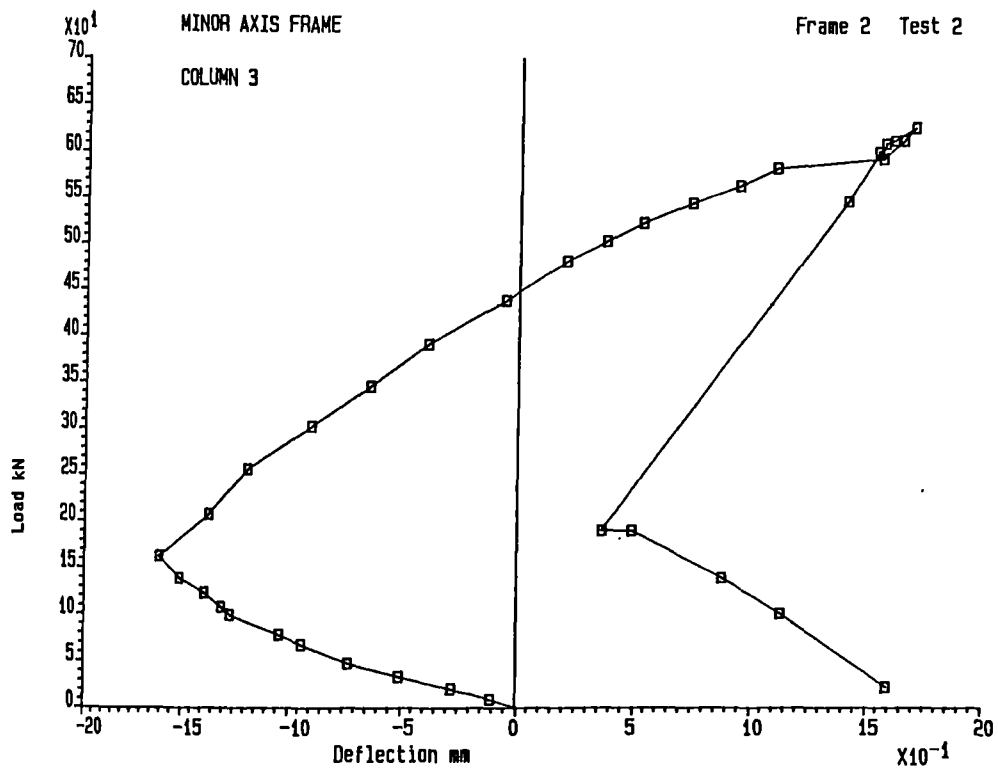
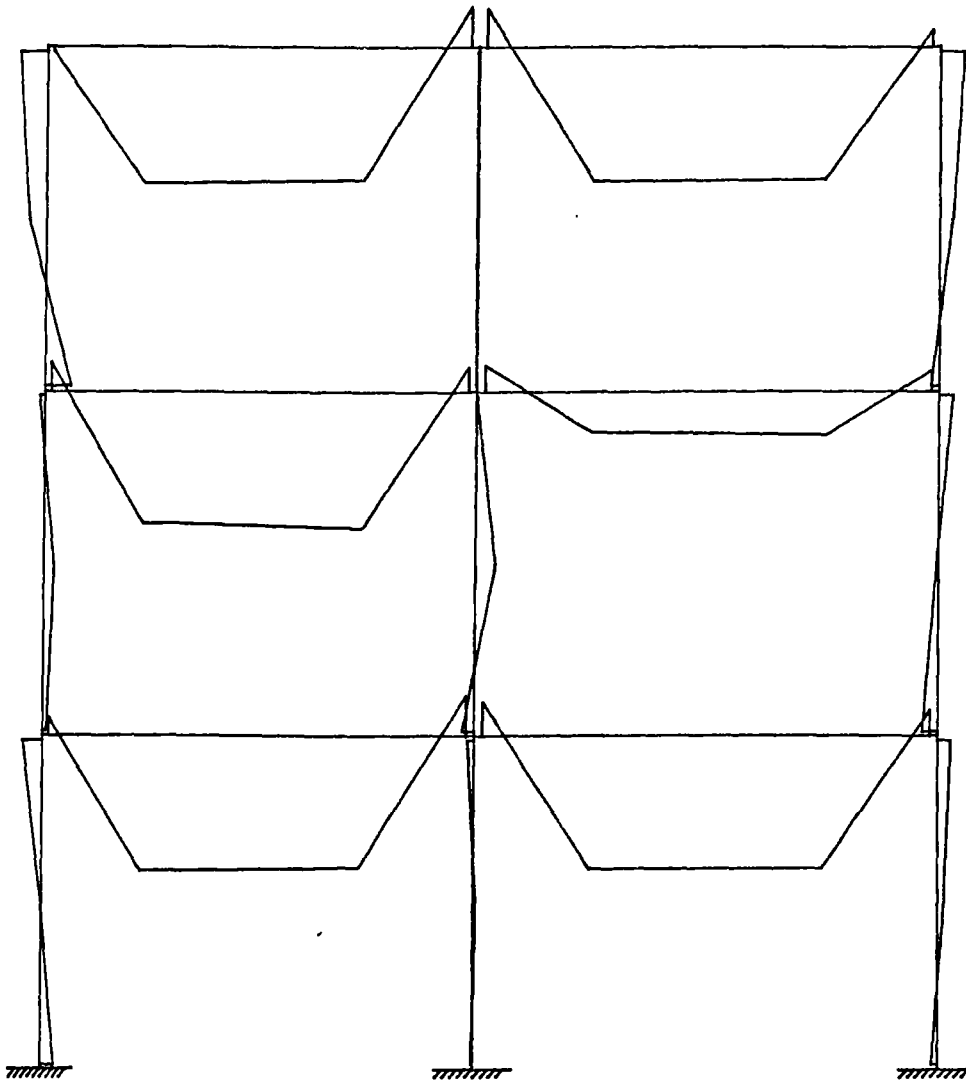


FIGURE 5.78 Total load in column against central deflection - column 3

MINOR AXIS FRAME

BENDING MOMENT DIAGRAM

MINOR AXIS COLUMN MOMENTS PLOTTED



Scale : 0.25mm/kN-m

Frame 2 Test 2

Run Numbers Plotted : 36

FIGURE 5.79 Moment distribution around frame 2 at failure of central column

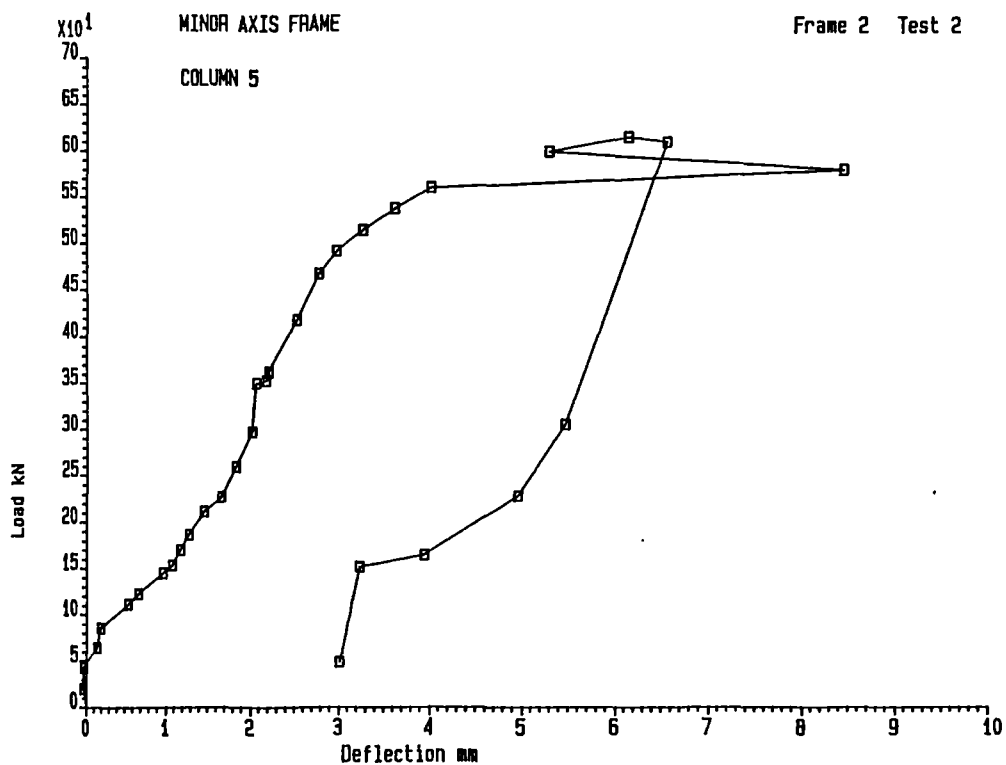


FIGURE 5.80 Total load in column against central deflection - column 5

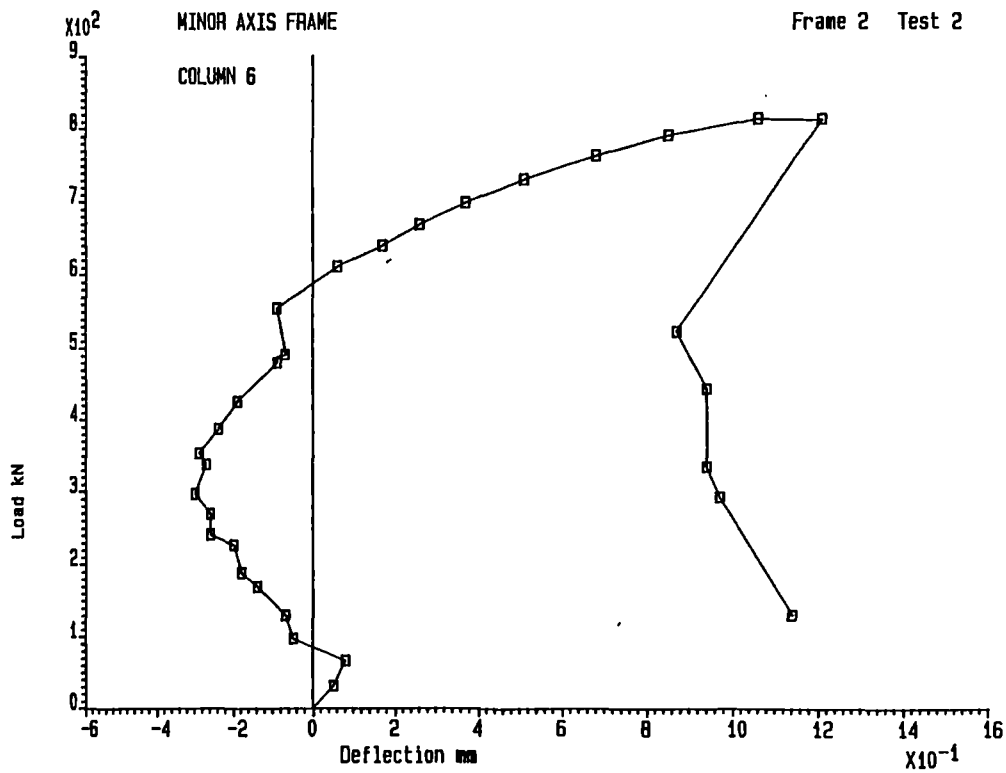


FIGURE 5.81 Total load in column against central deflection - column 6

6.0 COMPARISON OF EXPERIMENTAL BEHAVIOUR WITH ANALYTICAL PREDICTIONS

6.1 Declaration

In this chapter the behaviour of the subassemblage tests are compared with the response predicted by a computer program developed by A M Rifai at Sheffield University. Rifai conducted analyses of the subassemblage tests based on information provided by, and in discussion with, the author. A brief presentation of some of the comparisons between the tests and analysis is made herein but a more complete account is given by Rifai in reference 6.1.

Comparisons are reported between the frame test results and a semi-rigid analysis program (SERVAR) (6.2). The program was developed by C Poggi of the Politecnico di Milano, to whom gratitude is expressed for his permission for its use in this project.

6.2 Introduction

A principal objective of the experimental work conducted in this project was to provide results which could be used to verify computer programs capable of incorporating the effects of geometric non-linearity, plasticity and the influence of semi-rigid connections on column and frame stability. If such programs can be shown to accurately predict the behaviour of experimental tests then extended investigations to study the influence of many parameters may be conducted more conveniently by analytical methods than by extensive and expensive experimental studies.

6.3.1 Subassemblage Tests

An analysis of each subassemblage test was conducted using the best possible input data (measured section dimensions, static tensile yield stress, connection response from the joint test series and

loading history). An initial eccentricity of 2mm was assumed for the axial load; this was considered compatible with the experimental precision. In all cases an initial out-of-straightness of a sinusoidal shape with a maximum amplitude of 2mm was assumed. In those tests in which a larger initial deflection was introduced close to midheight a small lateral load was applied in the analysis to produce the same effect.

Figures 6.1 to 6.8 compare the analytical and experimental load central deflection curves for each test, and table 6.1 compares the maximum column load recorded in the subassemblage test and that predicted by the analysis. The comparison of predicted and tested load-deflection responses for tests ST2, ST3, ST4, ST8, ST9 and ST10 are very good, although the predicted failure loads in tests ST4 and ST10 are significantly lower than the test results (attributed by Rifai to numerical divergence). In tests ST6 and ST7 (flange cleat connections to the column web) the application of the beam loads produced much greater deflections in the test than the analysis predicted but the maximum load was predicted well in case ST7. In case ST6 the beam loads were of equal magnitude and placed symmetrically about the column centreline resulting in little or no moment transfer to the column in the analysis. In order to investigate the reason for the discrepancy two further analyses of test ST6 were conducted. In the first a lateral load was introduced at midheight to produce the deflection recorded in the test - see figure 6.9. In the second the moment-rotation response measured in ST6 was used as input data and residual stresses were also introduced. The resulting analysis was much closer as shown in figure 6.10.

In test ST7 the deflection of the column at midheight was modelled by the application of a lateral load, since the analysis incorrectly predicted the deflection produced by beam loading, and the resulting analysis produced a better load-deflection plot and maximum load - see figure 6.11.

In addition to the comparisons of load-deflection response the moments induced in the column and beams at the top connection throughout the test were studied in the experiment and the analysis. Figures 6.12 to 6.14 show the above comparison for tests ST4, ST8 and ST9. Bearing in mind the difficulty of measuring bending moments accurately, and at the desired locations, the correspondence in these cases was very good.

The above brief summary of the comparison between experimental and analytical results demonstrates that the computer program can accurately predict the response and failure load of columns restrained by semi-rigid connections. Exact correlation between tests and analysis for all cases will never be possible due to the complexity of the problem, the variability of the input parameters (material properties, residual stress, connection behaviour) the influence of experimental errors and the effects of friction, out-of-plane action etc which may be present in a physical test but are not readily accounted for in analysis. However the usefulness of such a program to study intimately the behaviour of restrained columns and to consider the influence of a wide range of parameters is clearly manifest.

6.3.2 Comparison of Frame 1 with SERVAR

A direct comparison of the results obtained in test frame 1 with the analytical predictions of SERVAR has been made. The measured

values of elastic modulus, yield stress and section properties were used (see Appendix C). The initial frame geometry, as reported in figure 5.13 was used in the model shown in figure 6.15. To compensate for the weight of the loading gear attached to the frame the yield stress of the beam sections was reduced to an effective value (approximately 17 N/mm^2 was deducted from the measured values). Table 6.2 shows the loading applied to the frame in the analysis. An eccentricity of 10mm was introduced to the axial loads applied to the columns. The moment-rotation curve, based on the behaviour of flange cleats connected to the column web, used in the analysis is shown in figure 6.16.

The bending moment distribution at the completion of the beam loading phase is shown in figure 6.18, and the deflected shape of the frame at this load level in figure 6.19. The shape and magnitude of the forces and deflections around the frame compare favourably with the test results - see figures 5.38 and 5.25. In figure 6.17 a comparison of the load deflection behaviour of beam 6 as predicted by the program and that recorded in the test is presented.

Referring to table 6.2, both three storey columns were loaded to just above 200kN before the column in position 2 was brought up to failure. In the analysis the column loading was stopped at 575kN in order that the execution could continue and load be applied to the external column. A previous run had indicated that the axial load on the central column at failure was 585kN. Figures 6.20 and 6.21 show the bending moment distribution and deflected shape just prior to failure of the central column. The correspondence with the test results (figures 5.44 and 5.25) is again good. However the value of the applied axial load was greater than the 483kN applied in the test.

Finally the external column was failed. An applied axial load of 650kN was sustained by the column before failure, which compares well with the test value of 623kN. The bending moment distribution and deflected shape are shown in figures 6.22 and 6.23, and may be compared with the test results illustrated in figures 5.38 and 5.25.

The analysis conducted and described above assumed a 10mm eccentricity in the application of the axial loads. This value would appear to be reasonable in view of the detail at the head of the column, where for practical reasons, no bearings of any description were used. As beam loads were applied deformation at the heads of the column was produced and some eccentricity appears to have been unavoidable. Further runs of the analysis program were conducted to investigate the sensitivity of the columns to eccentricity of the applied load. With perfectly axial loading applied to the column head the load required to cause failure of the central column increased from 585 to 609kN, and that for the external column increased from 650kN to a value between 725 and 750kN. The central column required only 502kN to initiate failure if the axial load was applied at an eccentricity of 30mm.

These results show that the collapse load of the column is quite sensitive to the degree of eccentricity of the applied axial load. Unfortunately the exact value in the test cannot be determined, and a short coming in the experiment has been identified. In future work it would be advisable to pay greater attention to the loading detail and it may be preferable to apply the load at a known eccentricity rather than estimate limits for the probable eccentricity of a notionally axial load.

In figure 6.24 the load-deflection plot for column 4 (the third storey lift of the central column) is shown for analyses assuming 10 and 30mm eccentricities along with the test results. The central deflection produced by the beam loads was recorded as 3.3mm and predicted by the program as 4.3mm. This could probably be improved by modelling the actual joint moment-rotation curves instead of using the idealised version from the joint test series. As load was applied to the column the deflections increased with the curve for the analysis assuming 10mm eccentricity at the column head more closely following the actual test results than that for an assumed 30mm eccentricity. In the test the column appears to soften at an axial load of about 450kN. This is not simulated by the computer model. The comparison of the results suggests that the test behaviour was influenced by yielding in the cross section at an earlier stage than that predicted by the analysis and that the discrepancies in the predicted and actual failure loads is due to material non-linearity and not extreme eccentricity at the column head. Though residual stresses were present in the off-cut from the head of the column they were partly removed by cold straightening of the sections (see Appendix C). It seems likely that a reduction in strength due to the presence of some residual stresses has occurred in the test which cannot, at present, be accommodated in the analysis.

6.3.3 Comparison of Frame 2 with SERVAR

A comparison of the tested performance of the minor axis frame with the predicted response was also made. The bending moment distribution and deflected shape under full beam loading are shown in figures 6.26 and 6.27 and may be compared with the test results illustrated in figures 5.73 and 5.58. In the analysis two moment-

rotation curves were used, one for the response of the connections to an external column and another for those connected to an internal column. As discussed in chapter 5, and illustrated in figure 6.25, the connections to the external column were much more flexible due to the absence of a similar connection on the other side of the column web. Notice that this is a difference in connection response due to the column web flexibility and is not attributable to the column's flexibility since the rotation of the connection was the difference between the column and beam rotation.

Figure 6.28 shows the comparison of the predicted and actual deflection of beam B3 as loads were applied. The correspondence is once again good and considerably better than that assumed by simple calculation based on pinned supports. A study of the failure loads of the column has not yet been undertaken because the SERVAP program accounts for minor axis sections by assuming they can be represented by an equivalent rectangular section. Where inelastic buckling is likely this limitation causes problems because a rectangular section can have the correct area or moment of inertia as the I section to be represented, but not both.

References

- 6.1 Rifai, A.M.
'Behaviour of columns in sub-frames with semi-rigid connections'
Ph.D. Thesis, University of Sheffield, 1987.
- 6.2 Poggi, C.
'A finite element model for the analysis of flexibly connected
plane steel frames'
In preparation.

TEST NO.	FAILURE LOADS			FIGURE NUMBER
	ANALYSIS (kN)	EXPERIMENT (kN)	$\frac{\text{ANALYSIS}}{\text{EXPERIMENT}}$	
ST2	671	682	0.984	6.1
ST3	537	520	1.033	6.2
ST4	683	762	0.896	6.3 (Numerical divergence)
ST6	594	518	1.147	6.4
ST7	524	526	0.996	6.5
ST8	499	518	0.963	6.6
ST9	511	485	1.054	6.7
ST10	597	743	0.803	6.8 (Numerical divergence)
ST6	570	518	1.100	6.9 (with applied horizontal load)
ST6	530	518	1.023	6.10 (with revised $M-\phi$ data and residual stress)
ST7	507	526	0.964	6.11 (with applied horizontal load)

TABLE 6.1 Comparison of test and analysis column capacities

TIME	TOTAL BEAM LOADS (kN)		APPLIED AXIAL COLUMN LOADS (kN)	
	BEAMS 2, 3, 4, 6	BEAM 5	INTERNAL COLUMN	EXTERNAL COLUMN
1	8.8	8.8	0.0	0.0
2	17.0	17.0	0.0	0.0
3	29.0	29.0	0.0	0.0
4	40.0	40.0	0.0	0.0
5	52.0	52.0	0.0	0.0
6	60.0	54.0	0.0	0.0
7	74.0	54.0	0.0	0.0
8	80.0	54.0	0.0	0.0
9	90.0	54.0	0.0	0.0
10	100.0	54.0	0.0	0.0
11	117.0	54.0	0.0	0.0
12	117.0	54.0	45.0	45.0
13	117.0	54.0	245.0	225.0
14	117.0	54.0	390.0	270.0
15	117.0	54.0	470.0	270.0
16	117.0	54.0	510.0	270.0
17	117.0	54.0	575.0	270.0
18	117.0	54.0	440.0	270.0
19	117.0	54.0	440.0	400.0
20	117.0	54.0	440.0	550.0
21	117.0	54.0	440.0	600.0
22	117.0	54.0	440.0	650.0

TABLE 6.2 Loading history for analysis of frame 1

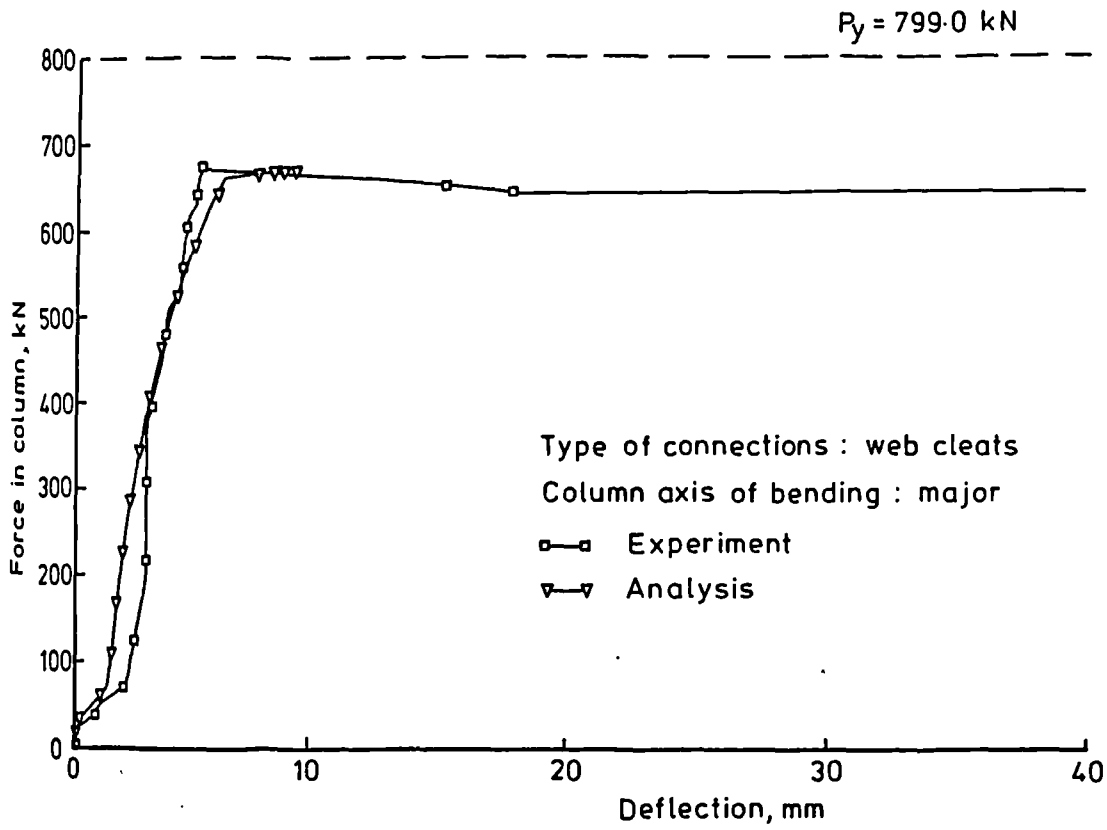


FIGURE 6.1 Comparison of analytical and experimental load-deflection response - ST2

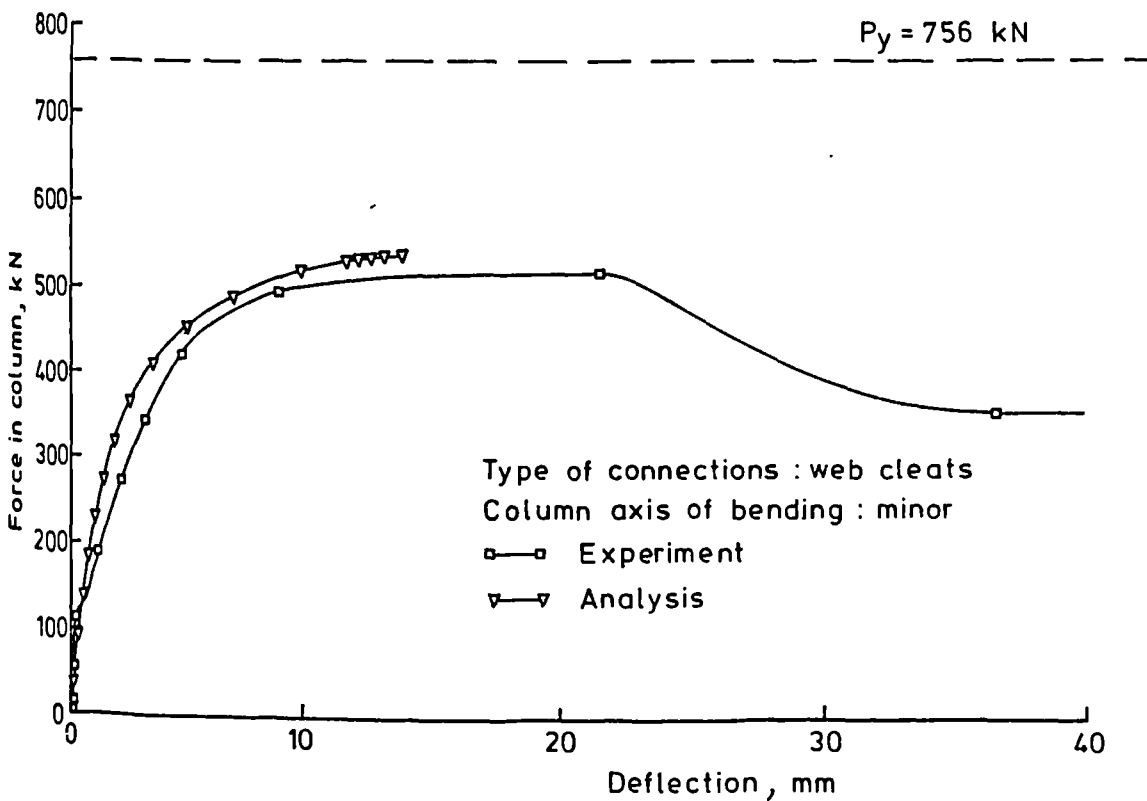


FIGURE 6.2 Comparison of analytical and experimental load-deflection response - ST3

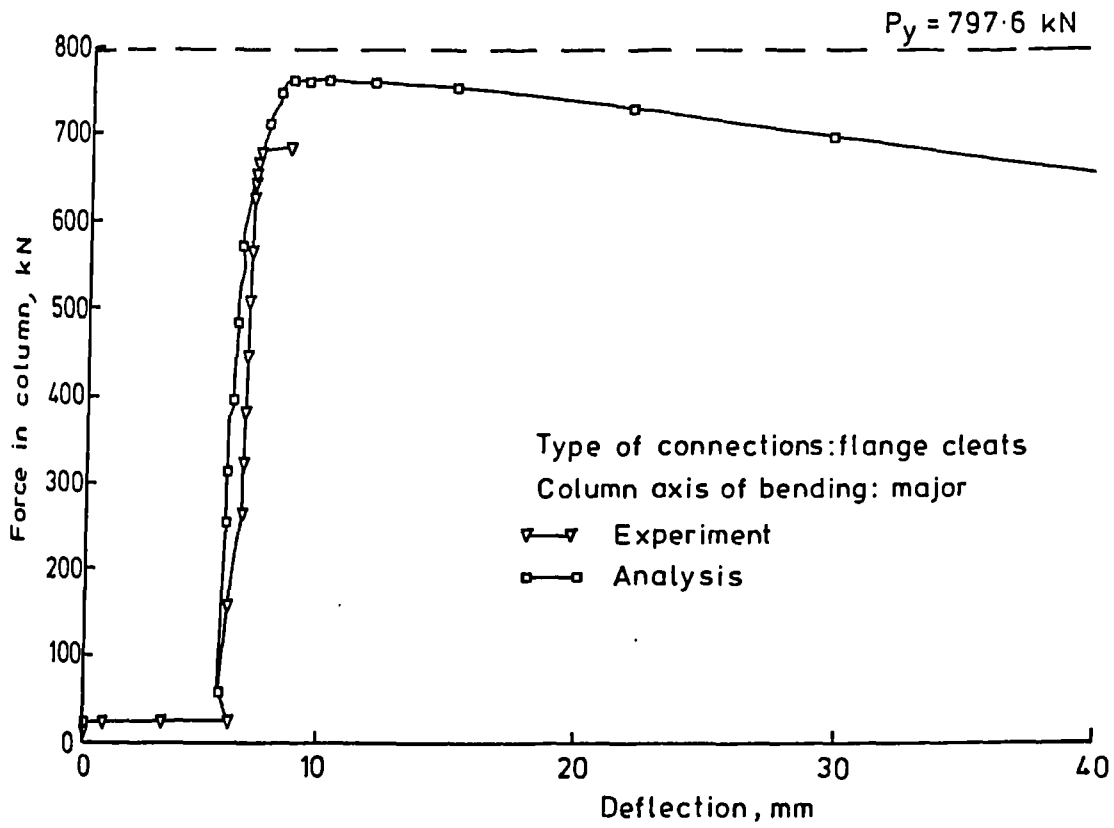


FIGURE 6.3 Comparison of analytical and experimental load-deflection response - ST4

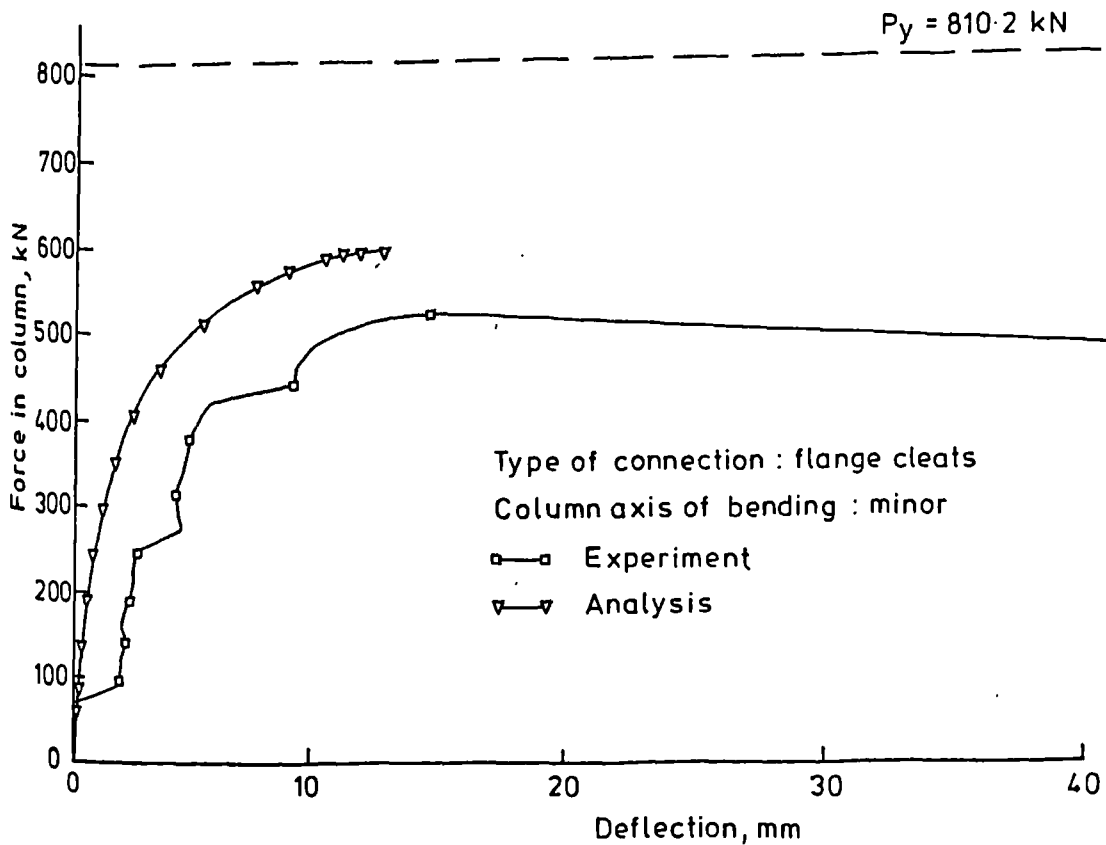


FIGURE 6.4 Comparison of analytical and experimental load-deflection response - ST6

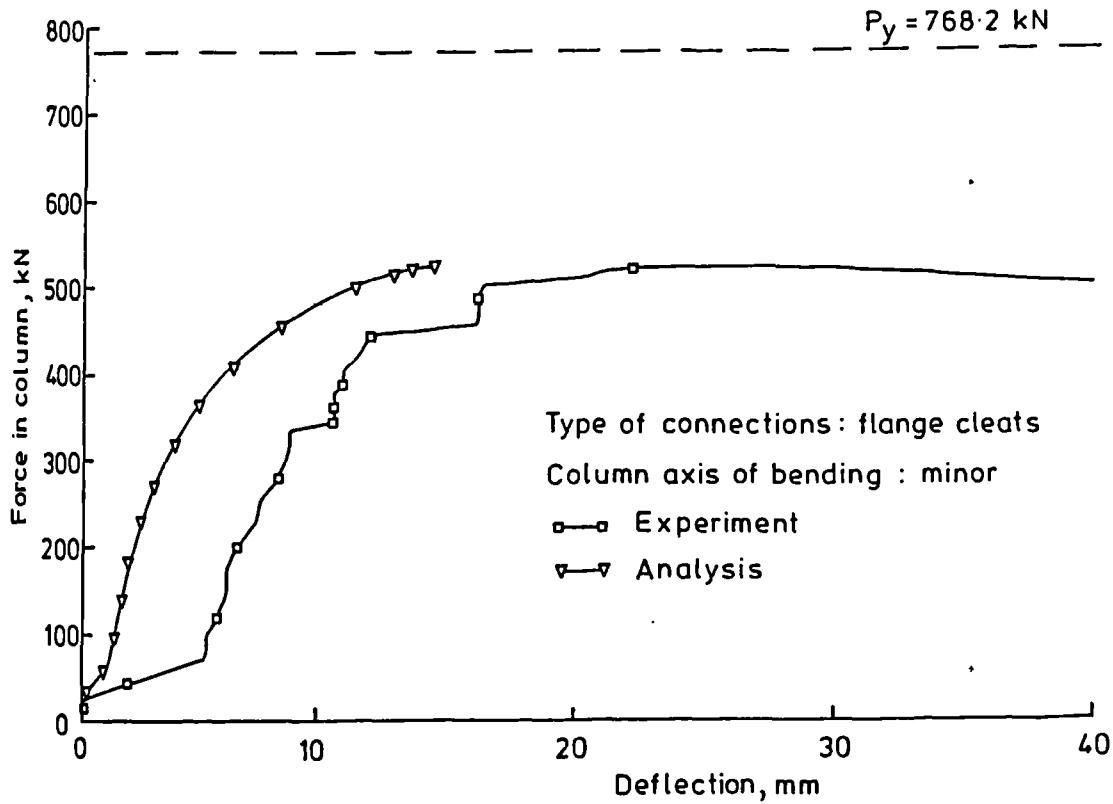


FIGURE 6.5 Comparison of analytical and experimental load-deflection response - ST7

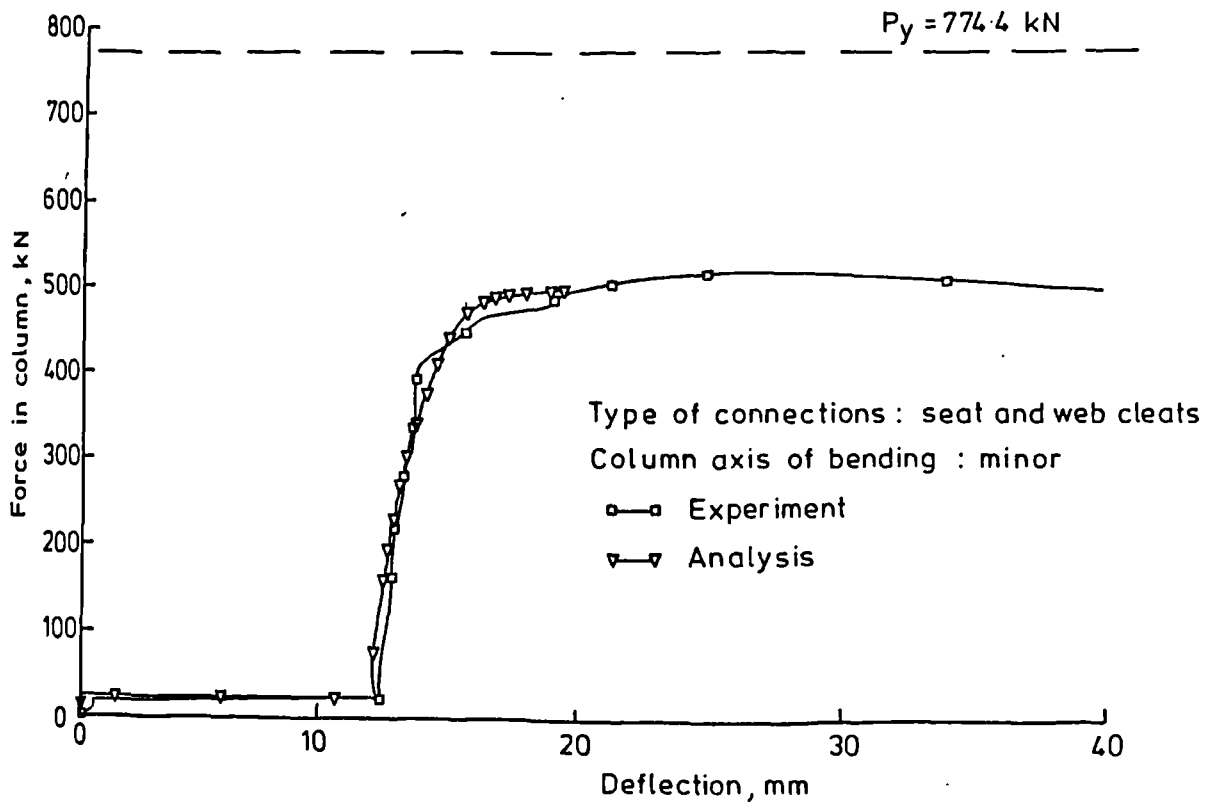


FIGURE 6.6 Comparison of analytical and experimental load-deflection response - ST8

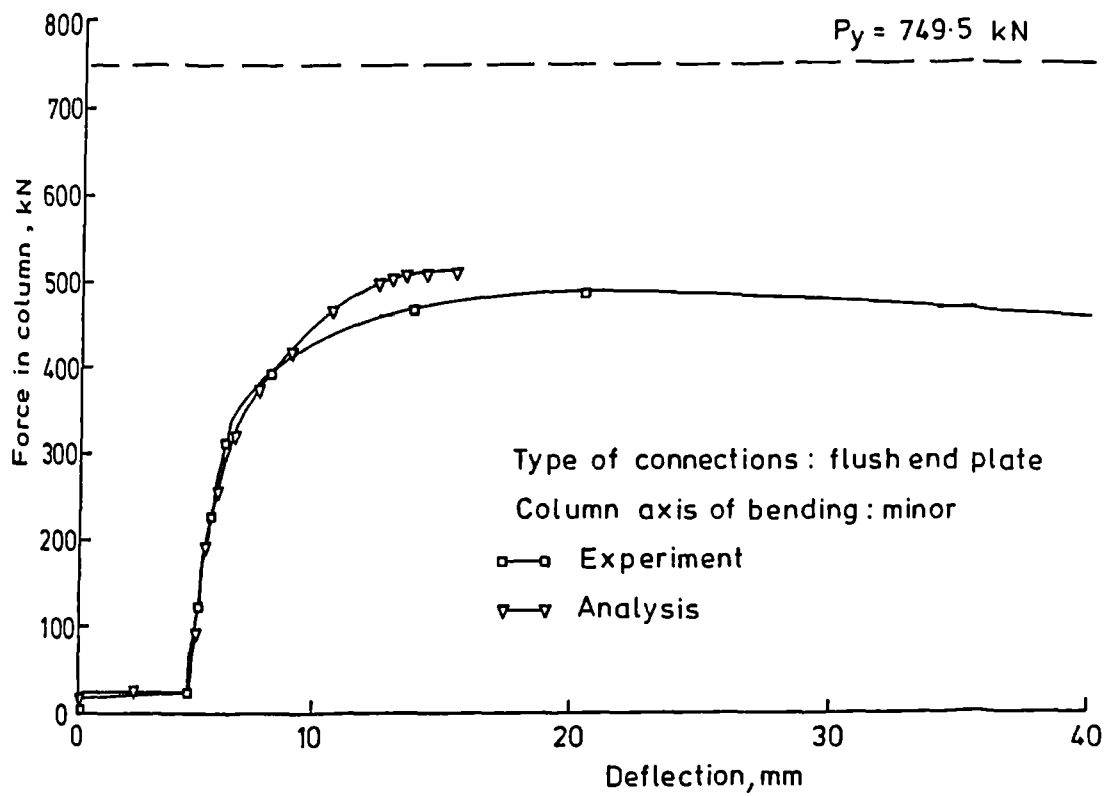


FIGURE 6.7 Comparison of analytical and experimental load-deflection response - ST9

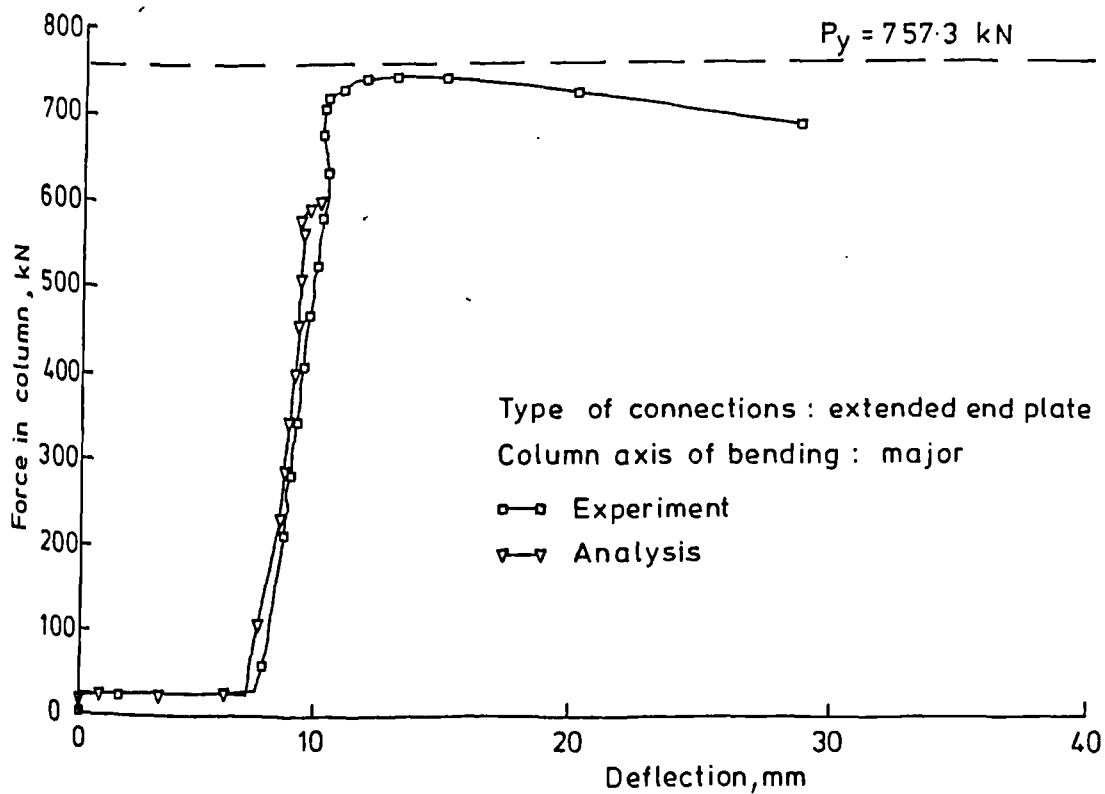


FIGURE 6.8 Comparison of analytical and experimental load-deflection response - ST10

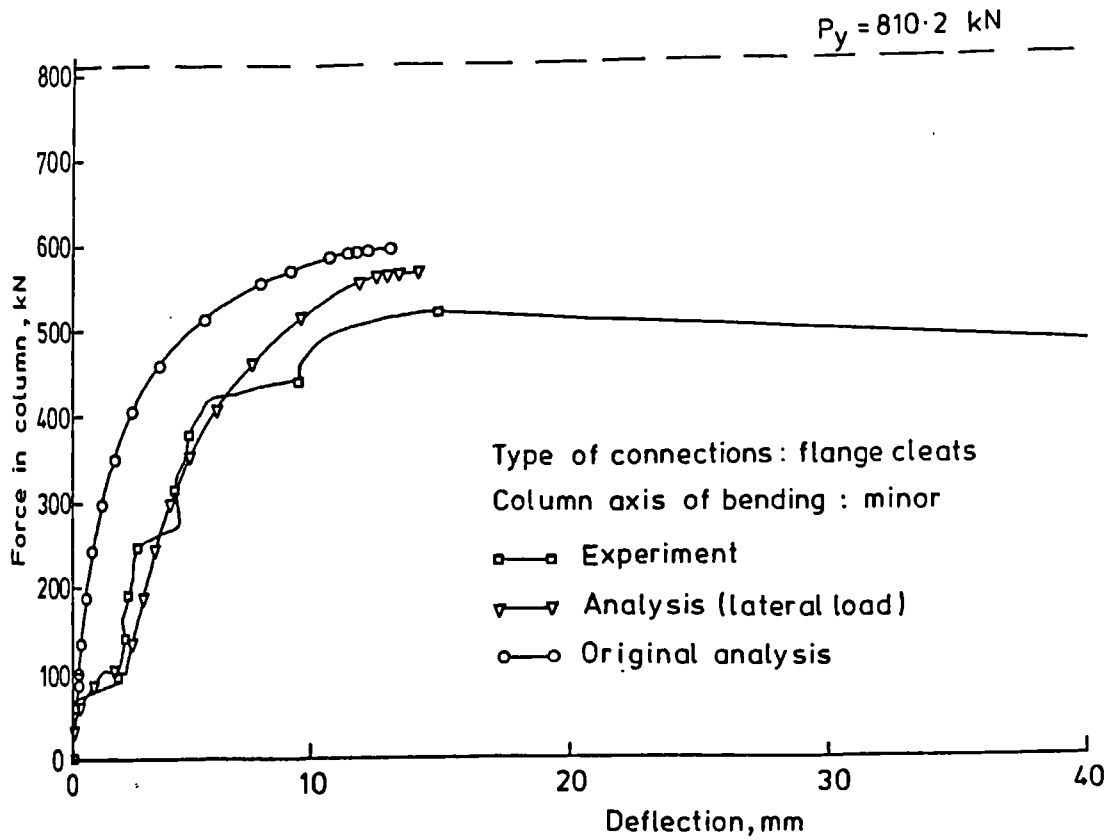


FIGURE 6.9 Comparison of analytical and experimental load-deflection curve for test ST6 with lateral load introduced at midheight

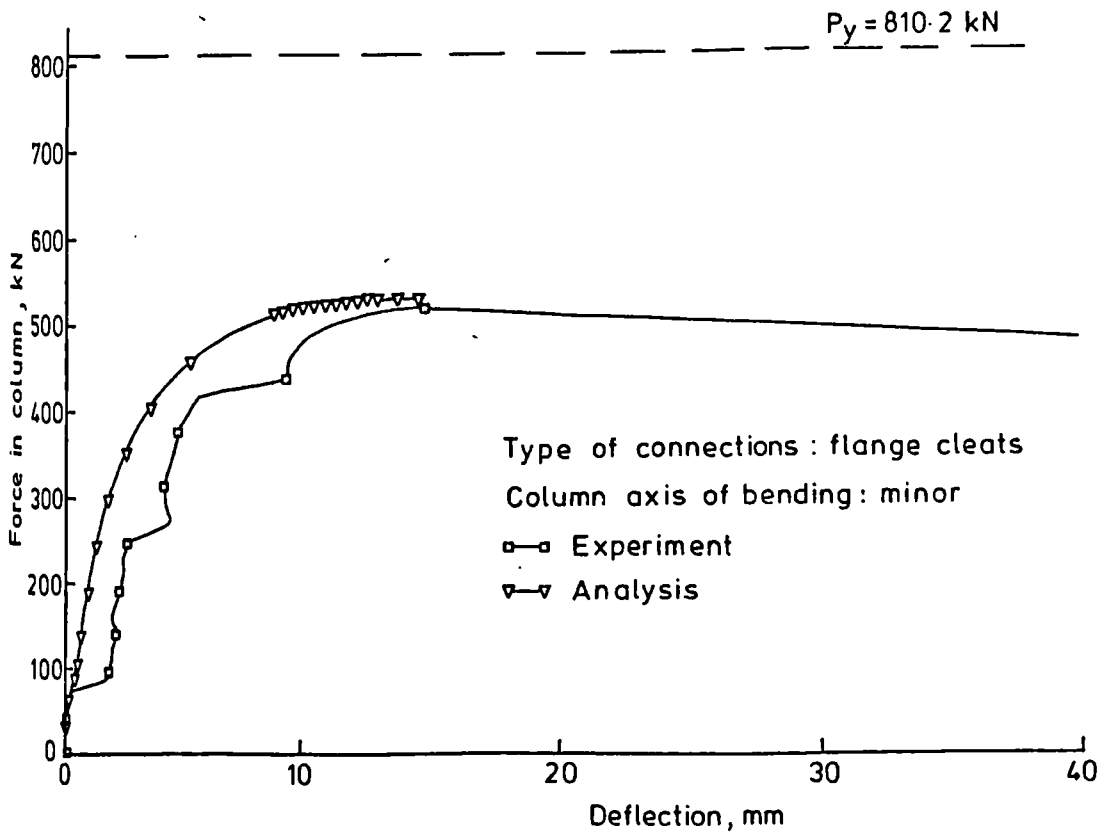


FIGURE 6.10 Comparison of analytical and experimental load-deflection curve for ST6 with residual stress and moment-rotation curves from test data

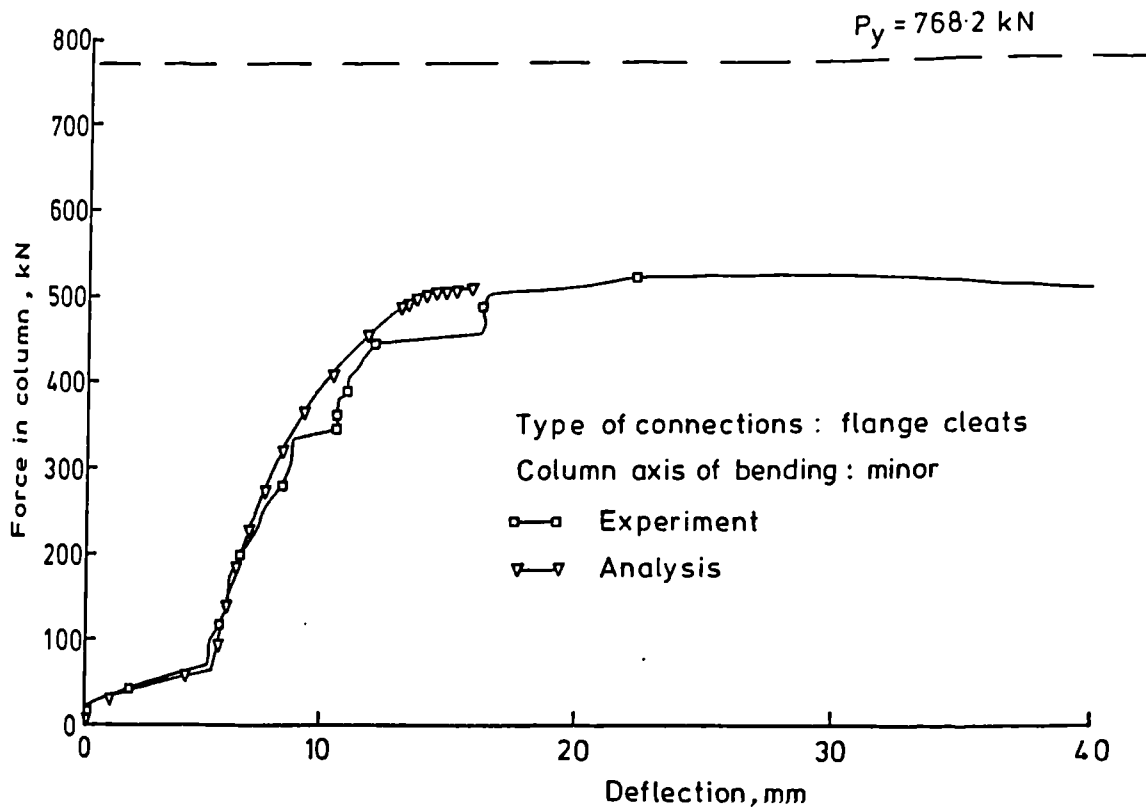


FIGURE 6.11 Comparison of analytical and experimental load-deflection curve for test ST7 with lateral load introduced at midheight

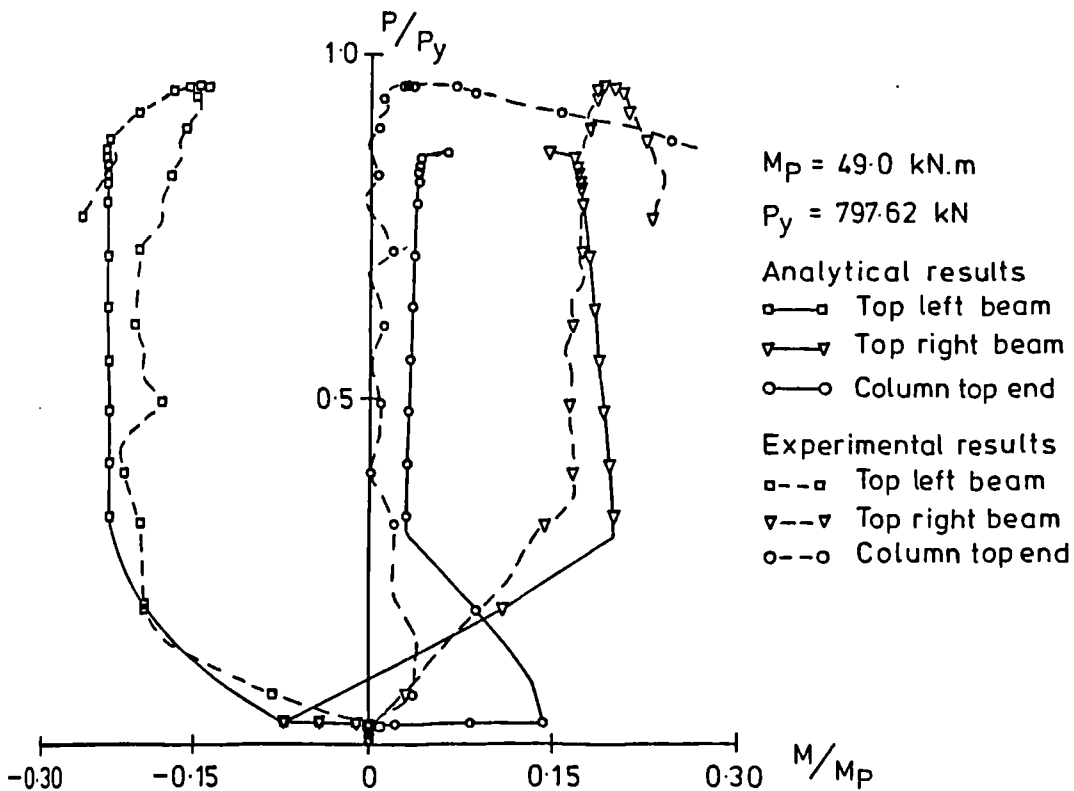


FIGURE 6.12 Moments at the head of column in test ST4

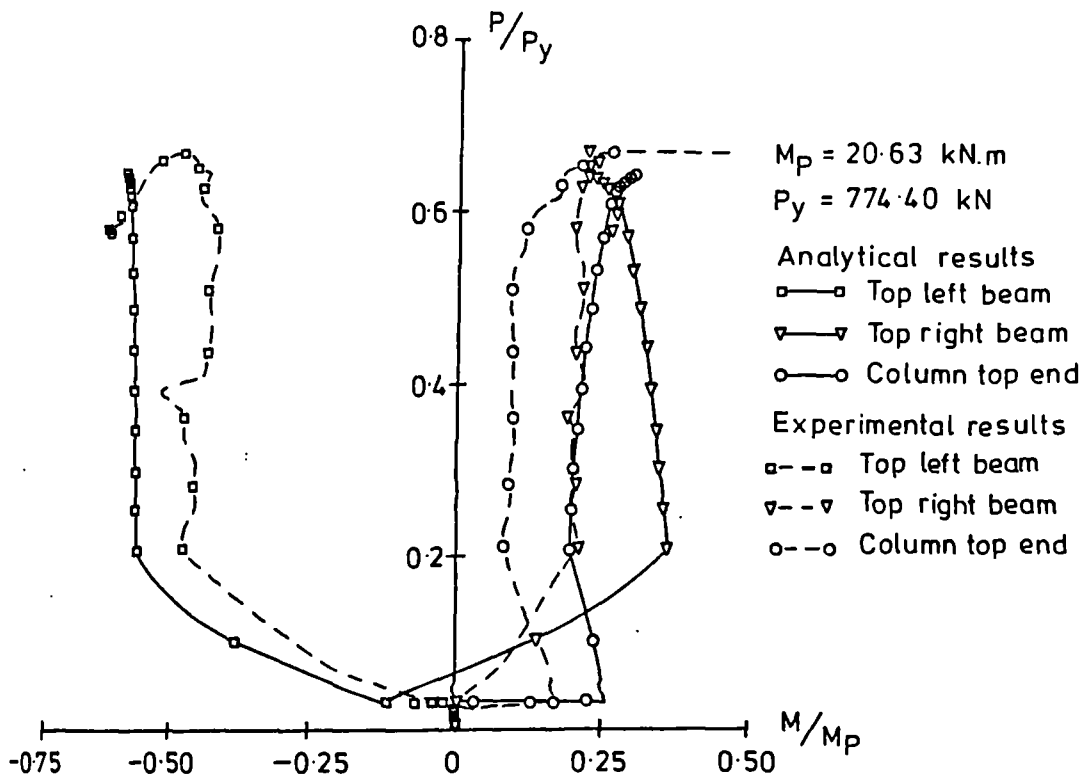


FIGURE 6.13 Moments at the head of column in test ST8

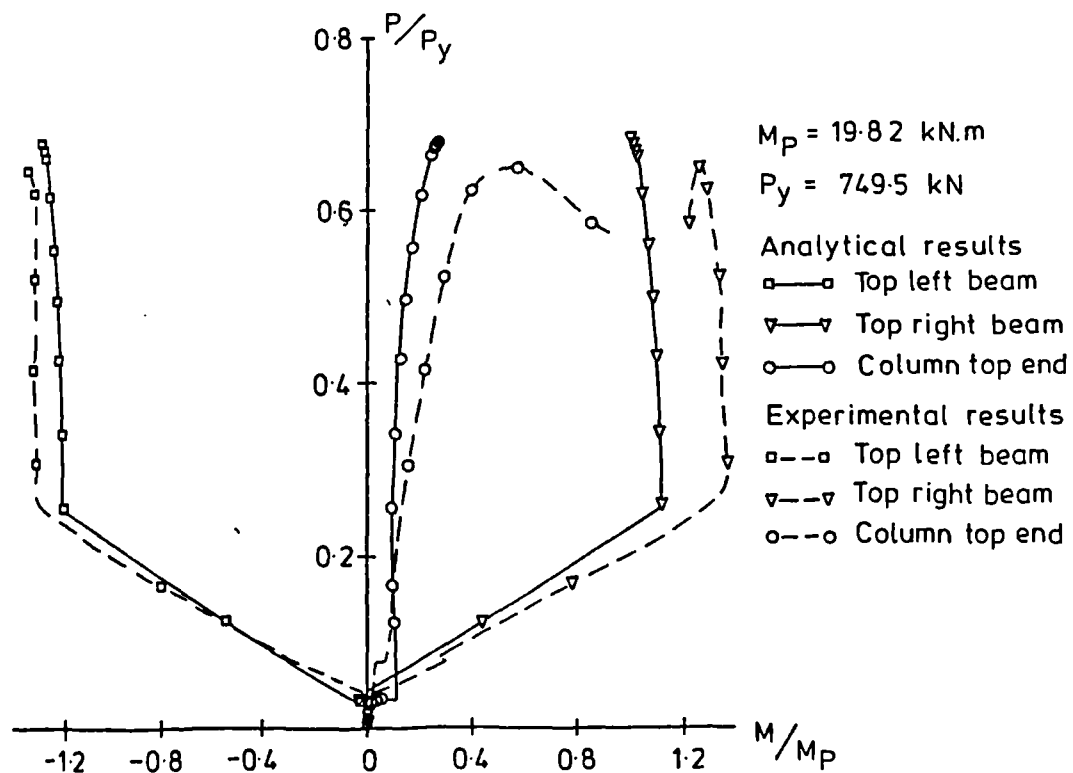
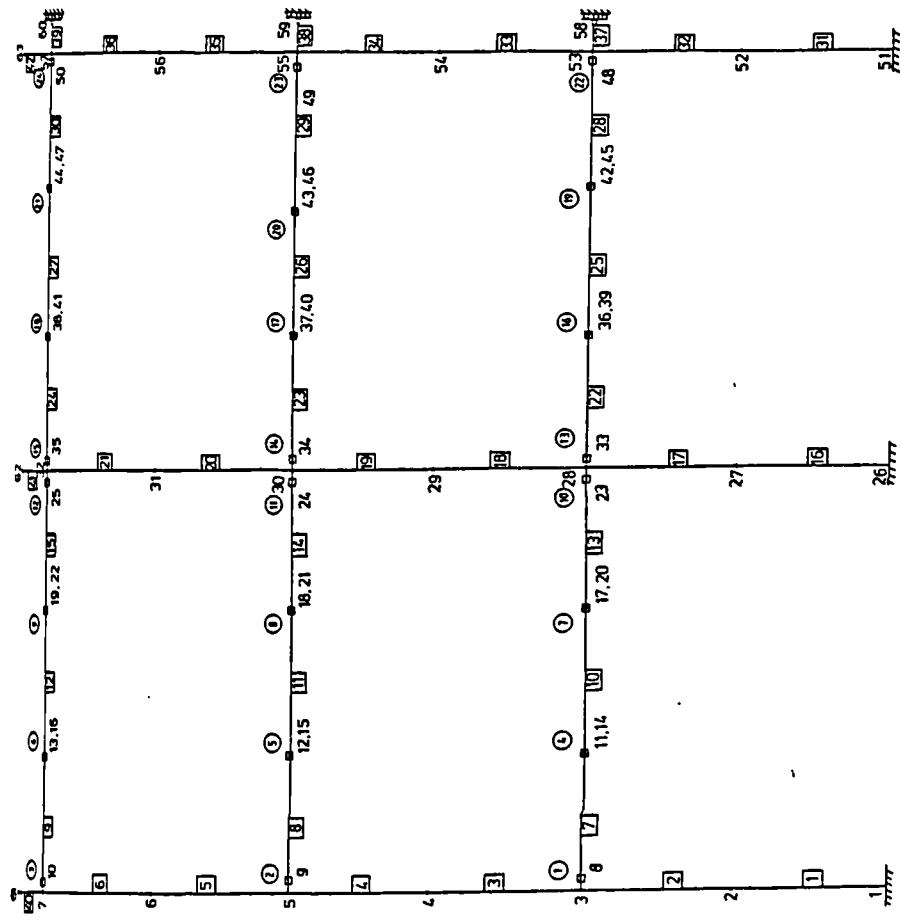
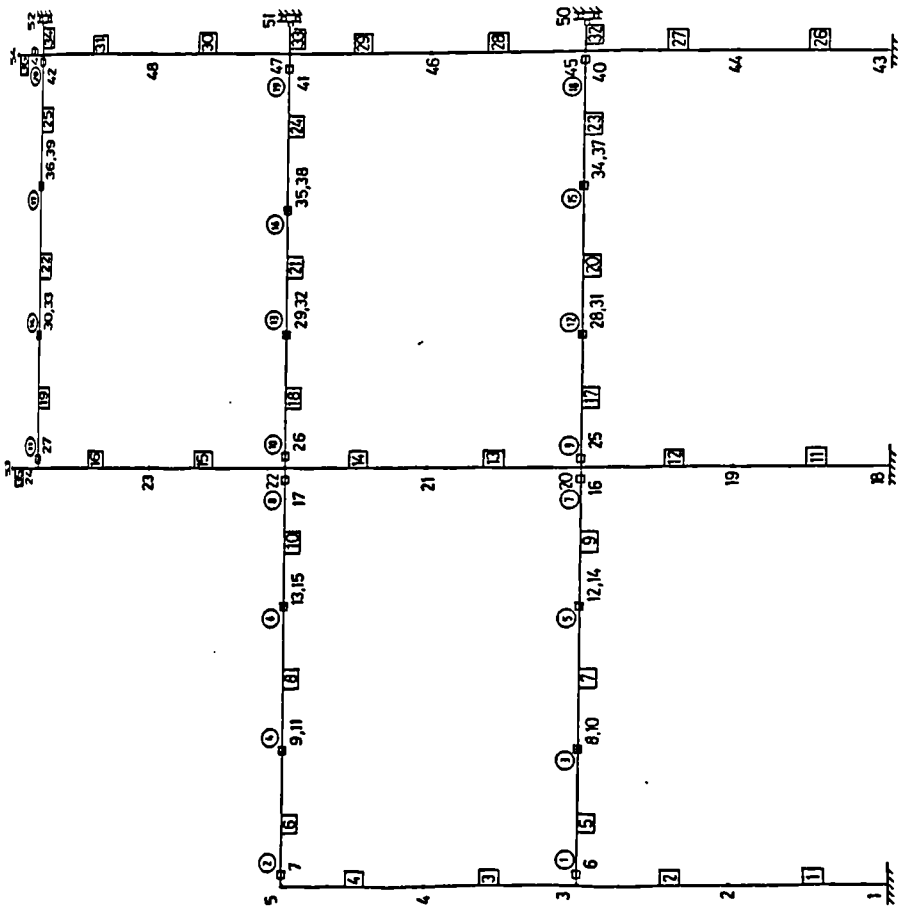


FIGURE 6.14 Moments at the head of column in test ST9



- ⊕ Semi - rigid node number.
- Semi - rigid node.
- Nodes.
- Fictitious semi - rigid node.
- ⊞ Member number.



- ⊕ Semi - rigid node number.
- Semi - rigid node.
- Nodes.
- Fictitious semi - rigid node.
- ⊞ Member number.

FIGURE 6.15 Computer models for frame 1 and frame 2

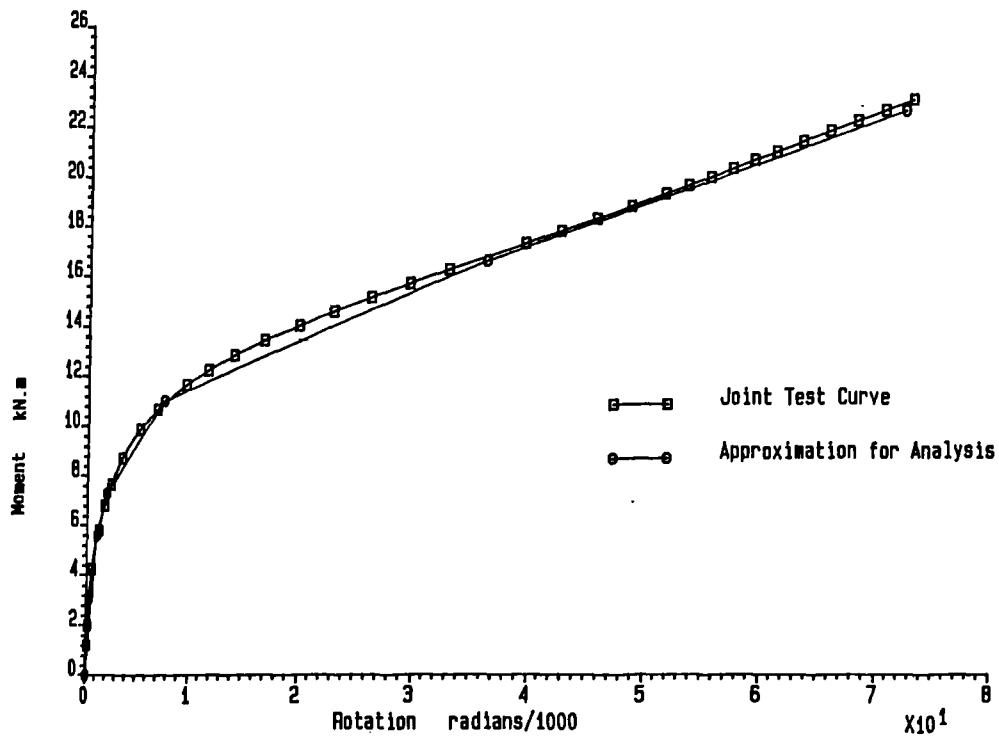


FIGURE 6.16 Linearised moment rotation characteristic used in the analysis of frame 1

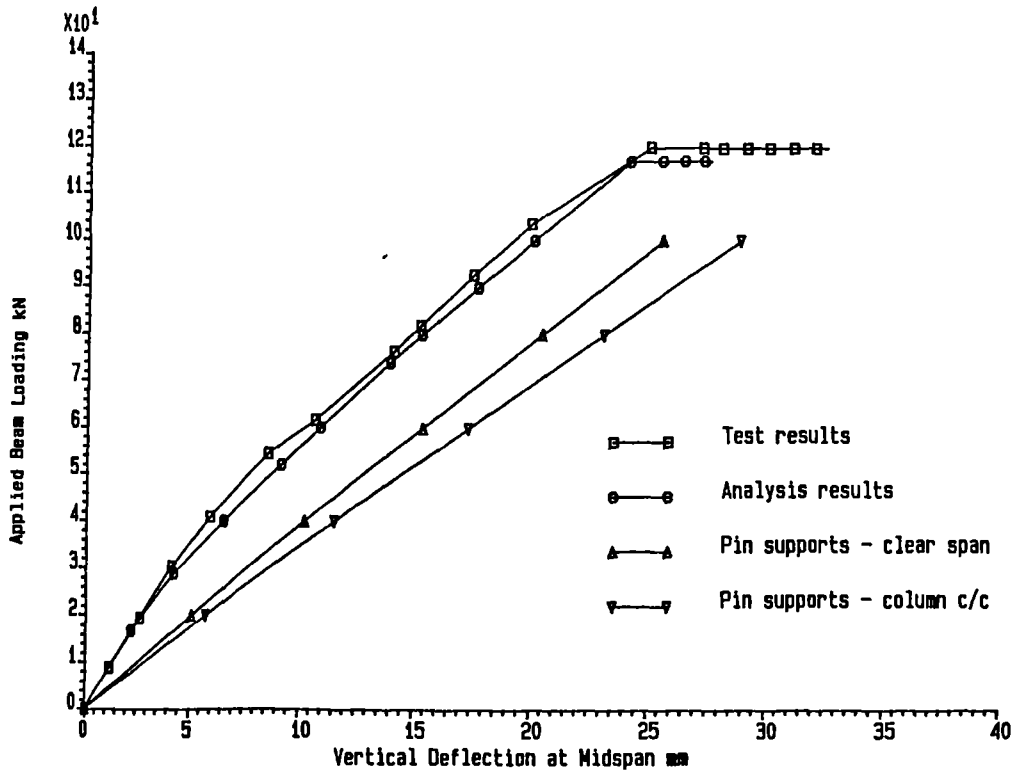


FIGURE 6.17 Comparison of predicted and test load-deflection response of beam 6

Frame 1 Flange cleats -major (analysis)
 STRESSES SCALE FACTOR = 0.004
 STEP NUM = 11 TIME = 11.0000
 bending moment Diagram

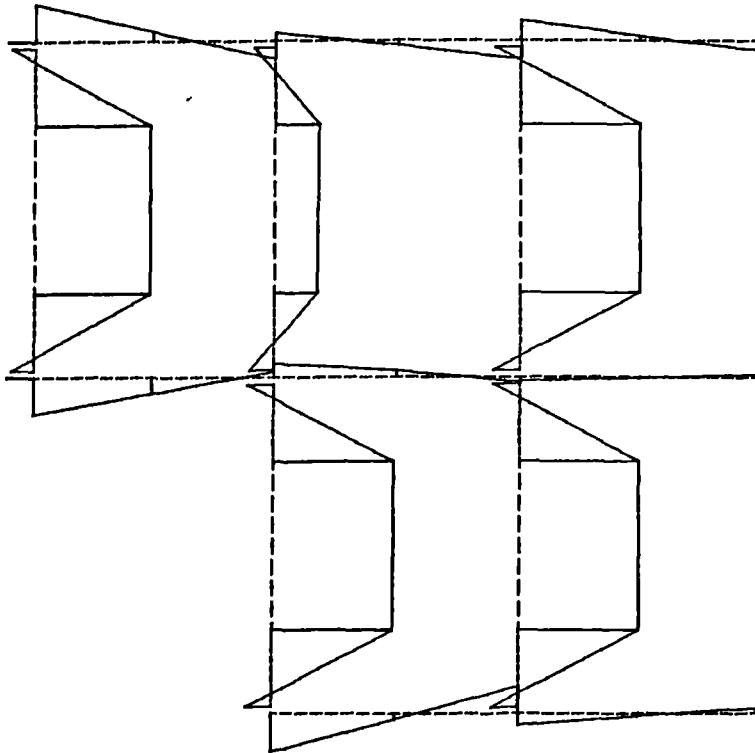


FIGURE 6.18 Bending moment distribution under full beam loading

Program SERVAR by C. POGGI
 Department of Structural Engineering
 Politecnico di Milano - ITALY

Frame 1 Flange cleats -major (analysis)
 DEFLECTIONS SCALE FACTOR = 5.000
 STEP NUM = 11 TIME = 11.0000
 Deformed structure Diagram

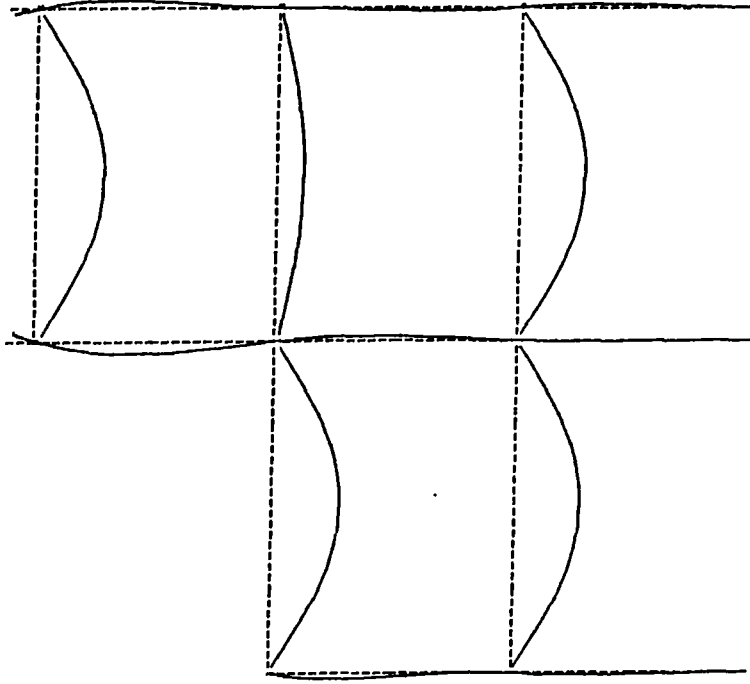


FIGURE 6.19 Deflected shape produced by beam loading

Program SERVAR by C. POGGI
 Department of Structural Engineering
 Politecnico di Milano - ITALY

Frame 1 Flange cleats -major (analysis)

STRESSES SCALE FACTOR = 0.004
STEP NUM = 16 TIME = 16.0000
bending moment Diagram

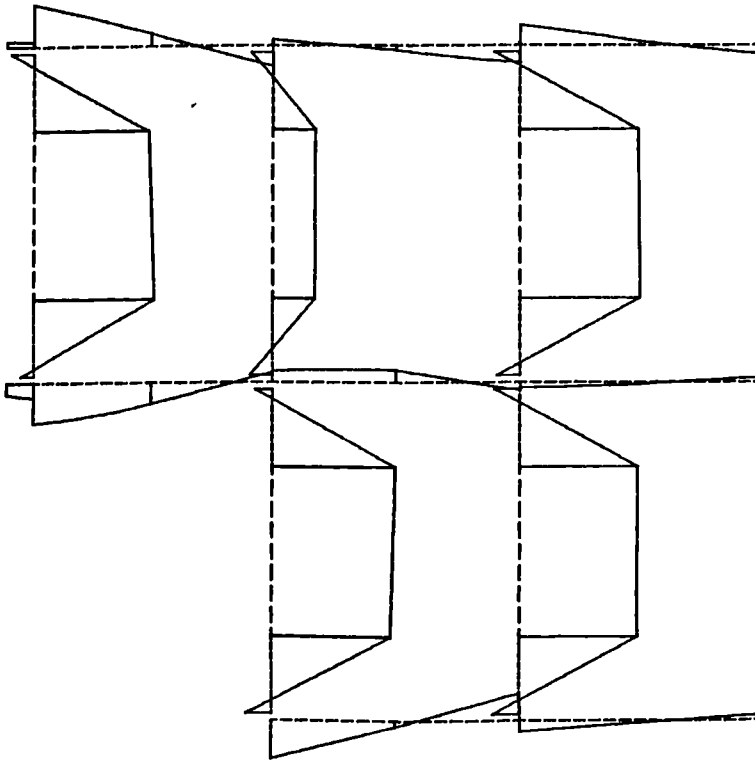


FIGURE 6.20 Bending moment distribution prior to failure of central column

Program SERVAR by C. POGGI
Department of Structural Engineering
Politecnico di Milano - ITALY

Frame 1 Flange cleats -major (analysis)

DEFLECTIONS SCALE FACTOR = 5.000
STEP NUM = 16 TIME = 16.0000
Deformed structure Diagram

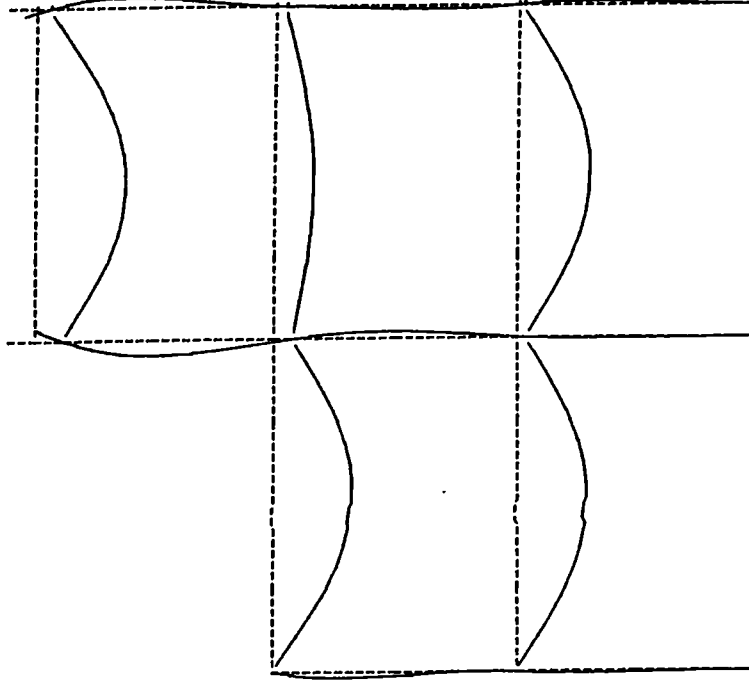


FIGURE 6.21 Deflected shape prior to failure of central column

Program SERVAR by C. POGGI
Department of Structural Engineering
Politecnico di Milano - ITALY

Frame 1 Flange cleats -major (analysis)

STRESSES SCALE FACTOR = 0.004
STEP NUM = 22 TIME = 22.0000
bending moment Diagram

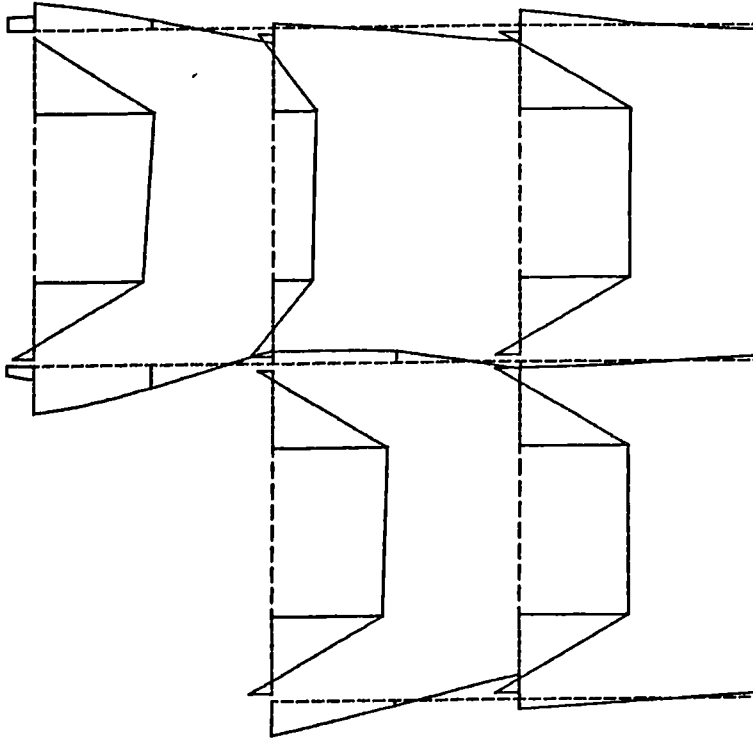


FIGURE 6.22 Bending moment distribution prior to failure of external column

Program SERVAV by C. POGGI
Department of Structural Engineering
Politecnico di Milano - ITALY

Frame 1 Flange cleats -major (analysis)

DEFLECTIONS SCALE FACTOR = 4.980
STEP NUM = 22 TIME = 22.0000
Deformed structure Diagram

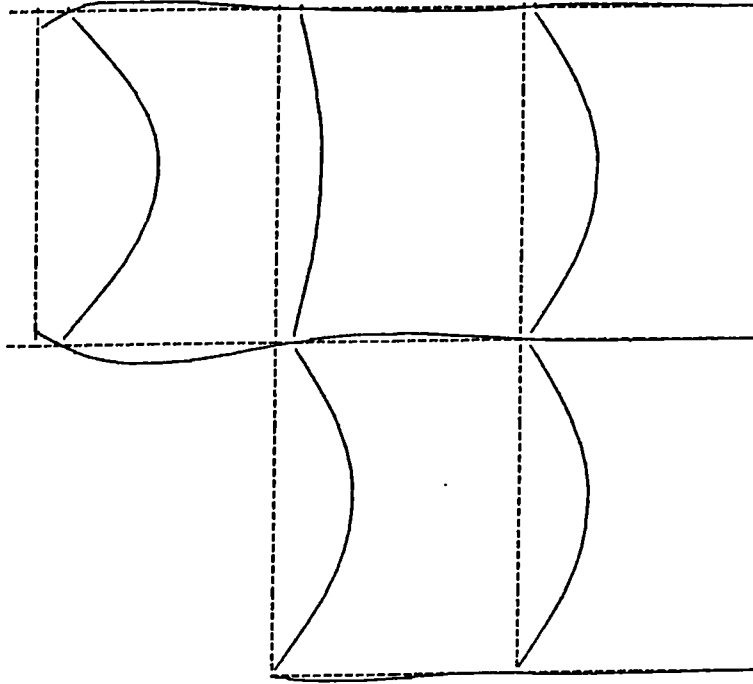


FIGURE 6.23 Deflected shape prior to failure of external column

Program SERVAV by C. POGGI
Department of Structural Engineering
Politecnico di Milano - ITALY

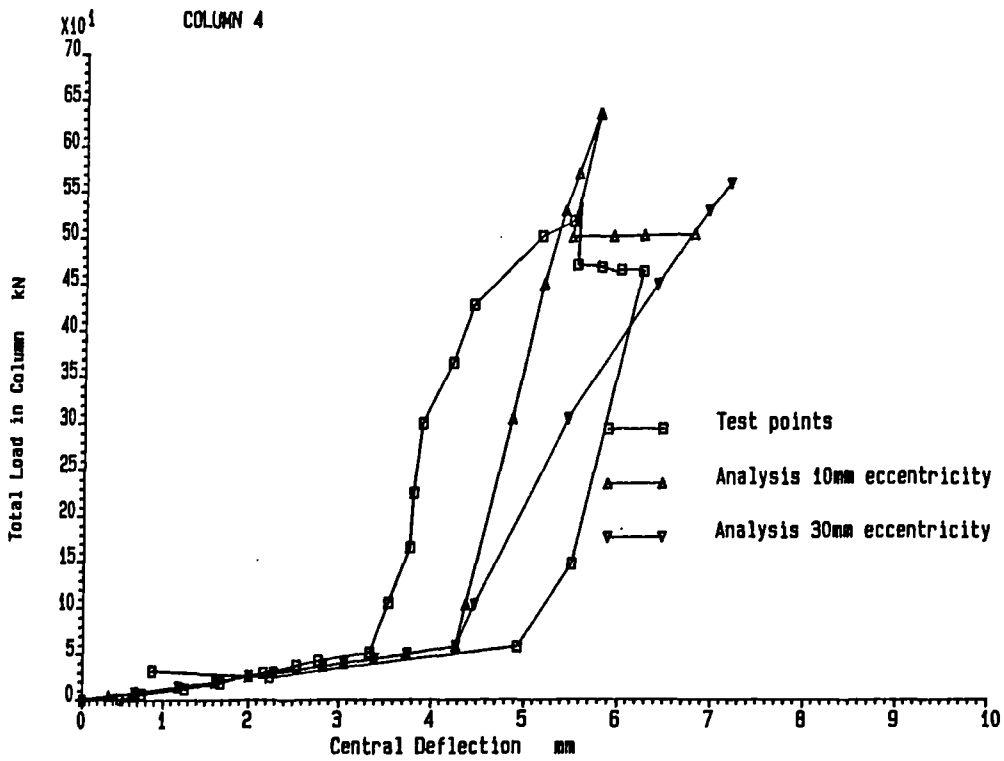


FIGURE 6.24 Load-deflection response of column 4 for 10mm and 30mm eccentricities at the column head

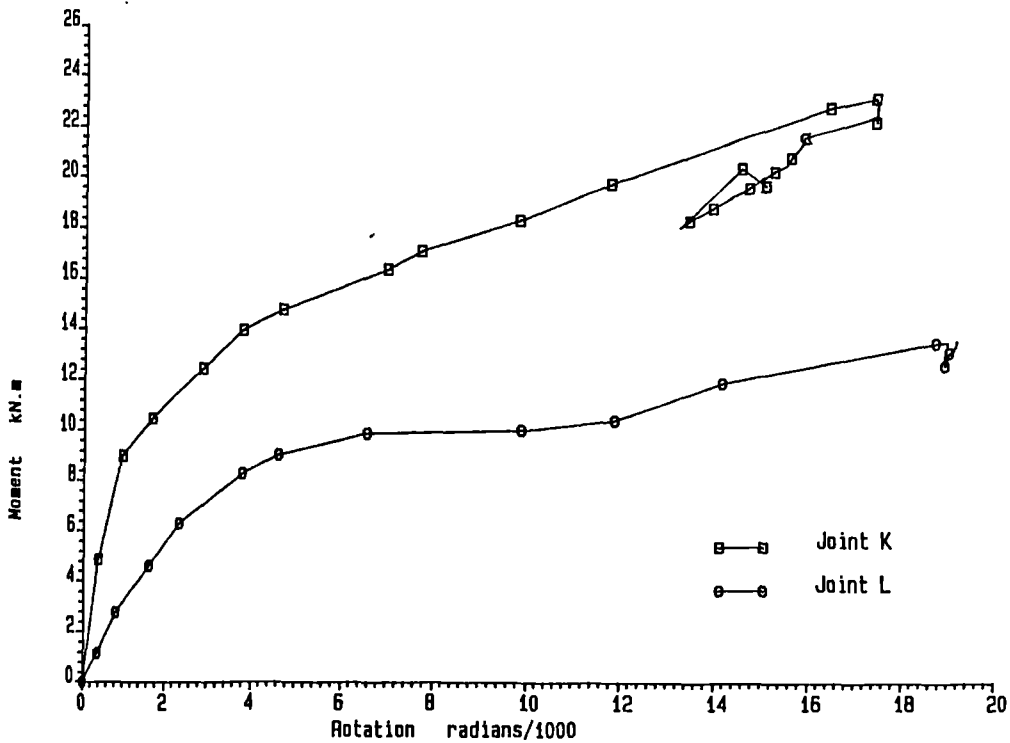


FIGURE 6.25 Comparison of moment-rotation response of connections to an internal and external column

Frame 2 Flange cleats -minor (analysis)

STRESSES SCALE FACTOR = 0.002
STEP NUM = 11 TIME = 11.0000
bending moment Diagram

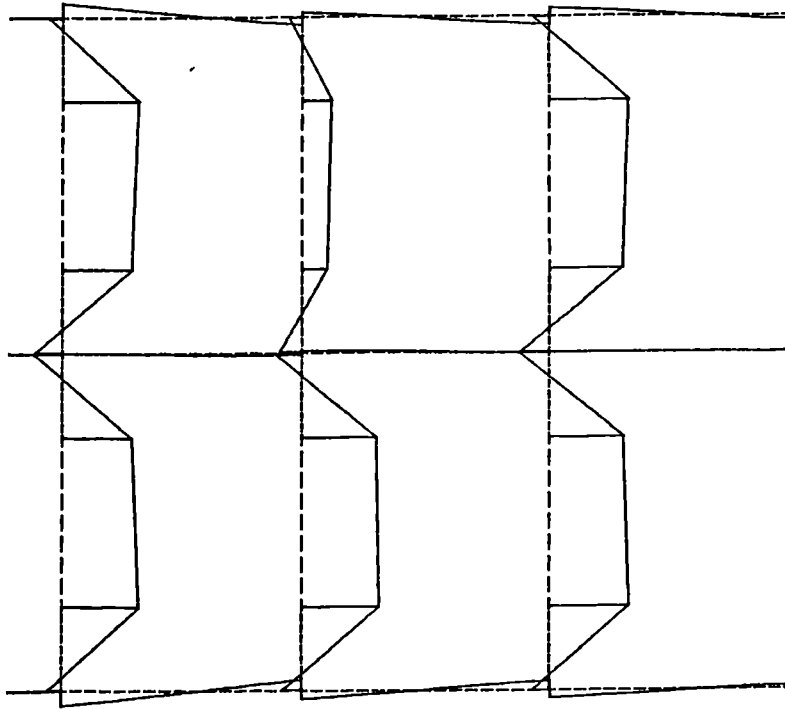
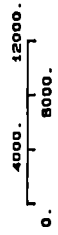


FIGURE 6.26 Bending moment distribution under full beam loading

Program SERVAR by C. POGGI
Department of Structural Engineering
Politecnico di Milano - ITALY

Frame 2 Flange cleats -minor (analysis)

DEFLECTIONS SCALE FACTOR = 7.500
STEP NUM = 11 TIME = 11.0000
Deformed structure Diagram

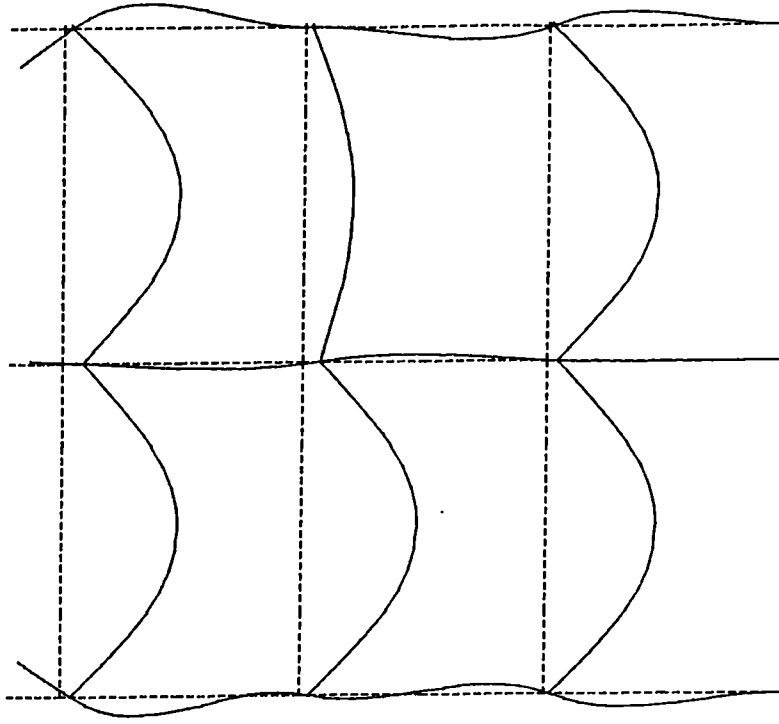
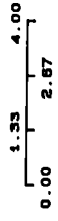


FIGURE 6.27 Deflected shape produced by beam loading

Program SERVAR by C. POGGI
Department of Structural Engineering
Politecnico di Milano - ITALY

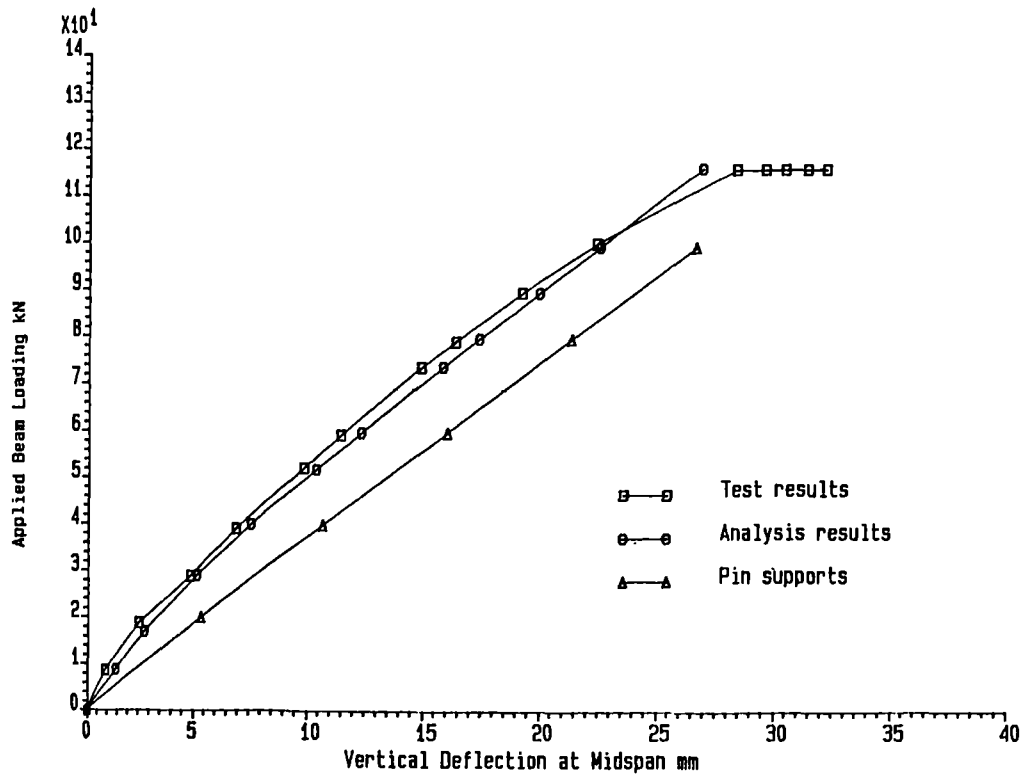


FIGURE 6.28 Comparison of predicted and test load-deflection response of beam 3

7.0 DESIGN OF STEEL FRAMES WITH FLEXIBLE CONNECTIONS

7.1 Availability of Connection Restraint Characteristics

The study of connection behaviour reported in Chapter 3 showed clearly that all connections possess some ability to resist moments, albeit modestly in some cases. Flush end-plates in particular can exhibit quite stiff moment-rotation behaviour but even so this type of connection is often designed to carry the beam end reaction only, i.e. the beam is assumed to be simply supported. However if the designer wishes to take account of the restraint available how can he quantify it? This question is fundamental to the development of design methods which take due account of the response of real connections.

At present it is very difficult to provide the designer with this information, for a number of reasons. Connections are usually designed for a specific situation, this leads to many similar but not identical designs for connections required to carry essentially the same loads. Research has shown that the moment-rotation response is affected by changes in bolt spacing, plate size, beam and column section etc and therefore it is not possible to predict the performance of a unique connection. If the particular connection has been studied in a research project then the designer needs to find details of the work - not an easy task due to the vast number of publications to be consulted, many of which are not readily available.

Attempts to alleviate this problem have been made by the Structural Stability Research Council (7.1) which established Task Force 25 - Connections Bibliography' with the aim "to collect and disseminate moment-rotation data on typical connections and quantify analytical models". At Sheffield University and elsewhere projects are underway to provide a computer data bank of moment-rotation curves

which will enable a designer to find the test behaviour of a particular connection or one with similar details. Another useful development is a move towards a rationalisation of connection design and selection.

Standardisation of connections has been proposed, and adopted in some countries, to reduce the design time used in repetitive re-design of very similar connections. Material costs are now relatively small and reductions in the time required to fabricate or design connections can lead to overall reductions in cost even if the material used in the joints is marginally increased. Standard connections would also enable researchers to more readily provide the needed moment-rotation data as the connections used in projects would conform to the standard. Allied to this the adoption of standard methods of connection design would lead to greater uniformity in the details of connections used. Currently a proliferation of methods exist for all types of connection although attempts to select the best as standard are being made (7.2) and inquiries to steel fabricators have suggested that such moves are welcome.

If the above suggestions and initiatives become a reality it is not so difficult to envisage moment-rotation data becoming widely available. Connections of a particular type could be grouped together and moment-rotation curves of the correct form, perhaps non-dimensionalised, presented based on past research possibly supplemented by additional testing work. Analytical prediction of moment-rotation curves has been only moderately successful in the past but some success in fitting a simple curve to a range of test data for end-plate connections was reported by Yee and Melchers (7.3) and

similar approaches for different types of connection could be implemented.

Once the designer has a reasonably accurate representation of the likely response of the connections to be used in the frame this may be incorporated into design.

7.2 Semi-Rigid Connections and Column Design

Column design involves the determination of the forces applied to the member—moments and axial loads — and an assessment of the member's ability to safely sustain the design loads. The semi-rigid nature of typical beam to column connections has an influence on both stages of design.

In chapter 5 the frame test results were reported. Here it was clearly demonstrated that the modest restraint provided by the simple top and bottom cleat connections transferred significant moments into the column. The traditional approach, first advanced in the 1930's, is to assume the moment in the column to be equal to a value obtained by multiplying the beam end reaction by a notional eccentricity of 100mm from the column face (either the web or flange depending on the axis of bending). These values were shown to be grossly in error in the frame tests. This is not surprising since the amount of moment transferred by the connection depends on the relative stiffness of the column, connection and beam and such interdependency conflicts with the use of a very simple design approximation.

The subassemblage tests reported in Chapter 4 showed conclusively that connection restraint influences the load carrying capacity of a column. This has been widely accepted for many years and BS 449 and BS 5950 take account of it by use of effective lengths. However the suggested values are based solely on the designer's estimation of

the ability of a particular joint to resist moment and or rotation at the column-beam intersection. Effective lengths considerably shorter than the values suggested by the two codes were evident in the experimental tests. Clearly if the columns are experiencing greater restraint than that assumed in design they are likely to be able to sustain higher loads.

When comparing the failure loads of the columns in the subassembly and frame tests the accuracy with which the interaction curve in BS 5950 (cl. 4.8.3) can predict the collapse load of a pin ended column must be borne in mind. Figures 7.1 and 7.2 (7.4) show the interaction between axial load and uniform bending moment for columns bent about their major and minor axis respectively. In both cases the ordinate is the value of applied axial load divided by axial capacity at a given slenderness (in the absence of applied moment) and the abscissa is the applied moment divided by the moment capacity of the section (ignoring lateral-torsional buckling in the major axis case). It can be readily seen from these figures that the interaction is not linear, but this is assumed by the interaction equation given in cl. 4.8.3.3.1 (if lateral-torsional buckling is prevented). For the major axis case the departure from a straight line interaction is most pronounced at high values of M/M_{Cx} for columns of low slenderness. In the minor axis case the interaction can be seen to be very poor for slenderness ratios less than about 70. The conservatism of this, and other interactions, was demonstrated by Nethercot in reference 7.4. The presence or absence of residual stresses also influences the interaction between axial load and bending moment. Ballio et al (7.5) present comparisons of the performance of struts under axial load and bending with and without residual stresses. For I section struts

about the major or minor axis the presence of stresses has a detrimental effect on the load carrying capacity of the strut. Since the column curves relating compressive strength to slenderness in codes of practice assume the presence of residual stresses in cases where the pattern is more favourable than that assumed or absent entirely the code predictions will be conservative.

However the two parts of the column design problem, the assessment of the loads and the calculation of capacity, cannot be divorced. It would be inappropriate to take account of the beneficial effect of connection restraint in reducing column effective lengths, and hence increasing capacity, if the corresponding increase in beam end moments transferred to the column was not properly incorporated. Conversely it would be inconsistent to design the column for the full moments applied by the connections if the influence of the connection restraint was guessed or estimated. Methods of incorporating connection stiffness, adjusted to account for beam flexibility, have been proposed by Bjorhovde (7.6) and Lui and Chen (7.7), but in both cases no assessment is made of the moments transmitted to the column and design is based on axial load capacity only. This shortcoming may not be as erroneous as it first appears since there is evidence to suggest that at collapse the connections restrain rather than load the column.

In view of the wide availability of mini computers and the complexity of the problem it appears retrogressive to be forced into developing design techniques which rely on easy to perform hand computation if these require over simplification of the real behaviour. Computer aided design for structural frameworks is already widely used, and the refinement of such methods to include the effects of semi-rigid connections does not present a radical change in design

philosophy. Computer programs could be used in one of two ways. Firstly they could be employed to provide the designer with a consistent set of forces, axial loads and bending moments, for which an element within a frame should be designed. With this information the trial section's capacity could then be checked using the interaction equations provided by structural codes of practice. In addition the program could provide the designer with a calculated value for the effective length of a column under consideration. Alternatively a sophisticated frame analysis program capable of checking the strength and stability of a trial design under design loading could be utilised. Compliance with codes of practice for resistance to local buckling, material strength and flexural buckling could be incorporated within the program.

A reluctance to pass design over to the computer programs is understandable, and desirable if the designer does not appreciate the limitations of the model, but if improved understanding of column behaviour is to be reflected in design the complexity of the problem forces the designer to consider the application of more sophisticated techniques than those currently in use.

7.3 Beneficial Effect of Semi-Rigid Joints on Beam Load Carrying Capacity

In a real frame the moments carried by a beam subjected to a uniformly distributed load, w , will lie somewhere between 0 and $\frac{wl^2}{12}$ at the supports and $\frac{wl^2}{24}$ to $\frac{wl^2}{8}$ at the centre, depending on the degree of restraint provided by the column to beam connection, and the relative stiffness of the connection, beam and column. In many cases the beams are assumed to carry no moment at their supports, an

assumption which is rarely true in practice. If the end restraint provided to the beam by simple connections can be quantified a more accurate picture of the real bending moment distribution along the beam may be obtained and more economic beam design performed. In addition to the economy in design due to the reduction in span moment there may also be improvements for beams which are laterally unsupported due to the beneficial effect of a bending moment diagram which reduces the length of the unrestrained compression flange (cf. BS 5950 cl. 4.3.7.6) (7.8). These economies, though at the expense of additional design time, require no increase in fabrication time or materials in heavier connections.

In many structural frames the beams are the primary structural element and take up a large percentage of the structural frame weight. In braced, simple frames, the columns may often be under designed for the sake of practicality. For example in a multistorey building it may not be practical to reduce the column section size for the upper lifts, or a larger column section may be required to accommodate the beam to column connections. Hence in many frames the beams are unable to transmit sufficient load into the columns to cause failure, and the ultimate capacity of the frame is limited by the capacity of the beams. In such cases the improvement in beam load carrying capacity due to the action of the connections results in an overall improvement in the capacity of the frame.

Improvements in the assessment of deflections at the serviceability limit state are also possible if the effect of semi-rigid joint response is recognised at the design stage. This could lead to the adoption of longer spans where serviceability is the controlling limit state.

assumption which is rarely true in practice. If the end restraint provided to the beam by simple connections can be quantified a more accurate picture of the real bending moment distribution along the beam may be obtained and more economic beam design performed. In addition to the economy in design due to the reduction in span moment there may also be improvements for beams which are laterally unsupported due to the beneficial effect of a bending moment diagram which reduces the length of the unrestrained compression flange (cf. BS 5950 cl. 4.3.7.6) (7.8). These economies, though at the expense of additional design time, require no increase in fabrication time or materials in heavier connections.

In many structural frames the beams are the primary structural element and take up a large percentage of the structural frame weight. In braced, simple frames, the columns may often be under designed for the sake of practicality. For example in a multistorey building it may not be practical to reduce the column section size for the upper lifts, or a larger column section may be required to accommodate the beam to column connections. Hence in many frames the beams are unable to transmit sufficient load into the columns to cause failure, and the ultimate capacity of the frame is limited by the capacity of the beams. In such cases the improvement in beam load carrying capacity due to the action of the connections results in an overall improvement in the capacity of the frame.

Improvements in the assessment of deflections at the serviceability limit state are also possible if the effect of semi-rigid joint response is recognised at the design stage. This could lead to the adoption of longer spans where serviceability is the controlling limit state.

Having discussed the beneficial effects of connection restraint on beam performance it is necessary to turn attention to methods of incorporating this present, but for the most part, ignored feature of frame action. Early attempts to codify a method of design (7.9) were not widely used and were based on work conducted in the 1930's on rivetted connections. Conservative approximations and assumptions which were necessary to formulate a design method for hand calculations produced solutions which impaired the benefits of beam end restraint and made the extra work involved appear to be in vain. The use of enhanced computational facilities which are now widely available would appear to be a sensible way of progressing.

7.4 Frame Analysis and Design with Semi-Rigid Joints

A steel frame comprises of beams and columns connected by some form of joint. The behaviour of the bare frame depends on the interaction of all these components. If an accurate analysis of an existing frame, or an economic design of a new frame is sought the analytical tools employed should take into account this interdependence. Frame analysis programs capable of incorporating the effects of member flexibility, joint stiffness, plasticity and instability are available (7.10). Chapter 6 compared the results of one such program, SERVAR, with the experimental results of two multi storey, two bay, braced frames. This type of program could be used in its present form to provide an indication of the force distribution around a frame under specified loading, from which key elements could then be checked against the design recommendations. With some modification these programs could perform the necessary checks and inform the designer of the results. Alternatively a given frame may be analysed to find the ultimate load it will sustain, which could then be checked against the

design loading. This second method would need careful calibration to ensure that the ultimate load predictions from the analysis model could be attained in real, imperfect buildings.

The above, though feasible, may not be practical due to the computer time required to run extensive frame analyses. A more practical proposition would be to consider the behaviour of limited subassemblages cut from the frame. Chapter 6 demonstrated the accuracy with which a subassemblage program can predict the inplane failure load of a column restrained by beams and semi-rigid connections. This type of program would enable a designer to find the force distribution around a limited subassemblage, or alternatively to check the ultimate capacity of a design.

The choice of subassemblage is important because it needs to incorporate a sufficiently large part of the frame to include the most dominant effects. A study of three subassemblies was conducted with the SERVAR program to check which most accurately predicted the failure load of a column within a more extensive frame. Figure 7.3 shows the details of the frame and subassemblages studied.

The study shows that the choice of boundary at the remote end of the beam has an influence on the collapse load of the column. Assuming pins at the remote end the column resisted an axial load of 475kN (in addition to the beam loading) and with fixed supports the additional axial load was 557kN. The central column in the more extensive frame sustained a load of 494kN, the same as that required to fail the column in case 4 where the remote ends of the beam were free to deflect but not rotate. Further work on the suitability of subassemblages in predicting the response of columns in more extensive frames is in progress.

A proposed design method for braced semi-rigid frames using micro/mini computers is outlined in figure 7.4. The designer calculates the loading to be applied to the structure and selects a number of subassemblages to be examined. He then chooses a connection type to be used in the structure and estimates the degree of fixity as a percentage of the free bending moment diagram. A beam section is then selected which can support a reduced midspan moment. A column section is also chosen. Next the moment-rotation relationship for a suitable connection is sought (from a data bank or other source). This information is used as input data for the program which calculates the force distribution around the subassemblage. The program calculates a column effective length based on the stiffness of the various elements and checks the member forces against the capacities permitted by the code of practice. The results are displayed and the designer may then adjust the sections, connection or loading as appropriate.

7.5 Simple Design Method to include the Benefits of Semi-Rigid Action

BS 5950 clause 2.1.2.4 allows the designer to use semi-rigid design in one of two ways. Firstly by satisfying "the strength, stability and stiffness requirements of all parts of the structure when partial continuity at the joints is to be taken into account in assessing moments and forces in the members". No guidance on the method to be used is given. The alternative is to assume the beam to column connection provides end restraint equal to 10% of the free bending moment applied to the beam. Beams may then be designed for the maximum net moment. The columns must be designed to resist the algebraic sum of the restraint moments from the beams at the same

level on each side of the column, in addition to moments due to eccentricity of connections. The code does not explicitly state what value of eccentricity should be taken, and it may be construed that a figure of 100mm from the force of the column is expected. The results of the frame tests suggest that the moments transferred to the column are equal to the moment in the connection plus that due to the end reaction acting some distance from the column centreline. In the case of the major axis test the end reaction appeared to act approximately 20mm from the column face and for the minor axis test at about 10mm from the column centreline. It would appear therefore conservative to use an all embracing figure for the eccentricity, but rather to take account of the joint detail. Furthermore the benefit of the beam end restraint is not accounted for in the reduction of the column's effective length.

The principal benefits of semi-rigid action appears to be in the reduction of beam span moments and hence section sizes. A possible modification to the BS 5950 method would be to take more account of this restraint where connections are capable of sustaining higher moments (and in reality do attract moment), as for example the two frame tests demonstrate where moments of 20-30% of the free bending moment were measured at the beam ends. Inclusion of the effect of joint flexibility is complicated because of the influence of beam stiffness. For design it would be acceptable to suggest limits for the restraint offered by a connection type depending on typical spans for multistorey construction. This would be considerably easier if standard connections were available. If it is assumed that such guidance could be provided in an acceptable form the design of beams would require an extra stage, that of selecting the relevant restraint

factor and determination of the net beam moment. It would be unwise to assume that such restraint could be developed at external columns due to column flexibility. This was illustrated by the frame tests where in some cases the column stiffness was insufficient to allow the joint to attain the same moment as that at the internal column where an adjacent beam balanced the induced moment. It would therefore be prudent to ignore the restraint at an external joint and ensure that the beam can sustain the design load when restraint is provided by one end only.

The effect of the connection restraint on reducing column effective lengths may be simply accounted for by assuming the connections act rigidly, thereby enabling the designer to use Figure 23 of BS 5950, and subsequently modifying the effective length so obtained by a factor to account for joint flexibility. The method is described below for the two test frames.

Consider the wholly internal column in figure 7.5. If the column buckles one connection at the top and bottom would be forced to close, the adjacent connection continuing to load. Hence effectively only one connection restrains the column. The behaviour of the restraining connection is assumed to be rigid the joint restraint coefficients k_1 and k_2 are calculated as,

$$k_1 = \frac{K_C + K_U}{K_C + K_U + 0.5 K_{TR}}$$

$$k_2 = \frac{K_C + K_L}{K_C + K_L + 0.5 K_{BL}}$$

where the 0.5 is required because the buckled shape puts the beam into single curvature (cl. E.4.1). The effective length ratio L_E/L may be readily found from figure 23. Table 7.1 shows the value of L_E/L which is obtained from the major and minor axis frames by this means.

By way of comparison table 7.1 shows the effective lengths that would be obtained from figure 23 of BS 5950 if various initial connection stiffness were used to modify the beam stiffness prior to calculating k_1 and k_2 . (The method used is that described in chapter 5 where the connection stiffness C , is modified to include the influence of beam flexibility, resulting in an effective connection stiffness, C^* .) Initial tangent stiffness ranging from 1000 to 50,000 kN.m/radian are shown in the table, which are representative of the range of stiffness likely for connections used with the sections under consideration. For all but the most flexible connections - less than about 5000 kN.m/radian, the effective length obtained by the more exact method lies within 10% of the value obtained assuming the connections behave rigidly. It would appear, from this example, that this relatively easy method of determining effective lengths gives a reasonable, and conservative, result.

7.6 Conclusion

This chapter has emphasised that all forms of beam to column connection have inherent stiffness. Efforts to standardise the design and fabrication of joints should help to ease the problem of obtaining a suitable moment-rotation response for a connection at the design stage. The benefits of the semi-rigid action of joints include enhancing the capacity of columns and, probably more importantly economically, reduction of beam span moments and deflections. Methods

of incorporating this as yet largely ignored beneficial characteristic of joints into frame analysis and design have been discussed. These design approaches need to be verified against data for a wide range of realistic frames of varied geometry, section size and loading. In this connection a further frame test incorporating flush and extended end plates is being prepared by BRE and analytical work is in progress in Sheffield and Milan.

References

- 7.1 STRUCTURAL STABILITY RESEARCH COUNCIL, TASK GROUP 25
'Connections Bibliography'
Third Draft, march 1987.
- 7.2 BARKER, H. and NETHERCOT, D.A.
Private Communication.
- 7.3 YEE, Y.L. and MELCHERS, R.E.
'Moment-rotation curves for bolted connections'
ASCE, Journal of Structural Engineering, Vol. 112, No. 3,
March 1986.
- 7.4 NETHERCOT, D.A.
'Evaluation of design formulae for beam-columns subject to
uniaxial bending'
Research Report No. R.75, April 1977.
- 7.5 BALLIO, G., PETRINI, V. and URBANO, C.
'The effect of the loading process and imperfections on the
load bearing capacity of beam columns'
MECCANICA, Journal of the Italian Association of Theoretical
and Applied Mechanics, No. 1, Vol. VIII, March 1973, p.
56-67.
- 7.6 BJORHOVDE, R.
'Effect of end restraint on column strength - practical
applications'
AISC Engineering Journal, First Quarter, 1984, p. 1-13.
- 7.7 LUI, E M and CHEN, W.F.
'End restraint and column design using LRFD'
AISC Engineering Journal, First Quarter, 1983, p. 29-39.
- 7.8 WANG, Y.C., EL-KHENFAS, M.A. and NETHERCOT, D.A.
'Lateral torsional buckling of end-restrained beams'
Journal of Constructional Steel Research (in press).
- 7.9 PD3343
'Recommendations for design'
Supplement No. 1 to BS 449 : Part 1 : 1970, The Use of
Structural Steel in Building, British Standards Institution,
1971.
- 7.10 POGGI, C and ZANDONINI, R.
'Behaviour and strength of steel frames with semi-rigid
connections'
Flexibility and Steel Frames, ed. W.F. Chen, ASCE, 1985,
p. 57-76.

INITIAL CONNECTION STIFFNESS kN.m/radian	β^*	MAJOR AXIS FRAME		MINOR AXIS FRAME	
		$K_1 (= K_2)$	L_E/L	$K_1 (= K_2)$	L_E/L
1000	0.172	0.934	0.95	0.819	0.87
5000	0.509	0.828	0.88	0.605	0.74
10000	0.675	0.784	0.85	0.536	0.71
20000	0.806	0.752	0.83	0.492	0.68
30000	0.862	0.739	0.82	0.475	0.67
40000	0.893	0.732	0.81	0.466	0.67
50000	0.912	0.728	0.81	0.461	0.67
Rigid	1.000	0.706	0.80	0.438	0.66

$$\beta^* = \frac{\beta}{\beta + 4}$$

where $\beta = \frac{\text{initial connection stiffness}}{\text{beam stiffness}}$ (see chapter 4)

TABLE 7.1 Comparison of effective length ratios from figure 23 of BS 5950

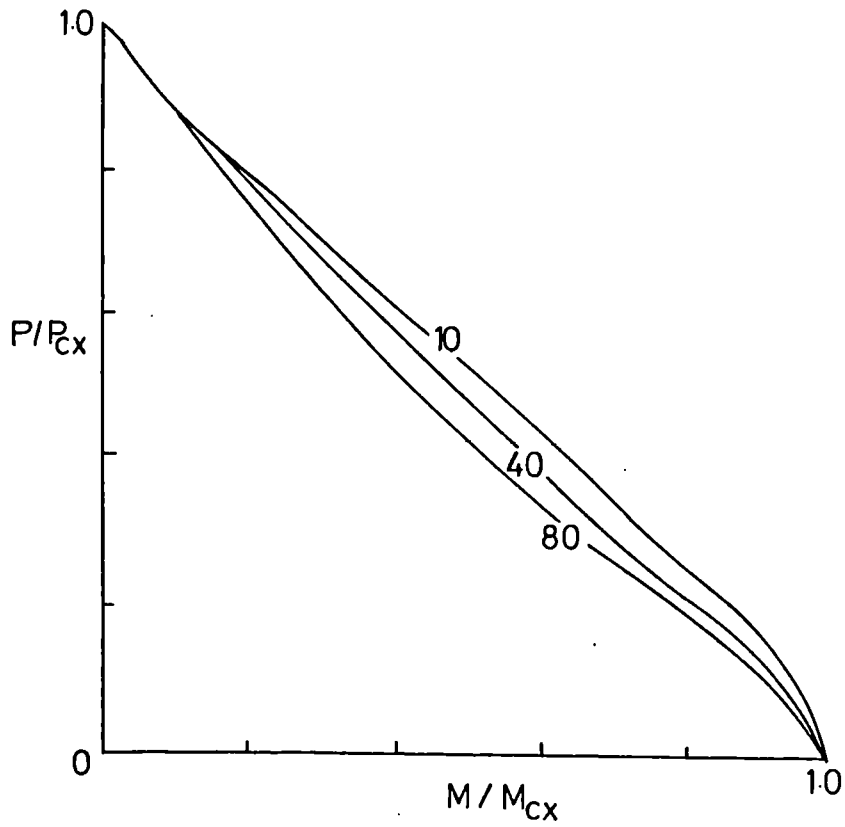


FIGURE 7.1 Interaction plot of axial load and moment for an I section bent about the major axis

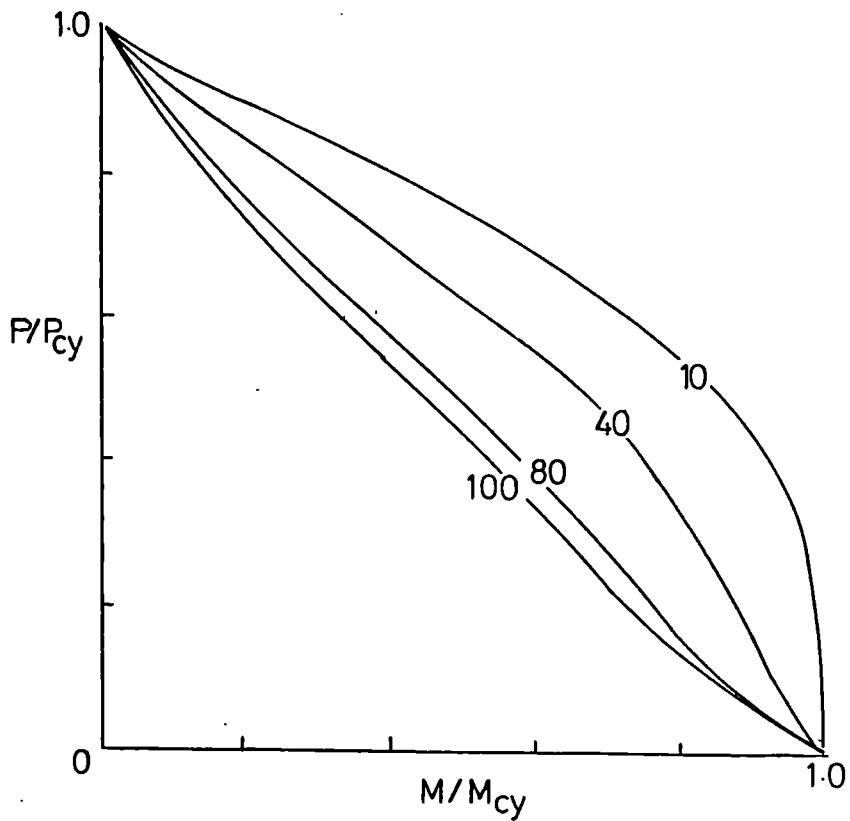
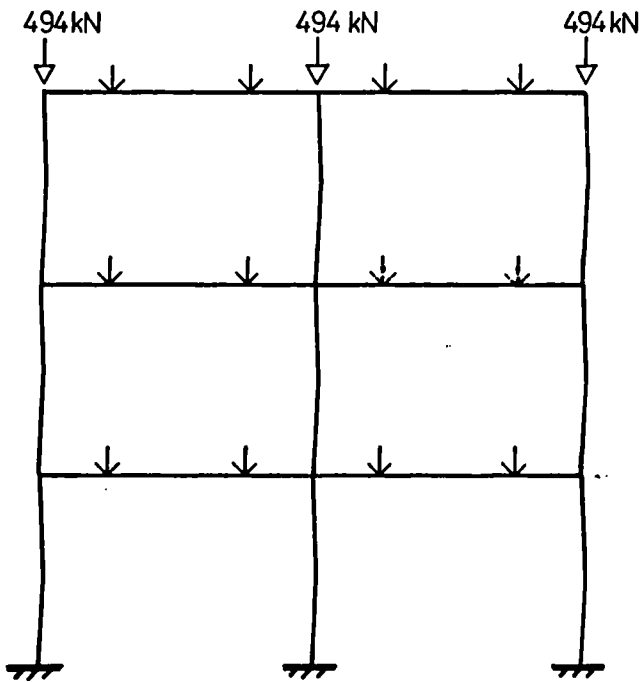
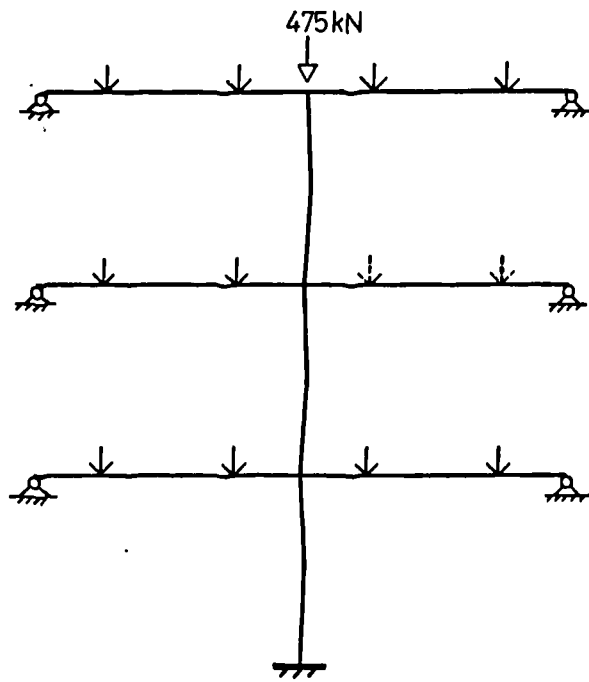


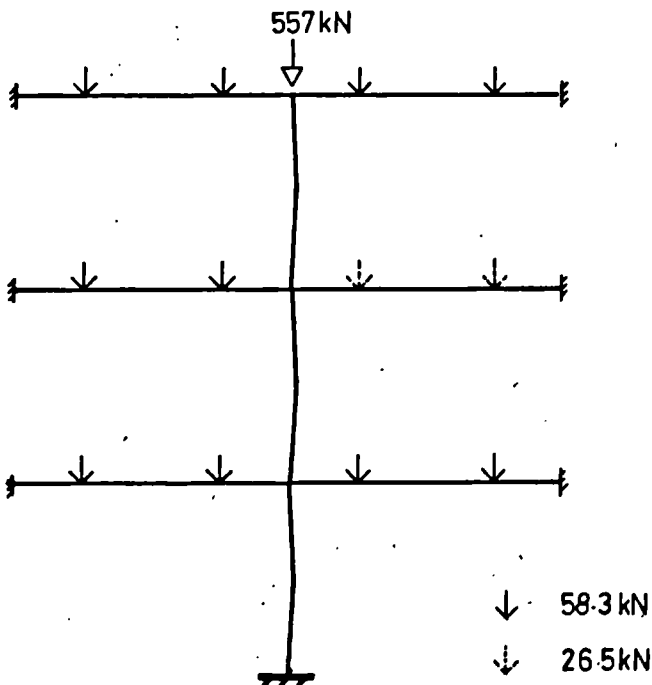
FIGURE 7.2 Interaction plot of axial load and moment for an I section bent about the minor axis



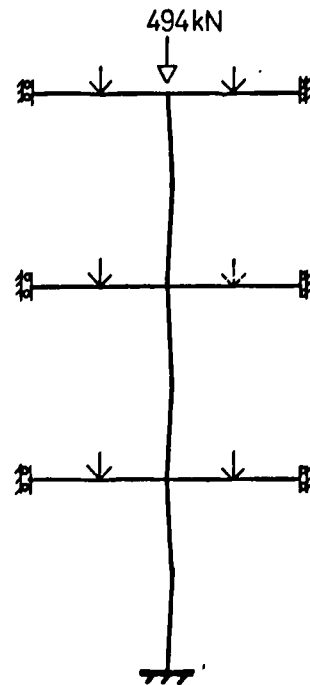
Case 1 Extensive frame



Case 2 Limited frame - pinned ends



Case 3 Limited frame - fixed ends



Case 4 Half beams free to deflect

FIGURE 7.3 Influence of boundary conditions at the remote ends of beams in limited subassemblages on the axial capacity of columns

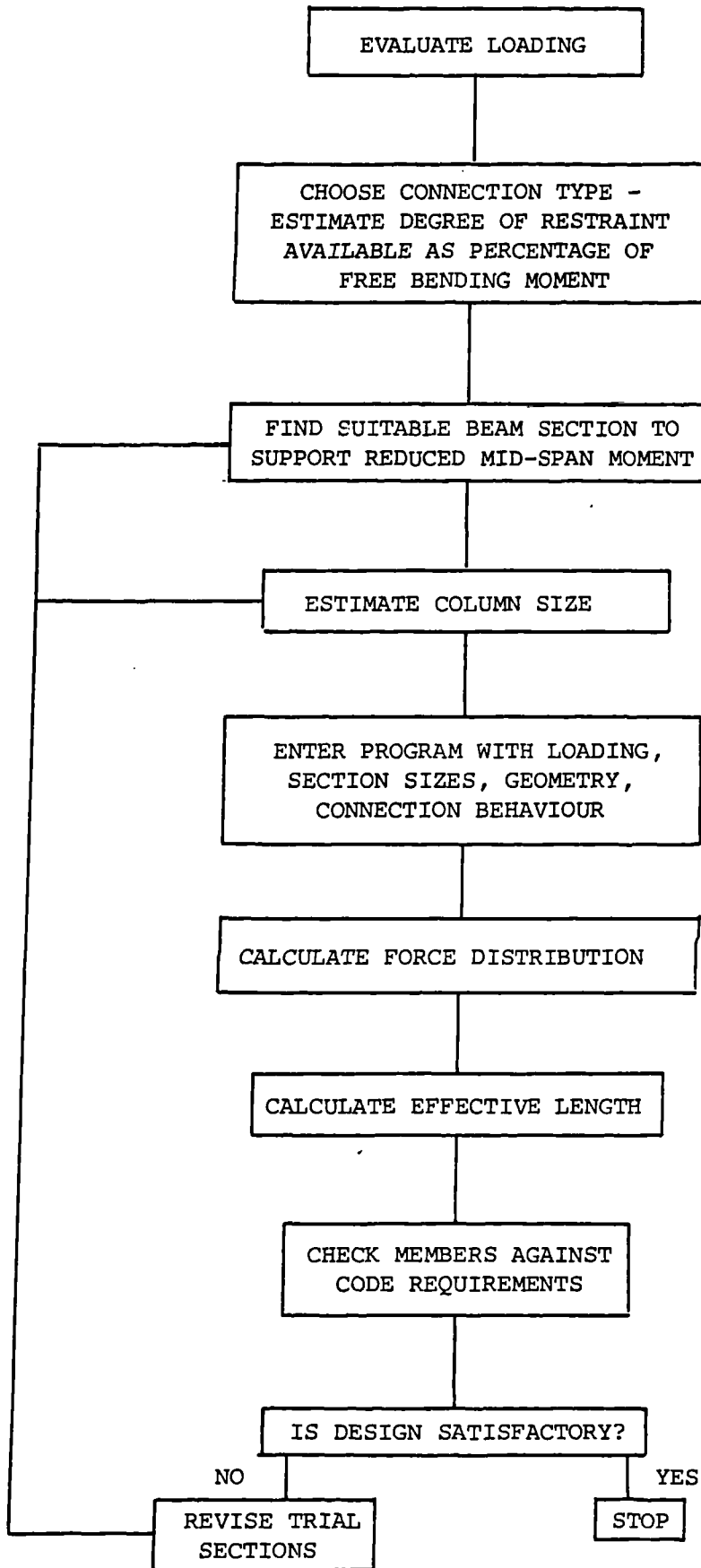


FIGURE 7.4 Flow chart for computerised design method for semi-rigid braced frames

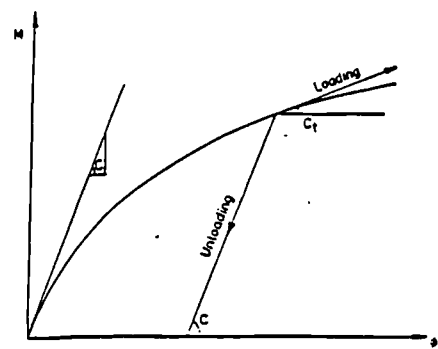
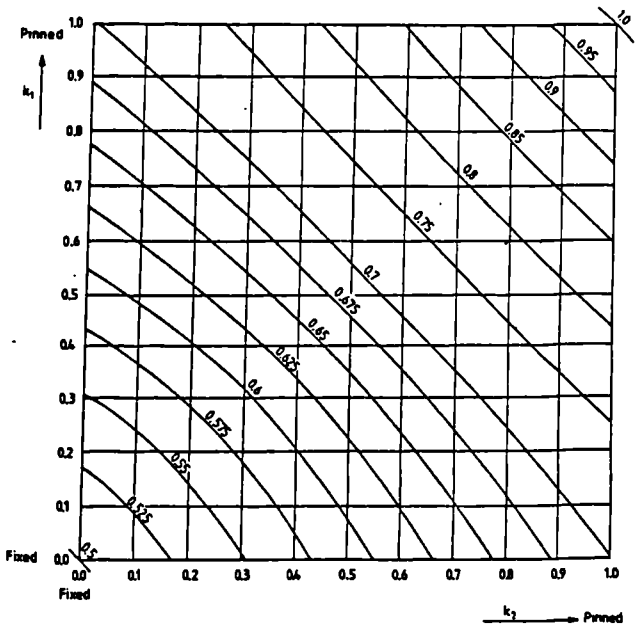
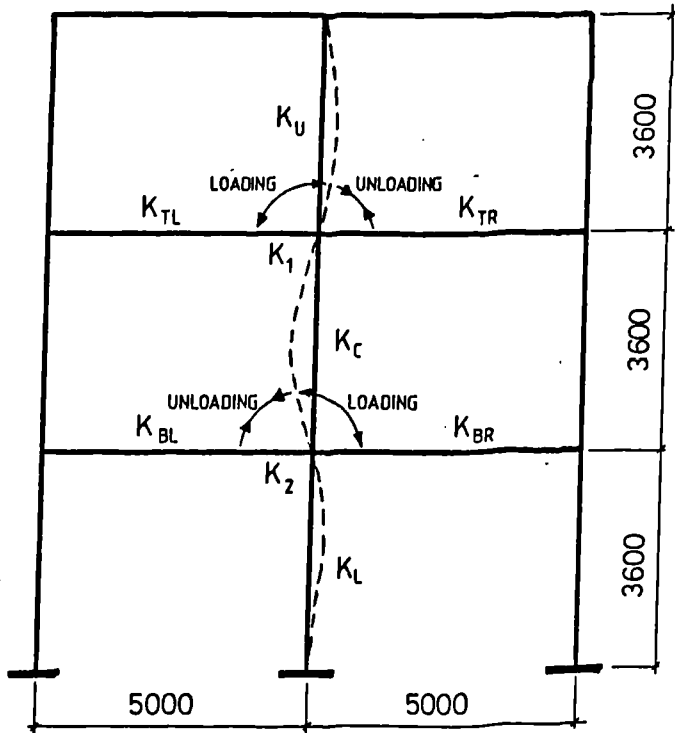


FIGURE 7.5 Determination of effective lengths using modifications to the method in BS 5950 appendix E.2

8.0 CONCLUSIONS

This thesis has detailed the results of an experimental investigation into the strength of flexibly connected steel beam-columns from which the following conclusions may be drawn.

1. 22 steel beam to column connections have been tested to determine their in-plane moment-rotation response. The behaviour of all the connections tested was found to be non-linear with some variability between identical connection arrangements. Seven of the tests incorporated some sort of lack-of-fit. In end-plate connections this was found not to be detrimental to the rotational characteristics. In cleated connections enlarged bolt holes permitted more slippage.
2. Eight end-restrained columns were tested to failure. The in-plane buckling resistance was found to be greatly enhanced by the rotational restraint provided to the column ends by simple beam to column connections.
3. The behaviour of the subassemblage tests has been successfully modelled by a finite element computer program developed at Sheffield University. The correspondence between failure loads, bending moment distribution and in-plane deflections was in most cases very good.
4. Two three storey, two bay, non-sway bare steel frames were tested at the Building Research Station, Watford. The frames' performance demonstrated that flange cleat connections provide restraint to the beams and hence reduce midspan moments and deflections. The connections also enhance the load carrying capacity of the columns.

5. The test frame results have been used to verify the accuracy of a finite element frame analysis program developed at the Politecnico di Milano.
6. Joint performance in isolated connection, restrained column and frame tests has been shown to be essentially the same.
7. The failure loads predicted by the new steelwork code, BS 5950, for an end-restrained column have been shown to be conservative in most cases. In part this is due to the straight line interaction of moment and axial load assumed in the code. It is also affected by the absence of a true cooling residual stress pattern in the test columns and the difficulty of assessing the moments in the column at failure.
8. Methods of incorporating the beneficial effects of inherent joint stiffness have been discussed. A simple method that assumes the connections to act rigidly in order to calculate an effective length, which is then modified to account for joint flexibility, for columns in braced frames has been presented.
9. Experimental verification of the benefits of joint resistance on the performance of columns and complete frames has been provided.

A principal objective of the tests conducted and reported herein was to provide data against which computer programs may be verified. Once programs have been proved accurate and reliable further numeric studies may be undertaken. Areas which need to be studied are the influence of the practical range of connection stiffness on steel frames of realistic geometry and section sizes, the sensitivity of frame behaviour to joint stiffness variations and the performance of subassemblages compared with that of complete frames. A further frame is to be tested at the Building Research Station which will incorpo-

rate flush and extended end-plate connections and will investigate the failure load of the columns restrained by these relatively stiff connections.

Design methods which utilize the benefits of semi-rigid joint action need to be developed. These may be verified against the test frames and against predictions made by computer models. It would appear that the benefits of semi-rigid design may well be in reduction of beam moments and hence section sizes rather than in reduction of column weights. This needs to be studied for a practical range of frame geometry, loading, section sizes and connection types.

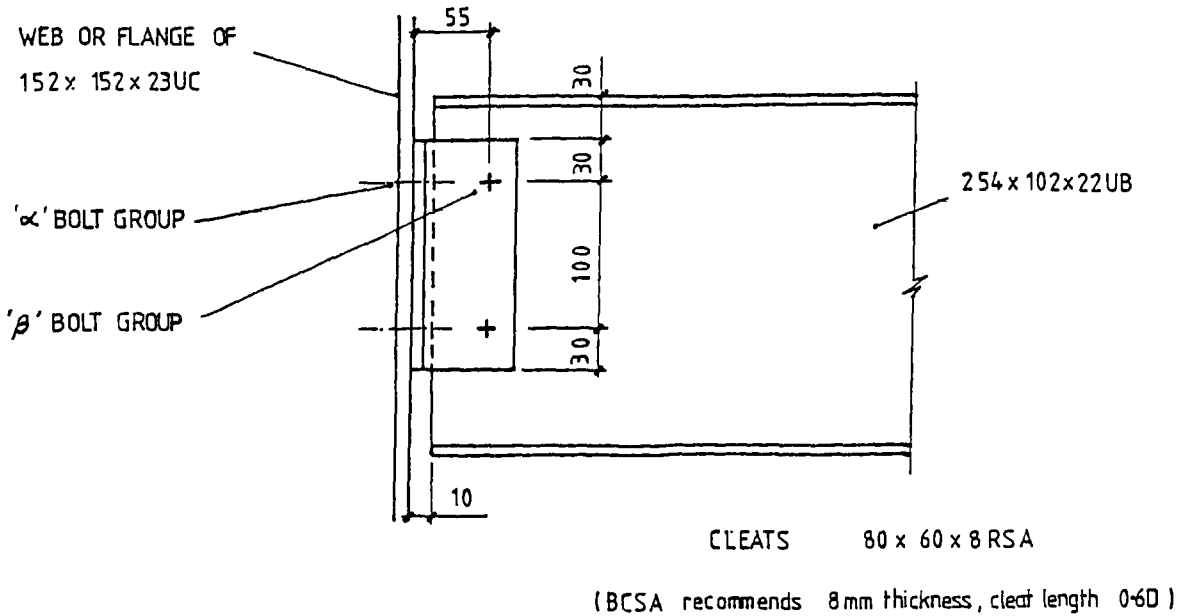
Further potential for incorporating the semi-rigid action into frame design lies in the field of composite construction. Joints which have a concrete decking are considerably stiffer than their bare steel counterparts and the reduction in beam span moments and deflections may be significant. Additionally the performance of columns in composite frames may at present be underestimated and some economy in column weights might be possible. Furthermore the stiffness of these composite joints may permit the omission of sway bracing.

The work reported in this thesis, and the comments made above, have concerned only the in-plane performance of steel frames and columns. Future experiments on the three dimensional response of end-restrained columns is of a high priority. This will supplement the analytical work already in progress and would enable the restriction of in-plane column failure, which is necessary in the current work, to be lifted.

APPENDIX A DESIGN OF CONNECTIONS

Design connections for end shear of 40 kN at working loads.

A.1 Double Angle Web Cleats



The design is based on AISC¹, 'Design of Structural Connections'

(A.1)

Bolt Strength

Bolt Strength (group α) $V_a = 2n \cdot B_v \cdot n_e / n$ (1)

Bolt Strength (group β) $V_b = 2Z_b \cdot B_v \cdot n_e / n$ (2)

where n = no. of bolts per angle leg

B_v = maximum permissible bolt force in shear, lesser of B_{VN} or B_{VX}, B_0

n_e = no. of effective bolts in one line, Table 3.1.3 gives

$n_e = 2.$

$$Z_b = \frac{n}{\sqrt{(1 + (6e/p)(n + 1))^2}} \quad (3)$$

¹Australian Institute of Steel Construction.

where e = eccentricity

p = bolt pitch

Now, B_{VN} , B_{VX} are given in Table 3.1.1.2, assuming M16 grade 8.8 untorqued bolts,

shear (threads in shear plane)¹ $B_{VN} = 29 \text{ kN (safe load)}$

shear (threads out of shear plane) $B_{VX} = 40 \text{ kN (safe load)}$

and, B_0 is given in section 3.1.1 as,

for group α , $B_0 = 1.35F_y.t.D$ (4)

for angle cleat to supporting member

$$B_0 = 2.1F_y.t.D \quad (5)$$

for supporting member

for group β , $B_0 = 1.35F_y.t.D$ (6)

for angle cleat attached to beam web

$$B_0 = 2.1F_y.t.D/2 \quad (7)$$

for supported beam web

where $F_y = 260 \text{ N/mm}^2$ for grade 43 (specified yield stress)

t = ply thickness (column web, beam web, cleat thickness, as appropriate)

D = bolt diameter

Substituting into eqns. (4) to (7) $B_0 = 44.9, 53.3, 44.9, 25.3 \text{ kN}$

ie $B_{0min} = 25.3 \text{ kN (for supported beam web)}$

Now, substitute B_{VN} into eqn. (1)

$$V_g = 2 \times 2 \times 29 \times 2/2 = \underline{116 \text{ kN}}$$

eqn. (3)

$$Z_b = \frac{2}{\sqrt{1 + (6 \times 0.055/0.1 (2 + 1))^2}} = 1$$

¹AISC advises that this case be assumed.

hence, eqn. (2)

$$V_b = 2 \times 1 \times 25.3 \times 2/2 = \underline{50.6 \text{ kN}}$$

Cleat Strength

$$V_p = (V_c, V_d) \text{ min}$$

where

$$V_c = 2 \times 0.3 \times F_y \cdot t \cdot l \quad (8)$$

$$V_d = \frac{2 \times 0.66 \cdot F_y \cdot t \cdot l^2}{6E} \quad (9)$$

and

l = cleat length

E = eccentricity

eqn. (8)

$$V_c = 2 \times 0.3 \times 260 \times 8 \times 160 = \underline{199 \text{ kN}}$$

Eqn. (9)

$$V_d = \frac{2 \times 0.66 \times 260 \times 8 \times 160^2}{6 + 66} = \underline{213 \text{ kN}}$$

Web Strength of Supported Member

$$V_{xx} = 0.37 D \cdot t \cdot F_y \quad (10)$$

where

V_{xx} = maximum permissible x-x shear strength of an unstiffened web (AS 1250, Rule 5.10.2)

D = beam depth

$$V_{xx} = 0.37 \times 245 \times 5.8 \times 260 = \underline{142 \text{ kN}}$$

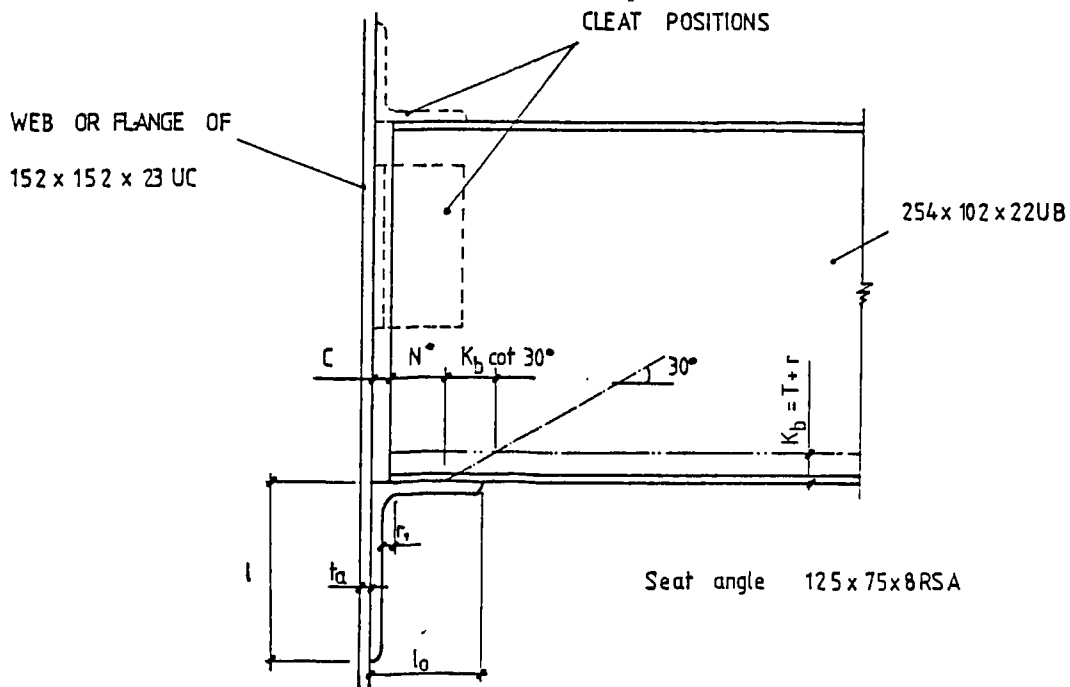
(Note - the Australian code allows a higher value to be taken for the web yield stress; this increase has been ignored in these cases)

Summary

Failure Mode	Maximum Permissible Load
V_a bolt strength - group α	116 kN
V_b bolt strength - group β	50 kN*
V_c cleat bearing	199 kN
V_d cleat bending	213 kN
V_{xx} beam web failure	124 kN

* likely mode of failure is that of bearing of the bolts in group β on the beam web.

A.2 Top and Bottom Flange cleats



Design based on AISC, Design of Structural Connections, (A.1)

$$V_a = 0.75F_y (N^* + k_b \cot 30^\circ)t$$

$$40 \times 10^3 = 0.75 \times 260 (N^* + 14.4.173).5.8$$

$$N^* = \frac{40.10^3}{0.75 \times 260 \times 5.8} - 144 \times 1.73 = 10.45\text{mm}$$

If $c + \frac{N^*}{2} < t_a + r_1$ bending of O/S leg of seat not critical

$$c + \frac{N^*}{2} = 10 + 5.2$$

$$t_a + r_1 = 8 + 11 \quad \therefore \text{bending of seat not critical}$$

Design condition $V_{des} = (\%V_{cap}, V_c)_{min}$

Capacity of Seat

$$V_{cap} = 0.375F_y.tz + \sqrt{y.l_s F_y t + (0.375.F_y.T.z)^2} \quad (1)$$

where

$$y = 0.1875 F_y t_a^2 \quad (2)$$

$$z = k_b \cot 30^\circ + 2(t_a + r_1) - 2c \quad (3)$$

calculate

$$y = 0.1875 \times 260 \times 8^2 = 3.1 \text{ kN}$$

and

$$z = (11 + 6.8) \cot 30^\circ + 2(8 + 11) - 2 \times 10 = 48.8 \text{ mm}$$

substitute into eqn. (1),

$$V_{cap} = 0.375 \times 0.260 \times 5.8 \times 48.8$$

$$+ \sqrt{3.12 \times 100 \times 0.26 \times 5.8 + (0.375 \times 0.260 \times 48.8)^2}$$

$$= 27.6 + \sqrt{470.5 + 22.6} = \underline{49.8 \text{ kN}}$$

Capacity of Fasteners

Consider bearing on column web

$$B_0 = 2.1F_y t D$$

$$= 2.1 \times 260 \times 6.1 \times 16 = 53.2 \text{ kN}$$

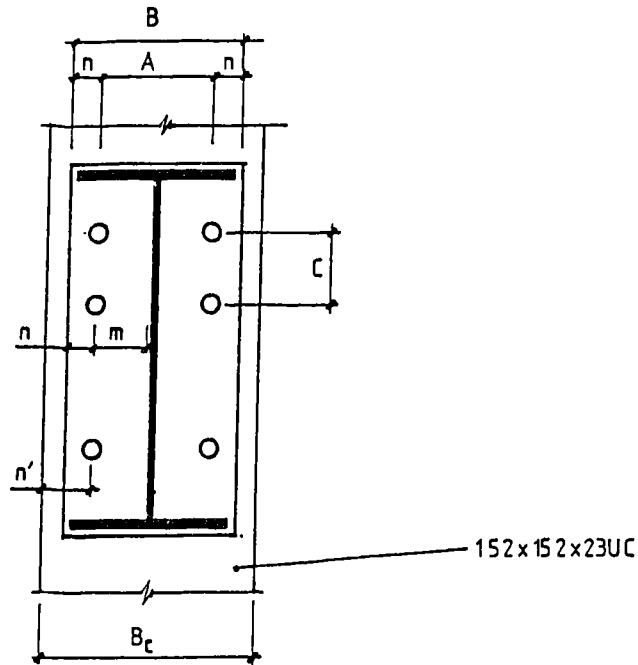
Check bolts in shear, $B_{yN} = 12 \text{ kN}$ (safe load, table 3.1.1.2)

$$4 \text{ bolts @ } 12 \text{ kN} = 48 \text{ kN} > 40 \text{ kN} \quad \therefore \text{O.K.}$$

(Note - this method of design is similar to that in BCSA publication No. 9/82. BCSA recommends that the end beam end clearance should not exceed 3mm. AISC states that the maximum end

clearance in practice should not exceed 10mm, but suggests 15mm for design. A value of 10mm has been used for these calculations).

A.3 Flush End Plate



This type of connection is often adopted for its neat appearance and not its moment capacity. Design may therefore be based simply on the shear load. By comparison with the seat cleat connection it can be clearly seen that provision of a 12mm thick end plate with 6 M16 (Grade 4.6) bolts will safely carry the shear load.

Limit State Design of Flush End-plate (A.2)

Moment Capacity

M16 grade 4.6 bolt, proof load, $P_L = 34.8$ kN

Connection capacity based on bolt strength, M_b

$$M_b = 2 P_L \Sigma \frac{y^2}{Y_{max}} = 2 \times 34.8 \left(\frac{200^2}{200} + \frac{150^2}{200} \right) = 21.75 \text{ kN.m}$$

End Plate Thickness

$$\text{End plate thickness } t_p = \sqrt{\frac{F^*tM}{P_{yp}l_e}} \quad (1)$$

where $F^*t = 4P_L$

P_{yp} = plate yield stress = 220 N/mm² (Grade 43A)

$$m = (A - t_b - 2 \text{ weld size})/2 \\ = (76 - 5.8 - 2 \times 4)/2 = 31.1\text{mm}$$

$$l_e = (\text{pitch of bolts} + 3.5m) \\ = (50 + 3.5 \times 31.1) = 158.9\text{mm}$$

substituting into eqn. (1)

$$t_p = \sqrt{\frac{4 \times 34.8 \times 31.1 \times 10^3}{220 \times 158.9}} = 11.1\text{mm} \quad \underline{\text{use 12mm M.S. Plate.}}$$

Weld Size

Horne and Morris (A.2) suggest a throat thickness of 0.5 × beam flange thickness; therefore required leg length 0.5 × 6.8 × 1.4 = 4.76mm.

4mm fillet weld was used.

Adequacy of Column Flange

$$F_{mb} = T_c^2 \left[\frac{3.14 (m+n^1) + 0.5C}{m+n} \right] P_{yc} + 4P_L \left[\frac{n}{m+n} \right] \quad (2)$$

where T_c = column flange thickness = 6.8mm

t_c = column web thickness = 6.1mm

P_{yc} = yield stress of column (grade 43A) 240 N/mm²

$$m = (A - t_c - 2 \cdot \text{root fillet})/2 \\ = (76 - 6.1 - 2 \times 7.6)/2 = 27.4\text{mm}$$

$$n = (B-A)/2 = (130-76)/2 = 27.0\text{mm}$$

$$n^1 = (B_c - A)/2 = (152-76)/2 = 38.0\text{mm}$$

substituting into eqn. (2)

$$F_{mb} = 6.8^2 \left[\frac{3.14 (27.4 + 8) + 0.5 \times 50}{27.4 + 22.5} \right] \times \frac{240}{10^3}$$

$$+ 4 \times 34.8 \times \left[\frac{27.0}{27.4 + 27.0} \right] = 96.86 \text{ kN}$$

$$\begin{aligned} F_{MC} &= T_c^2 [3.14 + (2n^1 + C - D^1)/m] P_{yc} \\ &= 6.82 [3.14 + (2 \times 38 + 50 - 18)/27.4] 240 \\ &= 78.6 \text{ kN} \end{aligned}$$

$$F^*t = 4P_L = 139 \text{ kN}$$

Since $F^*t > F_{MC}$, $F_{MC} < F_{Mb}$, column flange needs stiffening.

Leave flanges unstiffened, and limit F^*t to 78.6 kN

$$\therefore \text{max. capacity of connection} = \frac{78.6}{139} \times 21.75 = 12.3 \text{ kN}$$

Column Web in Tension

Horne and Morris require $F^*t \leq (C + 3.5m)t_c P_{yc}$

$$\text{and } F^*t \leq 7.0m t_a P_{yc}$$

$$(C + 3.5m)t_c P_{yc} = (50 + 3.5 \times 27.4) \times 6.1 \times 240 = 213 \text{ kN} > F^*t$$

$$7.0 m t_c P_{yc} = 7.0 \times 27.4 \times 6.1 \times 240 = 281 \text{ kN} > F^*t$$

Hence column web in tension zone O.K.

Column Web Compression Zone

$$F_{WC} = (T_b + t_p + d + 5K)t_c P_{yc}$$

where

$$K = (T_c + \text{root fillet})$$

$$F_{WC} = (6.8 + 12 + 0 + 5 \times 14.4) 6.1 \times 240 = 132.9 \text{ kN} < F^*t$$

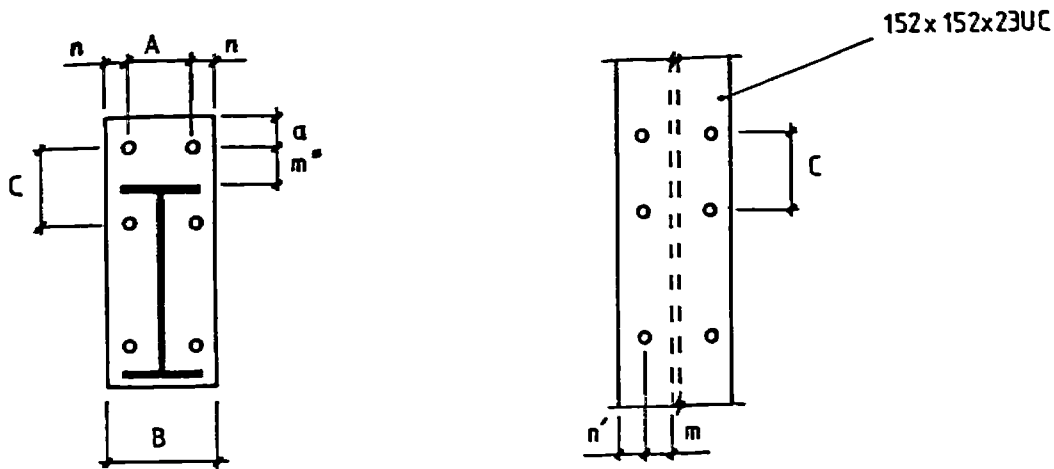
\therefore require web stiffeners - but since answers are close leave web unstiffened.

Connection to Column Web

Capacity of connection governed by bolt strength or end plate failure.

Since end plate is larger than required failure likely to be by bolt failure.

A.4 Extended End plate



Check connection to the method of Mann and Morris (A.3)

Base design on plastic moment of beam section,

$$M_p = Z_{bp} \cdot P_{yb} = 261.9 \times 240 = 62.8 \text{ kN.m}$$

$$\text{Max. tensile force } F_t = \frac{62.8}{0.2472} = 254 \text{ kN}$$

take max. bolt force as $P_u = F_t/3 = 85 \text{ kN}$

try M16 bolt grade 8.8, $P_u = 157 \times 800 = 125 \text{ kN}$.'. O.K.

Plate Thickness

$$t = \left[\frac{F_t m^*}{(P_{yp} B)} \right]^{\frac{1}{2}} = \left[\frac{254 \times 10^3 \times 46.6}{220 \times 135} \right]^{\frac{1}{2}} = 19.96 \text{ mm}$$

As a general rule end plate thicknesses equal to the bolt diameter are usually adopted, hence use a 15mm thick end-plate.

Weld Size

Recommended sizes are flange weld $\geq 0.5 T_b$

web weld $\geq 0.5 t_b$ use 4mm fillet weld all round

(Note: this recommendation is for minimum throat thickness, and hence the leg length should actually have been $1.4 \times 0.5 \times 6.8 = 4.76 \text{ mm}$).

Check Column Flange Tension Region

$$F_{mb} = T_c^2 P_{yc} \left[3.14 + \frac{0.5C}{m+n} \right] + \frac{4P_u n}{m+n} \quad (\text{note to ensure bolts do not fail limit } P_u \text{ to } 0.8P_u)$$

$$= 6.82 \times \frac{240}{1000} \left[3.14 + \frac{0.5 \times 100}{35 + 30} \right] + \frac{4 \times 100 \times 30 \times 10^3}{35 + 30} = 200.3 \text{ kN}$$

$$F_{mc} = T_c^2 P_{yc} \left[3.14 + \frac{(2n' + C - D')}{M} \right]$$

$$= 6.82 \times 240 \left[3.14 + \frac{(2 \times 38 + 100 - 18)}{35} \right] = 84.9 \text{ kN}$$

Since $F_{mc} < F_{mb}$ and $F_t > F_{mc}$ column flange requires stiffening

$$F_{mc} = T_c^2 P_{yc} \left[\left(\frac{1}{v} + \frac{1}{w} \right) (2m + 2n' - D') + \frac{2v + 2w - D'}{m} \right]$$

where $w = (m(m + n' - 0.5D'))^{\frac{1}{2}}$
 $= (35(35 + 38 - 9))^{\frac{1}{2}} = 47.3 \text{ mm}$

$$F_{ms} = 6.82 \times 240 \left[\left(\frac{1}{45} + \frac{1}{47.3} \right) (2 \times 35 + 2 \times 38 - 18) + \frac{2 \times 45 + 2 \times 47.3 - 18}{35} \right] = 114 \text{ kN} < F_t \therefore \text{require thicker flanges}$$

Rather than increase column size use 3 stiffeners in tension zone.

Check Column Web

$$F_c < A_s P_s + 1.63 P_{yc} T_c (b_c t_c)^{\frac{1}{2}}$$

$$\text{and } t_s < \frac{4.1 P_{yc} t_c (b_c t_c)^{\frac{1}{2}}}{P_{ys} b_s}$$

$$F_c = 150 \times 5 \times 240 + 1.63 \times 240 \times 6.8 (152 \times 6.1)^{\frac{1}{2}} = 261 \text{ kN O.K.}$$

$$t = \frac{4.1 \times 240 \times 6.8 (152 \times 6.1)^{\frac{1}{2}}}{240 \times 152} = 5.6 > 5 \therefore \text{O.K.}$$

References

- A.1 HOGAN, T.J. and THOMAS, I.R.
'Standardised structural connections'
Part B : Design of Structural Connections, Australian Institute
of Steel Construction, 2nd Edition, October 1981.
- A.2 HORNE, M.R. and MORRIS, L.J.
'Plastic design of low rise frames'
Constrado Monograph, Granada Publishing Ltd, 1981.
- A.3 MANN, A.P. and MORRIS, L.J.
'Limit design of extended end plate connections'
ASCE, Journal of Structural Division, Vol. 105, No. ST3, March
1979, p.511-525.

APPENDIX B DESIGN OF FULL SCALE FRAMES

B.1 Simple Design to BS 449

The following cross sectional properties, taken from the Structural Steelwork Hand book are assumed,

152 × 152 × 23 UC	area	$A_c = 29.8\text{cm}^3$
	gross moment of inertia	$I_{xx} = 1263\text{cm}^3$
	minor axis moment of inertia	$I_{yy} = 403\text{cm}^4$
	radius of gyration	$r_{xx} = 6.51\text{cm}$
	radius of gyration	$r_{yy} = 3.68\text{cm}$
	elastic modulus	$Z_{xx} = 165.7\text{cm}^3$
	elastic modulus	$Z_{yy} = 52.95\text{cm}^3$
	D\T ratio	= 22.3
254 × 102 × 22 UB:	gross moment of interia	$I_{xx} = 2356\text{cm}^4$
	radius of gyration	$r_{yy} = 2.095\text{cm}$
	elastic modulus	$Z_{xx} = 225.7\text{cm}^3$
	D/T ratio	= 37.2

Grade 43A steel throughout.

Beam Design

Point loads to be applied at 1/4 span from each column

$$\therefore \text{max. BM} = \frac{wL}{8} \quad \text{where } w = \text{total load per beam}$$

Assume beams restrained at 1/3 points,

$$\frac{l}{r_y} = \frac{5000}{3 \cdot r_y} = 81.3$$

Permissible bending stress, $f_{bc} = 165 \text{ N/mm}^2$ (Table 3a)

$$\text{Max. value of load/beam, } w = \frac{8 \times 165 \times 225.7}{5000} = 59.6 \text{ kN}$$

Hence, if dead:live ratio is 2:1

$$\text{Point dead load} = \frac{59.6}{6} = 19.8, \text{ say } 20\text{kN}$$

$$\text{Point live load} = \frac{59.6}{3} = 19.9 \text{ kN, say } 20 \text{ kN}$$

Column Design

If connections were designed as pinned effective lengths would be taken as 1.0, except base to 1st floor which would be 0.85. However most designers would provide seat and top cleats or flush end plate and reduce effective lengths to 0.85.

Worst case - bottom storey

$$\text{Maximum axial load} = 5 \times (10 + 20) + 20 = 170 \text{ kN}$$

$$\text{Maximum out of balance load} = 20 \text{ kN}$$

(i) Major axis column:-

$$\text{Bending moment} = (0.075 + 0.1) 10 = 1.8 \text{ kN.m}$$

distribute moment 50% to upper column, 5% to lower,

$$\text{hence column moment} = 0.9 \text{ kN.m}$$

$$l/r_y = 0.85 \times 3600/65.1 = 47, P_c = 136 \text{ N/mm}^2,$$

$$P_{bc} = 165 \text{ N/mm}^2$$

$$f_{bc} = 0.9 \times 10^3/165.7 = 10.8 \text{ N/mm}^2$$

$$f_c = 170 \times 10^3/2980 = 57.0 \text{ N/mm}^2$$

$$\text{For "failure" } \frac{f_c}{P_c} + \frac{f_{bc}}{P_{bc}} > 1$$

Now, f_{bc}/P_{bc}

$$= 5.4/165 = 0.033$$

so $f_c/P_c > 0.967$ i.e. $f_c = 132 \text{ N/mm}^2$ at failure

Additional axial load to cause "failure" =

$$(132-57).2980 = 223 \text{ kN.}$$

(ii) Minor axis column:

$$\text{Bending moment} = 0.1 \times 10 = 1 \text{ kN.m}$$

$$\text{Moment to lower column} = 0.5 \text{ kN.m}$$

$$l/r_y = 0.85 \times 3600/36.8 = 83.1 P_c = 100 \text{ N/mm}^2,$$

$$P_{bc} = 165 \text{ N/mm}^2$$

$$f_{bc} = 0.5 \times 10^3 / 52.95 = 9.5 \text{ N/mm}^2$$

$$f_c = 170 \times 10^3 / 2980 = 57.0 \text{ N/mm}^2$$

$$f_{bc} / P_{bc} = 9.5 / 165 = 0.058$$

$$\text{so } f_c / P_c > 0.94 \text{ for "failure" i.e. } f_c = 0.94 \times 100 \\ = 94 \text{ N/mm}^2$$

$$\text{Additional axial load to cause "failure"} = (94 - 57) \cdot 2980 \\ = 110.3 \text{ kN.}$$

Test Loading

If a factor of safety of 1.7 is assumed, then the working loads calculated above become the following ultimate test loads:-

Beam loads,

$$\text{dead point load} = 34 \text{ kN}$$

$$\text{live point load} = 17 \text{ kN}$$

Column loads,

$$\text{Major axis - additional column load} = 379 \text{ kN}$$

$$\text{Minor axis - additional column load} = 187 \text{ kN}$$

B.2 Semi-rigid Design

Assume beam-column connection transmits 20% of beam fixed end moment. Loading and frame as before.

Beam Design

$$\text{Beam end moment} = 0.2 \cdot 0.093W \cdot 5 = 0.09W \text{ kN.m}$$

$$\text{Free bending moment @ centre} = \frac{WL}{8} = 0.625W$$

$$\text{Moment at centre} = 0.625W - 0.09W = 37.2 \text{ kN.m (elastic moment of resistance)}$$

$$\text{so } W = 37.2 / 0.535 = 69.5 \text{ kN}$$

Assume dead:live ratio 2:1

$$\text{point dead load} = 23.2 \text{ kN}$$

point live load = 11.6 kN

Column Design

Maximum axial load = $5(11.6 + 23.2) + 23.2 = 196.8$ kN

Out of balance moment = $0.09 \times 69.6 - 0.09 \times 46.4 = 2.0$ kN.m

(i) Major axis

Distribute in proportion to I/L

$$I_b/L_b = 2867/5 = 573, I_c/L_c = 1263/3.6 = 351$$

$$\text{hence moment to column} = \left(\frac{351}{924}\right) \times 0.5 \times 2.0 = 0.4 \text{ kN.m}$$

$$P_{bc} = 165 \text{ N/mm}^2, P_c = 136 \text{ N/mm}^2$$

(as before)

$$f_{bc} = 0.4 \times 10^3 / 165.7 = 2.4 \text{ N/mm}^2$$

$$f_c = 196.8 \times 10^3 / 2980 = 66.0 \text{ N/mm}^2$$

$$f_{bc}/P_{bc} = 2.7/165 = 0.02$$

∴ at "failure" $f_c/P_c > 0.98$

Additional axial load to give "failure" $0.98 \times (136 - 66) \times$

$$2980 = 204 \text{ kN}$$

(ii) Minor axis

$$I_c/L_c = 403/3.6 = 112, I_b/L_b = 573$$

$$\text{hence moment to column} = \left(\frac{112}{685}\right) \times 0.5 \times 2 = 0.15 \text{ kN.m}$$

$$P_{bc} = 165 \text{ N/mm}^2, P_c = 100 \text{ N/mm}^2$$

(as before)

$$f_{bc} = 0.15 \times 10^3 / 52.95 = 2.9 \text{ N/mm}^2$$

$$f_c = 196.8 \times 10^3 / 2980 = 66.0 \text{ N/mm}^2$$

$$f_{bc}/P_{bc} = 2.9/165 = 0.02$$

so $f_c/P_c > 0.98$ @ "failure"

$$\text{Additional axial load required} = 0.98 \times (100-66) \times 2980 = 99.3 \text{ kN}$$

Test Loading

Again assuming a factor of safety of 1.7, test loads at ultimate limit state of the column are as follows:-

Beam loads,

$$\begin{aligned} \text{dead point load} &= 39.4 \text{ kN} \\ \text{live point load} &= 19.7 \text{ kN} \end{aligned}$$

Column loads,

$$\begin{aligned} \text{major axis - additional column load} &= 355 \text{ kN} \\ \text{minor axis - additional column load} &= 169 \text{ kN} \end{aligned}$$

B.3 Design to BS 5950

Beam Design

$$\text{Shear Capacity } P_v = 0.6 p_y A_v = 0.6 \times 275 \times 5.8 \times 254 = 243 \text{ kN (cl. 4.2.3)}$$

$$\frac{b}{T} = \frac{51}{6.8} = 7.5, \quad \frac{d}{t} = \frac{240}{5.8} = 41.4, \text{ table 7, plastic section}$$

$$\therefore \text{Moment Capacity} = p_y S = 275 \times 261.9 = 72 \text{ kN.m (4.2.5)}$$

Loads at quarter span,

$$\text{max bending moment} = \frac{WL}{8}$$

where W = total load,

$$\therefore W = 72 \times 8/4.953 = 116 \text{ kN}$$

if ratio of dead:live is 2:1 and load factors are 1.4 and 1.6, then

$$\text{unfactored dead load} = 53 \text{ kN}$$

$$\text{unfactored live load} = 26.5 \text{ kN.}$$

$$\text{and at ultimate loading condition total dead load per beam} = 74 \text{ kN}$$

$$\text{total live load per beam} = 42 \text{ kN}$$

Column Design

Cl. 4.7.7 says "in structures of simple construction it is not necessary to consider effects on column of pattern loading". In order to get some moment into the column assume pattern loading, as used in B.1 and B.2.

Minimum beam loading - end reaction = 26.5 kN

Major Axis Column Strength

Moment due to eccentricity = $(0.075 + 0.1)26.5 = 4.6$ kN.m

and = $(0.075 + 0.1)58 = 10.2$ kN.m

Maximum moment to column = $10.2 - 4.6 = 5.6$ kN.m

distributed 50% to top, 50% to bottom

Maximum axial load to column = $5 \times 116 \times 0.5 + 26.5$

= 316 kN

These tests prevent minor axis buckling therefore $\lambda_{LT} = 0$ and $M_b =$

$S_x P_y = 184 \times 275 = 50.6$ kN.m

$\frac{l}{r_x} = 0.85 \cdot \frac{3500}{65.1} = 46.9$, and from table 27 curve b ($P_y = 275$ N/mm²) $p_c = 241$ N/mm²

cl. 4.8.3.2 $\frac{F}{A_g P_c} + \frac{\bar{M}_x}{M_b} \leq 1$

$$\frac{\bar{M}_x}{M_b} = \frac{2.8}{50.6} = 0.005$$

$\therefore F \leq 0.945 \times 2.98 \times 241 = 678$ kN

Additional axial load required to give ultimate loading,

$678 - 316 = 362$ kN

Minor Axis Column Strength

Moment due to eccentricity = $0.1 \times 26.5 = 2.6$ kN.m

and = $0.1 \times 58 = 5.8$ kN.m

Maximum out of balance moment = 3.2 kN.m (distributed 50/50)

Maximum axial load as before = 316 kN.m

$$M_b = S_y \cdot P_y \text{ where } S_y \geq 1.2 Z_y$$

$$1.2 Z_y = 1.2 \times 52.95 = 63.54 < S_y$$

$$M_b = 63.54 \times 275 = 17.5 \text{ kN.m}$$

$$\frac{l}{r_y} = 0.85 \times \frac{3600}{36.8} = 83.1, \text{ from table 27, curve c, } p_c = 155 \text{ N/mm}^2$$

$$\text{using equality } \frac{F}{A_g p_c} + \frac{\bar{M}_y}{M_b} \geq 1$$

$$\frac{\bar{M}_y}{M_b} = \frac{1.6}{17.5} = 0.09$$

$$\therefore \frac{F}{A_g p_c} \geq 0.91 \quad \Rightarrow \quad F \geq 0.91 \times 2.98 \times 155 = 420 \text{ kN}$$

Additional axial load required to give ultimate loading

APPENDIX C MATERIAL AND CROSS SECTIONAL PROPERTIES

C.1 Cross Sectional Properties

Throughout the test series a careful record of the material used in each test was kept. Tables C.1, C.2 and C.3 log which beam, column and connection sections were used in the joint tests, subassemblages and frame tests respectively. Each column and beam section supplied was measured at regular intervals along its length. The average cross sectional dimensions and properties are presented in tables C.4, C.5 and C.6.

C.2 Tensile Tests

Tensile tests based on the procedure specified in TRRL Report 254 (C.1) were conducted on coupons from all material used in the testing programme (except the angles used in the frame tests). Specimens were cut from the sections as shown in figure C.1 and machined to a nominal gauge length of 140mm and width of 10mm. Tests were conducted in an Instron testing machine at its slowest strain rate, 0.005"/minute (0.127mm/minute) corresponding to a rate of change of strain in the specimen of approximately 0.1%/minute. A plot of load against cross head movement was plotted as the test proceeded and this trace was used in controlling the tests. Strain, at the rate specified above, was applied until the load against deflection trace flattened. The machine was then stopped for two minutes and the relaxation load in this time monitored. The test was restarted and the specimen strained further into the plastic region before stopping the test for a further two minute period. Ultimate strength tests were not conducted. Figure C.1 illustrates the test procedure and defines the dynamic and static yield stress. A summary of the test results is reported in table C.7.

C.3 Stub Column Tests

Stub column tests were conducted on short lengths of column cut from the six sections used in the two frame tests. The procedure detailed in reference C.2 was followed. A length of column of approximately 600mm was machined so that its ends were square to the longitudinal axis and parallel to within $\pm 0.025\text{mm}$. The cross sectional area was computed from readings around the section at four locations along the column length. Two high precision AC LVDT's were used to measure the change in length of the central 250mm portion of the stub column as load was applied using a 200kN Amsler testing machine - see figure C.2. An Orion Delta data logger was used to record the stress (computed from the load and cross sectional area) at strain intervals of $25\mu\text{s}$. Typical stress-strain curves are presented in figure C.3 and C.4. A value for the 0.2% yield stress (or proof stress) and Young's Modulus in compression for the six columns was thus obtained and is reported in table C.7.

C.4 Residual Stress Tests

In addition to the tensile and stub column tests residual stress testing was also undertaken using the sectioning method. A 600mm length of column was cut from the column used in the subassembly and frame tests and 1mm diameter indentations (columns 4, 11, 13-15A) or holes (columns 13B and 15B) were made over a 100mm gauge length at the locations around the section shown in figure C.5. The actual gauge length was measured for each pair of holes using a Cambridge Instruments Electronic Tenseometer. The column was then cut to a length of 120mm and sectioned as shown in figure C.5. The change in length of each pair of holes was then recorded and the stress

released by cutting the section calculated using an estimated value for Young's Modulus. Figure C.6 shows the residual stress patterns obtained.

Columns C.4 and C.11 were used in the subassemblage tests. Evidence of cold straightening was clear from the marks contained in the mill scale, and test C.11 shows the residual stress pattern had been almost eliminated. In test C.4 two adjacent lengths of the column were examined to see what variation in residual stress occurred along the column length. The patterns in C.4A and C.4B have been altered by the straightening process and therefore no set pattern could be selected as representative of the stress in the columns.

The columns in test frame 1 (C.13, 14, 15) were examined prior to testing the frame and the residual stress patterns in a length cut from the end of the column during fabrication are shown in C13A, C.14 and C.15A. The columns appeared to have been straightened but the process has not affected the column section near the end of the column. However tests conducted in the column length show a different pattern (C.13B and 15B) and again illustrate that the straightening process destroys the residual stress pattern caused by cooling.

References

- C.1 TRANSPORT AND ROAD RESEARCH LABORATORY
'Recommended standard practices for structural testing of steel models'
TRRL Supplementary Report 254.
- C.2 JOHNSTON, B.G.
'Guide to stability design criteria for metal structures'
Structural Stability Research Council, Third Edition, John Wiley & Sons, New York.

TEST	TYPE OF CONNECTION	AXIS	CONNECTION COMPONENTS	SOURCE OF COLUMN	SOURCE OF BEAMS	SOURCE OF CONNECTION	BOLT GRADE
JT/01	Web cleats	Minor	80x60x8 RSA	C1	B5	A1	8.8
JT/01B	Web cleats	Minor	80x60x8 RSA	C1	B5	A1	8.8
JT/02	Web cleats	Minor	80x60x8 RSA	C1	B6	A1	8.8
JT/03	Web cleats	Minor	80x60x8 RSA	C1	B6	A1	8.8
JT/04	Web cleats	Major	80x60x8 RSA	C1	B3	A1	8.8
JT/05	Web cleats	Major	80x60x8 RSA	C1	B2	A1 A2	8.8
JT/06	Web cleats	Major	80x60x8 RSA	C2	B1	A2	8.8
JT/07	Top and bottom flange cleats	Minor	80x60x8 RSA 125x75x8 RSA	C1	B1	A2 A5	4.6
JT/08	Top and bottom flange cleats	Major	80x60x8 RSA 125x75x8 RSA	C1	B5	A2 A5	4.6
JT/09	Bottom flange and web cleats	Minor	80x60x8 RSA 125x75x8 RSA	C2	Left B4 Right B3	A2 A5	4.6
JT/10	Bottom flange and web cleats	Major	80x60x8 RSA 125x75x8 RSA	C2	Left B2 Right B4	A2	4.6
JT/11	Flush end-plate	Minor	265x125x12 M.S. Plate	C2	B4	12mm plate	4.6
JT/12	Flush end-plate	Major	265x125x12 M.S. Plate	C2	B5	12mm plate	4.6

TABLE C.1 Material used in connection tests

TABLE C.1 cont'd

TEST	TYPE OF CONNECTION	AXIS	CONNECTION COMPONENTS	SOURCE OF COLUMN	SOURCE OF BEAMS	SOURCE OF CONNECTION	BOLT GRADE
JT/13	Extended end-plate	Major	350x135x15 M.S. Plate	C2	Left B3	15mm plate	8.8
JT/13b	Extended end-plate	Major	350x135x15 M.S. Plate	RE-TEST OF JT/13			8.8
JT/14	Header plate	Minor	265x125x12 M.S. Plate	C2	B6	12mm plate	4.6
CT/01	Web cleats	Major	80x60x8 RSA	C2	Left B1 Right B6	A2	8.8
CT/02	Top and bottom flange cleats	Major	80x60x8 RSA 125x75x8 RSA	C1	Left B3 Right B5	A2 A5	4.6
CT/03	Flush end-plate	Minor	265x125x12 M.S. Plate	C2	Left B4 Right B2	12mm plate	4.6
CT/04	Extended end-plate	Major	350x135x15 M.S. Plate	C1	Left B1 Right B4	15mm plate	8.8
CT/05	Flush end-plate	Minor	265x125x12	C1	B2/B5	12mm plate	8.8
CT/06	Extended end-plate	Major	350x135x15	C1	B1/B3	15mm plate	HSPG
CT/07	Extended end-plate	Minor	350x135x15	30mm plate	B1/B5	15mm plate	8.8
CT/08	Extended end-plate	Minor	350x135x15	30mm plate	B1/B3	15mm plate	8.8

TEST	TYPE OF CONNECTION	AXIS	CONNECTION COMPONENTS	SOURCE OF COLUMN	SOURCE OF BEAMS	SOURCE OF CONNECTION
ST1	-	Major Minor	-	C12	-	-
ST2	Web cleats	Major	80x60x8	C5	B9	A3
ST3	Web cleats	Minor	80x60x8	C7	B12	A4
ST4	Flange cleats	Major	80x60x8 125x75x8	C11	B15	A3
ST5	Flange cleats	Major	80x60x8 125x75x8	C3	B13	A3 A5
ST6	Flange cleats	Minor	80x60x8 125x75x8	C6	B14	A3 A5
ST7	Flange cleats	Minor	80x60x8 125x75x8	C8	B15	A3 A5
ST8	Web and seat cleats	Minor	80x60x8 125x75x8	C4	B11	A3 A5
ST9	Flush end-plate	Minor	265x125x12 M.S. plate	C9	B8	12mm plate
ST10	Extended end-plate	Major	350x135x15 M.S. plate	C10	B16	15mm plate

TABLE C.2 Material used in subassemblage tests

TEST FRAME NO	TYPE OF CONNECTION	AXIS	CONNECTION COMPONENTS	SOURCE OF COLUMN	SOURCE OF BEAMS	BOLT GRADE
				1 2 3	1 2 3 4 5 6	
FRAME 1	Top and bottom Flange cleats	Major	80x60x8 RSA 125x75x8 RSA	C13 C15 C14	B18 B17 B21 B22 B19	4.6
FRAME 2	Top and bottom Flange cleats	Minor	80x60x8 RSA 125x75x8 RSA	C16 C17 C18	B23 B24 B25 B26 B27 B28	4.6

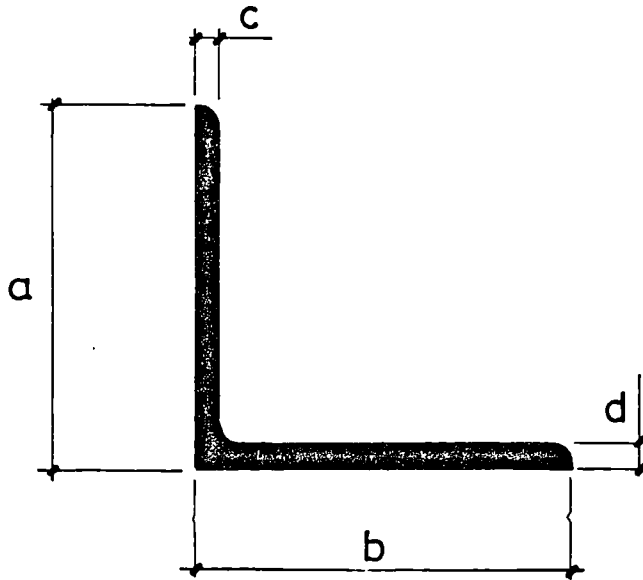
TABLE C.3 Material used in frame tests

REF	D MM	B MM	TW MM	TF MM	A CM2	IX CM4	IY CM4	ZX CM3	ZY CM3	ZPX CM3	ZPY CM3	RX MM	RY MM
C1	151.60	151.35	6.30	6.68	29.54	1228.9	387.9	162.1	51.3	180.6	78.5	64.5	36.2
C2	151.90	151.15	7.10	6.81	31.01	1268.5	393.9	167.0	52.1	187.3	80.1	64.0	35.6
C3	152.54	152.21	6.42	6.38	29.01	1211.8	376.9	158.9	49.5	177.3	76.0	64.6	36.0
C4	152.18	152.19	6.21	6.27	28.37	1185.1	370.2	155.8	48.7	173.5	74.6	64.6	36.1
C5	152.51	152.34	6.08	6.27	28.22	1188.7	371.3	155.9	48.7	173.5	74.7	64.9	36.3
C6	152.78	152.59	6.08	6.43	28.74	1218.0	382.6	159.4	50.1	177.4	76.8	65.1	36.5
C7	152.94	152.86	6.29	6.45	29.14	1230.3	385.8	160.9	50.5	179.3	77.4	65.0	36.4
C8	152.28	152.24	6.07	6.29	28.24	1186.8	371.7	155.9	48.8	173.4	74.8	64.8	36.3
C9	152.37	152.03	6.27	6.21	28.27	1180.1	365.6	154.9	48.1	172.7	73.8	64.6	36.0
C10	152.41	152.22	6.28	6.26	28.45	1189.4	369.9	156.1	48.6	174.0	74.5	64.7	36.1
C11	153.16	152.62	6.46	6.61	29.83	1259.4	393.5	164.5	51.6	183.5	79.1	65.0	36.3
C12	153.03	152.88	6.29	6.47	29.20	1234.9	387.2	161.4	50.7	179.9	77.6	65.0	36.4
C13	153.31	156.45	6.47	6.95	31.38	1339.4	445.5	174.7	56.9	194.6	87.1	65.3	37.7
C14	153.32	156.45	6.52	6.89	31.27	1331.9	441.6	173.7	56.5	193.6	86.4	65.3	37.6
C15	153.03	156.58	6.25	6.89	30.89	1321.3	442.7	172.7	56.5	192.0	86.4	65.4	37.9
C16	153.01	155.94	6.10	6.65	29.87	1277.9	422.1	167.0	54.1	185.6	82.8	65.4	37.6
C17	153.91	154.33	5.97	6.70	29.68	1287.0	412.3	167.2	53.4	185.7	81.7	65.9	37.3
C18	153.62	156.58	6.68	6.86	31.44	1337.8	440.8	174.2	56.3	194.4	86.3	65.2	37.4

TABLE C.4 Cross sectional properties of columns

REF	D MM	B MM	TW MM	TF MM	A CM2	IX CM4	IY CM4	ZX CM3	ZY CM3	ZPX CM3	ZFY CM3	RX MM	RY MM
B1	254.70	101.80	6.03	6.87	29.16	2935.4	122.0	230.5	24.0	268.2	38.2	100.3	20.5
B2	254.50	102.50	6.00	6.99	29.40	2974.9	126.6	233.8	24.7	271.4	39.3	100.6	20.8
B3	254.35	103.25	6.13	6.87	29.57	2968.4	127.2	233.4	24.6	271.6	39.3	100.2	20.7
B4	257.80	100.85	6.26	8.40	32.67	3449.9	144.8	267.6	28.7	309.5	45.5	102.8	21.1
B5	254.70	101.10	6.02	6.98	29.25	2949.8	121.4	231.6	24.0	269.3	38.3	100.4	20.4
B6	254.85	101.10	5.96	6.96	29.07	2941.2	121.0	230.8	23.9	268.2	38.1	100.6	20.4
B7						NOT USED							
B8	255.45	102.29	6.26	6.66	29.42	2933.4	120.0	229.7	23.5	268.6	37.6	99.9	20.2
B9	255.54	102.31	5.97	6.66	28.73	2901.9	120.0	227.1	23.5	264.5	37.4	100.5	20.4
B10						NOT USED							
B11	255.38	102.24	5.86	6.68	28.48	2888.9	120.1	226.2	23.5	263.0	37.4	100.7	20.5
B12	255.28	102.17	5.92	6.64	28.53	2880.8	119.2	225.7	23.3	262.7	37.2	100.5	20.4
B13	255.22	102.75	5.85	6.60	28.36	2871.5	120.5	225.0	23.5	261.6	37.3	100.6	20.6
B14	255.03	102.05	5.86	6.67	28.42	2873.3	119.3	225.3	23.4	261.9	37.2	100.6	20.5
B15	254.95	101.84	5.80	6.54	27.99	2823.4	116.3	221.5	22.8	257.6	36.4	100.4	20.4
B16	255.28	102.18	5.98	6.65	28.70	2890.9	119.4	226.5	23.4	263.8	37.3	100.4	20.4
B17	254.30	103.87	6.39	6.84	30.22	3001.8	129.0	236.1	24.8	275.6	39.8	99.7	20.7
B18	254.25	103.95	6.40	6.83	30.24	3000.5	129.1	236.0	24.8	275.6	39.8	99.6	20.7
B19	254.53	103.78	6.01	6.80	29.23	2950.5	127.9	231.8	24.6	269.4	39.2	100.5	20.9
B20						NOT USED							
B21	254.20	103.61	6.04	6.80	29.26	2941.8	127.2	231.5	24.6	269.0	39.1	100.3	20.9
B22	254.70	103.47	6.16	6.77	29.50	2957.5	126.2	232.2	24.4	270.6	39.0	100.1	20.7
B23	254.50	103.87	6.18	6.91	29.87	3002.5	130.3	236.0	25.1	274.5	40.0	100.3	20.9
B24	254.50	104.40	6.19	6.91	29.97	3014.9	132.3	236.9	25.3	275.6	40.4	100.3	21.0
B25	254.50	103.90	6.24	6.90	30.00	3007.3	130.2	236.3	25.1	275.2	40.0	100.1	20.8
B26	254.20	103.34	6.15	6.80	29.49	2948.9	126.3	232.0	24.4	270.2	39.0	100.0	20.7
B27	254.10	103.29	5.89	6.73	28.72	2895.4	124.8	227.9	24.2	264.5	38.4	100.4	20.8
B28	254.20	102.98	6.03	6.76	29.07	2916.3	124.2	229.4	24.1	266.9	38.5	100.2	20.7

TABLE C.5 Cross sectional properties of beams



	a	b	c	d
ANGLE 1	60.03	78.86	8.03	8.09
ANGLE 2	60.23	78.80	8.02	8.13
ANGLE 3	60.0	80.0	8.03	8.07
ANGLE 4	60.0	80.0	8.07	8.00
ANGLE 5	76.50	124.55	8.08	8.03

TABLE C.6 Cross Sectional Dimensions of Angles

SPECIMEN REFERENCE	DYNAMIC YIELD STRESS (N/mm ²)	STATIC YIELD STRESS (N/mm ²)	REMARKS
C1A	284.00	275.47	Joint Tests
C1B	280.11	270.77	"
C1C	290.33	281.81	"
C2A	278.68	270.90	"
C2B	N O T U S E D		"
C2C	274.50	266.26	"
C3A	294.84	286.53	Sub Assemblage
C3B	282.15	274.93	Tests
C3C	284.92	273.61	"
C4A	300.21	292.16	"
C4B	282.00	273.79	"
C4C	280.09	270.71	"
C5A	297.80	289.16	"
C5B	291.60	282.89	"
C5C	305.23	297.13	"
C6A	303.41	292.74	"
C6B	309.98	300.50	"
C6C	285.35	272.01	"
C7A	277.74	270.77	"
C7B	267.63	261.75	"
C7C	271.54	262.58	"
C8A	292.30	284.91	"
C8B	285.20	275.13	"
C8C	284.19	274.17	"
C9A	285.15	280.00	"
C9B	N O T U S E D		"
C9C	268.06	262.54	"
C10A	273.01	264.15	"
C10B	291.77	279.56	"
C10C	280.52	271.58	"
C11A	282.76	275.69	"
C11B	282.47	273.59	"
C11C	277.27	268.33	"
C12A	286.97	271.17	"
C12B	278.23	271.17	"
C12C	275.94	269.52	"
C13A	275.70	269.43	Frame Test Stub Column
C13B	251.60	243.66	No. 1 Test Result
C13C	253.00	244.42	" p _y = 295N/mm ² , E = 277kN/mm ²
C14A	277.15	268.33	" Stub Column
C14B	263.54	255.13	" Test Result
C14C	270.60	266.50	" p _y = 295N/mm ² , E = 222kN/mm ²

TABLE C.7 Material properties of columns, beams and connection components

TABLE C.7 continued

PECIMEN REFERENCE	DYNAMIC YIELD STRESS (N/mm ²)	STATIC YIELD STRESS (N/mm ²)	REMARKS	
C15A	278.85	271.28	Frame Test	Stub Column
C15B	268.31	261.01	No. 1	Test Result
C15C	262.04	254.56		$p_y = 300\text{N/mm}^2$, $E = 210\text{kN/mm}^2$
C16A	305.83	294.72	Frame Test	Stub Column
C16B	N O T	U S E D	No. 2	Test Result
C16C	311.11	302.78	"	$p_y = 304\text{N/mm}^2$, $E = 202\text{kN/mm}^2$
C17A	305.77	288.86	"	Stub Column
C17B	N O T	U S E D		Test Result
C17C	305.61	297.84	"	$p_y = 300\text{N/mm}^2$, $E = 207\text{ kN/mm}^2$
C18A	287.29	278.71	"	
C18B	286.46	277.43		
C18C	N O T	U S E D		
B1A	307.57	301.13	Joint Tests	
B1B	295.39	287.33	"	
B1C	298.20	288.26	"	
B2A	317.18	308.32	"	
B2B	306.04	295.66	"	
B2C	295.02	287.04	"	
B3A	306.84	297.06	"	
B3B	299.39	291.44	"	
B3C	301.10	293.25	"	
B4A	314.15	303.78	"	
B4B	296.10	291.11	"	
B4C	292.76	287.28	"	
B5A	321.28	310.60	"	
B5B	313.83	305.40	"	
B5C	317.84	308.53	"	
B6A	308.92	301.30	"	
B6B	311.97	302.32	"	
B6C	N O T	U S E D		
B8A	326.04	314.79	Sub Assemblage	
B8B	305.05	294.20	Tests	
B8C	294.42	287.88	"	
B9A	334.97	324.64	"	
B9B	304.35	297.87	"	
B9C	303.04	292.94	"	
B11A	288.23	281.82	"	
B11B	N O T	U S E D		
B11C	281.36	274.81	"	

TABLE C.7 continued

SPECIMEN REFERENCE	DYNAMIC YIELD STRESS (N/mm ²)	STATIC YIELD STRESS (N/mm ²)	REMARKS
B12A	322.37	314.96	Sub Assemblage
B12B	296.03	289.30	Tests
B12C	291.50	283.17	"
B13A	331.89	322.17	"
B13B	296.18	289.60	"
B13C	300.56	292.25	"
B14A	332.78	323.66	"
B14B	301.64	294.87	"
B14C	298.39	288.22	"
B15A	335.31	323.06	"
B15B	303.21	294.41	"
B15C	296.30	287.54	"
B16A	328.48	321.10	"
B16B	291.37	280.96	"
B16C	296.61	287.96	"
B17A	290.08	280.62	Frame Test
B17B	265.43	259.53	No. 1
B17C	268.71	262.74	"
B18A	290.95	283.01	"
B18B	264.39	258.54	"
B18C	266.81	260.75	"
B19A		N O T U S E D	
B19B	276.80	269.25	"
B19C	279.46	269.30	"
B20A	296.05	283.37	"
B20B	275.84	266.42	"
B20C	273.50	264.60	"
B21A		N O T U S E D	
B21B	283.01	272.63	"
B21C	275.71	266.30	"
B22A	296.51	286.85	"
B22B	253.14	244.21	"
B22C	280.54	270.63	"
B23A	319.84	311.15	Frame Test
B23B	296.28	287.26	No. 2
B23C	298.39	287.73	"
B24A	322.05	313.34	"
B24B	297.98	289.03	"
B24C	307.36	298.57	"
B25A	317.53	311.78	"
B25B	291.85	282.96	"
B25C	299.78	293.23	"
B26A	298.72	291.44	"
B26B	288.07	279.07	"
B26C	301.98	292.03	"
B27A	294.34	286.95	"
B27B	292.80	286.29	"
B27C	295.58	287.38	"
B28A	297.70	289.43	"
B28B	285.90	276.62	"
B28C	311.42	297.44	"

TABLE C.7 continued

SPECIMEN REFERENCE	DYNAMIC YIELD STRESS (N/mm ²)	STATIC YIELD STRESS (N/mm ²)	REMARKS
ANGLES			
1A	267.20	259.24	Joint Tests
1B	265.73	258.97	"
2A	265.03	257.35	"
2B	278.50	272.76	"
3A	269.09	259.80	"
3B	273.16	260.47	"
4A	281.10	270.10	"
4B	270.41	259.93	"
5A	N O T U S E D		
5B	294.99	286.29	"
12mm plate	298.28	290.43	Joint & Sub Assemblage
15mm plate	446.01	437.44	"
15mm plate	273.53	266.01	Lack of fit tests

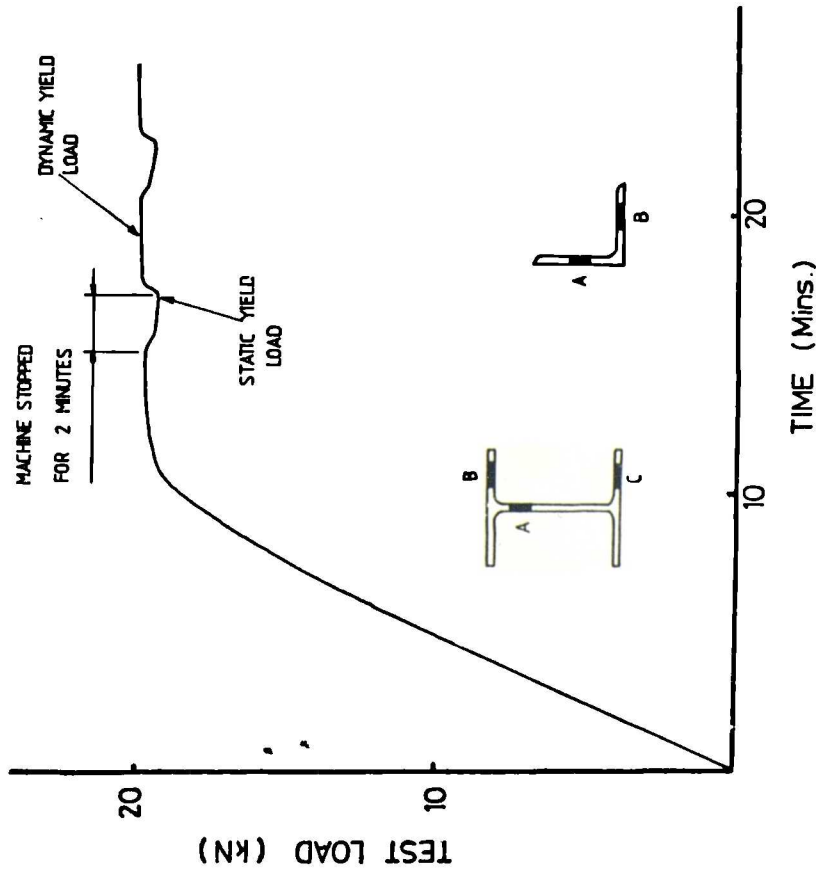


FIGURE C.1 Tensile test - load against time

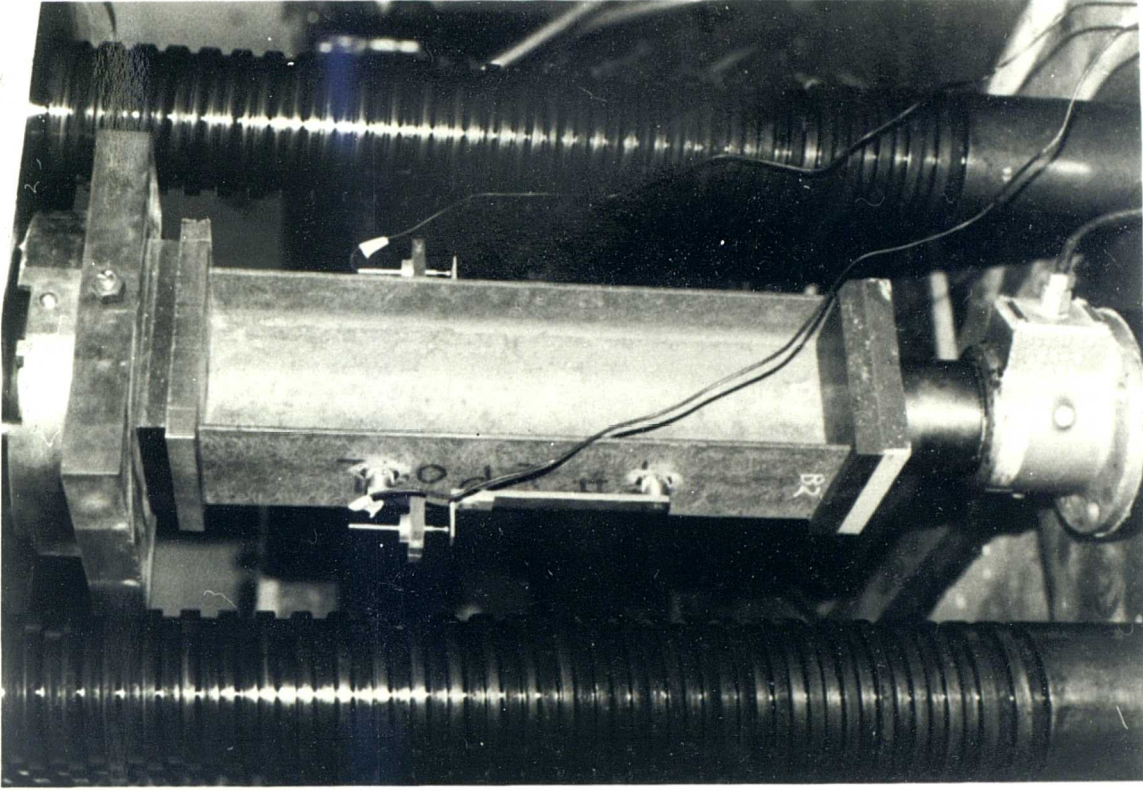


FIGURE C.2 Stub column test in progress

STUB COLUMN TEST

Column C16

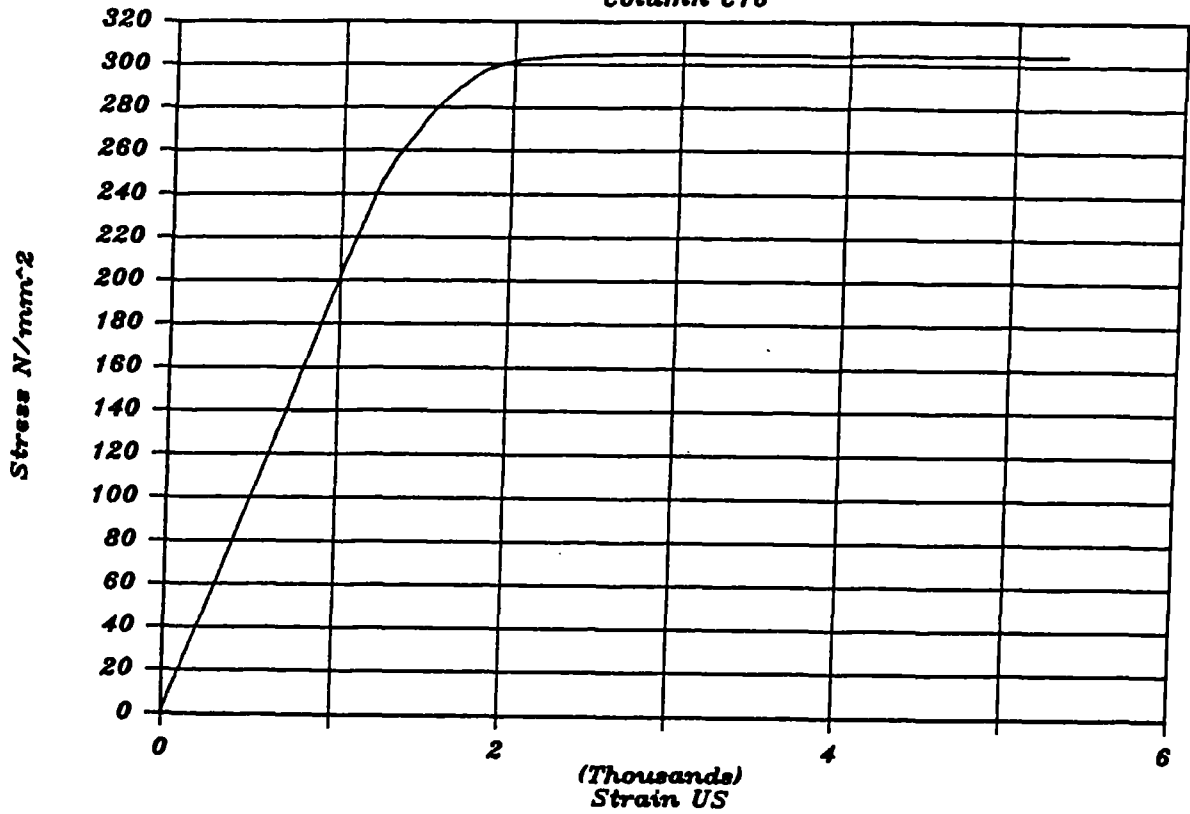


FIGURE C.3 Stress-strain curve for column C16

STUB COLUMN TEST

Column C17

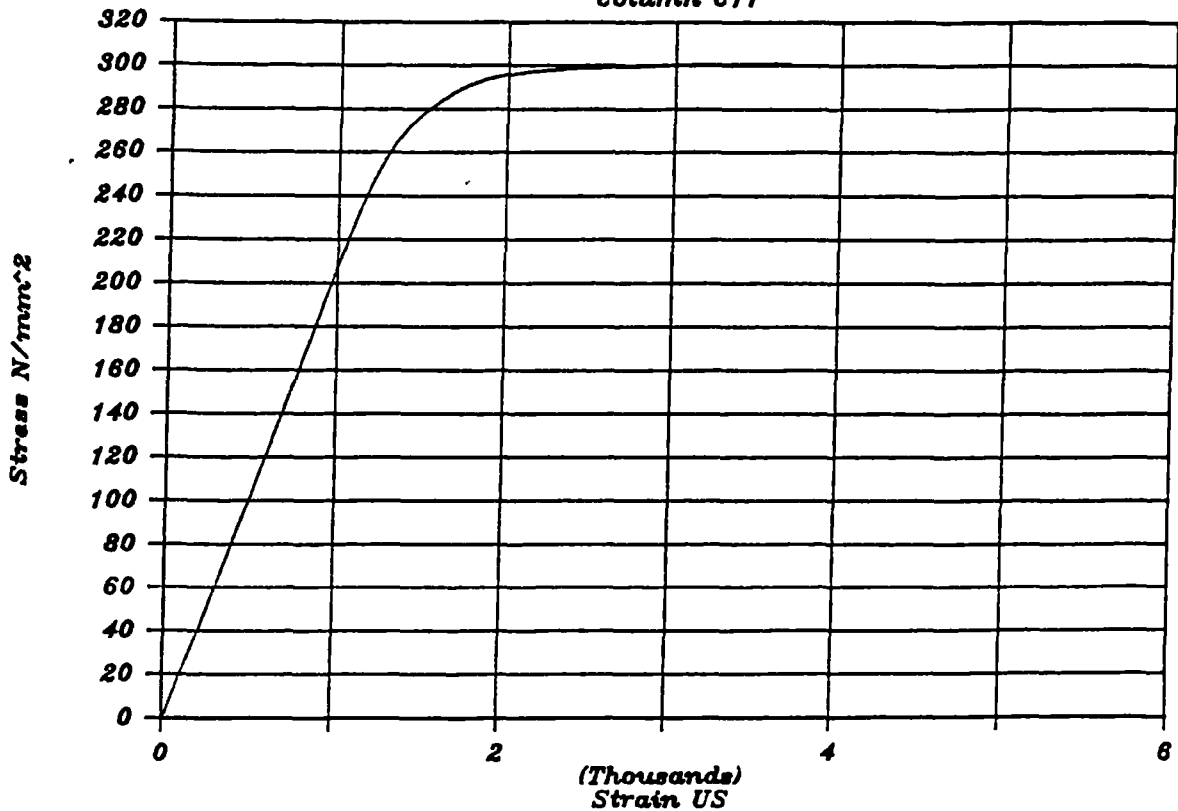


FIGURE C.4 Stress-strain curve for column C17

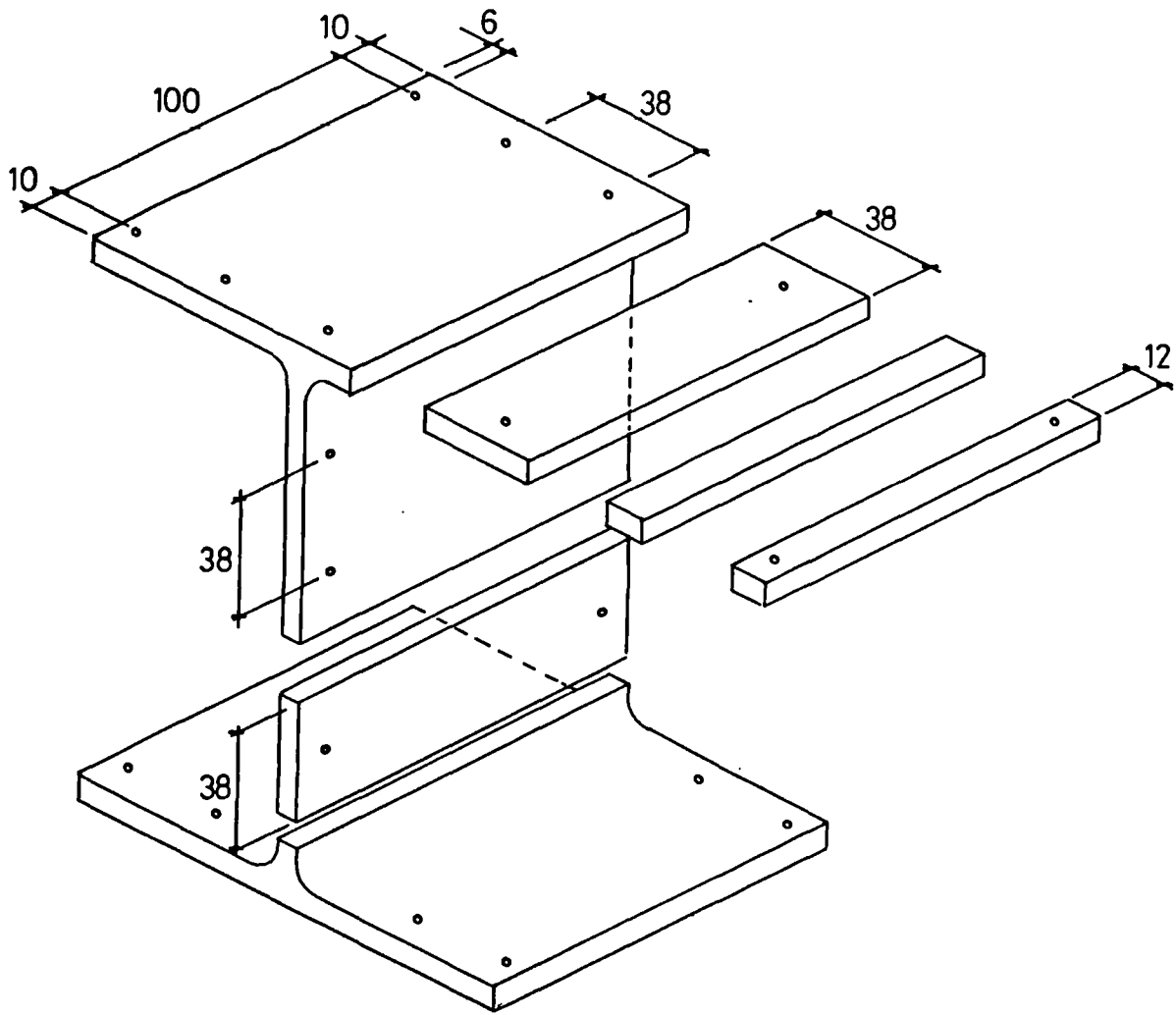


FIGURE C.5 Sectioning of universal column section to determine residual stress pattern

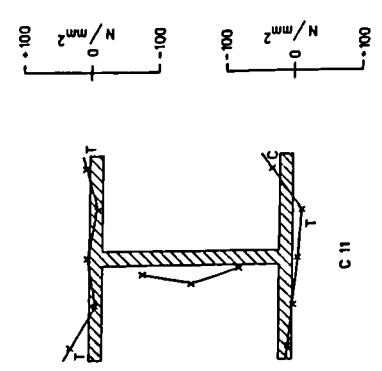
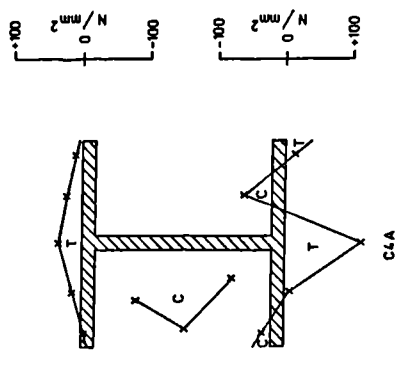
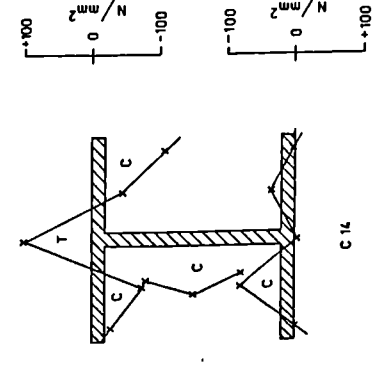
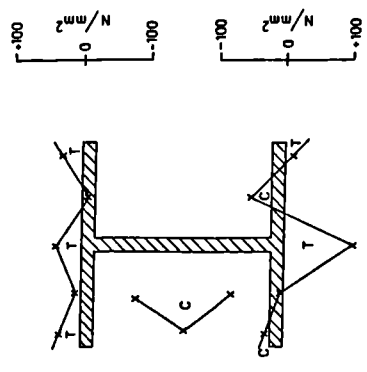
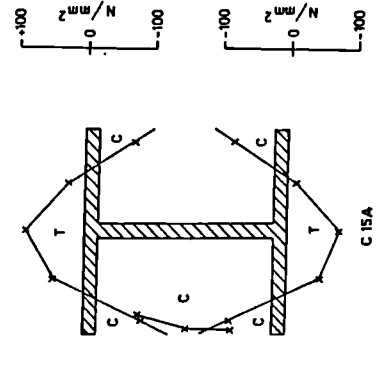
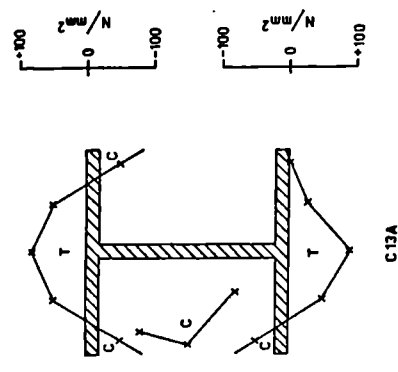
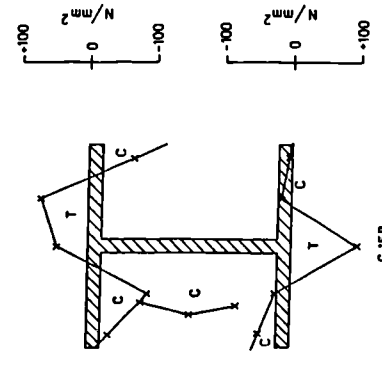
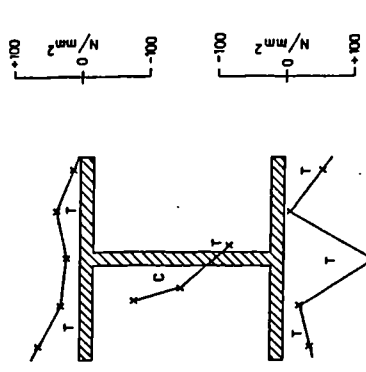


FIGURE C.6 Residual stress patterns for columns C4, C11, C13, C14 and C15